

NATO Science for Peace and Security Series - B:
Physics and Biophysics

Explosives Detection

Sensors, Electronic Systems and Data Processing

Edited by
Lorenzo Capineri
Eyüp Kuntay Turmuş

 Springer

*This publication
is supported by:*

The NATO Science for Peace
and Security Programme

Explosives Detection

NATO Science for Peace and Security Series

This Series presents the results of scientific activities supported through the framework of the NATO Science for Peace and Security (SPS) Programme.

The NATO SPS Programme enhances security-related civil science and technology to address emerging security challenges and their impacts on international security. It connects scientists, experts and officials from Alliance and Partner nations to work together to address common challenges. The SPS Programme provides funding and expert advice for security-relevant activities in the form of Multi-Year Projects (MYP), Advanced Research Workshops (ARW), Advanced Training Courses (ATC), and Advanced Study Institutes (ASI). The NATO SPS Series collects the results of practical activities and meetings, including:

Multi-Year Projects (MYP): Grants to collaborate on multi-year R&D and capacity building projects that result in new civil science advancements with practical application in the security and defence fields.

Advanced Research Workshops: Advanced-level workshops that provide a platform for experts and scientists to share their experience and knowledge of security-related topics in order to promote follow-on activities like Multi-Year Projects.

Advanced Training Courses: Designed to enable specialists in NATO countries to share their security-related expertise in one of the SPS Key Priority areas. An ATC is not intended to be lecture-driven, but to be intensive and interactive in nature.

Advanced Study Institutes: High-level tutorial courses that communicate the latest developments in subjects relevant to NATO to an advanced-level audience.

The observations and recommendations made at the meetings, as well as the contents of the volumes in the Series reflect the views of participants and contributors only, and do not necessarily reflect NATO views or policy.

The series is published by IOS Press, Amsterdam, and Springer, Dordrecht, in partnership with the NATO SPS Programme.

Sub-Series

A. Chemistry and Biology	Springer
B. Physics and Biophysics	Springer
C. Environmental Security	Springer
D. Information and Communication Security	IOS Press
E. Human and Societal Dynamics	IOS Press

- <http://www.nato.int/science>
- <http://www.springer.com>
- <http://www.iospress.nl>



Series B: Physics and Biophysics

Explosives Detection

Sensors, Electronic Systems and Data Processing

edited by

Lorenzo Capineri

Dipartimento Ingegneria dell'Informazione
Università degli Studi di Firenze
Firenze, Italy

and

Eyüp Kuntay Turmuş

Emerging Security Challenges Division
Science for Peace & Security (SPS)
Programme
BRUSSELS, Brussels Hoofdst.ge.,
Belgium



Springer

Published in Cooperation with NATO Emerging Security Challenges Division

Proceedings of the NATO Advanced Research Workshop on Explosives Detection,
Florence, Italy
17–18 October 2018

ISBN 978-94-024-1731-9 (PB)
ISBN 978-94-024-1728-9 (HB)
ISBN 978-94-024-1729-6 (eBook)
<https://doi.org/10.1007/978-94-024-1729-6>

Published by Springer,
P.O. Box 17, 3300 AA Dordrecht, The Netherlands.

www.springer.com

Printed on acid-free paper

All Rights Reserved

© Springer Nature B.V. 2019

This work is subject to copyright. All rights are reserved by the Publisher, whether the whole or part of the material is concerned, specifically the rights of translation, reprinting, reuse of illustrations, recitation, broadcasting, reproduction on microfilms or in any other physical way, and transmission or information storage and retrieval, electronic adaptation, computer software, or by similar or dissimilar methodology now known or hereafter developed.

The use of general descriptive names, registered names, trademarks, service marks, etc. in this publication does not imply, even in the absence of a specific statement, that such names are exempt from the relevant protective laws and regulations and therefore free for general use.

The publisher, the authors, and the editors are safe to assume that the advice and information in this book are believed to be true and accurate at the date of publication. Neither the publisher nor the authors or the editors give a warranty, expressed or implied, with respect to the material contained herein or for any errors or omissions that may have been made. The publisher and the editors remain neutral with regard to jurisdictional claims in published maps and institutional affiliations.

Preface

Mines, unexploded ordnances (UXOs), improvised explosive devices (IEDs) and other explosive remnants of war (ERW) pose a direct threat to the security of the citizens of NATO member and NATO partner countries and to regional development. Mines and UXOs are a persistent global threat, particularly in war-torn countries, and international cooperation is crucial to effectively address this challenge.

In modern times, IEDs are the weapon of choice for terrorists around the world, and as such, there is a growing need for methods to quickly and effectively detect explosives in both military and civilian environments. Explosive detection and removal are extremely challenging as devices become more sophisticated and deadly due to advancements in materials, shapes, sizes and varieties. The high cost and general inaccessibility of state-of-the-art explosives detection devices, combined with the high risk and inefficiency of classic demining activities, and a lack of information and education on detection and clearance in danger zones present considerable challenges to peace and security.

In line with the Brussels Summit Declaration in 2018, the Science for Peace and Security (SPS) Programme continues to support capabilities and technologies to address human, scientific and technological advancements in the field of Mine and UXO Detection and Clearance. Amongst others, SPS supports the development of new capabilities and technologies to tackle the significant threat posed by mines, UXOs and IEDs and to manage the consequences of their proliferation by cooperating with partners and international organizations to leverage the full potential of each stakeholder engaged in the global effort to manage explosive devices. Finally, the programme funds awareness-raising activities and the development of capabilities for long-term solutions.

The SPS Programme is an established NATO partnership tool that is based on the three pillars of science, partnership and security. In the spirit of cooperative security, SPS provides concrete, practical opportunities for cooperation to scientists and experts within NATO's wide network of partner countries based on security-related civil science, technology and innovation. All activities funded under the SPS

Programme address one or more of the programme's key priorities and have a link to security.¹ According to these priorities, the programme promotes cooperation, scientific research and innovation to address contemporary security challenges, enhances support for NATO-led operations and missions, increases awareness of security development including through early warning (e.g. mine and UXO detection and clearance) and is open to any other cooperation clearly linked to the field of security.

The SPS Programme has been contributing to the core goals of the Alliance for six decades. The origins of the programme date back to the 1950s, and its outlook has been successfully adapted to the changing security environment over the years. In 2018, we celebrated the 60th Anniversary of the SPS Programme at NATO, which gave us an opportunity to reflect upon the past several decades of SPS and to showcase prototypes built by SPS-funded experts at NATO headquarters. Today, the SPS Programme is fundamental to building bridges and fostering partnerships amongst NATO members and partners through tailored and targeted activities that promote capacity building and technological innovation through practical cooperation.

It speaks volumes that specialists from well over half of NATO's partner countries have been directors or co-directors of SPS-funded activities under the priority of counterterrorism. Many of these activities focused on explosives management in a variety of fields, including data analysis, developing new and advanced technologies as well as training, preparation, dissemination and capacity building, to name a few. These tailored SPS activities often build links between technological research and development of new capabilities and the human and social aspects of explosives management. For example, an SPS-funded multi-year project to support humanitarian demining in Ukraine was launched by the NATO Support and Procurement Agency and the State Emergency Service of Ukraine (SESU) after a request for support in demining operations in Eastern Ukraine by the Ukrainian government. The project provided a total of 53 types of equipment composing of 841 individual items, 4 vehicles and emergency trauma medical equipment and delivered training focused on the enhancement of SESU skills in clearing newly encountered IEDs.

In Iraq, the SPS Programme funded a training activity responding to a critical capability gap and an immediate Iraqi priority to implement the post-conflict search and clearance requirements, allowing the return of displaced populations. One hundred Iraqi explosive ordnance personnel were trained, and 154 kits of light-scale equipment were delivered through the project. Likewise, in Jordan, SPS has funded a multi-year project to deliver a series of cooperative events and training sessions to provide the Jordanian Armed Forces with more robust and resilient C-IED capabilities.

These activities, which support the human and social aspects of security, are complemented by projects that cultivate new and rapidly developing technologies.

¹The SPS key priorities are based on NATO's Strategic Concept agreed by Allies in the 2010 Lisbon Summit and the strategic objectives of NATO's partner relations agreed in Berlin in 2011.

An ongoing multi-year project led by Italy and Azerbaijan is preparing sensors for the detection of explosives, particularly nitroaromatic explosives like TNT, to be used in unmanned drones for the exploration of hazardous environments. This tool will reduce human-mine contact, thus saving lives. Meanwhile, Turkey and Ukraine are collaborating on a multi-year project to develop technology based on the application of two techniques of explosive detection: nuclear magnetic resonance and microwave sub-THz dielectric spectroscopy in order to create effective and fast methods of identifying explosive and illicit substances.

These are just some examples of many ongoing projects that the SPS Programme is currently supporting in the field of explosives management. The programme provides funding and expert advice for security-relevant activities in the form of workshops, training courses, or multi-year research projects, which foster practical cooperation by developing networks between academia, think tanks, civil society and government representatives. One of the specific objectives of the SPS Programme is to encourage applications that bring a lasting impact and have a thematic and geographical perspective. To this end, applications that promote long-term research in hard sciences, as well as in social disciplines, are encouraged. Social sciences applications may be in the form of long-term studies, case studies with practical applications and field studies. By connecting scientists, experts, government representatives and civil society on key issues of security, the SPS Programme makes a significant, positive impact upon society and achieves tangible and more immediate results.

Brussels, Belgium

Dr. Eyüp Kuntay Turmuş

Introduction

The extensive research on the detection of explosives has been continuously the subject of numerous books and publications [1–17]. This new book is, therefore, included in this line of research and follows others published in the NATO Science for Peace and Security Series by Springer.

This new book derives from the scientific and technological contributions presented at the NATO “Advanced Research Workshop on Explosives Detection,” held in Florence, Italy, on 17–18 October 2018. The workshop offered an opportunity for participants to diffuse the results of their projects and to compare the developed methods and find possible synergies for increasing the technological readiness level of the sensors, the electronics systems, and the detection methods.

The book structure reflects the organization of the workshop (see http://www.nato-sfps-landmines.eu/wp/wp-content/uploads/2018/08/NATO_workshop-.pdf) and consists of three sections.

The first section of the book reports the abstracts of seventeen NATO SPS projects and Three invited contributions to provide a concise information on the project aims and status. The developed methods and the achieved results are reported only for the completed projects.

The second section of the book includes a deep and more complete description also from the scientific point of view of thirteen NATO SPS projects and two from invited scientists who are actively involved in research on explosive detection.

The third section of the book summarizes the main outcomes derived from the final roundtable of the workshop. This section provides an assessment of the scientific and technical developments of the presented projects to determine the future directions of the NATO SPS program in the field of explosive detection.

Lorenzo Capineri

References

1. National Research Council (1998) Containing the threat from illegal bombings: An integrated national strategy for marking, tagging, rendering inert, and licensing explosives and their precursors. The National Academies Press, Washington, DC. <https://doi.org/10.17226/5966>
2. National Research Council (2004) Existing and potential standoff explosives detection techniques. The National Academies Press, Washington, DC. <https://doi.org/10.17226/10998>
3. National Research Council (2004) Opportunities to improve airport passenger screening with mass spectrometry. The National Academies Press, Washington, DC. <https://doi.org/10.17226/10996>
4. Morrison D, Milanovich F, Ivnitski D, Austin ThR (eds) (2005) Defense against bioterror: detection technologies, implementation strategies and commercial opportunities. In: Proceedings of the NATO advanced research workshop on defense against bioterror: detection technologies, implementation strategies and commercial opportunities, held in Madrid, Spain from 8 to 11 April 2004, Series: NATO science for peace and security series
5. Federici JF, Schukin B, Huang F, Gary D, Barat R, Oliveira F, Zimdars D (2005) THz imaging and sensing for security applications—explosives, weapons and drugs. *Semicond Sci Technol* 20(7). Published 8 June 2005, IOP Publishing Ltd
6. Combined devices for humanitarian demining and explosive detection. In: Proceedings of a technical meeting held in Padova, Italy, 13–17 November 2006. <https://www.iaea.org/publications/7769/combined-devices-for-humanitarian-demining-and-explosive-detection>
7. Use of nuclear and non-nuclear techniques for humanitarian demining and explosives detection. In: Proceedings of an IAEA technical meeting held in Vienna, Austria, 26–30 November 2007
8. Yinon J (ed) (Imprint) Counterterrorist detection techniques of explosives, 1st edn. Elsevier Science. Published Date: 3rd July 2007, Page Count: 454
9. Marshall M, Oxley J (eds) (Imprint) Aspects of explosives detection, 1st edn. Elsevier Science. Published Date: 17th October 2008, Page Count: 302
10. Fraissard J, Lapina O (eds) (2009) Explosives detection using magnetic and nuclear resonance techniques. In: NATO science for peace and security series B: physics and biophysics. Springer, Dordrecht. Number of Pages: 292. <https://doi.org/10.1007/978-90-481-3062>
11. David JD (2009) EM detection of concealed targets. Wiley series in microwave and optical engineering. Wiley. Date 14 Dec 2009. ISBN10 0470121696
12. Sun Y (ed) (2010) Field detection technologies for explosives. Format: Kindle Edition, Print Length: 328 pages, Page Numbers Source ISBN: 1906799024, Publisher: ILM Publications, 1 Oct. 2010

13. Marshall M, Oxley JC (eds) (2011) Aspects of explosives detection. Elsevier. ISBN0080923143, 9780080923147, 302 pages
14. Howards W (ed) (2016) Explosives detection canines & homeland security: background & analyses. Nova Science Publishers Inc, New York. Publication date: 01 Dec 2016. 80 pages, ISBN10: 1536101907
15. Pereira M, Shulika O (eds) (2017) THz for cbrn and explosives detection and diagnosis. In: NATO science for peace and security series, sub-series B. Physics and biophysics
16. Pellegrino PM, Holthoff EL, Farrell ME (2017) Laser-based optical detection of explosives, 1st edn. CRC Press. Published September 28, 2017. <https://doi.org/10.1201/9781315215280>. Pages: 409 pages
17. Beldowski J, Been R, Turmus EK (eds) (2018) Towards the monitoring of dumped munitions threat (MODUM). A Study of Chemical Munitions Dumpsites in the Baltic Sea

Contents

NATO Advanced Research Workshop on Explosives Detection	1
Scientific and Technical Contributions from Research Projects	33
Findings of the Advanced Research Workshop	325

NATO Advanced Research Workshop on Explosives Detection



www.nato.int/science
www.nato-sfps-landmines.eu



ADVANCED RESEARCH WORKSHOP ON EXPLOSIVES DETECTION

Florence, Italy | 17-18th October 2018



Under the Auspices of



UNIVERSITÀ
DEGLI STUDI
FIRENZE
DINFO
DIPARTIMENTO
DI INFORMATICA
E INGEGNERIA
DELL'INFORMAZIONE

ORGANIZING SECRETARIAT



**CONGRESS
PLANNERS**

www.congressplanners.com
info@congressplanners.com
Ph. +39 329 2154590



ADVANCED RESEARCH WORKSHOP ON EXPLOSIVES DETECTION

Florence, Italy | 17-18th October 2018

PROGRAM

DAY 1 | 17TH OCTOBER, 2018

08.30-09.00	UNIVERSITY OF FLORENCE Registration
09.00-09.20	Introductory Remarks <i>Lorenzo Capineri, University of Florence, Department of Information Engineering, Italy</i> Eyüp Kuntay Turmuş, NATO SPS Advisor and Programme Manager
09.20 -13.00	MORNING SESSION Moderator: Eyüp Kuntay Turmuş
09.20-09.40	Opening Address <i>Robert Weaver, Deputy Assistant General for NATO Emerging Security Challenges Division</i>
09.40-10.00	Overview of SPS Programme and Explosive Detection as a Key Priority <i>Eyüp Kuntay Turmuş, NATO SPS Advisor and Programme Manager</i>
10.00-10.20	Holographic and Impulse Subsurface Radar for Landmine and IED Detection (G-5014) <i>Lorenzo Capineri, University of Florence Gennadiy Pochanin, Usikov Institute for Radiophysics and Electronics of the NAS of Ukraine Tim Bechtel, Franklin & Marshall College, Department of Earth and Environment, USA</i>
10.20-10.40	Explosives Detection: Growing Threat and New Approaches <i>Pierre Charrue, SPS Independent Scientific Evaluation Group Member, France</i>
10.40-11.00	Coffee break Poster Session
11.00-11.20	Advanced Technology for Landmine Detection <i>Tor-Sverre Lande, Dept. of Informatics, University of Oslo, Norway</i>
11.20-11.40	Engineering silicon carbide for enhanced borders and ports security (E-SiCure) (G-5215) <i>Ivana Capan, Rudjer Boskovic Institute (RBI), Croatia</i>
11.40-12.00	Explosive Trace Detection for Standex (EXTRAS) (G-5526) <i>Antonio Palucci, Italian National Agency for New Technologies, Energy and Sustainable Economic Development (ENEA), Italy</i>

12.00-12.30	Q&A session Moderator: Tim Bechtel
12.30-12.50	Speech from the Rector of the University of Florence Luigi Dei, <i>University of Florence</i>
12.50-14.00	Lunch
14.00 -17.00	AFTERNOON SESSION Moderator: Eyüp Kuntay Turmuş
14.00-15.00	TECHNOLOGY DEMONSTRATIONS Holographic and Impulse Subsurface Radar for Landmine and IED Detection Project: G-5014 Lorenzo Capineri Engineering silicon carbide for enhanced borders and ports security (E-SiCure) Project: G-5215 Ivana Capan
15.00-15.20	Portable Sensors for Unmanned Explosive Detection (G-5423) Claudio Ferrari, <i>Institute of Materials for Electronics and Magnetism National Research Council (IMEM-CNR), Italy</i> Nahida Musayeva, <i>Institute of Physics, Azerbaijan National Academy of Science, Azerbaijan</i>
15.20-15.40	Standoff Coherent Detection of Warfare Chemicals via Photoacoustic Spectroscopy (G-5500) Seydi Yavas, <i>Bogazici University Physics Department, Turkey</i>
15.40-16.00	Coffee Break Poster Session
16.00-16.20	Ground penetrating radar attached to a Hexacopter for Automatic Mine Detection (G-5208) Dušan Gleich, <i>University of Maribor, Faculty of Electrical Engineering and Computer Science, Slovenia</i> Venceslav Kafedziski, <i>University SS Cyril and Methodius in Skopje, the former Yugoslav Republic of Macedonia (*)</i>
16.20-16.40	GPR Research for Military Search Daniela Deiana, <i>Electronic Defence, TNO Defence, Safety and Security, The Netherlands</i>
16.40-17.00	Q&A Session and Wrap-up Moderator: Tim Bechtel

(*) Turkey recognizes the Republic of Macedonia with its constitutional name.

DAY 2 | 18TH OCTOBER, 2018

09.00 -13.00

MORNING SESSION

Moderator: Lorenzo Capineri

09.00-09.20

Biological Method (Bees) for Explosive Detection (G-5355)

Sanja Vakula, Croatian mine action centre - Centre for Testing, Development and Training (HCR-CTRO), Croatia
Zdenka Babić, University of Banja Luka Research Fellow, Bosnia and Herzegovina
Ross Gillanders, University of St Andrew, UK

09.20-09.40

Magnetic resonance & MW detection of improvised explosive and illicit materials (G-5005)

Bulat Rameev, Gebze Technical University, Department of Physics, Turkey
Sergey Tarapov, O.Ya. Usikov Institute for Radio-physics and Electronics (IRE) , Ukraine
Bektaş Çolak, Alanya Alaaddin Keykubat University, Turkey

09.40-10.00

Comprehensive Package for strengthening Jordanian C-IED defence capabilities (G-5387)

Tabi Levente, C-IED Center of Excellence, Spain
Edoardo Cazorla Sarabia, C-IED Center of Excellence, Spain

10.00-10.20

Development of New Chemical Sensors and Optical Technologies for Fast and Sensitive Detection of Improvised Explosives (G-5536)

Tomas Torroba Perez, University of Burgos, Spain

10.20-11.00

Implementation of a Terahertz Imaging and Detection System (G-5396)

Jean-Louis Coutaz, Université Savoie Mont-Blanc, France
Mohamed Lazoul, Ecole Militaire Polytechnique, Algeria

11.00-11.20

Coffee Break | Poster Session

11.20-11.40

Technology of High-Selective Imprinted Nanoantenna for Explosives Detection (G-5361)

Volodymyr Chegel, V.E. Lashkaryov Institute of Semiconductor Physics, National Academy of Sciences of Ukraine
Juan Pastor Martinez, University of Valencia, Spain

11.40-12.00	Microwave Imaging Curtain (G-5395) Dmytro Tatyanko, IRE NAS, Ukraine
12.00-12.20	ALIS Dual sensor for Humanitarian Demining Motoyuki Sato, Institution Tohoku University, Japan
12.20-12.40	Development of mine and IED recognition system based on ultrawideband technology (G-5217) Iurii Voitenko, Norwegian University of Science and Technology (NTNU), Norway
12.40-13.00	Q&A Session Moderator: Tim Bechtel
13.00-14.00	Lunch Break
14.00-15.00	TECHNOLOGY DEMONSTRATIONS
	ALIS Dual sensor for Humanitarian Demining Motoyuki Sato, Institution Tohoku University, Japan
	Development of mine and IED recognition system based on ultrawideband technology Project: G-5217 Iurii Voitenko
15.00-16.00	Round Table Discussion: <ul style="list-style-type: none">• Contributions of SPS Programme to the Field of Explosives Detection;• Recommendations for future SPS Activities;• Call for Proposals
16.00-16.30	Wrap-up and Conclusions

GENERAL INFORMATION

CONFERENCE CHAIRS

WORKSHOP CHAIR

Dr. Eyüp Kuntay Turmuş

NATO

Science for Peace and Security

Advisor and Programme Manager

SCIENTIFIC CHAIR

Prof. Lorenzo Capineri

University of Florence

Department of

Information Engineering

THE VENUE

University of Florence

Department of Information Engineering

Via Santa Marta, 3

Firenze | Italy



SHUTTLE SERVICE

17th October	Hotel Donatello > University of Florence	08.00 am
	University of Florence > Hotel Donatello	05.00 pm
18th October	Hotel Donatello > University of Florence	08.30 am
	University of Florence > Hotel Donatello	04.30 pm



Holographic and Impulse Subsurface Radar for Landmine and IED Detection¹

Lorenzo Capineri (✉)

Dipartimento Ingegneria dell'Informazione, Università degli Studi di Firenze,
Firenze, Italy

Gennadiy Pochanin

O.Ya. Usikov Institute for Radiophysics and Electronics, National Academy of
Sciences of Ukraine, Kharkiv, Ukraine

Timothy Bechtel

Department of Earth and Environment, Franklin and Marshall College, Lancaster,
PA, USA

Project Description

As of 2017, there are an estimated 100 million abandoned land mines littered across 61 countries. Following the wars in Afghanistan, Libya, Syria, Yemen, and Ukraine, there has been a rise in casualties due to the triggering of previously-abandoned explosive devices. The above institutions combined specialties to develop a remotely-operable, multisensor, robotic device for the detection of land mines, UXO (1), and IEDs (2). The robotic detection device uses novel subsurface radar with imaging and target classification to differentiate between threatening landmines and innocuous clutter. The expected outcome of this research is the creation of a multi-sensor system on a semi-autonomous vehicle for detection and discrimination of explosive devices. This robotic platform will change the approach to detecting landmines in post-war zones, all the meanwhile lessening direct human-to-mine or animal-to-mine contact in detecting landmines. Architecture has a high potential to move the procedures of explosive detection toward completely remote and autonomous system.

¹Multi-year research project – Ref. no G5014. Status: Completed.



- *Robotic platform with UWB Ground*
 - *Penetrating Radar*
 - *Holographic Subsurface Radar*
 - *(2GHz) and 3D depth camera.*
- (1) “UXO” – unexploded ordnances
(2) “IEDs” is an abbreviation used improvised explosive devices

Engineering Silicon Carbide for Enhanced Borders and Ports Security (E-Sicure)²

Ivana Capan (✉)

Rudjer Bošković Institute, Zagreb, Croatia

Zeljko Pastuovic

Australian Nuclear Science and Technology Organization, Lucas Heights, NSW, Australia

Takeshi Ohshima

National Institutes for Quantum and Radiological Science and Technology, Takasaki, Gunma, Japan

Jose Coutinho

Universidade de Aveiro, Aveiro, Portugal

Luka Snoj

Jozef Stefan Institute, Ljubljana, Slovenia

²Multi-year research project – Ref. G5215. Status: Ongoing.

Project Description

Increasingly complex risks, like geopolitical instability or decentralized terrorism threats, have led to the urge for deploying nuclear screening systems for detection of illicit trafficking of nuclear materials, and from that, to a growing interest in the field of research and development of new radiation detection technologies suitable for homeland security applications. Unlike existing and commonly used neutron gasbased detectors, SiC-based devices have the potential to be simultaneously portable, operable at room temperature and radiation hard.

Recent progress in i) the manufacturing of high-quality bulk and epitaxial silicon carbide (SiC) and ii) processing technologies for fabrication of SiC-based electronic devices, could enable unprecedented detection properties of the future SiC-based detectors for neutron and alpha-particle emissions.

Our main objective is to combine theoretical, experimental and applied research towards the development of radiation-hard SiC-based detectors of special nuclear materials (SNM), and therefore to enhance border and port security barriers. This will be achieved through material modification processes in order to manipulate the most severe electrically active defects (which trap or annihilate free charge carriers), by specific ion implantation and defect engineering.

Explosive Trace Detection for Standex (Extras)³

Antonio Palucci (✉)
ENEA, Rome, Italy

Stoiljkovic Milovan
Vinča Institute of Nuclear Sciences, Belgrade, Serbia

Valentin Kolobrodov
National Technical University of Ukraine, Kiev, Ukraine

Bart Boonaker
TNO, The Hague, Netherlands

Frank Schnürer
ICT Fraunhofer, Pfinztal, Germany

Cristiano Stifini
ATAC, Rome, Italy

Luigi Carnevale
Ministry of Interior, Rome, Italy

³Multi-year research project – Ref. G5526. Status: Ongoing.

Project Description

The EXTRAS project has the intention to contribute to the development of a stand-off sensor to monitor trace components in a scanning mode to be compliant with the safety civil regulations, in the frame of the NATO STANDEX II programme.

ENEA has already successfully participated in the previous STANDEX programme, with the RADEX (Raman Standoff Detection of Explosives) apparatus, being also operated during the final demonstration in metro station Francois Mitterrand in Paris, July 2013.

The NATO project G5526 EXTRAS is a step forward from RADEX and the improvements will be introduced in order to enhance the overall performance of the apparatus and reduce the false alarm rate. Upgrades are scheduled in the optical scheme, in optical components, scanning in the two axes and in a new 3D vision capability and tracking capability.

EXTRAS apparatus will be implemented as confirmation sensor of information previously gained by other instruments (bulk analysis) and with the advantage to be installed in scenarios like an infrastructure with a high transit of people such as metro and train stations. Furthermore, a final test in a real environment has been included with the support of different end-users.

Portable Sensors for Unmanned Explosive Detection⁴

Claudio Ferrari (✉)

Institute of Materials for Electronics and Magnetism (IMEM-CNR), Parma, Italy
e-mail: claudio.ferrari@cnr.it

Nahida Musayeva

Institute of Physics, Azerbaijan National Academy of Sciences, Baku, Azerbaijan

Francesco Sansone

Department of Chemistry, Life Sciences and Environmental Sustainability,
University of Parma, Parma, Italy

Project Description

Technologies for explosive detection are characterised by sensitivity and selectivity. Portable devices, with the possibility of being carried by small drones, are required if the use has to be extended to dangerous environments.

⁴Multi-year research project – Ref. G5423. Status: Ongoing.

Sensors based on functionalised nanostructures, in particular those based on changes of conductivity of nanowire and nanotubes after interacting with explosive molecules are characterized by a very high sensitivity, with detection limit up to a few molecules per cm³, an enhanced selectivity, that can be achieved by combining nanostructures with different functionalization and an easy detection of the conductance signal, achievable with simple instrumentation (a signal amplifier). Therefore, functionalised nanostructure can offer a sensing solution to realise detectors offering a high sensitivity and combined with a very limited weight and electrical consumption. The favourable surface/volume ratio typical of nanostructure allow to realise sensitive, selective and small detectors suitable to be carried by drones.

In the present project we propose the preparation of sensors for explosive detection, in particular of nitroaromatic explosives such as TNT, based on germanium nanowires and carbon nanotubes as a starting point for the realization of to be used in unmanned drones for the exploration of hazardous environments.

Standoff Coherent Detection of Warfare Chemicals Using Photoacoustic Spectroscopy⁵

Mehmet Burcin Unlu (✉)

Department of Physics, Bogazici University, Istanbul, Turkey

Ihor Pavlov

Institute of Physics of the National Academy of Sciences of Ukraine, Kyiv, Ukraine

Yuriy Serozhkin

V. Lashkaryov Institute of Semiconductor Physics, Kyiv, Ukraine

Project Description

Remote detection of potentially dangerous chemicals or explosive materials is one of the top key priorities for the civil security. With the increasing rate of terrorist attacks, every year thousands of people are dying in terror attacks with explosives and chemicals. One of the ways to detect and identify potentially hazardous chemicals is recording their absorption spectra, which are known as a fingerprint for every material.

In this project, we will develop an integrated platform for remote detection of explosive materials and potentially hazardous gases from a distance up to 1 km, based on remote coherent vibrometry of photo-acoustic signal generated on the

⁵Multi-year research project – G5500. Status: Ongoing.

tested surface (or volume) by modulated light from excitation laser. We expect the developed methods, and the results of the measurements will have a significant impact on standoff detection technologies against the terrorist threat for explosive devices and other warfare chemicals including liquids and gases.

The results of the project will have a significant impact from two perspectives. Firstly, it will create know-how of a really safe contact-free remote detection method for potentially dangerous chemicals and explosive materials, which is one of the top priorities for the civil security. This know-how will be transferred to defense industry companies. Secondly, we expect the generation of important scientific data which will result several high impact publications. The revealed strengths and limitations of the system will create a background for future investigations and international project proposals. Besides, the obtained results from the project (including photo and video of real-time measurements) will be demonstrated on multiple international conferences and exhibitions.

Ground Penetrating Radar Attached to a Hexacopter for Automatic Mine Detection⁶

Dušan Gleich (✉)
University of Maribor, Maribor, Slovenia
e-mail: dusan.gleich@um.si

Venceslav Kafedziski
Faculty of Electrical Engineering, University of Cyril and Method, Skopje, Republic of Macedonia

Emir Skejic
Faculty of Electrical Engineering, University of Tuzla, Tuzla, Bosnia and Herzegovina

Project Description

This project deals with the methods and strategies for a land mine detection using a hexacopter. The goal is to develop a low-cost ground penetrating radar using standard radio frequency components. There exist two approaches, time domain and frequency domain approaches. The first one requires a pulse with short duration, typically few 100 ps and the other approach, which is easier to implement is to observe amplitude and phase between received and transmitted echoes. The

⁶Multi-year research project – Ref. G5208. Status: Ongoing.

developed radar will be attached to the hexacopter and a graphical user interface will be developed for the detected landmine localization in the graphical or GPS coordinated.

Landmines are made of metal or plastic, and there are many known detection principles or methods, which include also use of animals e.g. rats. Many of them have the disadvantage, that they cannot detect plastic landmines, but only metal. With use of electromagnetic (EM) radiation-microwaves this is not the case with suitable wavelengths, because the signal can penetrate through the ground surface and inside reflect from items with different dielectric constant or conductivity as the ground soil. This includes also explosive inside plastic landmines. The main objective addresses automatic land mine detection, which is a SPS key priority.

The proposed project is hardware and software oriented. The hardware will be developed using a standard component. It is known that the GPR hardware is very expensive, therefore our goal is to propose a low-cost solution and publish it on a web site, and that the end users can repeat experiments. Beside the hardware some new methods for land mine detection using a real time are under investigation. The compressed sensing, which can recover the original signal using less samples than theoretical bound are intensively researched. Those methods will enable landmine detection using a real time acquisitions.

Biological Method (Bees) for Explosive Detection⁷

Nikola Pavkovic (✉)

Croatian Mine Action Centre – Centre for Testing, Development and Training (HCR-CTRO), Benkovac, Croatia

e-mail: nikola.pavkovic@ctro.hr

Zdenka Babic

University of Banja Luka, Banja Luka, Bosnia and Herzegovina

Graham Turnbull

University of St Andrews, St Andrews, UK

Mario Muštra

Faculty of Transport and Traffic Sciences, University of Zagreb, Zagreb, Croatia

⁷Multi-year research project – Ref. G5355. Status: Ongoing.

Project Description

Mines are still present in Croatia, Bosnia and Herzegovina, and many countries through the world. Humanitarian demining is expensive, time consuming and presents high risks and threats. Besides well-developed techniques and procedures such as metal detectors and prodders, use of biological methods is recommended. Over the past decade, biotechnologies have had a significant place in scientific research, the results of which enable application in explosive detection. Within the EU FP7 TIRAMISU project, we developed procedures and methods for training honeybees and their colonies.

This follow-on project aims to develop innovative methods and technologies for detection of legacy landmines. This will be achieved through advancement and integration of state of the art techniques, namely, trained bee colonies in conjunction with organic semiconductor-based explosive vapor sensing films and UAVs with high definition and thermal imaging cameras and image processing and analyzing software. The application of these methods will enable both the passive sampling of an area in order to confirm presence of explosive materials and the active pinpointing of landmine locations. The main idea is to work with end users and experts in order to ensure high efficiency of project results and to reduce risks.

Magnetic Resonance & MW Detection of Improvised Explosive and Illicit Materials⁸

Bulat Rameev
Gebze Technical University, Gebze, Turkey

Sergey Tarapov (✉)
O.Ya.Uistikov Institute for Radiophysics and Electronics (IRE), Kharkiv, Ukraine
e-mail: tarapov@ire.kharkov.ua

İlhami Ünal
TUBITAK, Marmara Research Center, MILTAL Lab, Gebze, Turkey

Bektaş Çolak
Alanya Alaaddin Keykubat University, Alanya, Turkey

⁸Multi-year research project – Ref. G5005. Status: Ongoing.

Project Description

An issue of critical importance is to develop effective methods for detection of explosive and other dangerous substances in transport and at critical infrastructure objects. For addressing this issue, we proposed the combined use of two complementary methods of explosive detection: (1) time-domain (TD) nuclear magnetic resonance (NMR) technique; (2) MW & sub-THz dielectric spectroscopy.

In the project we proposed the development of the novel technology based on application of two techniques of explosive detection: (1) nuclear magnetic resonance (NMR) technique and (2) microwave & sub-THz dielectric spectroscopy. The main objective of the Project is to develop the effective and fast technique of identification of explosive and illicit substances by combined use of these (spectroscopic) techniques.

The project results are expected to be realized in the prototype of the device which will use both TD NMR and MW spectroscopy. The proposed device and methods, to the best of our knowledge, have not analogues in commercial devices available today. On the other hand, the main project results have been already presented at a number of national and international conferences and meetings.

Comprehensive Package for Strengthening Jordanian C-IED Defence Capabilities⁹

Levente Tábi (✉) 
C-IED Centre of Excellence, Madrid, Spain
e-mail: ltabi@ciedcoe.org

Ra'ed Salameh Alghyaline
Jordanian Armed Forces EOD-IEDD UNIT, Amman, Jordan

Raymond Lane
Defence Forces Training Center, Dublin, Ireland

Project Description

The aim of the project is to partner with the Jordanian defence and security officials and deliver a series of cooperative events and trainings. At the end of the project the Jordanian Armed Forces (JAF) will have all the critical Countering Improvised Explosive Devices (C-IED) capabilities. Upon the successful completion of this project, Jordanian Armed Forces would need only annual NATO C-IED Senior

⁹Multi-year research project – Ref. G5387. Status: ongoing.

leader Engagement with Subject Matter Experts to confirm continued progress of engagement to this would then be a task for Jordan to maintain their C-IED capabilities. The increasingly unstable security situation and increasing regional IED threat can be mitigated by this Multi-Year Project.

The Jordanian defence and security forces are likely capable of meeting the current threat, however, this program aims to assist in providing a more robust and resilient capability to the JAF and other Jordanian Security institutions to respond to the demonstrated increasing IED threat presented by Daesh/Islamic State and other violent Extremist Organizations.

This NATO Multi-Year Project will support the Jordanian defence and security forces in keeping and improving their flexible, highly-responsive force capability by meeting the current and more importantly the future IED threat.

Development of New Chemical Sensors and Optical Technologies for Fast and Sensitive Detection of Improvised Explosives¹⁰

Tomás Torroba (✉)
University of Burgos, Burgos, Spain
e-mail: totorroba@ubu.es

Israel Schechter
TECHNION, Haifa, Israel

Project Description

Over the past decade, the use of improvised explosive devices has increased, highlighting a growing need for a method to quickly and reliably detect explosive devices in both military and civilian environments before the explosive can cause damage. Conventional techniques have been successful in explosive detection, however they typically suffer from enormous costs in capital equipment and maintenance, costs in energy consumption, sampling, operational related expenses, and lack of continuous and real-time monitoring.

The goal of this project is to produce portable sensors that continuously monitor the environment, detect the presence of explosive compounds and alert the user. It will facilitate mutual beneficial cooperation on issues of common interest, including international efforts to meet emerging security challenges in counter-terrorism by the

¹⁰Multi-year research project – Ref. G5536. Status: ongoing.

implementation of detection technologies against the terrorist threat for explosive devices and other illicit activities.

The specific objective of this work will be to use chemical sensors combined with multiphoton electron extraction spectroscopy (MEES) in a platform that will consist of two independent sensing mechanisms, by chemical sensing and spectroscopy, which will take measurements from the same sample simultaneously and will provide a redundancy in response for positive explosive identification. By the system, TATP, HMDT and conventional explosives will be reliably detected. By the accomplishment of the project we will generate new knowledge and technology in counter-terrorism by generating new detection technologies against the terrorist threat for explosive devices and other illicit activities.

Implementation of a Terahertz Imaging and Detection System¹¹

Jean Louis Coutaz (✉)

Université Savoie Mont-Blanc, Chambéry, France

e-mail: Jean-Louis.Coutaz@univ-smb.fr

Mohamed Lazoul

Ecole Militaire Polytechnique, Bordj El Bahri, Algeria

Fredrik Laurell

Royal Institute of Technology, Stockholm, Sweden

Project Description

This project aims at designing and realizing a terahertz (THz) imaging and detection system that will be used to secure sensible places from terrorism and to fight against illegal traffic of dangerous materials. Indeed, THz radiations have strong penetrating capabilities. They potentially allow one seeing through many non-conductive materials (such as skin, clothing, paper, wood, cardboard, plastics ...). They are low energy and non-ionizing, unlike X-Rays, which makes them harmful. Furthermore, many molecules exhibit roto-vibrational resonances at THz frequencies, with unique fingerprints, which permits to detect them and even more to identify them, while it could be not possible in other spectral domains (vIS, IR).

The advantage of THz spectroscopy is to penetrate the packaging in which the explosives are potentially hidden. In this case, a unique and distinctive spectral

¹¹Multi-year research project – Ref. G5396. Status: Ongoing.

signature is recorded in transmission or in reflection mode, whether it is a pure explosive or associated with other chemical agents. Following this project, other NATOrelevant applications could be addressed, such as lethal gases or explosive detection in public areas or on the battlefields, or monitoring air pollution.

The goals of the project are first to install a THz spectroscopy laboratory at EMP, Bordj El Bahri, in Algeria, and then to build up a platform for THz imagery purpose. Secondly and simultaneously, fundamental researches will be performed in the domain of THz generation in periodic crystals.

Technology of High-Selective Imprinted Nanoantenna for Explosives Detection¹²

Sergey Piletsky

University of Leicester, Leicester, UK

Volodymyr Chegel

V.E. Lashkaryov Institute of Semiconductor Physics National Academy of Sciences,
Kyiv, Ukraine

Juan Martinez-Pastor (✉)

University of Valencia, València, Spain

e-mail: Juan.Mtnez.Pastor@uv.es

Project Description

Over the past decade, the use of improvised explosive devices has increased, highlighting a growing need for a method to quickly and reliably detect explosive devices in both military and civilian environments before the explosive can cause damage. Conventional techniques have been successful in explosive detection, however they typically suffer from enormous costs in capital equipment and maintenance, costs in energy consumption, sampling, operational related expenses, and lack of continuous and real-time monitoring.

The goal of this project is to produce portable sensors that continuously monitor the environment, detect the presence of explosive compounds and alert the user. It will facilitate mutual beneficial cooperation on issues of common interest, including international efforts to meet emerging security challenges in counterterrorism by the implementation of detection technologies against the terrorist threat for explosive devices and other illicit activities.

¹²Multi-year research project – Ref. G5361. Status: Ongoing.

The specific objective of this work will be to use chemical sensors combined with multiphoton electron extraction spectroscopy (MEES) in a platform that will consist of two independent sensing mechanisms, by chemical sensing and spectroscopy, which will take measurements from the same sample simultaneously and will provide a redundancy in response for positive explosive identification. By the system, TATP, HMDT and conventional explosives will be reliably detected. By the accomplishment of the project we will generate new knowledge and technology in counter-terrorism by generating new detection technologies against the terrorist threat for explosive devices and other illicit activities.

Microwave Imaging Curtain¹³

Florent Christophe
ONERA-DEMRA, Palaiseau, France

Kostantin Lukin (✉)
O.Ya. Usikov Institute for Radiophysics & Electronics, NASU, Xapki

Sangwook Nam
Seoul National University, Seoul, South Korea

Project Description

The project deals with radar design obtained by a combination of two approaches: stepped frequency radar and noise radar for the purposes of SAR imaging. Motivation for such combination is the need to overcome the drawback of noise radars such as necessity of using fast ADCs in order to provide high range resolution and drawbacks of stepped frequency radar such as presence of range ambiguities, low electromagnetic compatibility, high probability of interception and low interference immunity.

The objective of the project is to describe the approach, to present results of its preliminary experimental investigation and to confirm possibility of using this approach for SAR imaging.

Implementation of the Project will demonstrate possibility to design an efficient MIMO SAR system capable of generating high resolution 2D and 3D SAR images in real time scale, which will give the possibility of public area monitoring. As for implementation of our part of the Project, we have quiet long experience in design of Noise Radar, Ground Noise SAR, FPGA based digital generation and processing of

¹³Multi-year research project – Ref. G5395. Status: Ongoing.

random signals, fast algorithms for 3D SAR imaging and radar tomography. The related equipment and experiments have been done and the results have published. Implementing of fast antenna switching in Ku-band MIMO antenna array would be a challenge in Current project. However, with the help our partners and ONERA RF technology we will cope with all the problems.

Development of Mine and IED Recognition System Based on Ultrawideband Technology¹⁴

Iurii Voitenko

Norwegian University of Science and Technology, Trondheim, Norway

e-mail: iurii.voitenko@hig.no

Serhiy Bunin

Kiev Polytechnic Institute, Kyiv, Ukraine

Project Description

Land mines left behind from wars worldwide are one of the century's main unsolved problems and remain the focus of humanitarian mine detection and removal. Although the number of unexploded land mines globally is unknown, it is beyond doubt huge.

Today's mines and IEDs have different shape and varieties, which makes them more and more deadly sophisticated. There are even examples of pure plastic IEDs completely undetectable by classic mine detection technologies. Proposed project is aimed at development of the advanced mine and IED recognition system based on ultrawideband radars, that allow for more comprehensive detection along with 3D imaging of the underground objects up to 3 m in depth.

The system developed under this project will enhance effectiveness and quality of mine/ERW/IED recognition and clearance practices and thus increase protection of innocent people, servicemen, as well as equipment and infrastructure. It will also reduce considerably the cost and duration of such works. We expect to shorten the time needed to detect a mine or IED through quality 3D visualization and classification of the underground object. It will also be possible to achieve universality in application of mine/ERW/IED recognition devices by making them man-portable and mountable at the same time.

¹⁴Multi-year research project – Ref. G5217. Status: Completed.

Advanced Detection Equipment for Demining and UXO Clearance in Egypt¹⁵

Arnold Schoolderman
TNO, The Hague, The Netherlands
e-mail: arnold.schoolderman@tno.nl



Project Description

Egypt is regarded as one of the most contaminated countries in the world in terms of the number of mines and explosive remnants of war scattered across its territory. The issue poses a serious security challenge for local populations and hinders economic development and investment. As a result, large swathes of land are rendered unsafe and unusable.

In a coordinated effort to tackle this issue, NATO and Egypt completed a two-year project to introduce advanced detection systems suitable for demining in the Egyptian desert.

¹⁵Multi-year project – Ref. G4444. Status: Completed.

The majority of landmines in Egypt are remnants of military action during World War II. As these devices date back several decades, mapping and detection can be extremely difficult.

Today, it is thought that at least 10% of landmines and explosive remnants across Egypt are at depths of over 1.5 m. Another major problem is that these devices are often found in locations contaminated with metal fragments from former battlefields. The challenge is that widely-used manually operated metal detectors cannot discriminate between mines and harmless metal fragments, leading to false alarms. As each alarm signal must be investigated by the Egyptian authorities, this slows down demining operations considerably.

Launched in 2012, this project aimed to help Egyptian deminers to develop an operational capability for both dual-sensor and deep-search detectors.

The first phase of the project sought to develop dual-sensor technologies with a ground-penetrating radar (GPR), making it possible to not only detect metallic objects but also to deduce volume, allowing metal fragments to be distinguished from mines. GPR technology also facilitates mine-detection operations by enabling the mapping of the sub-surface, as it can detect objects, volumes and areas that have different electromagnetic properties.

As dual-sensor detectors are only able to detect mines and explosive remnants to a depth of between 0.5 and 1 m, specific deep-search detectors were employed during the second phase of the project. The Egyptian Military Engineers will benefit from the advanced detection equipment, which will result in better, safer and faster demining of the mine-affected areas in Egypt.

Identification and Neutralization of Chemical Improvised Explosive Devices¹⁶

Eyüp Kuntay Turmuş (✉)

Emerging Security Challenges Division, Science for Peace & Security (SPS) Programme, BRUSSELS, Brussels Hoofdst.ge., Belgium

Sławomir Neffe

Military University of Technology, Warszawa, Poland

Valery Kukhar

Institute of Bioorganic Chemistry and Petrochemistry, Kyiv, Ukraine

¹⁶Advanced Training Course – Ref. G4656. Status: Completed.

Description a Global Threat

IEDs are intended to cause maximum damage to life, both civilian and military, and are among the most deadly of terrorist acts. Increasingly, terrorists are using chemical, biological, radiological versions of these devices. Conventional IEDs are combined with highly toxic chemicals (Ch-IED), biological materials (B-IED) or radioactive materials (R-IED) – better known as “dirty bombs”.

Ch-IEDs, sometimes using chemical warfare agents (CWA), are designed to amplify the devastating effect of a classic IED, dispersing harmful and even lethal materials that cause more deaths and create a stronger psychological impact on their victims. The devices are deployed through unconventional means, such as mines and suicide bombers. This makes them more difficult to detect and they require a more complex response.

Many governments are not fully prepared for the response to the threat of Ch-IEDs. Whereas these procedures are well-developed for classical IEDs, this is not always the case for Ch-IEDs, which require a very specific approach, especially in procedures for recognition, and disposal/neutralisation of such devices. As such, there is a real need to train a maximum number of international and national experts in this field.



An advanced training course on “Identification and neutralisation of chemical improvised explosive devices” took place in Wroclaw, Poland from 26 to 30 May. Twenty-five commanders of military and civil emergency units, bomb squads and high-level officials responsible for the management of emergency situations joined experts from government, international organisations and academia. The trainees came from 11 NATO and partner countries: Algeria, Azerbaijan, the Czech

Republic, Egypt, Jordan, Kuwait, Mauritania, Poland, Turkey, Ukraine and the United Arab Emirates.

Designed to enhance public security through improving international awareness and preparedness for response to Ch-IED attacks, the course consisted of a series of lectures by high-level experts in the field, laboratory demonstrations and field exercises. Experts explained advanced technology and best practices to prevent and manage the consequences of these deadly devices. The field training introduced participants to light and heavy armoured bulldozers, robots, personal protection and decontamination on-site and off-site, and equipment.

The training intended to help decrease vulnerability and increase resilience in incidents involving Ch-IEDs and facilitate the development of specific procedures and specialised training on the recognition, handling and safe disposal of Ch-IEDs in NATO partner countries.

Increasing the Clearance Capability for Unexploded Ordnance in Montenegro¹⁷

Eyüp Kuntay Turmuş (✉)

Emerging Security Challenges Division, Science for Peace & Security (SPS)
Programme, BRUSSELS, Brussels Hoofdst.ge., Belgium

Arnold Schoolderman

TNO, The Hague, Netherlands

Mirsad Mulic

Ministry of Interior, Directorate for Emergency Management, Podgorica,
Montenegro

Milovan Joksimovic

Ministry of Interior, Directorate for Emergency Management, Podgorica,
Montenegro

Project Description

Due to the past wars in Montenegro and its region, large quantities of unexploded ordnance are present in Montenegro, for a large part in unsecured areas, where these dangerous items are found by citizens, tourists, farmers, children, etc., but they can also be found and used by terrorists. At the start of the project, the UXO clearance team from the Ministry of Interior, which acted as a rapid response team, lacked

¹⁷Multi-year project – Ref. G4754. Status: Completed.

suitable equipment for detection, transport and destruction of UXO, as well as standardized reporting procedures.

With this project the UXO clearance team was provided with a whole range of equipment for various aspects of UXO clearance: detection, investigation, transport and storage. With respect to detection, both handheld detectors for subsurface area scanning and for underwater use were selected and procured. For area scanning, the detection data can be recorded with data loggers for post-processing on ruggedized laptops with dedicated software. Suits, GPS devices, laser range finders, tables, mobile phones, etc. etc. for field work were bought, as well as small drones with cameras for reconnaissance. For underwater UXO detection, the team was equipped with appropriate diving equipment, such as complete suits, oxygen cylinders, regulators, as well as a compressor for filling the oxygen cylinders. Vehicles with a trailer were procured for transportation of the UXO team, the detection and diving equipment and the found UXO. For the investigation of found UXOs and suspected objects, the team was provided with a mobile X-ray system. As part of the project, the building used for temporary storage of found UXOs (before final destruction of the items) was renovated to achieve safe storage. For several of the procured detectors and other equipment, the UXO team members attended training courses. Moreover, EOD courses at level 2, 3 and 4, IMAS courses by GICHD and relevant conferences were attended.

As a result of the project, the clearance of UXO in Montenegro is enhanced, speeded up and done in a safer way, from survey to final destruction. The UXO clearance capacity built by the project has already resulted in substantial savings in recent clearance activities. The Ministry of Interior's Directorate for Emergency Management has been recognized as the equivalent to a national mine action centre (MAC) and has become member of the South-Eastern Europe Mine Action Co-ordination Council (SEEMACC), allowing it to enhance collaboration with similar services in the Balkan region. Montenegro has joined Protocol V of the Convention on certain Conventional Weapons (CCW), which sets out obligations and best practices for the clearance of UXO. This project was successfully live-tested as part of the NATO consequence-management field exercise organised by the Euro-Atlantic Disaster Response Coordination Centre in Montenegro in November 2016.

Advanced Technology for Landmine Detection

Tor-Sverre Lande

Department of Informatics, University of Oslo, Oslo, Norway

e-mail: bassen@ifi.uio.no

Landmine detection and removal is challenging and is getting even more difficult as non-metal (plastics) landmines are made. State-of-the-art landmine detectors are military systems with high production cost and unavailable to the general public. Acknowledging the fact that landmines are increasing in number as well as accidents

and fatalities due to landmines are increasing, action is required to reverse this trend. Making low-cost landmine detectors available for the general public may be a step towards increased landmine removal. Although such inexpensive systems may not perform as well as high-end systems, they may still prevent a significant number of accidents. In this talk I will indicate how modern technology may enable high-quality, low-cost landmine detectors and point at the challenges and identify potential solutions. Possibly adaptive (learning), community-based systems may improve detection quality and provide basis for detector refinements over time enable reliable landmine detectors.



ALIS Dual Sensor for Humanitarian Demining

Motoyuki Sato (✉)
Institution Tohoku University, Miyagi, Japan
e-mail: motoyuki.sato.b3@tohoku.ac.jp

Project Description

Dual Sensor ALIS is a combination of EMI sensor and GPR. It is a handheld sensor, working at 800 MHz-3GHz. The sensor position is estimated by an accelerometer, and Synthetic Aperture Radar (SAR) Processing is applied to the GPR data sets on an Android tablet PC to obtain 3-D subsurface images. ALIS is a compact hand-held

M. Sato
Institution Tohoku University, Miyagi, Japan
e-mail: motoyuki.sato.b3@tohoku.ac.jp

system, whose weight is 3 kg, which is almost the same as conventional EMI sensors. Its visualization capability drastically improve the discrimination ability of landmines from metal fragments. It works for 6 hours by using a rechargeable batteries. Now we are planning a SOP (Standard Operation Procedure) for ALIS.

Conventional EMI sensors detects small metal objects included in plastic mines, however, at the same time, too many fragments will be detected. Dual sensor ALIS can discriminate landmines from metal fragments by the shape of GPR images.

ALIS was evaluated in test site of Cambodian Mine Action center (CMAC) and we demonstrated that it can image buried landmines in almost real time, under the realistic conditions. Anti-personnel mines including PMN-2 and Type 72 buried up to 20 cm were clearly imaged. Then we conducted fundamental evaluation test in Colombia, where most of the mines are “handmade” and contain much less metal compared to other mines. We demonstrated that ALIS GPR can image these non-metal mines. After many fundamental tests and evaluation in laboratory and test sites, ALIS is now ready for deployment in real mine fields.

GPR Research for Military Search

Daniela Deiana

Electronic Defence, TNO Defence, Safety and Security, The Hague,
The Netherlands

e-mail: daniela.deiana@tno.nl

Project Description

In the framework of several projects commissioned by the Netherlands Ministry of Defence, TNO has carried out various studies on the application of the GPR technology for Military Search (MS). MS is defined as “the management and application of systematic procedures and appropriate tools to detect and locate specific targets, in support of a military operation”.

The projects address the SPS Key Priorities of point 3.c.i, specifically they focus on one side on the development of methodologies for the detection of IEDs and conventional mines, and on the other side on the development of advanced technologies to improve state-of-the-art GPR sensors.

The research studies the development methodologies, best practices and advanced technologies to improve the success rate of the goals of Military Search. Firstly, the safety of the soldiers is improved when the threats in the culverts can be detected with a sensor placed on the road, instead of carrying out an inspection that requires line-of-sight. Secondly, advanced technologies can help improving the imaging capabilities of the radar systems, decreasing in this way the efforts in the interpretation of GPR images.

Scientific and Technical Contributions from Research Projects



Multi-Year Project: Holographic and Impulse Subsurface Radar for Landmine and IED Detection

Lorenzo Capineri (✉)

Dipartimento Ingegneria dell'Informazione, Università degli Studi di Firenze,
Firenze, Italy

e-mail: lorenzo.capineri@unifi.it

Timothy Bechtel

Department of Earth and Environment, Franklin and Marshall College, Lancaster,
PA, USA

e-mail: tbechtel@fandm.edu

Gennadiy Pochanin

O.Ya. Usikov Institute for Radiophysics and Electronics, National Academy of
Sciences of Ukraine, Kharkiv, Ukraine

e-mail: gpp@ire.kharkov.ua

G. Borgioli

University of Florence, Florence, Italy

A. Bulletti

University of Florence, Florence, Italy

M. Dimitri

University of Florence, Florence, Italy

P. Falorni

University of Florence, Florence, Italy

N. Simic

Franklin & Marshall College, Lancaster, PA, USA

L. Varyanitza-Roschupkina

Usikov Institute for Radiophysics and Electronics, Kharkiv, Ukraine

V. Ruban

Usikov Institute for Radiophysics and Electronics, Kharkiv, Ukraine

O. Pochanin

Usikov Institute for Radiophysics and Electronics, Kharkiv, Ukraine

T. Ogurtsova

Usikov Institute for Radiophysics and Electronics, Kharkiv, Ukraine

Project Goals

The main goal of this project is to demonstrate the advantages of sensor integration on a remotely controlled robotic platform for increasing operator safety and improving the classification of explosive targets. This is accomplished by combining the imaging provided by radars and an optoelectronic sensor, a time-of-flight (ToF) depth camera. An additional aim is to demonstrate the operability and practicality of the system in a field with landmine simulants having plastic cases.

To reach these project goals, the partner institutions combined specialties to develop a remotely-operable, multi-sensor, robotic device for the detection of metal and plastic case land mines, unexploded ordnances (UXO), and Improvised Explosive Devices (IEDs). The robotic detection device uses a novel subsurface radar with imaging and target classification to differentiate between threatening landmines and innocuous clutter.

The expected outcome of this research is the creation of a multi-sensor system on a semi-autonomous vehicle for detection and discrimination of explosive devices.

Through the following steps, the holographic and impulse subsurface radar for landmine detection was developed:

- Identification of common explosive devices and their characteristics;
- Review of the literature and map review of local soils and their properties in the Donbass region of Ukraine;
- Measurement of soil electromagnetic properties within Donbass test sites;
- Field measurement of relief for analysis of vehicle accessibility;
- Implementation of a hologram reconstruction algorithm for landmine recognition and classification based on microwave holographic radar data;
- Development of a new impulse Ground Penetrating Radar (GPR) for real time detection of buried objects;
- Experimental results of detection and imaging of buried plastic landmines (PMN and PMN1) in natural soil.

Deliverables

The proposed robotic scanner is the first developed to integrate and jointly interpret data from three sensors:

- A. impulse radar, for fast, real-time detection of electromagnetic anomalies
- B. holographic radar, for high resolution imaging and identification/discrimination of buried targets (moved by a mechanical precision scanner)
- C. time-of-flight depth camera (Picoflexx by PMD), to obtain near-real-time, 3D digital elevation models for the terrain

We have adopted several technologies available in the framework of Industry 4.0 to develop a light, agile robotic scanner for clearing a lane width of about 30 cm, while a field operator monitors from a safe distance and a remotely-connected team of experts performs the detection.

The new approach for landmine detection based on a robotic scanner system is described by the system architecture shown in Fig. 1.

The robotic platform architecture allows experimentation and integration of different sensors. The internet connection allows sharing of the data to a remote server. A local operator can monitor the scanning phase at a safe distance from the robot while it is moving in the target area to be cleared. The front impulse GPR generates an alert and stops the robot, and the HSR scanning is activated together with the 3D depth camera. A team of experts examines the data from a control room

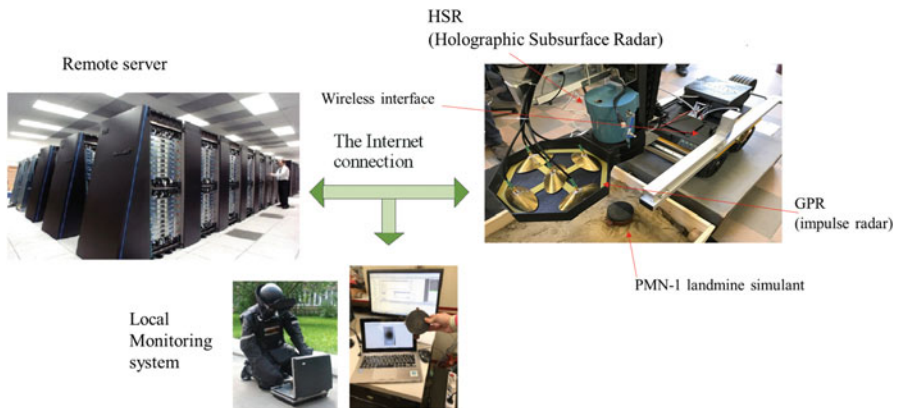


Fig. 1 The system architecture for landmines/UXO detection with a remotely controlled multi-sensor robotic scanner and remotely accessible data for image reconstruction and target classification

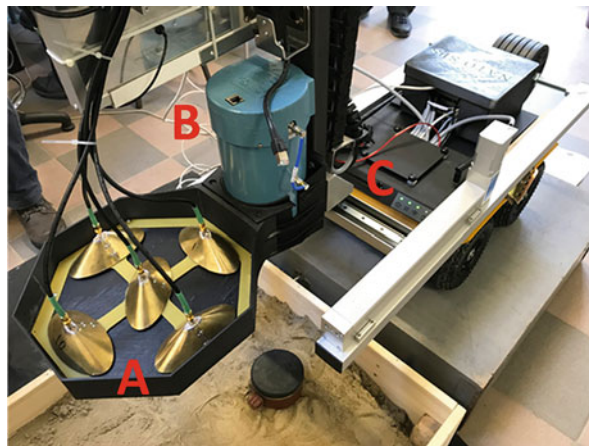


Fig. 2 The multisensor configuration installed on the robotic platform: (a) Impulse radar (1Tx-4Rx) for rapid target detection and location (1.9 GHz center frequency, 2GHz bandwidth@-6 dB), (b) Holographic radar for target discrimination with programmable (1.7–2.0 GHz) continuous wave operating frequency, (c) 3D camera scanner from PMD Technology for measuring the antenna-soil distance, useful for radar scan data interpretation

connected to the robot and the remote server and decides on the classification of a buried target.

The three main sensors and the data processing are described below and are shown in detail in Fig. 2. In the following sections, each sensor is described separately.

GPR Array (1TX – 4RX) for Fast Target Detection

This GPR was studied, simulated and constructed within this project with a fast detection algorithm for generating a stop command to the robot. In particular, the design of the two radars were specifically optimized to work with the electromagnetic characteristics of Donbass soils [1]:

The simulated algorithm with a central transmitter (1TX) and 4 receivers (4RX) considered the real antenna aperture and Ultra Wide Band signals generator/receivers and showed promising results. In Fig. 3 describes the coordinate system adopted for the calculation of targets according to the fast algorithm developed in this project [2, 3]. The low numerical complexity of the algorithm allows the implementation on low-power microcomputer boards to obtain a real-time response. The alarm is generated in few seconds to stop the robot movement when a suspicious target is detected.

The laboratory experiment with a plastic case PMN landmine simulant in air (see Fig. 4) always produced detected mine positions within the dimensions of the target. This result demonstrates that once the target is detected, its position is determined precisely enough for subsequent inspection with the holographic radar scan that covers an area greater than the target dimensions (typically a footprint of 10–20 cm).

The radar unit was contained [4] in a compact and robust box named “Odyiag Radar” and installed on the robotic platform with a connection to the antenna with a flexible coaxial cable (see Fig. 5). The central frequency is 1.9 GHz and the -6 dB bandwidth is 2.0 GHz. This ultrawideband (UWB) characteristic allows the emission of pulses short enough to detect targets in the soil with an accuracy of the order of few centimetres.

Fig. 3 Coordinate system for fast target detection with the 1Tx-4Rx antenna configuration for the impulse GPR radar. The antenna system lies on the XY plane and the target depth is Z_0 . The target central position is individuated by polar (r, θ) coordinates

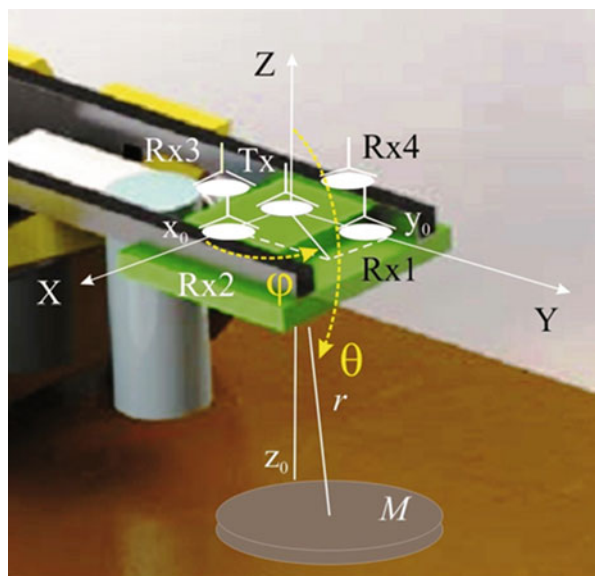


Fig. 4 Real time position estimation of a plastic PMN mine simulant on a flat surface in laboratory conditions. The representation of estimated target positions is on a portion of the X-Y plane defined in Fig. 2

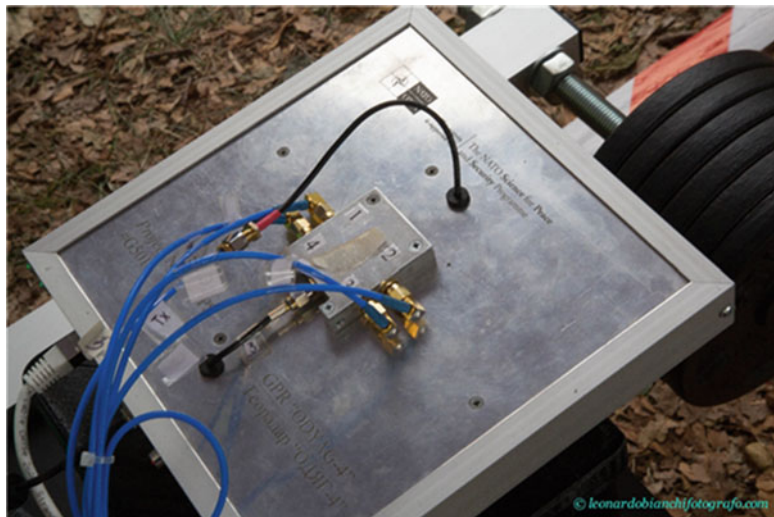
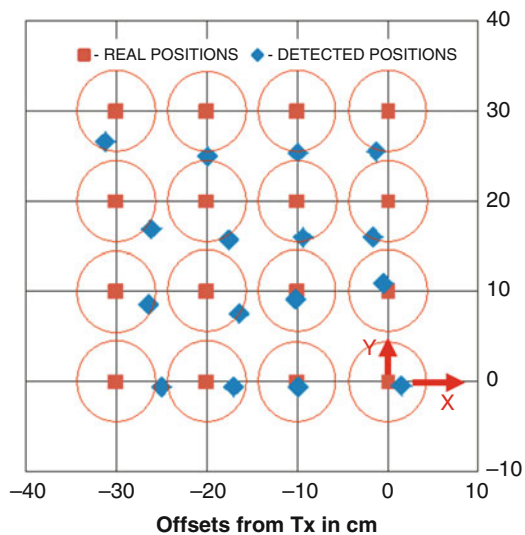


Fig. 5 Impulse GPR electronic unit connected by flexible coaxial cables to the antenna system placed in front of the robotic platform

The GPR electronic unit installed on the robotic platform was mechanically compatible with the other electronic and mechanical components that might influence each other (electromagnetic interference, vibrations, thermal gradient, etc.). In particular, the thermal gradients were examined to characterize the GPR time-of-flight characteristics: a thermal insulation block was provided to hold the GPR and



Fig. 6 Picture of the assembled system on a commercial robotic platform (*Jackal* model from Clearpath, Canada). The wi-fi router is installed on the rear side to avoid interference with the 2GHz microwave radar sensors

insulated it from the “hot” robot controller in the black box (see Fig. 6). Moreover, the electromagnetic compatibility with the wi-fi router and the holographic radar operating in close frequency range was verified (see the router on the left side of Fig. 6). The router can be used also to directly connect the impulse GPR to view the radargrams in real time on a remote terminal. It is interesting to see in Fig. 7 the outputs from the four receivers shown in real time on a remote laptop PC terminal: the top four traces show the signal before background removal, and the bottom four traces show the same signals after background removal.

Although this processing is simple and easy to implement, in practice there are issues to be considered regarding the long-term stability of the electronics and the variation in soil surface characteristics. In the present system, the acquisition of the background radargrams is repeated after the generation of an alarm event on a portion of the soil that is assumed to have no target.

This processing is necessary to increase the dynamic of the reflected signals from the shallow plastic landmines which otherwise overlaps with the impulse from the ground surface. The whole unit is supplied by the 12 V-DC power supply of the robot and the power consumption less than 6 W.

Holographic Radar for Target Discrimination 1.7–2.0 GHz

For target discrimination, the project employs a holographic radar that provides information (amplitude and phase) of the target response at each location covered by the center of antenna as it moves. The mechanical scan of the area provides high

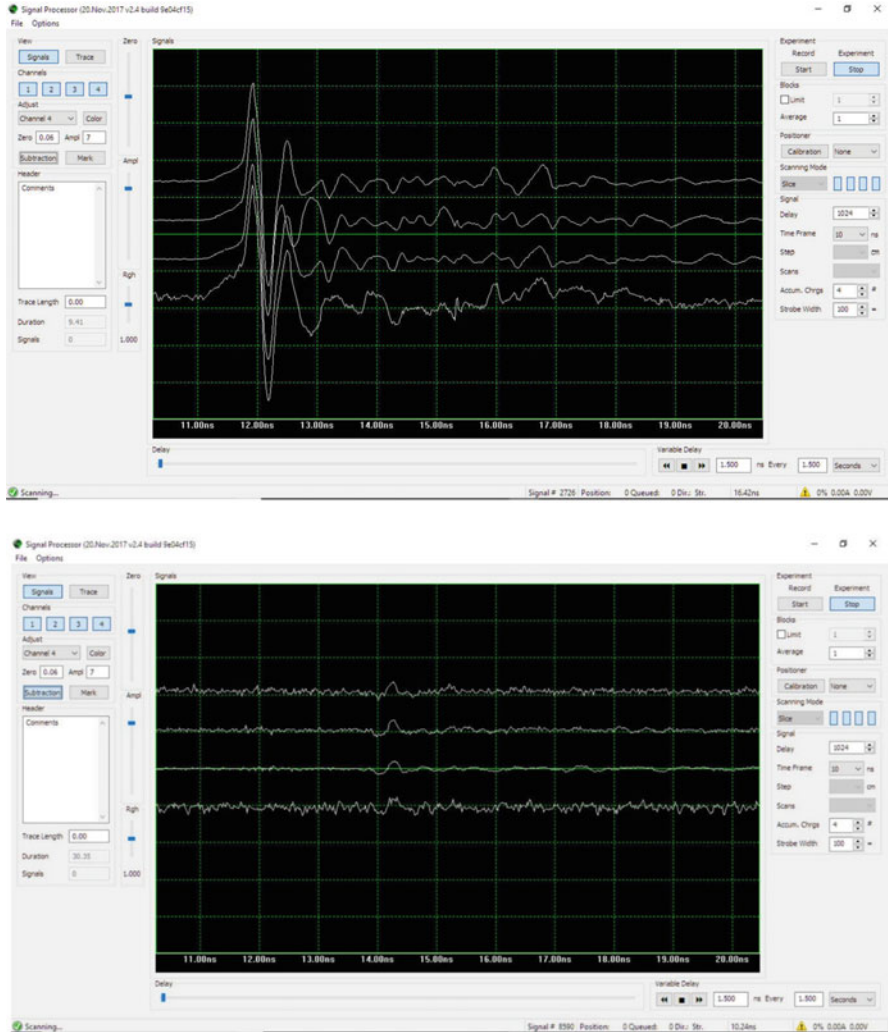


Fig. 7 Top: radargrams from the 4 radar channels showing the impulse signals reflected from the ground surface. The impulse duration is about 0.3 ns. Bottom: radargrams from the 4 radar channels reflected from a PMN-4 plastic landmines after background removal

spatial resolution images in real time for each activated frequency in the bandwidth (spanning 1.7–2GHz). The design antenna and the electronic unit box fixed on top provides a robust, directive antenna that is well coupled with the ground, even when operated at distance of 5–20 cm from the soil surface. The antenna design is based on a cylindrical cavity, and the two monopole feeds are used separately: the feeding TX excites the antenna and the receiving RX to generate the interference signal between the direct coupling from TX and the received signal from the shallow target. In Fig. 8

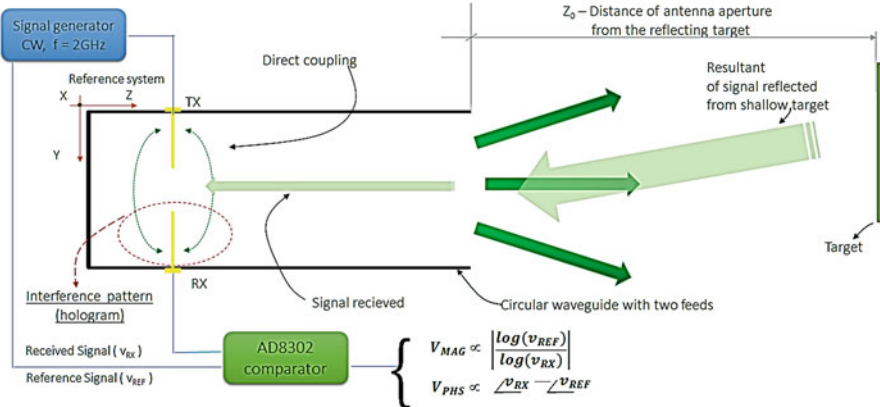


Fig. 8 Schematic diagram of the 2GHz holographic antenna with electronic front-end for the acquisition of the magnitude (V_{MAG}) and phase (V_{PHS}) voltage outputs. The electronics are integrated on the top of the antenna

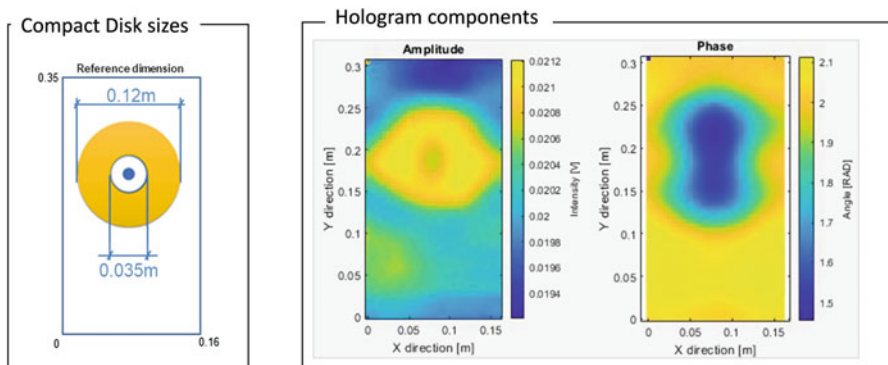


Fig. 9 On the left the reference dimension of the compact disk with coloured area of the metallization. On the right the raw data obtained with the holographic antenna scanned over an area of 0,18 m x 0,30 m with step 5 mm

shows the operating principle of the holographic antenna and the electronic unit that provide amplitude and phase information for each position of the antenna.

This new design was tested successfully at the beginning of the project and a large body of experiments has been carried out using different target shapes and soil conditions. For the latter, the influence of irregular surfaces was carefully analyzed [5] and an algorithm for post processing of the data has been developed [6]. An experiment of the image formation following the schematic description in Fig. 8 is reported which discusses the holographic antenna's ability to discriminate among shallow objects by shape and dimension. Figure 9 shows the raw data (V_{MAG} and V_{PHS}) obtained by the scan of a compact disk in air. The two images resemble the

dimension and circular shape of the compact disk, but some distortions are present. From an investigation of the distortion phenomenon, we conclude that the non-uniform illuminating field on the object and the finite size of the receiver antenna are the main causes of the distortion. Such aberrations can be corrected with some limitations by the deconvolution of the raw data. Some example of plastic mine images buried in natural soil will be presented in the next section. Among the limitations of the present holographic radar scanner we address the following:

- Trade-off between 20 cm penetration depth and 4 cm lateral resolution → frequency around 2GHz ($\lambda = 15$ cm in air)
- Antenna diameter (11.6 cm) comparable with small plastic landmines diameter (≈ 10 cm) → anisotropic radiation beam
- Mechanical constraints of robotic platform imply a limited scanning area → holograms recorded with limited diffraction fringes
- Layered medium due to air-soil interface → Antenna-ground distance must be considered

PMD Camera (Picoflexx) to Obtain Near-Real-Time Digital Terrain Models

The PMD depth camera has been integrated in the system and by processing and calibrating the data with a developed set of software, it can provide a soil surface profile in near-real-time. Moreover, the camera can map the volume where the Holographic Subsurface Radar (HSR) antenna is scanning, so it can measure the air gap from antenna to the soil. Both pieces of information are very useful in the HSR data processing for the removal the artefacts due to soil relief and the variable distance of antenna with soil. A laboratory experiment is shown in Fig. 10. Here a sandy soil profile was created with typical irregularities of real soil (Sinusoidal undulating sandy soil Height: 2 cm; Period: 7.5 cm). The results of the 3D point cloud shows a very good representation of the surface profile. This information is used later in the interpretation of HSR images.

In the same sand box we buried a PMN plastic mine and acquired an HSR image. The superposition of two images (see Fig. 11), the HSR image and the level curves of the soil profile, provides evidence to the classifier (either an operator or algorithm) that some patterns in the grey level HSR image are related to the surface relief instead of a buried object. The integration of the HSR image with the 3D depth camera is an important achievement toward the generation of a database with spatially correlated data.

The open system architecture allows for the addition of other sensors to complement the three main ones previously described. One of the sensors with which we have experimented is a thermal camera (FLIR type) that can operate in outdoor environments for obstacle detection, and in particular for image processing for tripwire detection. This is an important capability to develop to avoid blasts of the

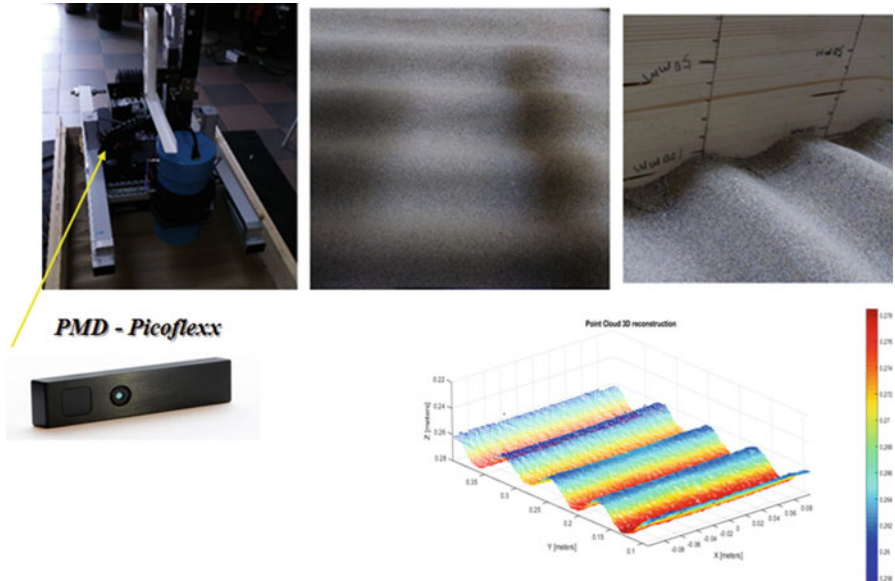


Fig. 10 Sandy soil sinusoidal profile reconstruction with a PMD Picoflexx camera

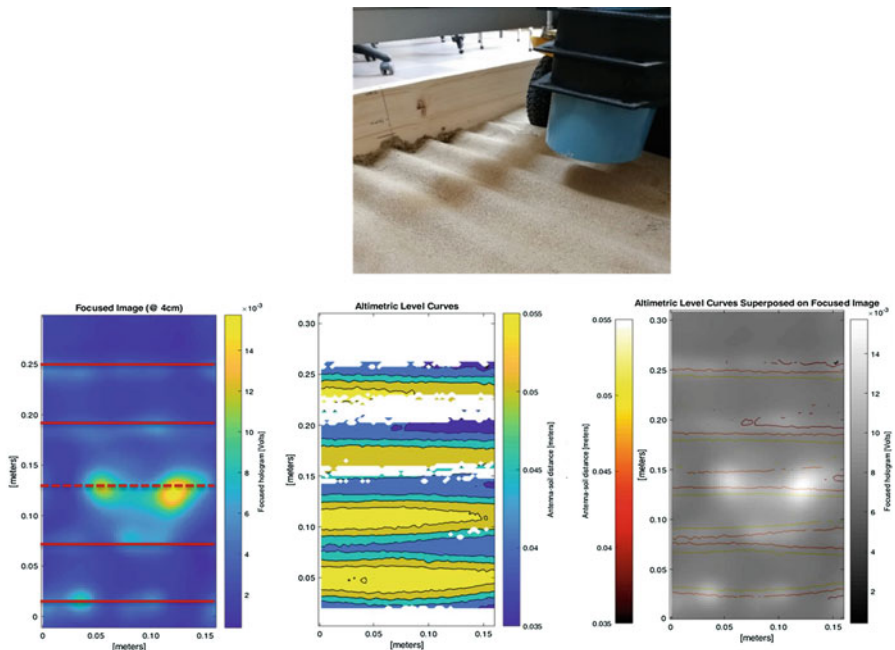


Fig. 11 Image fusion of holographic radar (Left) with altimetry soil profile (Centre) and resulting image in grey scale (Right), where the coloured horizontal patterns indicate the origin of the contrast variation due to height variation and not about buried objects

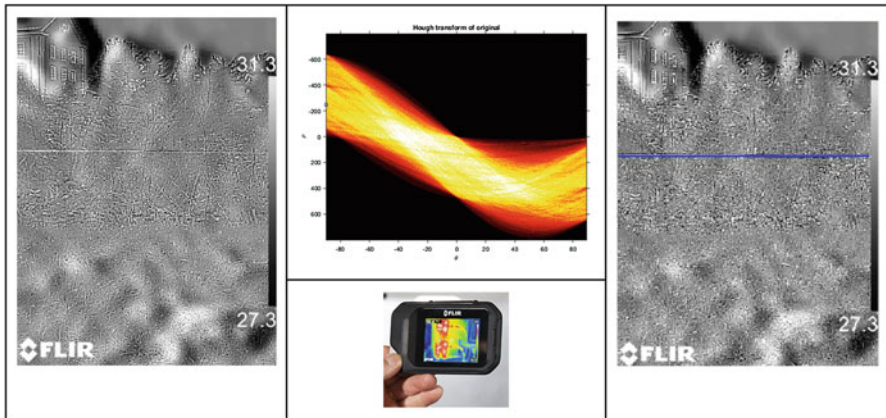


Fig. 12 (Left) Thermal image. A thin plastic tripwire is barely visible as on horizontal pattern even in the optical image. (Centre) On the bottom, a thermal infrared camera is used for trip wire detection by image processing with Hough Transform for the straight-line detection. On top, the Hough accumulator space is shown with high values in yellowish colour scale. (Right) The result is obtained by selecting the highest value in the accumulator space and the corresponding straight line is superimposed to the thermal image with blue colour

equipment and for IED detection. The processing by the Hough Transform for detecting straight lines is very computationally efficient, and the results are shown in Fig. 12.

Test Field Experiments

A series of tests were carried out with three targets buried in a garden rich soil for 3 months. The targets selected were the types of landmines for this project: a metal one and two plastic-case main PMN1 and PMN4 mines of about 10 cm diameter each buried at a depth of about 5 cm.

The operator on the field manoeuvres the robot along a straight path in the selected area to be cleared. A green light on the robot activated by the remote team at the control desk, indicates that the operator can move the robot. The team stops the robot and turns the light to red when an alarm is detected by the GPR. At this stage, the HSR scan is activated. When this is completed, the images of the HSR and the PMD camera data are examined, and if a shape and dimensions that are compatible with the target are recognized, this is marked as a detected target; otherwise it is considered a false alarm. The light is then turned green again and the detection process continues.

This procedure was applied to the test field in different weather conditions (lightly wet or dry days) and the three targets were always detected. The HSR images also provide an accurate estimate of the target position in the scanned area. The following pictures (see Fig. 13) show the different phases of the outdoor experiments.

An example of the post processing (step 4 in Fig. 13) to correct for the variable distance of the holographic antenna from the target due to natural soil irregularities is

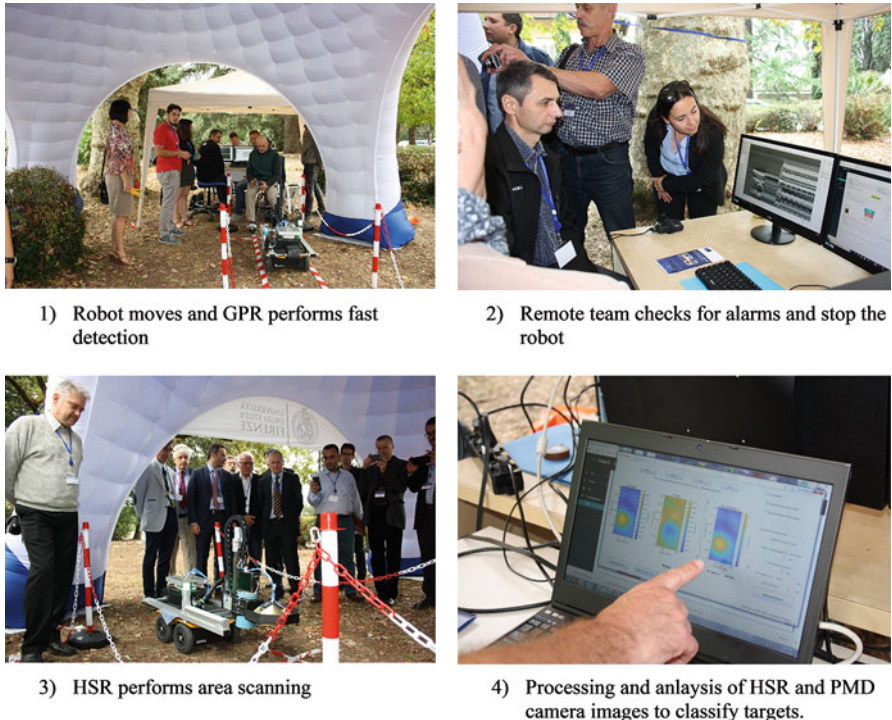


Fig. 13 Demonstration of the prototype for the detection of plastic mines in natural soil. The detection process includes four steps

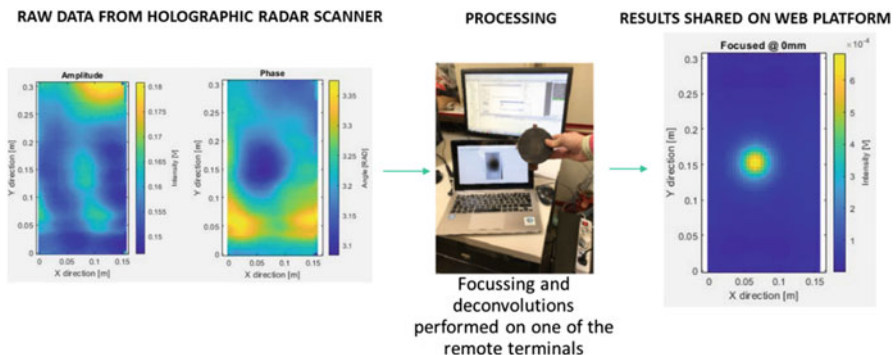


Fig. 14 Holographic radar raw data processing for image formation by focussing and deconvolution

shown in Fig. 14. In this figure, from left to right, we observe an increase in the image contrast and the buried circular shape PMN plastic case landmine is retrieved. The result (Fig. 14 on the right) is shared by all users connected to the robotic

platform, owing to the web-based software architecture installed. The processing time can be decreased by using a remote computer with more computational power while the other users can use portable terminals (Tablets, smartphones) in order to visualize the raw data and the results of post-processing.

Security Relevance

The produced prototype of the remotely controlled scanner has been designed to increase the safety of detection procedures during the clearing of terrain in post-conflict areas. This is an advantage for all NATO member and partner countries that are involved in such expensive, risky, and slow procedures that are performed by specially trained personnel. The country of Ukraine is a recent example among others illustrating the need for innovation in performing this task that is presently done with hand-held portable instruments. Figure 15 shows some of the standard methods for the landmine detection approved by United Nations (UN). These approaches combine human with hand-held electromagnetic sensors or human-animal interaction. Trained personnel are always close to threats during the detection and buried targets removal stage, increasing the risk of casualties.

The large problem of humanitarian demining has been monitored and assessed in several areas of the world. The relevance for security is outlined by some statistics/metrics shown in Table 1, which shows the time employed to find different types of



Fig. 15 Landmines detection methods. Images courtesy from, ICRC, Halo Trust, PM/HDP

Table 1 Data about mine clearance in Cambodia in 2000–2008. (Courtesy from Chap. 1, in Macdonald, Jacqueline et al. (2003) Alternatives for Landmine Detection, Rand Corporation, Santa Monica, CA)

Time Spent Detecting and Clearing Mines, Unexploded Ordnance, and Scrap in Cambodia, March 1992–October 1998

Type of Item	Total Number of Items Found	Time to Confirm (hours)	Time to Dig (hours)	Time to Neutralize (hours)	Total Time (hours)	Percentage of Total Time
Antitank mines	961	80	80	80	240	0.00074
Antipersonnel mines	89,327	7400	7400	7400	22,000	0.068
UXO	432,770	38,000	38,000	38,000	110,000	0.34
Scrap	191,737,707	16,000,000	16,000,000	0	32,000,000	99.6

Source: J. McFee, Defence R&D Canada (based on data from CMAC 2000 briefing package, assuming 3 min per item for confirmation, neutralization, or digging)

threats compared to the time employed to find innocuous scrap clutter. The latter takes 99.6% of the overall time.

Technological innovation occurred in the last decade with the introduction of a combined metal detector and GPR (e.g. Minehound, ALIS, HSTAMIDS). This has “improved” this to 70–80% of the time devoted to removing scrap.

Regarding the casualty metrics, according to Landmine-Monitor 2018 (http://www.the-monitor.org/media/2918780/Landmine-Monitor-2018_final.pdf), civilians represented the vast majority of casualties compared to military and security forces, continuing the well-established trend of civilian harm that influenced the adoption of the Mine Ban Treaty: 87% of casualties were civilians in 2017 where the status was known. The recorded casualties in 2017 counts a total of at least 7239 people killed or injured by antipersonnel and antivehicle landmines, including improvised landmines, as well as unexploded cluster submunitions, and other explosive remnants of war (ERW)—henceforth mines/ERW.

Science Relevance

The technological innovation undertaken in the previous section for the security of detection procedures of landmines and IEDs has been achieved in this project owing to the fertilization of different technical and scientific competences (geophysics, electronics, electromagnetism, computer science, robotics, informatics) of the groups involved in different NATO countries and partner countries. The networking established by the SPS program has been demonstrated to be effective in advancing the research with tangible results.

Partnership Relevance

This research has the capability of establishing worldwide partnerships due to the direct impact in reducing human and animal interaction for explosives detection by the use of the newly developed instrument. There are several competences needed to fill the gaps still present in the project that are available in the scientific community of NATO countries and partner members.

During the 36 months of the project duration, the three teams have developed an efficient collaboration for sharing the design of the sensor integration and the training of young researchers for the innovative web-based architecture adopted in this project. The regular reciprocal visits have made this partnership operational and very rewarding for the many young researchers participating in the project. The number of members of the three teams increased from the project start continuously, reaching in the end six researchers/experts for each team. Paradigms of Industry 4.0 are adopted as a useful tool to reach the decentralized electronic/mechanic/software design, and make updates easy during the successive phase of system integration. This approach to the system design and scientific investigation helps the partners to continue the collaboration even while remaining in their own countries. Many system components (electronic and mechanical) are easy to reproduce by CAD programs and 3D printing from almost everywhere in the world.

This research has the capability for limitless worldwide partnerships due to the direct impact of reducing human and animal interaction during explosive detection using the newly developed system.

End Users

The two end users Colin King of Phoenix (UK) and State Emergency Service of Ukraine (SESU) have been actively involved at the beginning of the project for the target selection and providing plastic landmine simulants for testing. In the mid-term of the project, the collaboration with experts such as Prof. Colin Windsor (UK) and Dr. Masaharu Inagaki of Walnut (Japan) for target classification strategy by imaging has been important in addressing the efforts for image contrast enhancement and the selection of classifiers based on artificial neural networks.

Finally, the feedback about the usability of the prototype on the field will be assessed by meeting with the SESU or other interested institutions. This step is very important to fill the usability gaps before a certification of performance in terms of Receiver Operating Characteristic (ROC).

Technical Summary

The main outcome of this research is the creation of a multi-sensor system on a semi-autonomous vehicle for detection and discrimination of explosive devices. The list of deliverables is as follows:

- Measurement of soil electromagnetic properties within actual Donbas test sites;
- Field measurement of relief for analysis of vehicle accessibility and microwave radar image enhanced interpretation;
- Development of a new impulse GPR for real time detection of buried objects;
- Hologram reconstruction algorithm for landmine recognition and classification based on microwave holographic radar data;
- Enhanced detection using multi-sensor data from a team of experts remotely connected;
- Preliminary tests for automated IR detection of tripwires;
- Experimental results of detection and imaging of buried plastic landmines (PMN and PMN1) in natural soils;

The system architecture is described in Fig. 16. It shows the complexity of integration required by the multisensory robotic platform and how the Industry 4.0 methodology [7] can help solve any reliability, flexibility and usability issues of this new equipment.

With reference to the schematic of the architecture in Fig. 16, the full system is composed by the following fully integrated components:

- 1. Impulse GPR
- 1.1 GPR antennas (5 total); 1 transmitter (Tx) and 4 receivers (Rx)

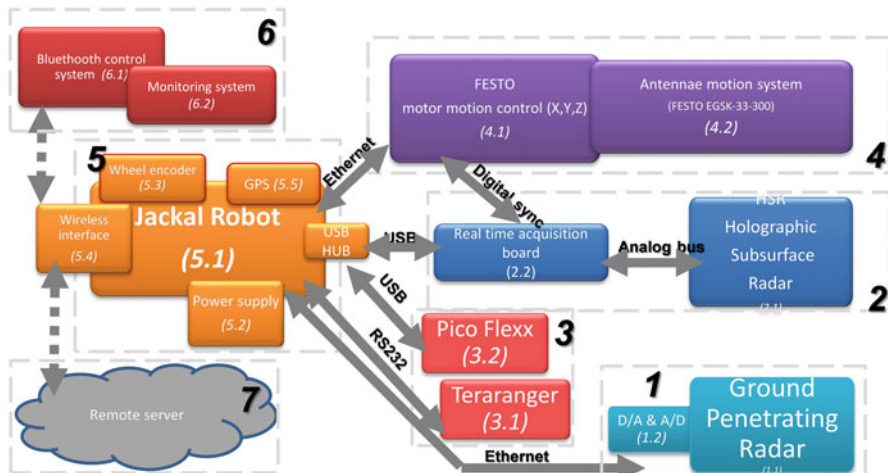


Fig. 16 Robot scanner architecture: sensors and electronics interconnected, remotely controlled by web-based software

- Impulse Subsurface Radar for Rapid Landmine and IED Detection
- 1.2 Signal decoder and A/D converter
- 2. Holographic Subsurface Radar (HSR)
- 2.1 HSR antenna system
- Holographic Subsurface Radar for Landmine and IED Detection
- 2.2 Real-time acquisition board
- 3. Sensors of position/distance/visualization
- 3.1 Time-of-flight (TOF) laser rangefinder (TeraRanger)
- 3.2 3-D camera/scanner (PMD Pico Flexx)
- 4. Dedicated interface motor system (FESTO)
- 4.1 Proprietary electronic controller with external COM interface
- 4.2 Three-axis moving system FESTO EGSK-33-300
- 5. Jackal unmanned ground vehicle
- 5.1 On-board standard computer (with ROS OS)
- 5.2 Power unit/power reserve meter
- 5.3 Wheel actuators
- 5.4 WiFi interface
- 5.5 GPS
- 6. Wireless remote controls
- 6.1 Remote control system (joystick)
- 6.2 Control and monitoring data
- 7. Remote Server for control system and post-processing of sensor and navigational data.

Broader Impacts

As of 2017, there are an estimated 100 million abandoned landmines littered across 61 countries. Following the wars in Afghanistan, Libya, Syria, Yemen, and Ukraine, there has been a rise in casualties due to the triggering of previously abandoned explosive devices. Current annual clearance is approximately 230,000 anti-personnel (AP) and 30,000 anti-tank (AT) mines per year, indicating that it could take 1100 years to clear all the landmines across the globe. Success in this project would entail widespread use of this technology and reduce the number of civilian casualties in addition to a reduction in risk and casualties of those detecting and removing the landmines.

This robotic platform will change the approach to detecting landmines in post-war zones, while also reducing direct human-to-mine or animal-to-mine contact in detecting landmines. The design approach is based on the new paradigm of Industry 4.0 that allows us to implement new cyber-physical systems that are reproducible everywhere and which are expandable with different sensors and actuators. Robot remote control and data sharing are achieved by a sophisticated web-based software architecture and has a high potential to move the procedures of explosive detection toward completely remote and autonomous systems.

Young Researcher Participation

The research teams have been formed with young researchers (Researchers, PhDs, PhD and MS Thesis students), supported by young/senior technicians and coordinated by professors/senior scientist. The project management has continuously monitored team members' involvement during the 3 years of the project.

The distributions of roles and their % time dedicated to the project is as follows:

	# of heads	% time
Students (master thesis or PhD students)	7	3,1
Young researchers	4	0,65
Senior researchers	6	1,23
Technicians	4	0,62
Professors/senior scientists	5	1,0
Total	26	6,6

It can be observed that the involvement of students and young researchers is large for this project. Three masters theses have been dedicated to this project and one Best Student paper award has been awarded at the PIERS 2018 conference [5].

Contributions

1. Pochanin G et al. (2017) Field measurement of permittivity, electrical conductivity, magnetic susceptibility, and topographic relief of soils in Donbass, Ukraine for robotic, multi-sensor, humanitarian demining system design. In: Abstracts of XXXII International Union of Radio Science General Assembly and Scientific Symposium (URSI 2017), Montreal Canada, August 2017
2. Pochanin O et al. (2018) Estimation of lane width for object detection using impulse GPR with “1Tx and 4Rx” antenna system. In: 2018 17th International Conference on Ground Penetrating Radar (GPR), Rapperswil, Switzerland, August 2018. Publisher: IEEE. pp. 1–5
3. Ogurtsova T et al. (2018) Criteria for selecting object coordinates at probing by the impulse UWB GPR with the “1Tx + 4Rx” antenna system. In: 2018 ninth International Conference on Ultrawideband and Ultrashort Impulse Signals (UWBUSIS), Odessa, Ukraine, September 2018. Publisher: IEEE. pp. 161–164
4. Pochanin G (2017) Design and simulation of a “single transmitter – four receiver” impulse GPR for detection of buried landmines. In: 2017 ninth International Workshop on Advanced Ground Penetrating Radar (IWAGPR), Edinburgh, UK June 2018. Publisher: IEEE. pp. 1–5
5. Qin T et al. (2018) Influence analysis of uneven surface on landmine detection using holographic radar. In: 2018 Progress in Electromagnetics Research Symposium (PIERS-Toyama), Toyama, Japan, August 2018. Publisher: IEEE. pp. 683–691
6. Borgioli G et al. (2018) A hologram reconstruction algorithm for landmine recognition and classification based on microwave holographic radar data. In:

- 2018 Progress in Electromagnetics Research Symposium (PIERS-Toyama), Toyama, Japan, August 2018. Publisher: IEEE. pp. 1938–1944
7. Pochanin G et al. (2018) Application of the industry 4.0 paradigm to the design of a UWB radiolocation system for humanitarian demining. In: 2018 ninth International Conference on Ultrawideband and Ultrashort Impulse Signals (UWBUSIS), Odessa, Ukraine, September 2018. Publisher: IEEE. pp. 50–56

Engineering Silicon Carbide for Enhanced Borders and Ports Security

Ivana Capan (✉)

Rudjer Bošković Institute, Zagreb, Croatia

Tomislav Brodar

Rudjer Bošković Institute, Zagreb, Croatia

Željko Pastuović

Australian Nuclear Science and Technology Organisation, Lucas Heights, NSW, Australia

Jose Coutinho

Universidade de Aveiro, Aveiro, Portugal

Vladimir Radulović

Jožef Stefan Institute, Ljubljana, Slovenia

Luka Snoj

Jožef Stefan Institute, Ljubljana, Slovenia

Takeshi Ohshima

National Institutes for Quantum and Radiological Science and Technology, Takasaki, Gunma, Japan

Introduction

Recent progress in the manufacturing of high-quality bulk and epitaxial silicon carbide (SiC) and processing technologies for fabrication of SiC-based electronic devices, could enable unprecedented detection of neutron and alpha-particle sources. Unlike existing and commonly used neutron gas-based detectors, SiC-based devices have the potential to be simultaneously portable, operable at room temperature and radiation hard.

Our main objective is to combine theoretical, experimental and applied research towards the development of radiation-hard SiC-based detectors of special nuclear materials (SNM), and therefore to enhance border and port security barriers. This will be achieved through material modification processes in order to manipulate the most severe electrically active defects (which trap or annihilate free charge carriers), by specific ion implantation and defect engineering [1, 2].

Deliverables

We developed a simple prototype of a neutron detection system and demonstrated its capability to detect thermal neutrons generated in a low power nuclear reactor. The whole prototype system is modular. By entirely eliminating a requirement for mains power, our system is fully portable and operable in the field. The prototype detection system consists of: (1) a silicon carbide detector, (2) a neutron conversion layer, (3) a modular electronic system for low amplitude signal detection and processing, (4) a standalone battery powered voltage source and (5) a laptop computer.

Thermal neutrons are detected indirectly using a neutron conversion layer for generation of secondary charged particles. The detector of secondary charged particles is configured as a simple Schottky barrier diode (SBD) and realized using high-resistivity electronic-grade epitaxial 4H-SiC layers. The sensing volume of a prototype detector is defined by the thickness of a thin epitaxial layer which is grown onto a thick substrate, and the surface area of the electrical contacts. The optimization of the epitaxial layer thickness to achieve the best signal to noise ratio is an ongoing project activity. A detector assembly consists of a SBD, surface-mounted onto a chip carrier with wire bonded electrical contacts. A chip carrier bearing an SBD is enclosed in a 3D-printed plastic holder in order to completely enclose the electrical contacts under bias voltage and prevent any accidental contact during handling. The plastic holder had an aperture above the detector to enable charged particles to reach the detector surface. A short coaxial cable with a BNC connector was used to connect a detector to the electronic detection system. The plastic detector holder was placed in a two-piece aluminium enclosure in order to minimize electronic noise which can negatively affect spectroscopy measurements of ionizing radiation. The enclosure lid also provided support for a foil used as a neutron converter layer for indirect detection of thermal neutrons.

The modular electronic system for particle detection and spectroscopy using the prototype detector is designed to be: (1) adjustable and simple to use; (2) applicable in the field and not only in laboratory environment; (3) serviceable during field testing and (4) of low cost.

The current version of electronic system consists of a preamplifier and a shaping amplifier PCB modules (CR-150-R5 and CR-160-R7) manufactured by CREMAT, and a digital signal processing multichannel analyser (DSP-MCA) manufactured by AMPTEK (model No. 8000D), connected to a laptop computer. The DSP-MCA is USB powered by a laptop.

A standalone battery-powered voltage source was made in-house to provide electrical power for the preamplifier, the amplifier, and to a separate high voltage module with adjustable bias output for the detector. The reverse negative potential is connected to the front Schottky contact, while the back Ohmic contact of SBD detector is grounded.

Security Relevance

Increasingly complex risks, like geopolitical instability or decentralized terrorism threats, have led to the urge for deploying nuclear screening systems for detection of illicit trafficking of nuclear materials, and from that, to a growing interest in the field of research and development of new radiation detection technologies suitable for homeland security applications.

Our main goal is to develop a SiC-based detector for special nuclear materials (SNM), and therefore to enhance border and port security barriers.

Science Relevance

Owing to many advantages over silicon, silicon carbide is becoming a mainstream material for the industry of high-power electronics [3–5]. Due to its wide band gap, radiation hardness, high breakdown field and melting point, SiC is also a promising semiconductor for the fabrication of nuclear radiation detectors working in harsh environments, including at high temperature and in high intensity radiation fields [6].

In the past 10 years we have seen tremendous development in the area of SiC substrate growth and epitaxy. Today, high-quality single-crystalline SiC wafers with diameters of 150 mm (6 in.) are commercially available, providing the opportunity for developing devices with unprecedented performance.

SiC-based diodes for radiation detection are extremely sensitive to defects that introduce deep carrier traps, especially to those with large capture cross section for minority carriers which hold the actual impact signal. Besides the point defects already present in the as-grown material, defects in SiC are also created during device processing, as well as during operation under harsh conditions. In the first case, defects are formed upon e.g., thermal treatments or ion-implantation steps, whereas in the second case they appear due to atomic displacements upon collisions with high-energy impinging particles.

It is therefore crucial to understand the effects of lingering defects already present in SiC as the material comes from the production line, to monitor the accumulated radiation damage under operation conditions, and assess the respective impact to the electrical performance of devices. Hence, a major part of the scientific relevance of this project relates to important advances in the fundamental physics of SiC materials.

Among the intrinsic defects (i.e. those which do not involve foreign chemical species), the carbon vacancy (V_C) displays the lowest formation energy, ranging from 4.5 eV to about 5 eV in carbon-poor and carbon-rich growth conditions, respectively. The defect gives rise to a conspicuous signal observed by deep level transient spectroscopy (DLTS), commonly referred to as $Z_{1/2}$, which allows to measure its concentration. The low formation energy explains why in as-grown epi-layers of SiC, the V_C defect is present with a concentration in the range 10^{12} – 10^{13} cm $^{-3}$. Other defects show concentrations below the detection limit when employing highly sensitive space-charge techniques. The concentration of the carbon vacancy is prominently increased upon irradiation of 4H-SiC with electrons and neutrons. It is the major recombination and trapping center in 4H-SiC, and importantly, it interacts strongly with both electrons and holes. Given the above, it is mandatory to have a detailed understanding of the properties of this defect.

The electronic structure of the V_C defect was thoroughly investigated. From hybrid density functional calculations, we found that the defect exhibits a rich catalogue of structures that depend on the sub-lattice site and charge state. Their occurrence was rationalized on the basis of several effects, namely the character of the occupied one-electron states, the site-dependence of the crystal-field, and the magnitude of a pseudo-Jahn-Teller effect.

We also investigated the V_C defect by combining experimental and theoretical studies of the electronic properties of $Z_{1/2}$. The study addressed the location of individual acceptor transitions in the band gap, as well as the capture and emission kinetics of electrons between these traps and the conduction band of 4H-SiC. The experiments were carried out by conventional and high-resolution Laplace-DLTS, whereas the calculations employed a plane-wave based density functional theory method using a semi-local approximation to the exchange-correlation energy. We were able to connect Z1 and Z2 levels with the carbon vacancy at the hexagonal and pseudo-cubic sites of the lattice, respectively. We also reported direct capture cross section measurements for the levels. These show minute (or vanishing) capture barriers, confirming the calculated strong coupling between initial and final states involved in the transitions. Based on the calculated capture and transformation barriers, detailed mechanisms were proposed for the first and second electron capture.

Partnership Relevance

Partnership is one of the most important aspects of the E-SiCure project. Institutions from three NATO nations (Croatia, Portugal and Slovenia) and two NATO partner countries (Australia and Japan) are working together on a SiC material engineering project for enhanced borders and ports security.

Developing new state-of-the-art, low-cost, radiation hard detectors is a difficult challenge which can be tackled only by a multidisciplinary group of scientists and engineers from various fields having access to different infrastructure. In our project,

each working package is carried out by different partners, i.e. device fabrication is performed by partners from Japan (QST) and Croatia (RBI), SiC material engineering is performed by Australia (ANSTO) and Japan (QST), modelling of various physical processes in the detector as well as irradiation fields is carried out in Portugal (UA), Australia (ANSTO) and Slovenia (JSI); characterization of detectors is performed in Croatia (RBI, Australia (ANSTO) and Japan (QST) and irradiation testing in representative radiation environment is done in Slovenia (JSI) and Australia (ANSTO). Irradiation tests were carried out at the JSI TRIGA Mark II research reactor in Slovenia as well as at accelerator facilities at ANSTO (Australia) and Japan Proton Accelerator Research Complex, J-PARC. In addition to the abovementioned infrastructure, each lab also provided their infrastructure for modelling (such as computer clusters) and for device fabrication, material engineering and sample characterization (such as alpha-particle/heavy-ion beam induced charge transient spectrometer, electronic system for particle detection and spectroscopy please add).

The established partnership was beneficial not only from the point of view of joining multidisciplinary knowledge and various facilities to develop SiC material, but also to promote collaboration among the countries and institutions, which resulted in international exchange of personnel, exchange of knowledge and technological innovation as well as joint applications to other international research programs. This project connected research groups and countries with little previous collaborations to an intensively collaborative group that will work together also in the future and tackle various multidisciplinary challenges.

It is planned to prepare common proposals to the EU H2020 programme. In comparison to the EU H2020 Research and Innovation programme, which is aimed at securing Europe's global competitiveness is very broad in terms of research fields and is mostly limited to EU member states and, the NATO SPS programme promotes security related cooperation between NATO member states and partner nations based on scientific research, technological innovation and knowledge exchange. The SPS Programme offers funding, expert advice and support to tailor-made, security-relevant activities that respond to NATO's strategic objectives. It has been working also as a mean for parallel diplomacy.

End Users

The main goal of this project is to find effective SiC modification methods based on defect engineering, towards the development of SiC neutron detectors for security applications at borders and customs. In order to achieve our goal, it is important to receive real-life feedback from technology End-Users. The best candidate for our project is the Customs Administration, which is in charge of supervising the trafficking of illicit materials. Our End-User, Customs Administration of Republic of Croatia is the ideal partner. They are continuously showing a strong interest in the new technology which will be provided, and which could significantly improve their

capabilities. As they are in charge of controlling the “outside” border of EU they are facing many challenges. From them, we are receiving important information regarding the required specifications for effective neutron detectors which helps us with the optimization of engineering processes and establishing an effective modification method for enhanced SiC-based detectors.

Technical Summary

Neutron detectors were made from n-type silicon carbide Schottky barrier diodes (SBDs), which were fabricated onto nitrogen-doped epitaxial grown 4H-SiC single crystal layers approximately 25 μm thick [7]. The lateral dimensions of the diodes was 1 mm by 1 mm. The Schottky barriers were formed by evaporation of nickel through a metal mask with patterned square apertures of 1 mm \times 1 mm, while Ohmic contacts were formed on the backside of the SiC substrate by nickel sintering at 950 °C in Ar atmosphere [8]. Figure 1 shows a SiC-based SBD used in the neutron detector. The quality of the SBDs was assessed by current-voltage (I-V) and capacitance-voltage (C-V) measurements.

Defects in as-grown and in irradiated diodes were investigated by highly sensitive space-charge methods, namely DLTS and high-resolution Laplace-DLTS [9] to determine their concentrations, activation energies for carrier emission and respective capture cross sections. For studying the capture kinetics, capacitance transients were measured with different pulse widths, while keeping the other parameters constant [10].

Defect modelling was carried out by first-principles using density-functional theory methods. Core and valence states were described by pseudo-potentials and a plane wave basis set, respectively. The many-body electronic potential was evaluated using the hybrid density functional of Heyd-Scuseria-Ernzerhof [11]. To large extent, this approach mitigates the well-known underestimated gap syndrome affecting conventional density-functional calculations. Defects, vacancy-related and interstitial-related defects were inserted in 576-atom hexagonal supercells. The

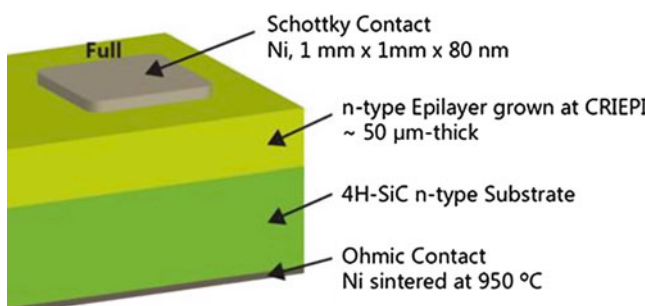


Fig. 1 Schematic drawing of the n-type 4H-SiC Schottky barrier diode

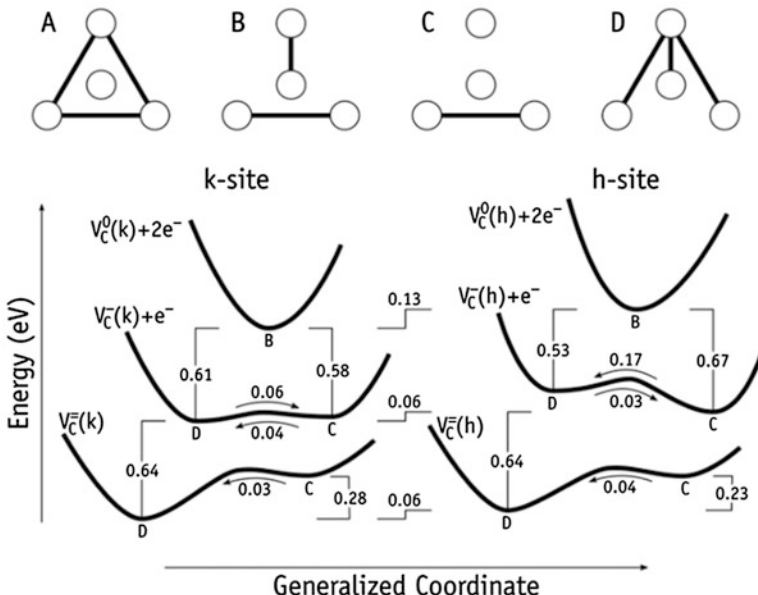


Fig. 2 (Top) structures of the carbon vacancy in 4H-SiC. The [0001] axis is perpendicular to the plane of the figure. Outer circles forming a triangle are basal Si atoms, whereas the central circle represents an axial Si. Thick lines indicate the formation of reconstructed bonds between Si second neighbours. (Bottom) configuration coordinate diagram for the neutral, negative, and double negative VC defect in 4H-SiC located on k- and h-sites. Transformation barriers are indicated next to the arrows. All energies in eV

outcome from the calculations were the electrical levels of defects and respective capture barriers. These quantities can be directly compared to the DLTS observations. Other calculated quantities include migration barriers, hyperfine- and g-tensors of paramagnetic defects. One of the main results from the modelling tasks is the configurational coordinate diagram of the carbon vacancy in 4H-SiC shown in Fig. 2, illustrating its negative-U character and relative energies in different crystallographic positions.

The Schottky diodes were tested for neutron irradiation-induced defects upon bare exposure or inside cadmium (Cd) thermal neutron filters with a wall thickness of 1 mm in the 250 kW JSI TRIGA reactor in Ljubljana, Slovenia. A photograph of the reactor core and a diagram of the core configuration are shown in Fig. 3. The irradiations were performed in the Pneumatic Tube irradiation facility, with neutron fluences ranging from $10^8 \text{ n} \cdot \text{cm}^{-2}$ to $10^{15} \text{ n} \cdot \text{cm}^{-2}$. The neutron spectrum was obtained from Monte Carlo neutron transport calculations with the MCNP6 code [12] in conjunction with the ENDF/B-VII.1 nuclear data library.

For prototype testing, four detectors were assembled, enclosed in 3D-printed plastic holders, and housed in turn in custom-made aluminium enclosures. The detector prototypes were equipped with thermal neutron converting materials for

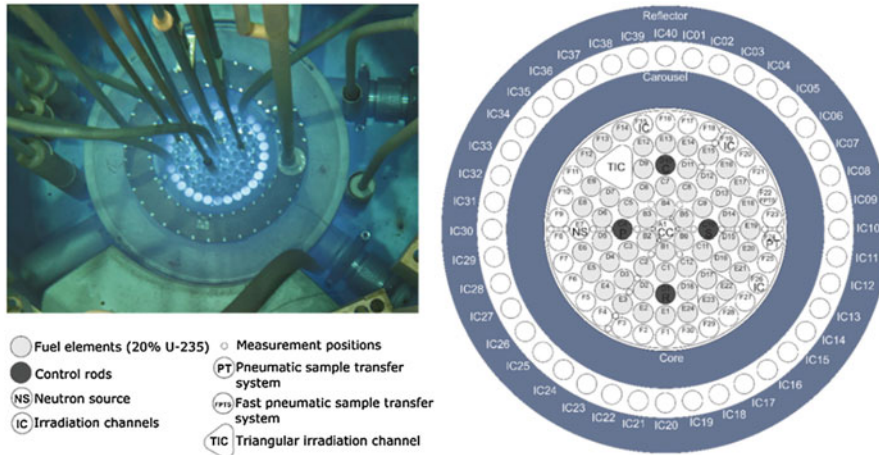


Fig. 3 Core of the 250 kW JSI TRIGA Mark II reactor in Ljubljana, Slovenia

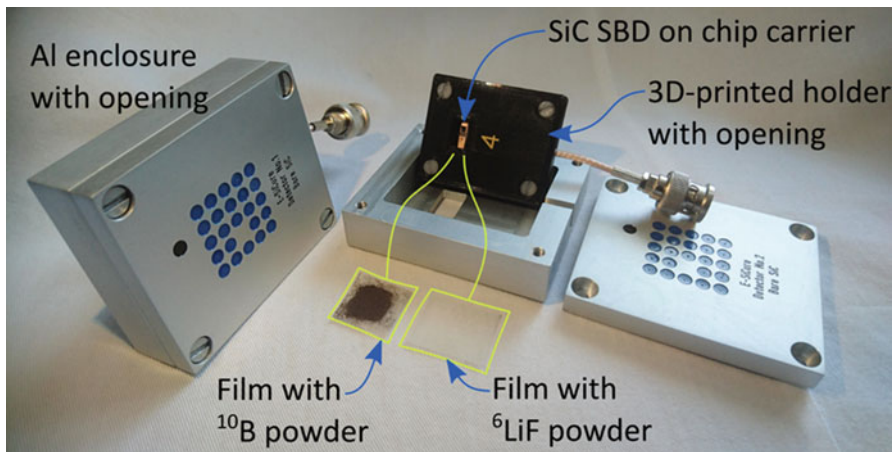


Fig. 4 E-SiCure prototype detectors. Left: assembled detector prototype in aluminium enclosure. Right: prototype detector components: SiC SBD mounted onto chip carrier with contacts, installed in 3D printed holder with opening, converter films (with ^{10}B and ^6LiF powder), open aluminium enclosure with opening [13]

neutron detection. Due to the very large thermal neutron cross sections of ^{10}B and ^6Li isotopes (around 3843 b and 938 b respectively, at an incident neutron energy of 0.0253 eV), the chosen converting materials were enriched ^{10}B , ^6LiF and $^{10}\text{B}4\text{C}$ powders. The ^{10}B and ^6LiF powders were applied onto a plastic film and mounted above the openings of the 3D-printed SBD holders. Figure 4 shows two prototype detectors employed during the experimental tests (fully enclosed and open).

Following the functioning tests, the neutron converter films were applied to the detectors and neutron irradiations were performed in the Dry Chamber of the JSI TRIGA reactor. The Dry Chamber is a large irradiation room in the concrete body of the reactor, connected with the reactor core by a graphite thermalizing column. It is mostly used for radiation hardness testing of detectors, electronic components and systems. Measurements were taken at power levels of 10 kW, 50 kW, 100 kW, 180 kW and 250 kW. In all the recorded spectra we observed a significant number of counts at higher energy channels, attributed to alpha particles and recoil ^7Li particles originating from ^{10}B (n,α) reactions. We also observed a distinctive structure in the spectra, attributed to the different energies of the secondary particles. The testing results confirmed the ability of the developed prototypes to detect thermal neutrons.

Broader Impacts

This project is expected to trigger the widespread use of solid-state SiC technology for neutron detection by means of significant improvements in efficiency, radiation hardness and long-term performance of SiC-based detectors. It will provide a crucial contribution towards the development of advanced, cheap and scalable radiation detectors for homeland security applications. The use of SiC-based in-core detectors in nuclear power plants is expected to increase the safety margins of nuclear reactors by providing high counting rates. Further, the results delivered by this project will provide important contributions to ongoing developments on SiC-based technologies for power conversion, fast electronics, ultra-violet detection and solid-state lightning.

Young Researcher Participation

e-SiCure project has attracted considerable interest among young researchers, and a number of diploma, master, doctoral and post-doctoral students have been or are still involved in the project research activities.

Three (3) diploma theses focused on electrical characterization of our devices have been completed at RBI. Four (4) Master students have been working on device fabrication and testing at QST. One (1) PhD thesis has been completed at UA, while research in the framework of three (3) PhD theses is still ongoing, two at RBI, and one at JSI. One (1) post-doctoral student is working at UA.

All together, twelve (12) young researchers have been involved in e-SiCure project, so far.

Contributions

The citations for journal articles and conference paper. Arising from e-SiCure project.

1. Z. Pastuovic, I. Capan, S. Sato, T. Ohshima, T. Brodar, R. Siegele, Deep level defects in 4H-SiC introduced by ion implantation: The role of single ion regime, *J. Phys.: Condens. Matter* 29 (2017) 475701.
2. José Coutinho, Vitor J. B. Torres, Kamel Demmouche, and Sven Öberg, Theory of the carbon vacancy in 4H-SiC: Crystal field and pseudo-Jahn-Teller effects, *Phys. Rev. B* 96 (2017) 174105.
3. Ivana Capan, Tomislav Brodar, Takeshi Ohshima, Shin-ichiro Sato, Takahiro Makino, Željko Pastuović, Rainer Siegele, Luka Snoj, Vladimir Radulović, José Coutinho, Vitor J. B. Torres, Kamel Demmouche, Deep level defects in 4H-SiC epitaxial layers, *Materials Science Forum* 924 (2018) 225.
4. Ivana Capan, Tomislav Brodar, Takeshi Ohshima, Shin-ichiro Sato, Takahiro Makino, Željko Pastuović, Rainer Siegele, Luka Snoj, Vladimir Radulović, José Coutinho, Vitor J. B. Torres, Kamel Demmouche, Double negatively charged carbon vacancy at the h- and k- sites in 4H-SiC: Combined Laplace-DLTS and DFT study, *Journal of Applied Physics* 123 (2018) 161597.
5. Vladimir Radulović, Klemen Ambrožič, Luka Snoj, Ivana Capan, Tomislav Brodar, Zoran Ereš, Željko Pastuović, Adam Sarbutt, Takeshi Ohshima, Yuichi Yamazaki, José Coutinho, “E-SiCure Collaboration Project: Silicon Carbide Material Studies and Detector Prototype Testing at the JSI TRIGA Reactor”, Oral presentation, International Conference “Nuclear Energy for New Europe 2018”, (NENE2018, September 10–13, Portorož, Slovenia).
6. Tomislav Brodar, Ivana Capan, Vladimir Radulović, Luka Snoj, Željko Pastuović, José Coutinho, and Takeshi Ohshima, Laplace DLTS study of deep defects created in neutron-irradiated n-type 4H-SiC, *Nuclear Inst. and Methods in Physics Research B* 437 (2018) 27.
7. Ivana Capan, Tomislav Brodar, Jose Coutinho, Takeshi Ohshima, Vladimir Markevich, Anthony Peaker, Acceptor levels of the carbon vacancy in 4H-SiC: combining Laplace deep level transient spectroscopy with density functional modeling, *Journal of Applied Physics* 124 (2018) 245701.

References

1. Ayedh HM, Nipoti R, Hallén A, Svensson BG (2015) Elimination of carbon vacancies in 4H-SiC employing thermodynamic equilibrium conditions at moderate temperatures. *Appl Phys Lett* 107:252102. <https://doi.org/10.1063/1.4938242>
2. Storasta L, Tsuchida H, Miyazawa T, Ohshima T (2008) Enhanced annealing of the Z1/2 defect in 4H-SiC epilayers. *J Appl Phys* 103:013705. <https://doi.org/10.1063/1.2829776>
3. Brezeanu G, Draghici F, Craciunioiu F, et al. (2011) 4H-SiC Schottky diodes for temperature sensing applications in harsh environments. *Mater Sci Forum*

- 679–680:575–578. <https://doi.org/10.4028/www.scientific.net/MSF.679-680.575>
- 4. Mazzillo M, Sciuto A, Roccaforte F, Raineri V (2012) 4H-SiC Schottky photodiodes for ultraviolet light detection. *IEEE Nucl Sci Symp Conf Rec* 1642–1646. <https://doi.org/10.1109/NSSMIC.2011.6154652>
 - 5. Ostling M, Ghandi R, Zetterling C-M (2011) SiC power devices – Present status, applications and future perspective. In: 2011 IEEE 23rd International Symposium on Power Semiconductor Devices and ICs. IEEE, pp. 10–15
 - 6. Nava F, Bertuccio G, Cavallini A, Vittone E (2008) Silicon carbide and its use as a radiation detector material. *Meas Sci Technol* 19:102001. <https://doi.org/10.1088/0957-0233/19/10/102001>
 - 7. Ito M, Storasta L, Tsuchida H (2008) Development of 4H–SiC epitaxial growth technique achieving high growth rate and large-area uniformity. *Appl Phys Express* 1:015001. <https://doi.org/10.1143/APEX.1.015001>
 - 8. Han SY, Kim KH, Kim JK, et al. (2001) Ohmic contact formation mechanism of Ni on n-type 4H–SiC. *Appl Phys Lett* 79:1816–1818. <https://doi.org/10.1063/1.1404998>
 - 9. Dobaczewski L, Peaker AR, Bonde Nielsen K (2004) Laplace-transform deep-level spectroscopy: The technique and its applications to the study of point defects in semiconductors. *J Appl Phys* 96:4689–4728. <https://doi.org/10.1063/1.1794897>
 - 10. Capan I, Brodar T, Coutinho J, et al. (2018) Acceptor levels of the carbon vacancy in 4H-SiC: combining Laplace deep level transient spectroscopy with density functional modeling. 245,701:. <https://doi.org/10.1063/1.5063773>
 - 11. Heyd J, Scuseria GE (2004) Efficient hybrid density functional calculations in solids: assessment of the Heyd-Scuseria-Ernzerhof screened Coulomb hybrid functional. *J Chem Phys* 121:1187–1192. <https://doi.org/10.1063/1.1760074>
 - 12. Goorley T, James M, Booth T, et al. (2012) Initial MCNP6 release overview. *Nucl Technol* 180:298–315. <https://doi.org/10.13182/NT11-135>
 - 13. Radulović V, Klemen A, Snoj L, et al. (2018) E-SiCure collaboration project: silicon carbide material studies and detector prototype testing at the JSI TRIGA reactor. International Conference “Nuclear Energy for New Europe 2018,” Portorož

Multi-Year Project: Explosive Trace Detection Sensor (Extras)

Antonio Palucci (✉)
ENEA, Rome, Italy
e-mail: antonio.palucci@enea.it

Francesco Colao
ENEA, Rome, Italy
e-mail: francesco.colao@enea.it

Stoiljkovic Milovan
Vinča Institute of Nuclear Sciences, Belgrade, Serbia
e-mail: missa@vinca.rs

Valentin Kolobrodov
National Technical University of Ukraine, Kiev, Ukraine

Bart Boonaker
TNO, The Hague, Netherlands
e-mail: bart.boonacker@tno.nl

Frank Schnürer
ICT Fraunhofer, Pfinztal, Germany
e-mail: frank.schnuerer@ict.fraunhofer.de

Cristiano Stifini
ATAC, Rome, Italy
e-mail: cristiano.stifini@atac.roma.it

Luigi Carnevale
DCA-SPS, Rome, Italy
e-mail: luigi.carnevale@poliziadistato.it

Lieutenant Colonel Luigi Cassioli
RTMAS (AM), Rome, Italy
e-mail: luigi.cassioli@aeronautica.difesa.it

Stefano De Muro
FS, Rome, Italy
e-mail: s.demuto@rfi.it

Pasquale Antuofermo
MERMEC Group, Rome, Italy
e-mail: pasquale.antuofermo@mermecgroup.com

Project Goals

The EXTRAS (Explosive Trace Detection Sensor) project has the intention to contribute to the development a stand-off sensor to monitor trace components in a scanning mode to be compliant with the safety civil regulations.

This project relates to the development of a proximal trace explosive detection on surfaces implementing the Raman spectroscopy to investigate in real time a wide range of surfaces of a potential bomber that might be contaminated with energetic materials.

In EXTRAS, improvements will be introduced in order to enhance the overall performance of the apparatus and reduce the false alarm rate. Upgrades are foreseen in the optical scheme, in optical components, scanning in the two axes and in a new 3D vision and tracking capability.

EXTRAS apparatus can be implemented as confirmation sensor of information previously gained by other instruments (bulk analysis) and with the advantage to be installed in scenarios like an infrastructure with a high transit of people such as metro and train stations.

Furthermore, a final test in a real environment has been included with the support of different end-users.

Deliverables

In this frame, the EXTRAS project has the intention to addresses the NATO Science for Peace technical requirements addresses issues related to identifying IED explosive substances, providing end users with a new tool that will improve the efficiency of security forces in crime prevention. The requirements are wrapped-up below:

- Screening selected individuals and suspect items;
- Screening selected individuals either without restricting their motion;
- Real-time response;
- Public deployment; all EU regulations;
- Integration into a multi-sensor integration platform;
- Screening carried items such as bag packs;
- Screening a wide range of threat materials, including HME's;
- Discriminating among threat materials;
- Covert operation such that selected individuals are not aware that they have been selected.

Therefore, the sensor will be based on an optoelectronic scanning system (laser, telescope and send/receiving optics), optical discrimination (filters and monochromator, assisted by a 2D + 3D vision to track and select the targeting area and the control setting electronics able to communicate with the external Command & Control system.

Security Relevance

The development of a scanning and stand-off sensor devoted to the detection of energetic materials is of high relevance to security and remarkably in the protection of people travelling everyday on mass transports and in turn in the contrast of possible terroristic attacks.

The project fits properly in the SPS Key priorities, in detail falls in the first area.

Facilitate mutually beneficial cooperation on issues of common interest, including international efforts to meet emerging security challenges.

Counter-Terrorism

- (i) Methods for the protection of critical infrastructure, supplies and personnel
- (ii) Detection technologies against the terrorist threat for explosive devices and other illicit activities

Science Relevance

EXTRAS has the intention to develop a new laser scanning optical sensor to be installed in different scenarios and operate under the eye-safe regulations. The laser scanning apparatus will be based on the Raman spectroscopic technique and will adopt new technical solutions for a better performances.

The expected improvements concern the following fields:

- Track the subjects;
- Scanning remotely critical parts of the body;
- Operate with non-invasive and respectful laser system for the safety of eye-safe people;
- Establish an iterative process to strengthen coordination between the Command and Control Centre with field staff.

Partnership Relevance

The partnership is based on different expertise, ranging from optical ray tracing and design, mechanical scanning capabilities, frame design, 3D vision algorithms, calibrated targets, complex control software. A remarkable support of different end users will drive the project from the beginning to the final test, being included police forces and high transit manager operators.

The EXTRAS partnership holds expertise from technical competences (software and hardware), to Law Enforcement Agencies and end-users that will support the project from the beginning and during its activities.

In particular, the design and development of the apparatus will be followed jointly among ENEA, VINCA, NTUU and TNO. ENEA will take care of the overall

software complexity. Conversely, ENEA and ICTF will work together on the target samples and relative data analysis. TNO will supply a spectrometer dedicated for this application, which should allow for a better detection limit of the overall system.

Furthermore, the involvement of Law Enforcement Agencies (DCA_SPS, AM) will contribute to define the appropriate modus operandi and will support in the selection of energetic materials. The end-users (ATAC, FS and Mermec) will be a valuable support for the logistic selection and operation in future applications.

The EXTRAS partnership holds expertizes as technical competences (software and hardware), to Law Enforcement Agencies and end-users that will support the project from the beginning and during its activities.

In particular, the design and development of the apparatus will be followed jointly among ENEA, VINCA, NTUU and TNO. ENEA will be responsible of the overall software complexity. Conversely, ENEA and ICTF will work together on the target samples and relative data analysis.

Furthermore, the involvement of Law Enforcement Agencies (DCA_SPS, AM) will contribute to define the appropriate modus operandi and will support in the selection of energetic materials. The end-users (ATAC, FS) will be a valid support for the logistic selection and operation in future applications.

End Users

EXTRAS project takes on board end-users for their valuable expertise and competences. The end-user included are ATAC, DCA-SPS, AM, FS and Mermec. Some of them are institutional end-users (DCA-SPS, AM) while the other are stakeholders. Both, institutional and stakeholders, will be member of the Advisory Board and involved in support of the project from the beginning.

The role of the Advisory board will be to guide the definition of the initial requirements, being expert in the selection of the materials to be investigated, on the possible body area to be scanned, as well as procedures, protocols to be adopted in the sensor for the operation. Furthermore, the advisory board should consider also the logistic offered by ATAC and FS as interested in possible future installation of this class of sensors in their structures.

Mermec group is interested in manufacturing this new class of sensor being deeply introduced in the worldwide network of transport suppliers.

Technical Summary

Explosive stand-off detection is still an extreme important issue for homeland security. Although many explosive detection techniques are well established, there is still the need and technological challenge for development of fast, in-situ screening sensors to be camouflaged in the critical infrastructures without harming people.

To this respect, lasers and optical systems are of critical importance to standoff detection technology for their ability to passively and actively probe threats near and far the possible threat.

The detection of dispersed particles is one of the possibilities to recognize hidden explosives. The handling and transportation of explosives has been shown to generate explosive traces on surfaces, which may subsequently be detected.

Optical spectroscopy techniques are good candidates for early detection and trace of IED evidence due to their ability to analyze different types of samples in a few seconds and operate in the field.

One of the techniques for ultra-rapid, in-situ identification of materials is the laser-induced breakdown spectroscopy (LIBS) [1, 2], as it does not require any sample preparation. LIBS analyses demand no contact, making stand-off detection possible from up to 130 m⁵. LIBS is based on plasma generation by an intense laser pulse, which leads to atomization and ionization of the sample material. Spectral emission from the excited species in plasma is used for the identification and eventual quantification of the sample composition. This particular feature, even if very sensitive, returns as a drawbacks in the MPE (Maximum Permissible Energy). Thus to not be applicable in public displacement.

Conversely, the Raman based spectroscopy [3] has gained consensus as a potential tool for detecting trace explosives because of its high discrimination capabilities and extremely appealing application in remote sensing due to highly discriminant capability, being based on molecular detection where each substance holds its peculiar spectra [4–6].

The Diagnostics and Metrology (DIM) Laboratory have successfully investigated the Raman technique, developing a proximal LIDAR trace detection of explosives (10 cm – 200 m, NATO classification) technique for a handheld device [7–9]. The RADEX (Raman Detection of Explosives) apparatus, developed in the frame of the NATO STANDEX programme, was successfully operated in the BCT (Big City Trial) test (June 2013; Metro Station Francois Mitterrand Paris).

With the RADEX apparatus has been achieved the ability to realize a system with the following performances:

- proximal detection (6–7 m)
- real time investigation
- operation in respect to MPE
- remotely controlled
- integrated in a sensor's network
- preliminary algorithms for data retrieval
- tested in a real environment

In the layout of the control software (Fig. 1), are shown to the user the following information: streaming video centered on the point to analyze (1), the collected Raman spectrum (2), the logging data and messages to the operator (3), the small field of view camera snapshot of the analyzed rea (4) and the real time result of the analysis in form of a traffic light showing the alarm level (5).

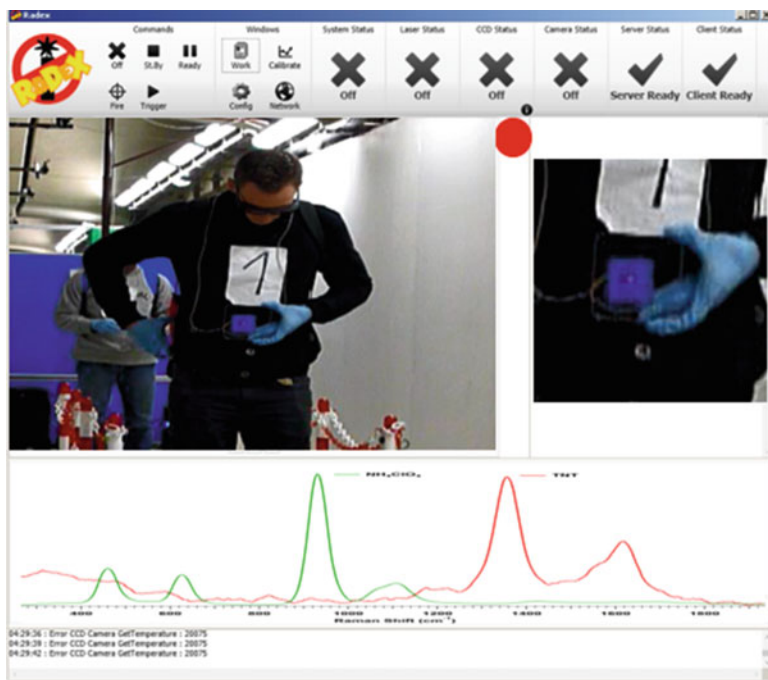


Fig. 1 Layout of the RADEX acquisition software: streaming video centred on the point to analyse (1); the acquired Raman spectrum (2); the logging data and messages to the operator (3); the small field of view camera snapshot of the analyzed area (4); and the real time result of the analysis in form of a traffic light showing the alarm level (5)

The video camera adopted is a special device with overlapped a red laser beam for pointing the invisible laser spot.

Different algorithms for data analysis developed with the main aim to release in real time the presence of suspicious substances and designed to remove uncorrelated noise and subtract the fluorescence contribution. To this respect, a discrete wavelet routine were introduced to retrieval the spectral signature and assign to the respective substance (Fig. 2).

The previous apparatus was calibrated with reference samples of explosives realized at Fraunhofer Institute for Chemical Technology, (ICT Pfintzal, Germany). Details of the preparation are reported elsewhere [10]. Several microscope slides, covered with different fabrics were prepared, depositing the explosive material on a squared area of $1 \times 1 \text{ cm}^2$ of these substrates to have a surface density between 100 and $800 \mu\text{g}/\text{cm}^2$. TNT, UN, PETN and AN in proper solutions supplied by ICT were deposited on the fabrics as a regular array of microdroplets so that, after the solvent evaporation, explosives are released as micro-particles homogeneously distributed on the surface.

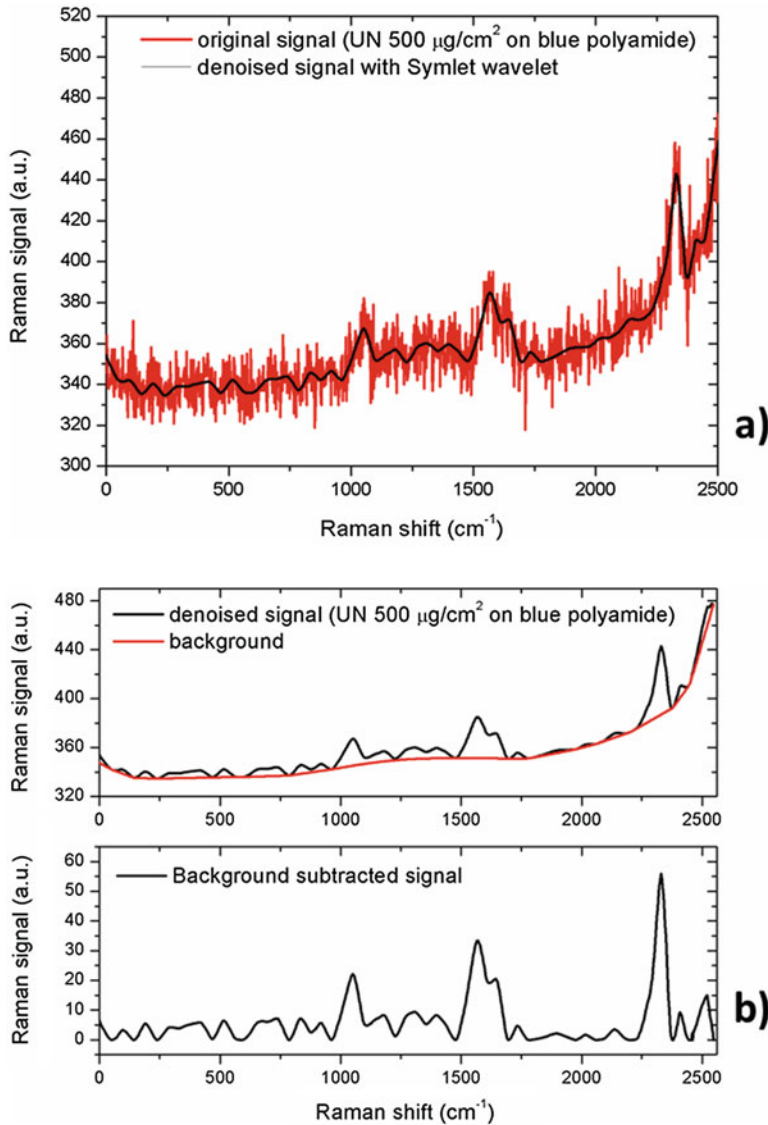


Fig. 2 Raw Raman spectrum of a single shot eye-safe UV laser (redline) compared to the denoised spectrum (blackline) obtained with a CWT Daubechies least symmetric wavelet (Symletwavelet). (b) (Top) Plot of the denoised Raman signal (blackline) and fluorescence background (redline) after the application of the subtraction algorithm. (Bottom) Plot of the background subtracted signal

Implementation of PCA statistical tool allowed to retrieve the discrimination ability of the data analysis algorithm with the use of different fabrics (Blue polyamide, Black polyester, Brown leather)⁹. As an example, in Fig. 3 are shown the score plots of the three principal components, which explain about 80% of the spectral

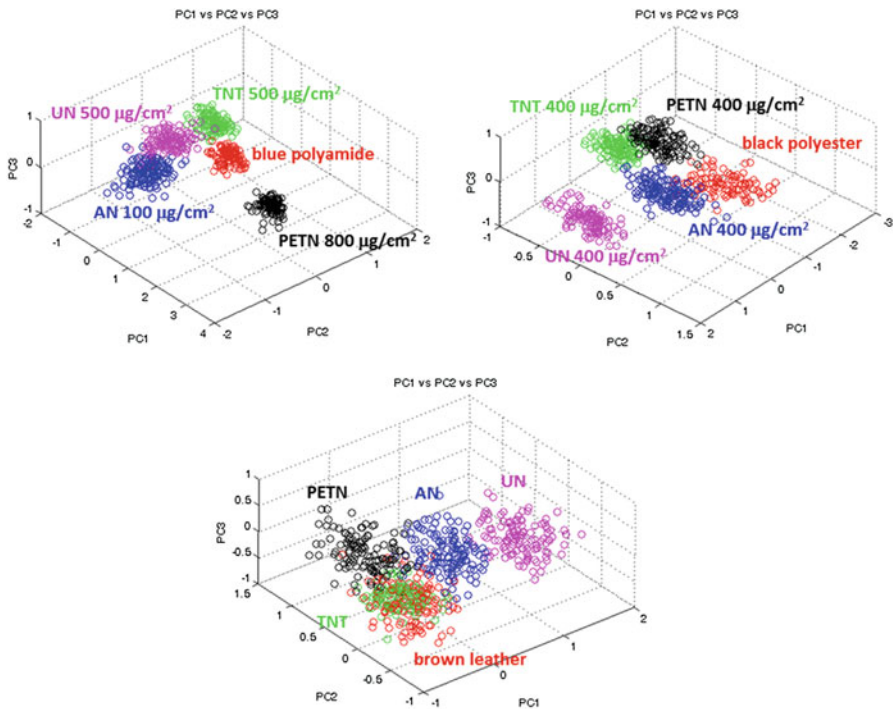


Fig. 3 PCA score plots showing discrimination between explosives compounds and clean substrates of different fabrics or tissues. The superficial concentration of each explosive is reported in the first two figures, the third figure show discrimination of explosives deposited on brown leather simulating a single fingerprint

variance of the three datasets. Looking at the PC score plots the selected samples seem to agglomerate satisfactorily into distinct groups except for the latter case, in which the TNT cluster is superimposed to the clean brown leather cluster (green and red dots) and the PETN cluster is barely distinguishable from the previous two. The main difference in this case is that the first principal component accounts for more than 64% of the total variance of the spectra, while the other components give a relatively low contribution, whereas in the previous cases the second principal component accounts for a larger contribution (about 13%), allowing for a better clustering in the plane delimited by the PC1 and PC2 axes. The third component is relatively irrelevant in this analysis, accounting for almost the same, residual variance, in all the PC scores.

In order to retrieve the detection capabilities of the apparatus, a data evaluation program was developed and tested on the experimental data to explore the potentialities for an automatic recognition of explosives. It is based on the comparison between the intensity of the stronger band of each explosives versus a reference threshold. Its performances have been evaluated via ROC curves [11, 12].

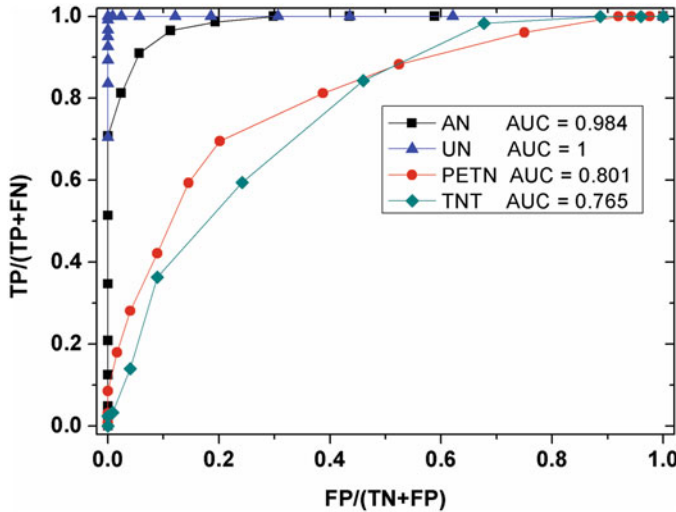


Fig. 4 ROC curves for the examined explosives deposited on brown leather in fingerprint concentration. In the legend are reported the corresponding area under the curve

Receiver operating characteristic (ROC) curves were used to discuss and quantify the sensitivity and the selectivity of the proposed recognition procedure. In Fig. 4, ROC curves are reported in terms of selectivity, or true positive rate (TPR), i.e. the $TP/(TP + FN)$ ratio, as a function of $(1 - \text{specificity})$ or false positive rate (FPR), i.e. $FP/(TN + FP)$ ratio¹¹. About 120 spectra of fingerprints of explosives were processed, together with 120 spectra of the clean leather, changing each time the threshold values from 0 to 0.2, in step of 0.01 and getting the corresponding TPRs and FPRs, to build the ROC curves for each compound (Fig. 4). The qualifying parameter considered for the presented binary classifier is the Area Under the ROC Curve (AUC), reported in the graph legend for each explosive. The higher the AUC the better is the classifier.

To our knowledge, the developed device is at the highest sensitivity nowadays achievable in the field of eye-safe, Raman devices for proximal detection.

A new optical lay-out is presently under investigation from the optical ray tracing theoretical model of the main optical components by a devoted software (e.g. Zemax or similar) in order to simulate and maximize the collecting performances. In the simulation, all the laser optical parameters (laser diameter), laser spot at the target distance, sensor active area etc., the telescope design should maximize the radiation collection to be forwarded to the entrance of a monochromator either by direct coupling or by a fiber optic.

A new light monochromator is foreseen in the system. Presently, commercially available monochromator is used but this is unlikely the most effective. The spectrometer is big: 30 liters, can collect light of relatively small angles, and requires a slit to obtain a good resolution.

TNO will design and manufacture a novel monochromator based on their previous work using free form optics. Free form optics are mirrors that can take an arbitrary shape, a bit like distorting mirrors at funfairs. However, now the mirrors are used to improve the performance. TNO has ample experience with design and manufacture of these mirrors, for example in the Tropomi instrument that was recently launched [13]. These mirrors are also used in the Raman spectrometers that TNO develops.

In this project, first a requirement analysis will be made to assess how the light can be used most efficiently. This will depend on the performance of the newly developed telescope, as well as the overall illumination and collection strategy. The TNO monochromator could have several benefits:

1. A larger collection angle.
2. Lightweight and low volume.
3. High resolution:

In all these aspects, an approach dedicated to the application and adapted to the other parts of the system are required.

There are many benefits to a freeform monochromator (Fig. 5). However, a challenge lies at the production of the mirrors. The UV light used in this application is very sensitive to roughness of the mirrors. This is why often spherical mirrors are used, which are created by polishing glass and then coating it. TNO has ample experience in designing and manufacturing free form optics using single point diamond turning and high precision milling. Nevertheless, production will be a challenge that should not be underestimated.

The extraction of the most areas to be investigated will be obtained with ad-hoc software composed by customized algorithms for the automatic engaging of the target and EXTRAS sensor positioning (Fig. 6), allowing estimating different scanning priorities especially in presence of crowd.

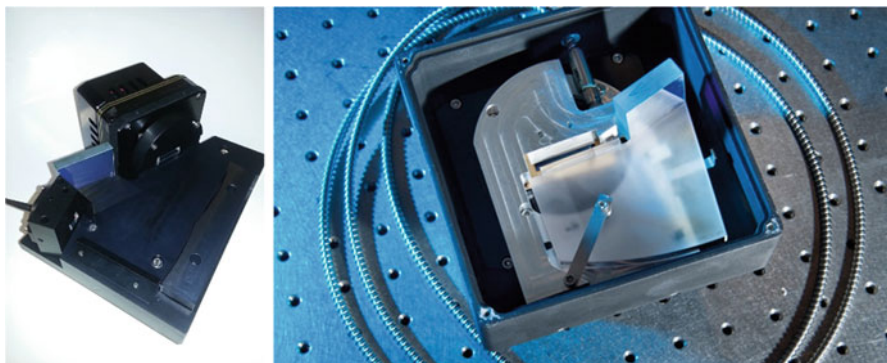


Fig. 5 View of the freeform monochromator

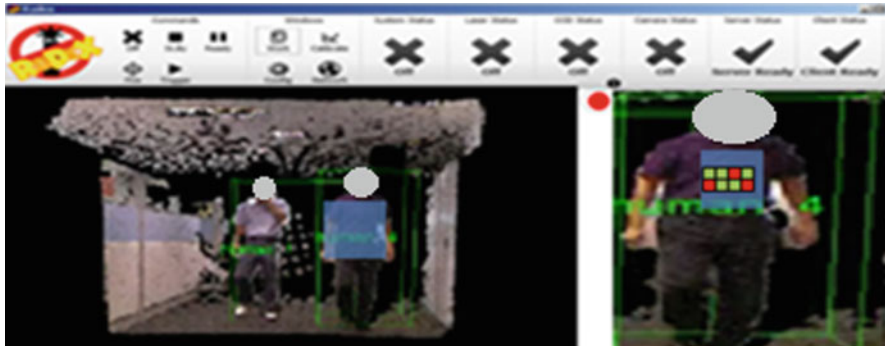


Fig. 6 The expected upgrade of the EXTRAS video detection with the addition of the 3D apparatus: left – person identification as block; right – the selected area to be scanned and the different spots coloured the possible positive or null detection

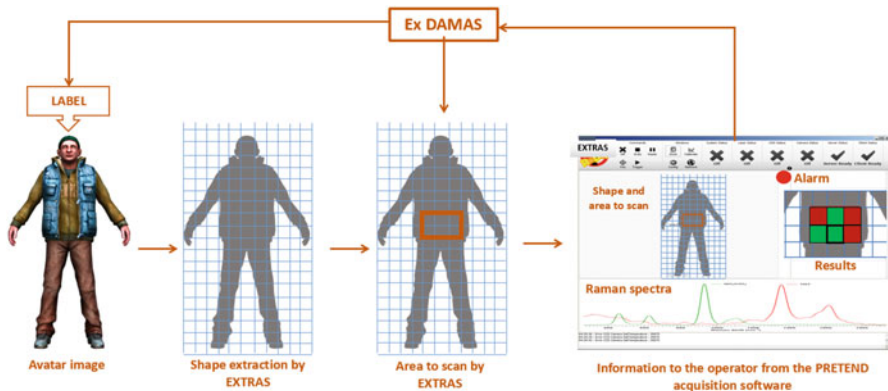


Fig. 7 The modus operandi of the 3D image software linked to the sensor's control software

The apparatus will analyze in real time an area of around 50–60 cm² through a fast laser scan. The laser scan will be performed respecting the actual regulations concerning laser exposure for humans [14].

The real-time data processing and fast response (in less than few seconds) will allow for the identification of explosive issues such as a potential suicide bomber before he/she reaches the target providing more time for an adequate action from law enforcement agencies. The software of the 3D camera will allow to reconstruct an avatar from the shape of the person and extract the areas to be investigated by the sensor (Fig. 7). This information will be released in the control setting and operation software of the system.

The 3D video-surveillance and alert system will base its functionalities on the cross-correlation between 2D and 3D data sensors, with the aim to support and make

more robust the weakness of the two techniques, if considered separately. Most of the development will be focused on the integration of algorithms for real-time monitoring, data transmission and machine/human support. Actually, body detection and small crowd segmentation algorithms are quite slow, 2 Hz, (e.g. deformable part models) or unprecise (e.g. cascade classifier), due mainly to the nature of the most common techniques: in our project will try to mix these techniques and test new one for a precise, robust and real-time implementation of these algorithms [15]. One of the features offered by these 3D video system based on structured light is the possibility to have in real time a 3D points cloud with XYZ coordinates of the entire investigated scene: this feature is used for solving another issue of this project, which is to extrapolate the target coordinates and determine the area where to address the Raman scanning system. As first approach to solve the problem a simple geometric area extrapolation based on the bounding box surrounding the person will be approached. As second step, a segmentation and classifier algorithm will be implemented for a more accurate localisation of the area to scan (e.g. backpacks, belts). During normal operations of the Raman scanner, accidental events have to be considered, like blockage or interception of the laser beam caused by person passage: in this case, algorithms based on distance and morphological threshold will be implemented for pausing or stopping the scanning. The entire software will be equipped with a user interface for inspecting, in a 3D virtual environment, the entire monitored zone and highlighting possible suspects with easy understandable tags.

The 3D scene recreation, the communication and positioning of the tracking system are highly dependent processes. In particular, their interaction takes place on three complementary levels:

- The 3D reconstruction module and target identifier provides the areas to test with the sensor;
- Reference points and target areas can be identified by the 3D recreation process;
- The area is scanned by selected technologies and the raw data captured are processed and forwarded by the communication module to the control center.

Consequently, the correct integration of the 3D model with communication and tracking system is extremely crucial to the application we imagine. In this sense, we must make sure that the geometry and references are correctly identified by all cooperating sub-systems and that the data format and software interfaces are properly defined and not ambiguous. In order to ensure maximum interoperability between scene reconstruction and track system, the compliance to Open Geospatial Consortium (OGC) standard will be evaluated.

Within this activity, we will perform functional tests of the derived prototype to verify its proper functioning and that the application requirements in terms of precision, delay and overhead are met.

Hardware testing and software testing, validation of localization and 3D models, and data exchange will be performed. It will also be verified that the performance of the communication system is appropriate in terms of volume of data exchanged and transmission latency to meet operational requirements: in particular, appropriate

arrangements will be made to limit transmission delays so that they have acceptable performance for operation in a real environment.

Data analysis will be implemented with various methods available for data reduction including principal component analysis, noise reduction, base line correction and emission band identification. The problem of false positives and false negatives will be addressed by considering different approaches including neural networks, vector support machines, and Gaussian mixing patterns.

The final apparatus will released as preindustrial system in order to increase the TRL in compliance with the following relevant standards.

Within the project implementation, the Consortium will take into account the issues about privacy and data protection according to EU and Italian regulation:

- Privacy code
- Directive IEC 60825
- Directive 95/46/CE
- Regulation (EU) 2016/679
- And the Directive 2016/680/CE
- Resolution of the EU Parliament of the 6° of July 2011

This, in order to meet all needs connected with data protection legislation, and using technologies in a realistic and optimal way.

Broader Impacts

The development of a scanning and stand-off sensor devoted to the detection of energetic materials is of high relevance in the protection of people travelling everyday on mass transports and in turn in the contrast of possible terroristic attacks. The installation of new sensors in critical scenarios will have, both camouflaged or noticeable, a deterrent effect on possible suicide terrorists with the feeling to be pinpointed and successively interdicted by the authority intervention. Such sensor can be operated stand-alone and in real time advise the operator of the superficial presence of suspected material and address the alarm to the intervention squads. Moreover, the sensor can be integrated in a more complex network of sensors and controlled from a remote operator. EXTRAS will have a strong impact in NATO public diplomacy due to the high value added in developing innovative sensors and furthermore in the media visibility.

Furthermore, end-users are interested to the outcomes of the project for the possible installation in large area scanning of metro or train stations.

Young Researcher Participation

Partners as Vinca Institute of Nuclear Science and the National Technical University of Ukraine “Igor Sikorsky Kyiv Polytechnic Institute” will involve young researchers in the project activities.

Contributions

1. Winefordner JD, Gornushkin IB, Correll T, Gibb E, Smith BW, Omenetto N (2004) Comparing several atomic spectrometric methods to the super stars: special emphasis on laser induced breakdown spectrometry, LIBS, a future super star. *J Anal At Spectrom* 19:1061–1083
2. López-Moreno C, Palanco S, DeLucia F Jr., Mizolek AW, Rose J, Walters RA, Whitehouse A, Laserna JJ (2006) Test of a stand-off laser-induced breakdown spectroscopy sensor for the detection of explosive residues on solid surfaces. *J Anal At Spectrom* 21:55–60
3. Gardiner DJ (1989) Practical Raman spectroscopy. Springer-Verlag, Amsterdam
4. Wallin S, Pettersson A, Östmark H, Hobro A (2009) In *Anal Bioanal Chem* 395:259–274
5. Chance Carter J, Michael Angel S, Marion Lawrence-Snyder, Jon Scaffidi, Richard E. Whipple, John G. Reynolds (2005) Standoff Detection of High Explosive Materials at 50 Meters in Ambient Light Conditions Using a Small Raman Instrument. *Appl Spectroscopy* 59(6):769–775
6. Gaft M, Nagli L (2008) UV gated Raman spectroscopy for standoff detection of explosives. *Optical Materials* 30(1):1739–1746
7. Garibbo A, Palucci A. Photonics for Detection of Chemicals, Drugs and Explosives. Photonics for Safety and Security edited by: Antonello Cutolo (University of Sannio, Italy) and Anna Grazia Mignani (CNR – Institute of Applied Physics ‘Nello Carrara’, Italy) edited by: Antonella Tajani (CNR, Italy). 2013 World Scientific Publishing Co. ISBN: 978-981-4412-96-4
8. R. Chirico, S. Almaviva, F. Colao, L. Fiorani, M. Nuvoli, W. Schweikert, F. Schnürer, L. Cassioli, S. Grossi, D. Murra, I. Menicucci, F. Angelini, A. Palucci. Proximal Detection of Traces of Energetic Materials with an Eye-Safe UV Raman Prototype Developed for Civil Applications, *Sensors* 2016, 16, 0008; doi:<https://doi.org/10.3390/s16010008>. I.F. 2.245.
9. Almaviva S, Chirico R, Nuvoli M, Palucci A, Schnürer F, Schweikert W (2015) A new eye-safe UV Raman spectrometer for the remote detection of energetic materials in fingerprint concentrations: Characterization by PCA and ROC analyzes, *Talanta* 144: 420–426. I.F. 3.545
10. Almaviva S, Botti S, Palucci A, Puiu A, Schnürer F, Schweikert W, Romolo FS (2014) Application of micro-Raman Spectroscopy for fight against terrorism and smuggling. *Opt Eng* 53(4):044113-1–044113-7
11. Fawcett T (2006) An introduction to ROC analysis. *Pattern Recognit Lett* 207:861–874

12. Jander P, Noll R (2009) Automated detection of fingerprint traces of high explosives using ultraviolet Raman spectroscopy. *Appl Spectrosc* 63:559–563
13. <https://time.tno.nl/en/articles/tropomi-will-help-us-answer-pressing-questions-about-climate-change/>
14. IEC 60825-1:2014 Safety of laser products – Part 1: Equipment classification and requirements <https://webstore.iec.ch/publication/3587>
15. Benenson R et al. (2012) Pedestrian detection at 100 frames per second – Computer Vision and Pattern Recognition. <https://doi.org/10.1109/CPVR.2012.6248017>

Multi-Year Project: UnExploDe: Portable Sensors for Unmanned Explosive Detection

G. Attolini

IMEM-CNR Institute, Parma, Italy

S. Beretta

IMEM-CNR Institute, Parma, Italy

M. Bosi

IMEM-CNR Institute, Parma, Italy

C. Ferrari (✉)

IMEM-CNR Institute, Parma, Italy

e-mail: ferrari@imem.cnr.it

C. Frigeri

IMEM-CNR Institute, Parma, Italy

P. Frigeri

IMEM-CNR Institute, Parma, Italy

E. Gombia

IMEM-CNR Institute, Parma, Italy

L. Lazzarini

IMEM-CNR Institute, Parma, Italy

F. Rossi

IMEM-CNR Institute, Parma, Italy

L. Seravalli

IMEM-CNR Institute, Parma, Italy

G. Trevisi

IMEM-CNR Institute, Parma, Italy

Rovshan Hasanov

Institute of Physics, Azerbaijan National Academy of Sciences, Baku, Azerbaijan

Chingiz Sultanov

Institute of Physics, Azerbaijan National Academy of Sciences, Baku, Azerbaijan

Gulnaz Gahramanova

Institute of Physics, Azerbaijan National Academy of Sciences, Baku, Azerbaijan

Nahida Musayeva

Institute of Physics, Azerbaijan National Academy of Sciences, Baku, Azerbaijan

e-mail: nmusayeva@physics.ab.az

Teymur Orujov

Institute of Physics, Azerbaijan National Academy of Sciences, Baku, Azerbaijan

Francesco Sansone

Department of Chemistry, Life Sciences and Environmental Sustainability,
University of Parma, Parma, Italy

e-mail: francesco.sansone@unipr.it

Laura Baldini

Department of Chemistry, Life Sciences and Environmental Sustainability,
University of Parma, Parma, Italy

Francesco Rispoli

Department of Chemistry, Life Sciences and Environmental Sustainability,
University of Parma, Parma, Italy

Zahra Sadre Momtaz

NEST laboratory, Scuola Normale Superiore, Pisa, Italy

Pasqualantonio Pingue

NEST laboratory, Scuola Normale Superiore, Pisa, Italy

Stefano Roddarò

NEST laboratory, Scuola Normale Superiore, Pisa, Italy

Project Goals

The project's aim is to prepare portable sensors for explosives based on semiconductor nanowires or carbon nanotubes. Nanostructures permit the preparation of sensitive, very compact and lightweight chemical sensors able to detect the air presence of molecules of explosives emitted by solid explosives, such as Tri-Nitro-Toluene (TNT).

Devices based on functionalised nanostructures have the advantage of very low electrical consumption, high chemical sensitivity, and simple technology.

This will allow the mounting of the sensor on unmanned aerial vehicles such as drones able to explore hazardous environments without the direct human intervention.

Deliverables

The expected deliverable of the project started on 15 February 2018 are:

Functionalised Germanium Nanowires or Carbon Nanostructures

The nanostructures prepared during the first part of the project, namely germanium nanowires and carbon nanostructures, will be functionalized with proper sensitizers containing amino groups (Lichtenstein et al. 2014), or other electron rich organic compounds, able to selectively interact with the molecule of explosives to be revealed. The sensitizer will establish a weak chemical bond with explosive molecules present in air, through acid-base and electrostatic interactions. This bond will modify the electrical field near the surface of the nanostructure (carbon nanotube or semiconducting nanowire) and will change the electrical carrier's concentration inside the nanostructure.

Functionalised nanowires will behave as field effect transistors (FET) in which the explosive molecules modify the gate potential (Schnorr et al. 2013) and change the conductivity of the FET channel making it sensitive to the presence of explosive molecules.

Functionalized carbon nanotubes will be made sensitive to the presence of explosive molecules in the air by binding the explosive molecules and by changing the contact resistivity between nanotubes (Cognet et al. 2007).

These deliverables of the project will be the base for the TNT sensor. They will permit in future the realization of sensors for different type of explosives and the study of sensor physical properties, such as the sensitivity (minimum detectable explosive concentration), the selectivity, the promptness of the sensor, the method to recover the initial state after the detection of the explosive (Fig. 1).

Trinitrotoluene Sensor

The second deliverable of the project is the sensor itself. This will be realised by using the functionalized nanowires or carbon nanostructures; then they will be attached on a insulating substrate and contacted.

An important feature of the sensor will be the system to recover the initial sensitivity after the detection of the explosive. This can be performed in two different ways:

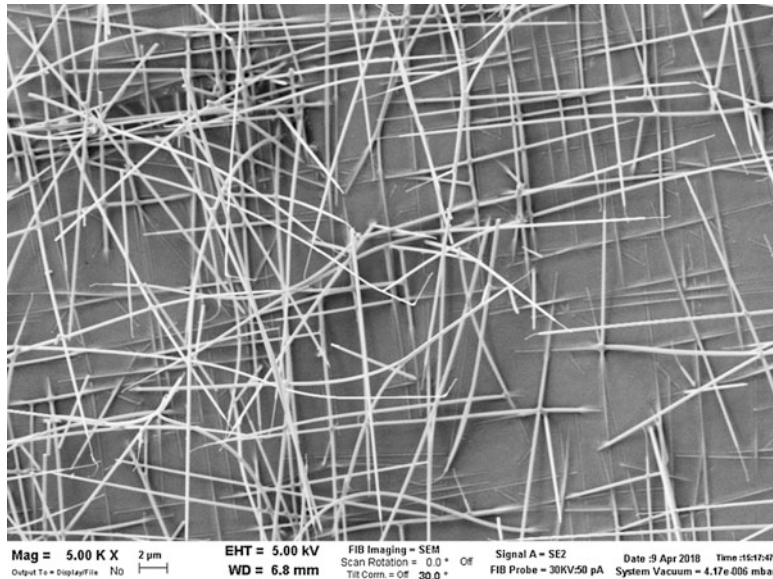


Fig. 1 straight 10 μm long monocrystalline Ge nanowires grown along (111) directions of the Si (100) substrate. Also demonstrated by x-ray diffraction and transmission electron microscopy

- By overheating the sensor some tens centigrade in order to break the weak chemical bonds with explosive molecules, in the same way as artificial noses work
- By fluxing pure air or other inert gases on the sensor itself.

In this way the sensor will operate by periodically detecting the signal and purging the sensor surface. The sensor itself should operate standalone and show the result of the measurement on a display (Fig. 2).

Due to the reduced dimensions and current consumption the overall system will be portable, of limited weight and should have a better sensitivity compared to detectors already available on the market and based on different technologies (Fig. 3).

System Made by Sensor Mounted on a Drone and Wireless Connection

The last deliverable will consist in the first prototype of sensor mounted on a drone. This prototype will be realised by adding a wireless communication system. This will permit the remote, unmanned detection of explosives by communicating the explosive concentration in the air and other parameters affecting the sensitivity of the instrument, such as the temperature and (possibly) the presence of air turbulence near the detector (Figs. 4 and 5).

Fig. 2 Carbon nanotubes gown by aerosol chemical vapour deposition technique and Fe as catalyst observed by electron microscopy

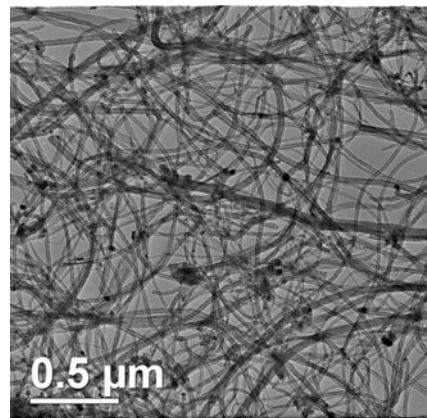


Fig. 3 Scheme of the field effect transistor based on a single functionalised germanium nanowire

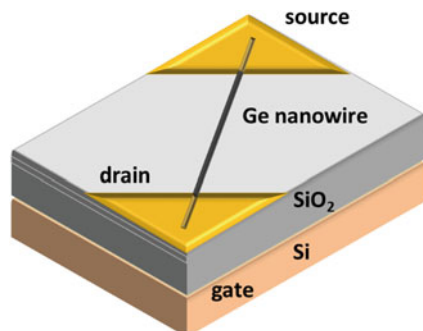


Fig. 4 Scheme of the sensor based on the conductivity of carbon nanotubes

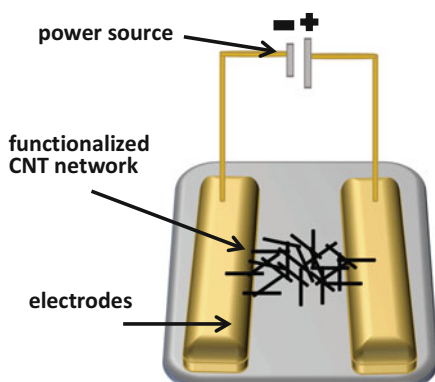
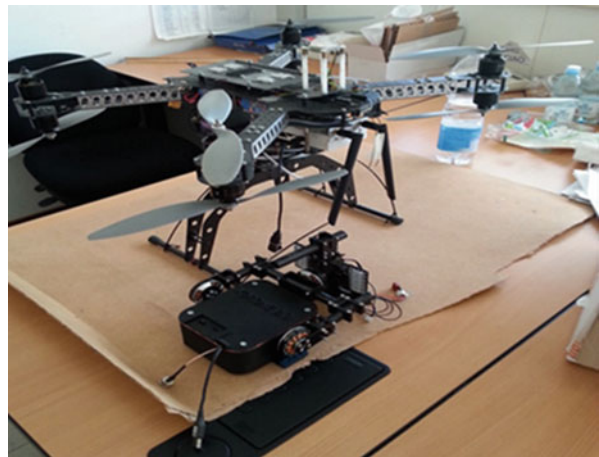


Fig. 5 Sensor mounted on a drone similar to that to be realised by the project



Security Relevance

The expected final result of the UnExploDe project is the realization of an ultra-sensitive and lightweight explosive detector based on nanostructures that, thanks to its much reduced weight, current consumption, and sensitivity can be easily mounted on unmanned vehicles permitting to explore hazardous environments without the direct human intervention.

The existing portable instrumentation with weight of the order of one kilogram usually needs human intervention and therefore is not suitable for the exploration of dangerous sites.

If successful the impact of the project on the security problems related to the presence of explosives will be relevant.

In particular the device can be employed for Counter-Terrorism:

- For protecting critical infrastructures, supplies and personnel;
- For detecting explosive devices against the terrorist threat activities;
- For detecting improvised explosive devices (IED) without the direct human intervention
- Depending on the achieved sensitivity, to detect mines and unexploded ordnance.

Science Relevance

The entire project is based on the use of nanotechnology for the preparation of chemical sensors able to detect explosives.

The research on nanostructures and on nanotechnology to realize electronic devices or sensors is one of the most active in the field of solid state physics and thousands of new international publications appear every year on physics, chemistry and electrical engineering scientific journals.

The part of the project devoted to scientific research in the UnExploDe project is more relevant than that devoted to technological developments.

The scientific research will concern the physical properties of the nanostructures realized. Even if a large literature is available in the field of semiconducting nanowires and carbon nanotubes, the mechanisms that make nanostructures sensitive to explosive molecules are still not completely clear and contradictory results are reported in scientific publications.

An important part of the project is the publication of results on high impact factor international journals, such as Nanotechnology, Applied Physics Letters, and Journal of Applied Chemistry.

The project involves relevant Italian and Azerbaijan Academic institutes such as

- Istituto per Materiali per Elettronica e Magnetismo (IMEM) belonging to National Research Council, the Italian largest research organization
- The department of Chemistry, Life Sciences and Environmental Sustainability, University of Parma, one of the most active scientific departments in the field of Chemistry in Italy
- The Institute of Physics, Azerbaijan National Academy of Sciences, the largest scientific organization in Azerbaijan.

The idea of the project arose from the long lasting cooperation between Institute of Physics and IMEM Institute with tens of common publications in the field of nanostructures and nanotechnology.

Partnership Relevance

Starting from the existing cooperation between Italian and Azerbaijan research institutions, based on the complementarity of the scientific expertise of the groups (growth and characterization of materials at the Italian side and technological applications at the Azerbaijan side), this project will strengthen the scientific collaboration and the mutual knowledge between partners.

Science will permit to enhance the security of populations vulnerable to the threat of a terrorist attack. A great attention is put to this theme in all the European countries, in which many terrorist attacks occurred in the last years with several tens victims, but also in Azerbaijan due to the situation of conflicts and not well established borders between Azerbaijan and Armenia, in particular near the Nagorno-Karaback enclave.

At the same time the close cooperation between Azerbaijan and Italy, two Mediterranean countries, will deepen mutual cultural and social understanding.

End Users

The Research and Development Center for High Technologies (RDCHT) was established in 2009 by the Government of Azerbaijan to encourage high technologies research and development.

The Center's research and production facilities include a state of the art clean room, optical spectroscopy equipment, electron microscopy lab, as well as carbon nanotechnology labs.

Several projects, as environmental friendly, energy-saving and cost-effective colour and white LEDs (chip on board) for indoor and outdoors applications, carbon nanotubes based nanocomposite materials for nanoelectronics, military, construction industry, mechanical engineering et all. Are realized in the RDCHT.

Azerbaijan was among the first countries which supported the war against terrorism. Azerbaijan joined all 12 international convention of counter-terrorism and reinforces regional cooperation on fighting against terrorism through signing numerous agreements.

In order to put the results of the Project into practical use, RDCHT researchers and engineers are involved in the project to carry out testing of the sensors, elaborated during the project.

If the result product will be effective and the devices will perform as expected, the end user will plan to obtain the patent, the fabrication of such sensors in large quantity, promote pilot study on production of such sensors and will advertise the application in Azerbaijan.

RDCHT has cooperation with ministry of defences of Azerbaijan, and some joint projects have been realised. They are also interested in this project and in its testing. If the results of testing will be successful, there is a possibility of using such sensors in explosive-searching devices, including drones.

If the project is successful, RDCHT as the end user will take tasks to produce such sensors in much quantity and try to advertise for the application in the Azerbaijan (detection of explosive in metro stations, in the places with many people, control of cargo on the border, protection of oil rings and gas pipelines et al.).

Technical Summary

Preparation of Sensors Based on Nanotechnologies

Preparation of Carbon Nanotubes (CNT)

CNTs Aerosol- are syntetised using an Aereosol-CVD system with horizontal quartz reactor (2 m length quarts tube) covered by movable electric furnace, 35 cm long and 22 cm in diameter with Ar/H₂ as a transport gas,. This technology is based on the injection of the solution in the reactor as an aerosol and its decomposition at high

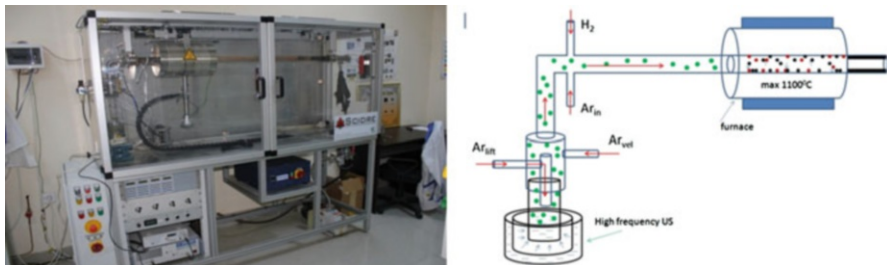


Fig. 6 aerosol CVD system picture (left) and principal scheme (right)

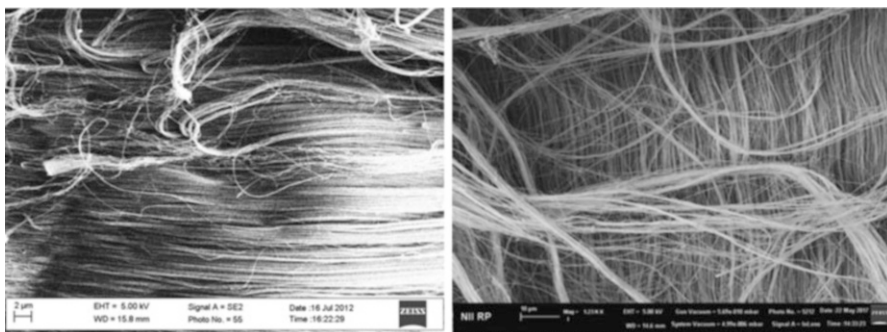


Fig. 7 SEM pictures of the CNTs obtained by Aerosol –CVD system

temperature (830–1000 °C). As a solution for the aerosol organic solvents such as cyclohexane, heptane, hexane, acetonitrile, alcohol, acetone, benzene mixed with ferrocene ($\text{Fe}(\text{C}_5\text{H}_5)_2$) catalyst in different concentrations are used (Fig. 6).

From the start of the Project (SPS G5423) in February 2018 we have performed more than 300 experiments to find the optimal conditions to grow high quality CNTs. Each sample of the CNTs with different synthesis condition has been analyzed by Raman spectroscopy, SEM, X-Ray diffraction and the more interesting samples were further characterized by Transmission Electron Microscopy (TEM).

After testing different solutions and different synthesis condition we concluded that cyclohexane and heptane are the best solvents for our Aerosol CVD, which permitted to synthesize long (650 micron) and very smooth Multi Wall CNTs with diameters between 5 and 50 nm (Fig. 7).

Raman spectroscopic analysis confirms the high quality of the CNTs. TEM observations show that such CNTs are either empty or partially filled with catalyst nanoparticles that affect their electrical resistivity, which is an important factor in our study (Fig. 8).

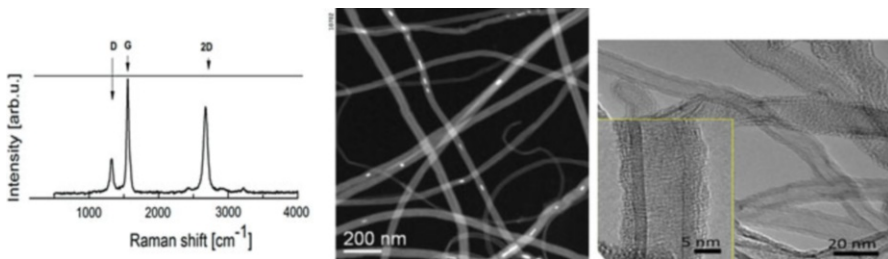


Fig. 8 Raman spectroscopy (left) and TEM analysis results (right) of the grown CNTs

Preparation of Germanium Nanowires

Ge NWs are routinely grown using a standard hot wall MOVPE system on Si or Ge substrates, either (001) or (111) oriented. The process is performed at 100 mbar, with a total of 500 sccm of ultra-pure H₂ as carrier gas.

The most common precursor reported in literature for the growth of Ge NW is germane (GeH₄), a highly flammable, potentially pyrophoric and highly toxic gas. In order to reduce the risk factor in the research environment, we chose Isobutyl germane (iBuGe) as a liquid metal organic precursor. This precursor is in liquid form, non-pyrophoric, does not react with water, atmospheric oxygen and moisture and it does not generate germane as by-product. It was successfully used to deposit Ge epitaxial layer for photovoltaics and electronics, SiGe, SiGeC, strained silicon, GeSb, and GeSbTe layers. It has high vapour pressure at room temperature, starts to decompose at 350 °C, has a low background impurity level and is considerably less toxic than GeH₄.

The successful use of Isobutylgermane for the growth of Ge NW was reported in literature for the first time by our group (Bosi et al. 2018).

Gold nanoparticles (Au NP) with diameter ranging from 20 to 80 nm are used a catalyst: the Au NP are dispersed on the substrate prior to the growth with the aid of poly-l-lysine to get a better NP adhesion. The Au NP size reflects the diameter of the grown NW with a very good approximation.

The growth process is performed at a temperature range of 340–445 °C with iBuGe flows ranging from 0.4 to 0.7 sccm. We have studied the influence of temperature, iBuGe flow and growth time (5 min – 3 h) on NW morphology.

In the following figure we show the typical morphology of Ge NW grown on Ge (111) substrates (Fig. 9).

The Ge NWs grow along the (111) axis, as confirmed by TEM analysis, and are vertically aligned to the Ge (111) substrate. NWs up to 25 µm long were obtained by tuning the growth conditions and the growth time.

TEM investigation confirms the excellent crystallographic structure of the NW, that are free from extended defects.

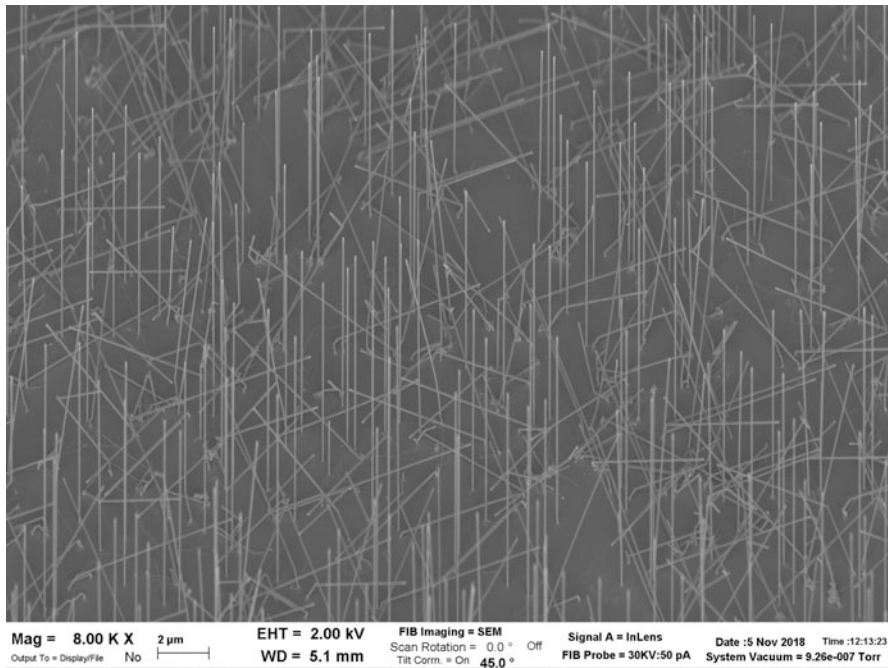


Fig. 9 SEM picture of Ge NW grown on Ge (111) substrates

The NW were detached from the substrate by ultrasonication in aqueous solution, then dispersed on a carrier substrate to perform further processing such as further analysis and metal contact deposition.

Functionalization

In order to impart high selectivity and sensitivity to the sensor, the nanostructures are decorated with chemical moieties able to interact with the explosive molecules. In particular, the electron-poor aromatic ring of TNT is well known to strongly bind electron rich, basic and nucleophilic amino groups through the combination of two types of interactions (Figs. 10, 11 and 12):

1. the formation of Meisenheimer complexes by nucleophilic addition of the amino group to the aromatic ring (Zang et al. 2011, Hughes et al. 2015), which takes place even in the gas phase (Yinon et al. 1995).
2. acid–base pairing interaction that involve the deprotonation of the slightly acidic TNT methyl group by the basic amino group followed by a charge-charge interaction between the ammonium group and the negatively charged aromatic

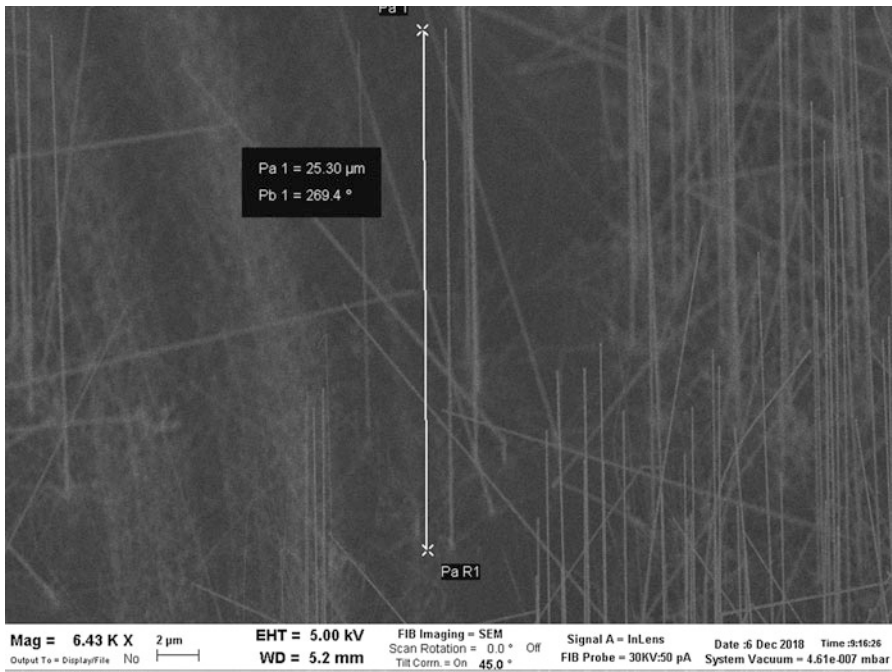


Fig. 10 SEM picture of Ge NW up to 25 μm long

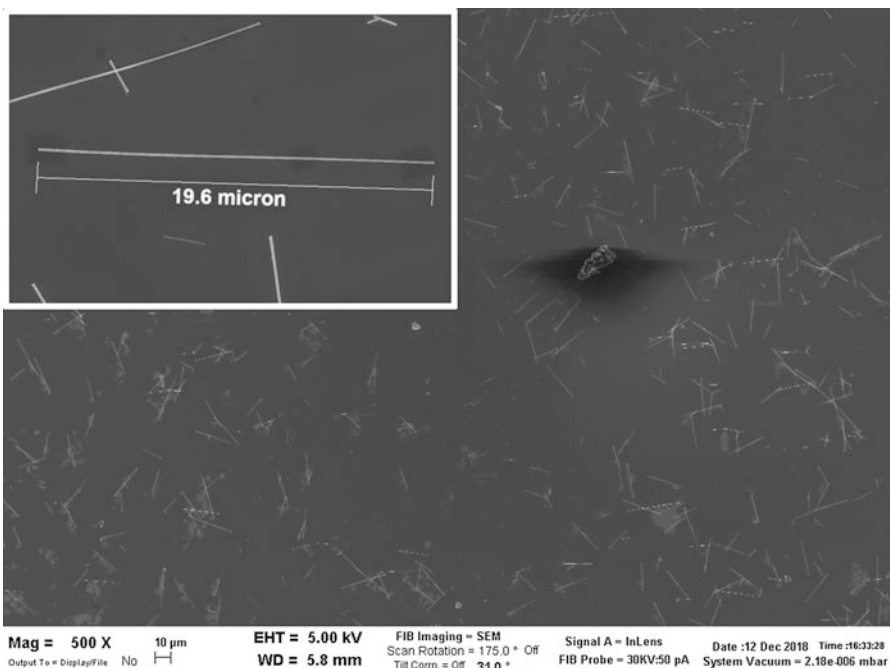


Fig. 11 NW dispersed on a silicon substrate. In the inset we report the magnification of a single NW

Fig. 12 Possible modes of interaction between amino groups and the TNT molecule: left, Meisenheimer complex; right, acid-base reaction followed by charge pairing

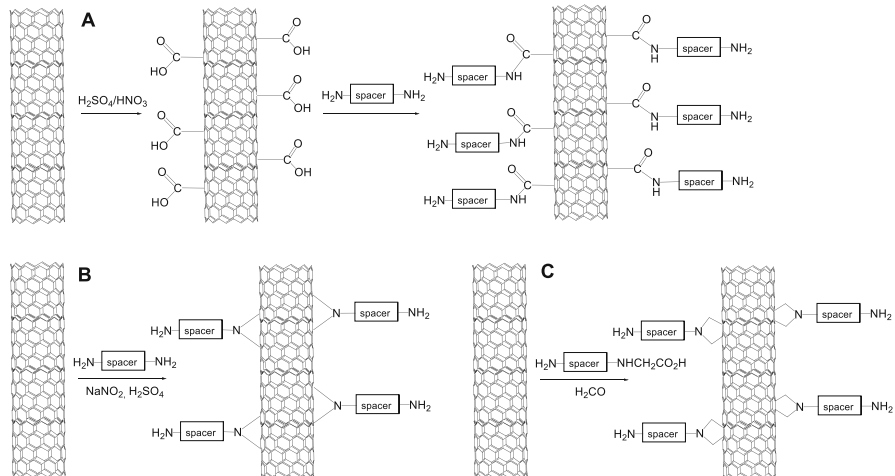
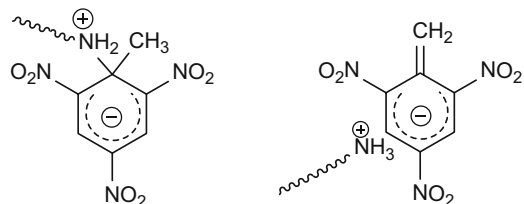


Fig. 13 Possible strategies to decorate CNTs with amino groups: (a) through an amide bond; (b) through the reaction of CNTs with amines; (c) Prato reaction

ring where the charge is delocalized through resonance by the three nitro groups. (Walker et al. 2007, Xie et al. 2008).

Amino groups can conveniently be installed on carbon nanotubes (CNT) and germanium nanowires (GeNWs) with specific methodologies that take into account the chemical nature of the nanostructure.

For the functionalization of CNTs with amino groups three different approaches are available (Fig. 13).

The first one is based on the preliminary oxidation of the CNT surface by treatment with H_2SO_4/HNO_3 to generate carboxylic acid moieties (Yan et al. 2007, Mallakpour et al. 2011) that are subsequently exploited to anchor the sensing group through the formation of ester or amide bonds.

The second strategy of functionalization involves the reaction between the aromatic rings of the CNT and amines (Schnorr et al. 2013).

The third approach consists in the Prato reaction between the CNT, an amino acid and an aldehyde (Georgakilas et al. 2002). The amino terminating chain can be linked either to the nitrogen of the amino acid or on the aldehyde.

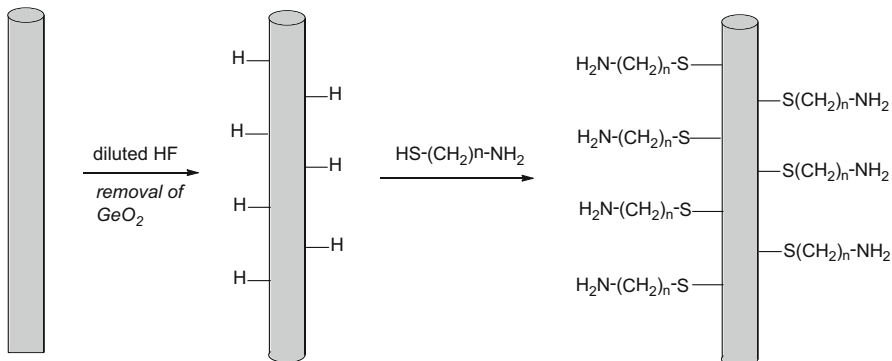


Fig. 14 Functionalization of GeNWs with aminoalkanethiols

The functionalization of the GeNWs can be performed by their reaction with aminoalkanethiols of C12–C18 length performed after a preliminary acid treatment to remove the Ge oxide layer (Fig. 14). In this way, the resulting nanowires are covered by a self-assembled monolayer that, besides performing the analyte recognition, ensures the protection of the nanowire surface from oxidation (Wang et al. 2005).

In addition to simple primary amino groups, other basic electron-rich groups can be installed on CNTs and GeNWs to be tested as explosive binders, with the aim of improving the sensor performances in terms of sensitivity and selectivity. For example, linkers bearing multiple amino groups can give an added value in binding and selectivity exploiting a multivalency effect (Mammen. et al. 1998) through their cooperation in the recognition process.

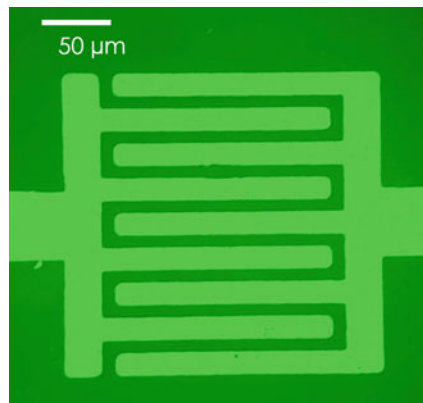
Aromatic amino acids (Dasary et al. 2009) and nucleotides are also promising active moieties, being able to establish additional interactions with TNT and other aromatic compounds through π - π stacking. Finally, the presence of additional cationic groups like guanidinium in combination with the amino groups could improve the recognition efficiency by interacting with the negatively charged ring through base-pairing interactions.

Contact Preparation and Electrical Characterization of Nanostructures

In order to characterize the nanostructures from the electrical point of view, it was necessary to prepare new electrical contact pads with spacing of the order of the nanowire or carbon nanotube length. By using a proper lithography mask we obtained suitable pads with spacing of 5–10–15 μm between electrodes, one of them is shown in Fig. 15.

The connection between NWs and contact pads was realised by using a Focused Ion Beam (FIB). FIB systems offer great potentialities in this field, as they allow the high resolution SEM analysis of nanostructures and, at the same time, the deposition

Fig. 15 contact pad obtained by a lithography mask realised in the frame of the project with 6- μm spacing between electrodes



of nm-sized metallic -Pt layers through Focused Ion Beam Induced Deposition (FIBID) or Focused Electron Beam Induced Deposition (FEBID) (De Teresa et al. 2013). To this aim, precursor molecules containing the metal (Pt in our case) are delivered to the surface through a gas-injection system (GIS). Then the ion beam (for FIBID) or the electron beam (for EBID) scans the surface, dissociates the precursor molecules and creates a metal deposit with the shape of the beam scan (Fig. 16) (De Teresa et al. 2013).

As known from the literature, one of the main problem of this technique is the so called “halo effect” that is the contamination of the surface (included the NW) due to implantation of Ga and undesired deposition of Pt outside the selected area (De Teresa et al. 2013).

This effect could lead to a partial overlapping of the contacts when their separation is too small (Lan et al. 2015, D’Ortenzi et al. 2016). In order to reduce the halo effect, we used Ga + ion beams with low probe currents of 20 pA and 50 pA. Under these conditions, we deposited several Pt stripes on Au pads designed with photolithography on SiO₂ substrates. The Pt stripes were interrupted with separation ranging from 2 μm to 8 μm , one of these is shown in Fig. 15. The I-V measurements confirmed the electrical separation of the stripes suggesting that, for probe currents ≤ 50 pA, the halo effect extends for less than 2 μm . Since Ge NWs are as long as 20 μm , our FIBID conditions are adequate for the deposition of contacts on NWs. Our activity will proceed studying the electrical properties of FIBID Pt stripes with different geometrical parameters (section and length); some of these are shown in Fig. 17.

The feasibility of contacting single Ge NWs has been tested on samples with NWs dispersed on Au pads deposited with lithography on SiO₂ substrates, as shown in Fig. 18. The effect of Pt deposition on the morphology of the NW and the measurement of its electrical characteristics are ongoing activities.

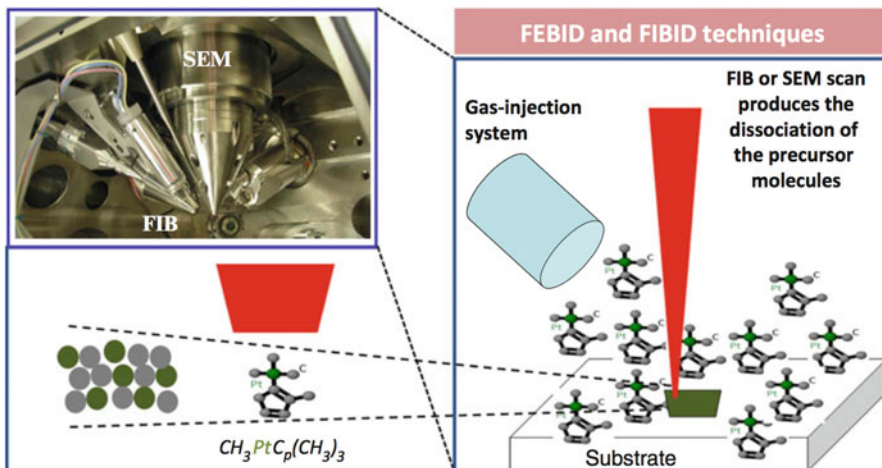
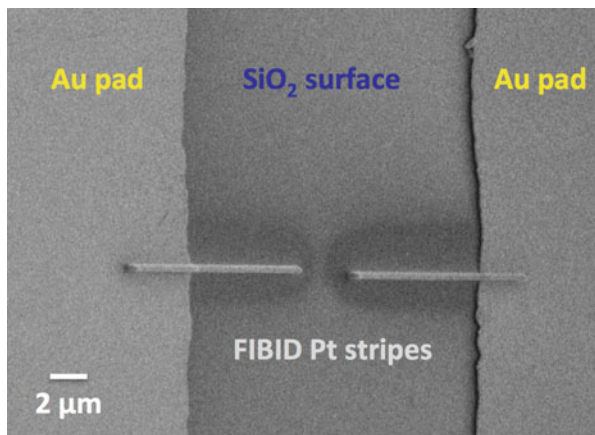


Fig. 16 scheme of fabrication of Pt wires and contacts by using SEM or FIB beams

Fig. 17 SEM image of FIBID Pt stripes (nominal parameters: $0.3 \times 0.3 \mu\text{m}^2$ section, $10 \mu\text{m}$ length) with $2.4 \mu\text{m}$ separation. The stripes are deposited with 50 pA current and 30 kV acceleration of the ion beam on Au pads deposited by lithography on SiO_2 substrates



Broader Impacts

The most important impact of a successful project is on security of environment. The expected compactness, lightweight, low cost and high sensitivity of explosive sensor will enable its widespread use, thus significantly upgrading the defenses against security threats.

Other expected impacts are: promotion of high quality applied research, increased ability towards problem solving in science and security, fostering scientific co-operation among scientists from NATO and EAPC partner countries, participation of young scientists, ability to promote collaboration among scientists and

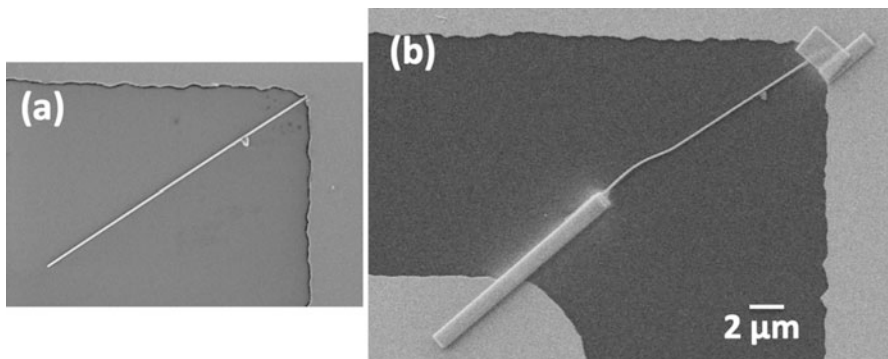


Fig. 18 SEM images of (a) single Ge NW dispersed on a SiO₂ substrate with Au pads, and (b) the same Ge NW after FIB deposition of Pt stripes (30 kV acceleration, 50 pA current) that connect the wire to the Au pads. The scale bar is the same for both images. The structure is ready for the electrical characterization

end-users, possibility of spin-off companies oriented to the production of devices and security related products or services.

Young Researcher Participation

IMEM Institute

Dr. Sara Beretta started her activity at IMEM in July 2018.

She is involved in all the activities carried at IMEM Institute:

- Growth of germanium nanowires
- X-ray diffraction and microscopy characterization
- Electrical characterization of nanostructures

She attended the European edition of Maker Faire exposition held in Rome from 12 to 14th of October 2018, in which the project attracted a large interest.

She also attended the conference “Nanostructures technology and research for sensor application “in Baku at the Institute of Physics and gave a talk “Germanium nanowires growth ”” at the conference.

Department of Chemistry, Life Sciences and Sustainability of Parma

Dr. Francesco Rispoli started his activity in the department of Chemistry, Life Sciences and Environmental Sustainability of the University of Parma in June 2018 and is in charge of the chemical functionalization of the nanostructures and of the characterization of the functionalised samples using spectroscopic techniques.

In particular, he explored different reactions to introduce amino groups on the CNTs and GeNWs through a proper linker and optimized the conditions to detect the presence of the new functionalities through InfraRed (IR) absorption spectroscopy.

Institute of Physics of the Azerbaijan Academy of Sciences

From Azerbaijan side four young scientists are involved in the project.

In accordance with the main objective of the project, each of the YS has a task and their implementation is monitored by the PPD Dr. Nahida Musayeva.

Rovshan Hasanov	– Task: Synthesis of SWCNTs and characterization by XRD
Chingiz Sultanov	– Task: A-SEM microscopic analysis of the samples
Gulnaz Gahramanova	– Task: Purification, functionalization of CNTs and Raman spectroscopic analysis
Teymur Orujov	– Task: IR spectroscopy analysis of functionalized CNTs. Analysis of their sensitivity to explosive traces

R.Hasanov is participating in all synthesis process of CNTs and characterization by XRD.

For synthesis of SWCNTs YS Rovshan Hasanov has an idea to put the A-CVD reactor Sulphuric particles, which play role of promoter (Fig. 19).

Using of Sulphur makes it easy to decrease the diameters of grown CNTs. By SEM CNTs with 5 – 7 nm diameters are observed and from RBM (Radial Breathing Mode) peaks of the Raman spectra it is calculated that there are SWCNTs with 1 – 1.4 nm diameter. It is planning the observation of the samples by TEM.

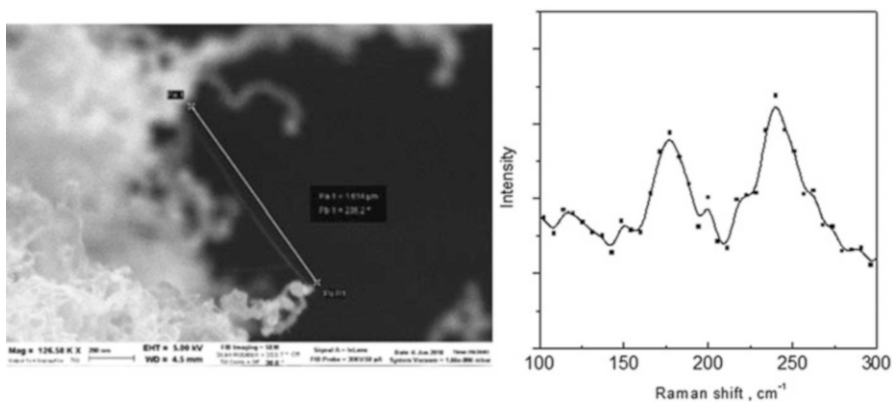


Fig. 19 Left: SEM picture of the CNTs of Sulphuric promoted synthesis process. Right: Raman BM bands of the Raman spectrum of the CNTs, specific of single walled CNTs

It is expected R.Hasanov will be trained in third Milestone on XRD machine in NPD -Dr.C.Ferrari's laboratory in IMEM-CNR (Parma).

Ch. Sultanov analyses of the samples by Analytic-SEM in the Institute of Physics (sector of Radiation Problems) NOTE: some of CNTs samples have been analyzed by Dr.G.Trevisi in IMEM-CNR (Parma). Ch. Sultanov has 12 engineer certificates on different microscopes.

He traveled 1 week to IMEM-CNR on June 2018. It is expected in forth Milestone Ch.Sultanov will be trained on Transmission Electron Microscope in the IMEM-CNR (Parma).

One of main and not easy task of the project is the functionalization of CNTs. From YS to this task is involved Gulnaz Gahramanova. She had 1 year YS fellowship in Ulm University in the laboratory of Prof. Ferdinand Scholz (Germany) by DaaD program. She carries out such chemical experiments under leadership of chemists of the RDCHT. All samples are analysed by Raman spectroscopy method.

G. Gahramanova traveled 1 week to IMEM-CNR on June 2018. It is expected that she will have training in third Milestone by help of our colleagues in Parma University – Department of Chemistry, group of prof. Francesco Sansone.

Teymur Orujov is involved to the project to analyze functionalized CNTs by IR spectroscopy method. He had 1 week training in January, 2019 on FTIR from Perkin Elmer in the Department of Chemistry, Parma University by support of group of prof. Francesco Sansone.

After functionalization it is important to make the structures to put contacts, to connect it to electrical circuitry and testing. To this task also is involved Chingiz Sultanov and Teymur Orujov. Teymur has trained and has a good experience work on Wire and Die bonding automatic machines in the laboratory, and of course e – beam evaporator to put contacts on the structures. They will test sensing of obtained structures.

Contributions

Presentations

Presentations performed in June in IMEM and in Bruxelles by the co-directors are available. Other presentations made during the periodical meeting are also available.

Some of our joint activities and meetings are published in media:

<http://science.gov.az/news/open/7483>

[http://inform.az/index.php?newsid = 28,424.](http://inform.az/index.php?newsid=28,424)

www.xalqqazeti.com/az/news/education/98487

[http://tehsil-press.az/index.php?newsid = 30,660.](http://tehsil-press.az/index.php?newsid=30,660)

<http://inform.az/index.php?newsid=33416>

Newspapers

“Il naso elettronico che fiuta la presenza di esplosivi nascosti”, Libero, 28 Giugno 2018, author Egidio Bandini.

“Tecnologie: Il naso elettronico che scova le bombe? Made in Parma”, Gazzetta di Parma 25 Giugno 2018.

Publications and Conferences

“Growth of germanium nanowires with isobutyl germane”, Matteo Bosi, Luca Seravalli, Sara Beretta and Claudio Ferrari, Published 31 December 2018 • © 2018 IOP Publishing Ltd., Nanotechnology, Volume 30, Number 8.

“Portable sensors for unmanned explosive detection”. Sara Beretta, Matteo Bosi, Claudio Ferrari, Cesare Frigeri, Paola Frigeri, Laura Lazzarini, Luca Seravalli, Giovanna Trevisi, Francesco Sansone, Laura Baldini, Nahida Musayeva, Rasim Jabbarov. Oral contribution to Advanced Research Workshop on Explosives Detection, Florence, Italy, Oct. 17–18th 2018.

Participation to “MAKER FAIRE 2018: Call for Universities”, held in Rome 22–24 of October 2018 “Progetto NATO GS5423 SENSORI PER LA RIVELAZIONE IN REMOTO DI ESPLOSIVI” Sara Beretta, Matteo Bosi, Claudio Ferrari, Cesare Frigeri, Paola Frigeri, Laura Lazzarini, Luca Seravalli, Giovanna Trevisi, Francesco Sansone, Laura Baldini, Nahida Musayeva, Rasim Jabbarov.

Oral contribution: “Synthesis of germanium nanowires and carbon nanotubes tailored to explosive detection”, Bosi Matteo, Beretta Sara, Ferrari Claudio, Frigeri Cesare, Frigeri Paola, Gombia Enos, Lazzarini Laura, Rossi Francesca, Seravalli Luca, Trevisi Giovanna, Baldini Laura, Sansone Francesco, Musayeva Nahida, Jabbarov Rasim, Teymur Orujov, Hasanov RovshanNano2Sense workshop, 6–7 November 2018, Grenoble, France.

Acknowledgments

This work has been supported by the NATO project G5423 UnExploDe: Portable Sensors for Unmanned Explosive Detection.

Dr. Claudio Ferrari (NPD).

IMEM-CNR Institute; Parco Area delle Scienze 37/A, Parma, Italy, NATO Country.

Prof. Nahida Musayeva (PPD).

Institute of Physics, Azerbaijan National Academy of Sciences, H. Javid ave.131 Az-1143 – Baku; Azerbaijan, Partner Country.

Prof. Francesco Sansone (Codirector).

Department of Chemistry, Life Sciences and Environmental Sustainability, University of Parma, Parco Area delle Scienze, 11/A, Parma, Italy.

References

1. Bosi M, Seravalli L, Beretta S, Ferrari C (2018) Growth of germanium nanowires with isobutyl germane. Published 31 December 2018 • © 2018 IOP Publishing Ltd., *Nanotechnology* 30(8)
2. Cognet L, Tsybouski DA, Rocha JDR, Doyle CD, Tour JM, Weisman RB (2007) *Science* 316:1465–1468.
3. Dasary SSR, Singh AK, Senapati D, Yu H, Ray PC (2009) Gold nanoparticle based label-free SERS probe for ultrasensitive and selective detection of trinitrotoluene. *J Am Chem Soc* 131:13806–13,812
4. De Teresa JM, Córdoba R, Fernández-Pacheco A, Sangiao S, Ibarra MR (2013) Chap. 5: Nanoscale Electrical Contacts Grown by Focused Ion Beam (FIB)-Induced Deposition, In: Wang ZM (Ed) *Fib nanostructures*. Springer 95
5. D'Ortenzi L, Monsù R, Cara E, Fretto M, Kara S, Rezvani SJ, Boarino L (2016) Electrical Contacts on Silicon Nanowires Produced by Metal-Assisted Etching: a Comparative Approach, *Nanoscale Research Letters* 11, 468
6. Georgakilas V, Kordatos K, Prato M, Guldi DM, Holzinger M, Hirsch A (2002) Organic Functionalization of Carbon Nanotube. *J Am Chem Soc* 124:760–761
7. Hughes S et al. (2015) Meisenheimer complex between 2,4,6-trinitrotoluene and 3-aminopropyltriethoxysilane and its use for a paper-based sensor. *Sens Bio-Sens Res* 5:37–41
8. Lan Y-W, Chang W-H, Chang Y-C, Chang C-S, Chen C-D (2015) Effect of focused ion beam deposition induced contamination on the transport properties of nano devices. *Nanotechnology* 26(5):055705
9. Lichtenstein, Havivi E, Shacham R, Hahamy E, Leibovich R, Pevzner A, Krivitsky V, Davivi G, Presman I, Elnathan R, Engel Y, Flaxer E, Patolsky F (2014) *Nature Comm* 5:4195.
10. Mallakpour S, Soltaniana S (2016) Surface functionalization of carbon nanotubes: fabrication and applications. *RSC Adv* 6:109916–109,935
11. Mammen M, Choi S-K, Whitesides GM (1998) Polyvalent interactions in biological systems: implications for design and use of multivalent ligands and inhibitors. *Angew Chem Int* 37:2754–2794
12. Schnorr Jan M, van der Zwaag D, Walish JJ et al. (2013) Advanced Functional Materials 23(42):5285–5291. Published: NOV 132013 Sensory Arrays of Covalently
13. Xie, Liu B, Wang Z, Gao D, Guan G, Zhang Z (2008) Molecular Imprinting at Walls of Silica Nanotubes for TNT Recognition. *Anal Chem* 80:437–443
14. Yan X, Han Z, Yang Y, Tay B (2007) Fabrication of Carbon Nanotube–Polyaniline Composites via Electrostatic Adsorption in Aqueous Colloids. *J Phys Chem C* 111:4125–4131
15. Yinon J, Johnson JV, Bernier UR, Yost RA, Mayfield HT, Mahone WC, Vorbeck C (1995) Reactions in the mass spectrometry of a hydride Meisenheimer complex of 2,4,6-trinitrotoluene (TNT). *J Mass Spectrom* 30:715–722

16. Walker NR, Linman MJ, Timmers MM, Dean SL, Burkett CM, Lloyd JA, Keelor JD, Baughman BM, Edmiston PL (2007) Selective detection of gas-phase TNT by integrated optical waveguide spectrometry using molecularly imprinted sol-gel sensing films, *Anal. Chim. Acta* 593:82–91
17. Wang Y-L, Chang Z, Liu, Dai H (2005) Oxidation resistant germanium nanowires: bulk synthesis, Long Chain Alkanethiol Functionalization, and Langmuir–Blodgett Assembly. *J Am Chrem Soc* 127:11871–11,875
18. Zhang K, Zhou H, Mei Q, Wang S, Guan G, Liu R, Zhang J, Zhang Z (2011) Instant visual detection of trinitrotoluene particulates on various surfaces by ratiometric fluorescence of dual-emission quantum dots hybrid. *J Am Chem Soc* 133:8424–8427

Multi-Year Project: Standoff Coherent Detection of Warfare Chemicals Via Photoacoustic Spectroscopy

Mehmet Burcin Unlu (✉)

Physics Department, Bogazici University, Istanbul, Turkey

Ihor Pavlov

Institute of Physics of the National Academy of Sciences of Ukraine, Kiev, Ukraine

Yuriy Serzhkin

V. Lashkaryov Institute of Semiconductor Physics, Kiev, Ukraine

e-mail: yuriy.serzhkin@isp.kiev.ua

Project Goals

In this project, we will develop an integrated platform for remote detection of explosive materials and potentially hazardous gases from a distance up to one km, based on remote coherent vibrometry of photo-acoustic signal generated on the tested surface (or volume) by modulated light from excitation laser. We expect the developed methods, and the results of the measurements will have a significant impact on standoff detection technologies against the terrorist threat for explosive devices and other warfare chemicals including liquids and gases.

Deliverables

In order to reach the main aim, fundamentally three tasks will be performed within the project:

1. Development of high power (30 W) narrow linewidth (10 kHz) detection laser operating at 1.5 mm. The wavelength of the detection laser is chosen specifically at the eye-safe region, and it is less sensitive to scattering on small contaminations in the air like fog, smoke or dust compared with visible or 1 mm wavelength lasers. This laser will be completely fiber integrated and closely packaged to ensure stable and robust operation, allowing usage of the laser outside of the lab at different environmental conditions. The main challenge during development and packaging of this laser is expected from thermal degradation and damage of the gain fibers, due to the low conversion efficiency of Er ions pumped by 976 nm commercially available diodes, as a result of a significant quantum defect. To overcome these undesired effects detailed numerical simulations based on solving rate equations together with heat transfer equation will be performed to define final optical and mechanical design of the laser. This part of the project will be done at Institute of Physics of the NAS of Ukraine (IOP).
2. Development of tunable in a wide spectral range, high power excitation part based on a combination of several quantum cascade lasers. Since most of the potentially dangerous explosive materials and gases contain organic O-H-, C-O-H- groups they have vibrational absorption lines in the infrared spectral range near 10 mm. The absorption and photoacoustic spectrum for different chemical agents as well as relative intensities for the photoacoustic signal will be characterized using a gas/liquid chamber. Optimization of the signal level and the decision for the pulse repetition rate for the low-noise operation to obtain high signal-to-noise ratio will be accomplished in these studies. This part of the project will be done at Bogazici University (BU).
3. Development of high sensitivity low noise remote coherent detection platform. This platform will include a narrow linewidth detection laser (at the last stage the laser will be replaced by the high power detection laser developed in IOP), low loss optical receiver designed to receive the scattered from the target light, heterodyne mixing scheme, high sensitive low-noise photodetector, lock-in-amplifier, and analyzing scheme. The main challenge of this part is to amplify extremely low signal in the presence of high noise level caused by mechanical vibrations of the setup and the target, air turbulences, electrical and electronic noise of detection electronics. In order to increase the signal-to-noise ratio, different types of initial detectors (including balanced detectors) will be applied together with lock-in amplification scheme. The noise spectrum of the system at various environmental conditions will be recorded before the measurements to choose the optimal modulation frequency of the lock-in amplification. This part of the project will be performed at V.E. Lashkaryov Institute of Semiconductor Physics of the NAS of Ukraine (ISP).

4. Integration of the developed parts into a single platform, tests of the system and final measurements. During this stage, the excitation part will be delivered from BU, and the detection part will be delivered from ISP to IOP. The system will be mounted on a single platform with an external power supply allowing it to move outside of the lab space for the measurements in a natural environment. During the final measurements, absorption spectra of the investigated explosive materials will be recorded remotely, and the minimal detectable amount and the maximal detectable distance, i.e. the limitations of the system, will be defined.

Security Relevance

The project aims for developing a technology for the detection of explosive materials from a safe distance with high sensitivity, high speed, and high accuracy. If the project will be successful and the outcomes will be as expected and planned, the developed technology will enable a safer environment for everyone.

Science Relevance

The project is highly scientific and challenging the state-of-the-art methods that have been developed. So there is an excellent potential for new academic papers as an outcome of the project. Since the SPS Programme is aiming for performing research activities of innovative ideas with the potential of addressing global security challenges, we are of the mind that this project fits for the science pillar of SPS.

Partnership Relevance

In the project, there is one institute from a NATO member country and two institutes from NATO partner countries. The project brings together different experts, academicians, students with different backgrounds, knowledge, and culture. Despite the differences, the aim is the same; making the world a safer place via science and using all our knowledge, profession and abilities for this purpose.

End Users

There are many potential end user for the project. Since the output of the project will be a standoff detection system for the explosives, the security institutions from both governmental and private sectors are potential end users. If we can reach our goals

and detect the explosives from the trace of chemicals using the system we proposed, it will be a device that can be deployed to especially crowded areas such as airports, train station, subway stations, and mobile security vehicles. Besides, it can also be used for the detection of leakage or hazardous gases in industrial facilities.

Background Information and Technical Summary

Introduction

Early detection of threats, especially explosives, is one of the top priorities of homeland security. Studies are increasingly focusing on developing new detection techniques of the explosives from a few aspects; more sensitive, more accurate, faster and less expensive. Through this effort, it has become possible to detect even traces of explosives.

Security is of utmost importance in crowded places, such as airports, and traditional methods for detecting weapons and explosives are mostly based on X-ray machines and metal detectors. While these methods provide a quite good detection, especially for hand luggage, most terrorist groups now avoid traditional metal-based approaches when preparing explosives. Thus, new methods that can detect particularly from the volatile substances from a distance are gaining importance. A method that keeps the operator and the valuable assets at a sufficient distance from the possible threats is always desired. Such a method is called stand-off detection. The sufficient length in stand-off detection is between 50 and 100 meters; however, in the case of dangerous poisonous gases or powerful explosives, it extends to several hundreds of meters.

Detection of explosive materials from such distances brings two technical challenges: Sensitivity and selectivity. Unlike the spectroscopic measurements with analyses in laboratory conditions, the measurements with explosive traces are very low in concentration in open air measurements which is in the order of parts per million or parts per billion. Besides, since the composition of the chemicals includes sulfur, phosphorous, fluorine and chlorine in addition to organic compounds, it is harder to recognize narrow spectral patterns because they may interfere with the contributions from background signals. Detecting spectral features from big molecules is difficult.

This section is focused on giving a review of the background of the ideas that led to the proposed project. After summarizing the explosive detection techniques, we are going to introduce photoacoustic spectroscopy and its abilities in explosive detection. Then, we are going to introduce a method to detect photoacoustic signals using a fiber-based laser doppler vibrometer that will enable standoff detection.

Bulk Detection

The direct detection of the explosives from the material of the explosive itself can be defined as bulk detection. Most of the methods currently in use are bulk detection methods. Most important ones are:

- X-ray and gamma ray systems [45],
- Neutron methods [23],

Since the applied radiation levels are hazardous for human health, most of these methods are generally not applicable for direct scanning of people.

Trace Detection

The materials at solid and liquid form release vapor depending on the pressure and temperature of the environment. The quantity of the vapor emitted is called the volatility of the material. Using certain methods, it is possible to sample and analyze the vapor near the material without directly contacting the material. The efficiency of the analysis depends on several factors; collection efficiency and the pressure of the vapor, and, temperature and strength of the wind. Trace detection methods can be classified under three main branches; electronic/chemical sensors, optical sensors, and biosensors (Figs. 1 and 2). We are going to cover these methods briefly in this section.

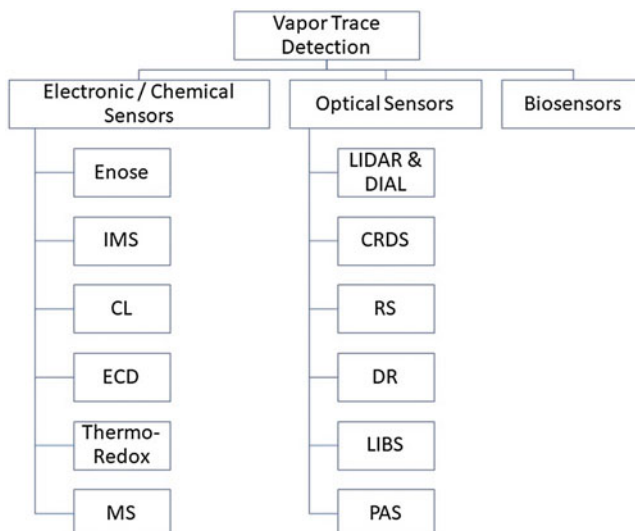


Fig. 1 Trace detection methods for explosives

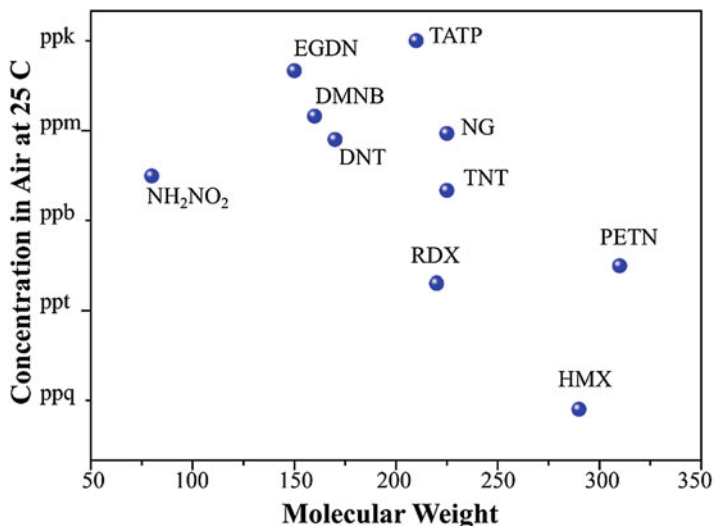


Fig. 2 Vapor concentration of different chemical

Trace detection methods are intrinsically non-invasive and based on direct detection of the vapor emanating from the explosive. The detection ability is hence directly dependent on the volatility of the explosive. Some examples of the concentrations of chemicals, that are commonly found in different explosives at room temperature, are; nitroglycerine – 4.1×10^{-2} ppb, PETN – 18 ppt, RDX – 6 ppt, TNT – 0.7 ppb [41]. However, these are the values for the chemicals near the surface of the material in a saturated condition, and the values reaching the sensor are at much lower. These values also drop when the package is sealed or packaged to hide the explosive. Most trace detectors are good at detecting concentration levels around ppm to hundreds of ppt levels and for the levels lower than that necessitate further studies.

Trace detection methods can be examined under three main titles;

- Electronic/chemical sensors
- Optical sensors
- Biosensors

Electronic/Chemical Detection

Electronic/Chemical Sensors are the biggest family of trace detection methods. Numerous results have been shown using the ability to sense gases using electronic and chemical detectors. To name a few of them;

- Electronic Nose or ENose, is a system based on chemical sensors specific to different chemicals. They are generally used as arrays, and by analyzing the

pattern of the data collected by these arrays, it is possible to detect and distinguish different gases' signal patterns. Various sensor types such as fiber optic cables [76], micro electro mechanical systems [51], piezoelectric sensors [58] and conducting polymers [40] are utilized to be used as electronic noses. By combining these sensors and analyzing the data using smart algorithms such as neural networks, it is possible to sense gases in the orders of ppm levels [18].

- Ion Mobility Spectrometry (IMS), is a method that is widely used in gas detection. A typical IMS have four parts; ion source, ion gate, drift region and detector. A radioactive source first ionizes the molecules in the samples, and the generated ions are mobilized using an applied electric field. Mass/charge ratio determines the drift time of the ion, and the detector at the end of drift region accumulates the time data of different molecules inside gas. The advantage of this method is relatively lower (seconds) detection time; however it has the disadvantage of low selectivity [21].
- ChemiLuminescence is an effective method to detect nitro-based explosives. When the vapor of the NO₂ group explosives mixed with ozone, they react, and a characteristic light is emitted. It is based on the detection of light as a result of this chemical reaction [22]. The disadvantage of this method is the lack of selectivity.
- Electron capture Detector (ECD) detects the concentration of the analyte based on how many electrons it absorbs to use in an electron capture event. Thus, it can detect the vapor of substances that strongly capture thermal electrons. It should be used with gas chromatography since it cannot distinguish certain types of explosives from each other by itself. Typical sensitivity level for an ACD is on the order of 1 ppb [25].
- Thermo-Redox method is based on an electrochemical reaction of explosive materials. In this method, first the explosive vapor is trapped inside a tube which is heated and NO₂ is released from the vapor proportional to explosive vapor concentration. The biggest drawback of this method is the inability of detecting non-nitrogen group explosives [49].
- Mass Spectrometry is a method based on ionizing the molecules in the vapor and passing them through a filter. Hence, ions are identified according to their charge/mass ratio. Using a method named Direct Analysis in Real Time (DART), a high voltage is applied to a carrier gas, and the molecules resulting from the excited state of the sample are then coupled to the mass spectrometer to analyze [14].

Biosensors

A biosensor can be defined as a self-contained analytical device that incorporates utilizes a biologically active element in contact with a suitable transduction element to detect the concentration or activity of chemical species [2]. The first biosensor, which was an enzyme-based glucose sensor, was shown by Clark and Lyons [13]. Since then many biosensors are developed and utilized for the detection of different

chemicals [16]. A biosensor is composed of two elements, the bio-receptor and the transducer. Bioreceptor is a biomolecule that is responsible for recognizing a specific type of analyte while the transducer converts this process into an electrical signal. The most significant advantage of biosensors is the simplicity of use and the measurement duration [49]. Using biosensors detection of TNT and DNT has been shown using immobilized proteins on electrodes [52]. Another good result for TNT detection has been shown with a sensitivity of 31 ppb using electrochemiluminescent immunoassays [89]. In order to find concealed explosives using the vapors some animals are also trained and utilized for detection and they can be counted under the category of biosensors as well [26].

Optical Methods

Since the trace levels are very low, the detection via laser-based techniques needs to use beams with high average power. It is known that some of the samples of interest in homeland security are shock sensitive and that they can be ignited with laser pulses. Thus, the spectral method, laser source and the sample of interest are essential operational security features. There is another problem that many spectroscopic methods need some sampling. In the remote detection of explosive chemicals applications, the method should detect the analyte with no sampling. Several spectroscopic methods that can do this task are well described in Caygill et al. [11] and Wallin et al. [83] together with the advanced methods. Some of these were described to have stand-off capabilities which are summarized below:

Differential Reflectometry(DR) DR is a surface examination technique that gives information regarding the electron structure in the vicinity of Fermi Energy [30]. It detects the electrons that absorb the energy of photons and excited into a higher energy state. Differentiation is based on the fact that different materials have different electron structure and hence different electron transitions which can be used as fingerprints to recognize different substances. So the DR modulates the electron structure of different materials and subsequently measures the spectral reflectivity with respect to perturbation [30]. Using the dielectric constant/wavelength relation, which is unique for every material, DR can be used to classify explosives. Using this method 66 nanograms of TNT was detected from 35 cm range [30].

Laser Induced Breakdown Spectroscopy(LIBS) This method necessitates a laser with very high peak power to be focused on the sample. Due to the high intensity in the focal region, the sample breaks down into diatoms and triatoms that can be measured using an atomic spectroscopic method and a spectral analysis method. Materials such as black powder, cyclotrimethylenetrinitramine (RDX) and air were analyzed using this method [15]Using single shot laser pulses in LIBS analysis on explosive detection, they have formed a library to detect with an accuracy of more than %95. Although the system works fine in the laboratory environment, there are challenges to overcome in open fields such as interference and undesired substances.

One method is to use double pulses instead of a single pulse [3]. Here, closely spaced (milliseconds) two pulses are sent to the sample. The first pulse generates a vacuum in the sample that enables the clean signal generation using the second pulse. It has been shown that 45 meters of standoff distance is possible using LIBS [43]. Limit of detection was around 100 ppm.

LIDAR and DIAL LIDAR is the acronym for Light Detection and Ranging. It is based on illuminating a target with a laser and analyzing the reflected light to obtain distance information by using time-of-flight information of the sent light. In order to obtain high resolution, generally narrow laser beams are preferred. A LIDAR consists of three main parts; transmitting beam, receiving optics and signal processing. One example of usage of LIDARs in standoff detection is for hydrogen leak gas detection [71]. Using LIDAR mechanism combined with Raman effect, concentration hydrogen less than one percent was measured. Differential Absorption LIDAR is also a technique for remote sensing atmospheric gases. In this technique, two laser beams at different wavelengths are used. One of these wavelengths is chosen to be absorbed by the gas to be measured and the other one is chosen to be transmitted. The difference between the two lights is used as a quantification of the concentration of the absorbent gas [17].

Cavity Ringdown Spectroscopy(CRDS) CRDS is a technique that a short pulsed laser is coupled into a resonator cavity which is formed of highly reflective mirrors and an aperture for gas intake. After enough laser energy is built up inside the cavity, the resonator turns off and the decay of the laser intensity is measured over time. The decay time is then compared with an empty cavity and the cavity filled with a substance of interest. The concentration and the molecular absorbance can be derived using this method. Detailed information on CRDS can be found in ([5]; [54]).

Raman Spectroscopy Vibrational methods such as IR and Raman spectroscopy are complementary techniques that need no sampling and give essential information from the sample of interest since the molecular vibrational energy levels are investigated. Among these, Raman spectroscopy is a weak spectroscopic method considering that the probability of inelastic scattering is low (Ratio of inelastically scattered photons to elastically scattered photons is 10^{-6}). Despite this, both approaches are widely used for stand-off explosive detection. The first remote Raman measurements had the stand-off distance of 10 meters and the detection limit of several ppm [27]. After the development of the fiber lasers and miniaturization of the spectrographs, many portable Raman systems were developed to detect possible hazards or to reach samples that are difficult to reach ([1]; [8]; [68]; [79]). The ambient light and fluorescence contributions were reduced by using an optimal gating width of the spectrometers [9]The detection distance in Raman spectroscopy is up to 100 meters. Limit of detection is in the order of ppm. Selectivity in this method is very high.

Photoacoustic Spectroscopy This is the method that we will use in our project for standoff detection of explosives and we will analyze it thoroughly in the next section.

Photoacoustic Spectroscopy

Photoacoustic Effect

Graham Bell is well known for his invention of the first practical telephone. However, one of his other great inventions is the production of sound waves by illuminating an absorber sample by chopped sunlight [4]. They reported that rapidly interrupted beams generated the loudest sounds which led them to design the device we call “chopper” nowadays. In this work, he and co-authors described the effect as the response of the illuminated material to cyclic heating and cooling., and Lord Rayleigh brought another physical explanation 1 year after the article: The unequal heating by intermittent radiation on thin plates of material creates mechanical motion of the solid. That generates un-electric sounds [62].

On the other hand, Preece came out with the idea that the solid does not move; however, it absorbs the photon energy and transforms it into kinetic energy which accelerates the atoms of the substance and leads to temperature rise [61]. After laser was invented, the interest in the photoacoustic field was stimulated. The name “photoacoustic” has been used more widely to replace optoacoustics in order not to confuse with the “acoustic-optic” effect. High powered state-of-the-art continuous wave (CW) lasers-were adapted to the experiments mentioned above. Kerr and Attwood were the first to apply laser photoacoustic spectroscopy in [35]. They named the device as spectophone which is used to measure absorptivity of gases. As the initial applications proposed, chopped light reveals the most intense acoustic waves. Development of the pulsed laser brought the idea to use these lasers as similar as chopped light sources to adapt in the photoacoustic setups. Patel et al. demonstrated the use of pulsed laser in their article published in 1979 [55]. This study showed that pulsed lasers in the photoacoustic setup allow more sensitive measurements of absorptivity. The same group followed up this demonstration with a new study in 1981 [56] to increase the detection limit and accuracy of the absorption amplitude.

A comprehensive theoretical model came out for photothermally induced acoustic waves in solids by Rosencwaid and Gersho in 1976 [63]. The physics of photoacoustic is built on the thermal expansion of the illuminated material as a result of absorption processes as mentioned in previous sections. We are going to brief the theory of photoacoustic taking considering the source as pulsed laser since the modern applications commonly use it. Since the heat diffusion equation behaves according to Helmholtz equations, one can call the temperature term as a “thermal wave”. Following the well-documented theory of photoacoustic with pulsed lasers [20, 85], the common expression of the photoacoustic wave equation in an inviscid medium is given in Eq. (1).

$$\left(\nabla^2 - \frac{1}{v_s^2} \frac{\partial^2}{\partial t^2} \right) p(\mathbf{r}, t) = -\frac{\beta}{\kappa v_s^2} \frac{\partial^2 T(\mathbf{r}, t)}{\partial t^2} \quad (1)$$

where β , v_s and κ are thermal coefficient for volume expansion, speed of sound and isothermal compressibilities, respectively. The isothermal compressibility is expressed as given in Eq. (2):

$$\kappa = \frac{C_p}{\rho v_s C_V} \quad (2)$$

The wave equation is reduced to Eq. 3 using the heating function $H = \mu_a \Phi$ and Eq. (2):

$$\left(\nabla^2 - \frac{1}{v_s^2} \frac{\partial^2}{\partial t^2} \right) p(\mathbf{r}, t) = -\frac{\beta}{C_P} \frac{\partial H(\mathbf{r}, t)}{\partial t} \quad (3)$$

One needs to quantify the heating function since it is related to the pulse duration of the laser. The pulse duration also determines the laser fluence. When a pulsed laser hits a substance, due to the local heating, a fractional expansion in volume is observed at the position of \mathbf{r} . This volume expansion can be expressed as

$$\frac{dV}{V} = -\kappa p(\mathbf{r}) + \beta T(\mathbf{r}) \quad (4)$$

In diffusive phenomenon, a sudden temperature change, where the heating pulse occurs, can be used to solve the Helmholtz equation in the temperature field to obtain the Gaussian spread of thermal energy [46].

$$q(x, t) = \frac{T_1 - T_0}{\sqrt{\pi t}} \exp \left(-\frac{x^2}{d_c^2} \right) \quad (5)$$

d_c is the thermal diffusion length (TDL) in Eq. 4. Considering α_{th} as thermal diffusivity constant, TDL is defined as:

$$d_c \sqrt{4\alpha_{th}\tau} \quad (6)$$

One condition to acquire photoacoustic signals is that the pulse duration of the laser should be shorter than the acoustic confinement time which should be less than thermal confinement time.

$$\tau < \frac{d_c}{v_s} < \frac{d_c^2}{4\alpha_{th}} \quad (7)$$

Using these relations, the pressure change upon pulsed laser illumination can be defined as in Eq. 8:

$$p_0 = \frac{\beta}{\kappa\rho C_V} A_e \quad (8)$$

The first term on the right side of equation eight is dimensionless and defined as Gruneisen parameter Γ whereas A_e is volumetric optical absorption. Using these terms, we can re-write the pressure expression:

$$p_0 = \Gamma A_e \quad (9)$$

Substituting constants in this equation, one can find that each milikelvin of temperature change results in an 800 Pa of pressure increase.

The sound waves propagating due to these pressure changes were first detected by microphones. Generally, a capacitance sensor which is sensitive to the deflection of a diaphragm in contact with the sample was used as microphones in the photoacoustic experiments. Commercial microphones could provide a sensitivity of about 100 mV/Pa and a bandwidth of 100 kHz. A laser schlieren microphone was designed by Choi and Diebold in 1982 which increased the sensitivity of the microphone by using a He-Ne laser [12]. However, these devices are not useful neither in the field of biomedicine nor in the gas sensing since the acoustic impedance mismatch decreases the signal intensity down to 10–4. To overcome this issue, ceramic piezoelectric transducers are used. These transducers can be produced from lead zirconate titanate (PZT), lead metaniobate, lithium niobate, crystalline quartz. Jackson and Amer reviewed the photoacoustic signal collection using transducers [31]. Although the sensitivity of transducers (about 3 V/Pa) is much worse than the commercial microphones, their fast rise times and better acoustic impedance matching properties make them more preferable.

Photoacoustics can be used as a spectroscopic or an imaging method. In the latter case, it is called photoacoustic spectroscopy (PAS), and it requires point by point measurements using the detectors described above. The imaging technique is multiplexed where one should scan many wavelengths or positions simultaneously. An image reconstruction algorithm is needed to form an image from these scanned wavelengths or positions.

Imaging of biological tissues using pulsed lasers is very common in the recent applications of photoacoustic. Wang led this kind of applications with many aspects of biological imaging. Among the group's studies, miniaturized photoacoustic tomography for cell and organelle imaging [86], use of nanoparticles in biomedical imaging [90] and their reviews on photoacoustic imaging [84, 85] are notable examples.

Since this chapter is dedicated to explosive detection using PAS, we will explain the studies on gas sensing wider in the section below.

Photoacoustic Spectroscopy for Gas Sensing

Photoacoustic spectroscopy is a molecular spectroscopic technique based on the absorption mechanisms of the molecules in the targeted sample. The strong absorption spectral lines of gases present in the mid-IR window. These experimental spectra are deposited in the US National Institute of Standards and Technology (NIST) database and can be reached freely [70].

When a narrow bandwidth light source is used, Beer-Lambert rule for absorption is valid which is given below:

$$I = I_0 \exp(-\mu_a x) \quad (10)$$

μ_a is the absorption coefficient in the equation above. For small values of μ_a ,

$$\frac{\Delta I}{I} \approx -\mu_a x \quad (11)$$

PAS signals are directly related to the ΔI value instead of I . This decreases the noise effects stem from the intensity of the absorption signal. Besides, the scattering of the photons from the target does not reduce the PA signal. On the other hand, many spectroscopic techniques use CCD cameras whose sensors are blind in the IR range. No camera is necessary for PAS; an ultrasonic transducer is enough for detection which is independent of the wavelength of the source.

Veingerov published the first ever photoacoustic study on gas detection in 1938 [80]. In his work, he used charged capacitive microphone diaphragms and a Nernst glower for sensing CO₂ in N₂ with a concentration of 0.2% (v/v). Pfund proposed an apparatus to measure temperature instead of pressure using a thermopile to detect CO₂ concentrations [60]. Luft measured trace gas absorption as sensitive as ppb level [44]. His measurement was important since laser was not invented and he illuminated the gas chamber with a low power lamp. Photoacoustic spectroscopy (PAS) was suggested as a new measurement technique for gas sensing after this work. Following his previous study, Veingerov published another study in 1946 [81]. He sent infrared beams into a closed chamber containing a gas mixture. He detected the pressure changes using a microphone whose membrane is disturbed when the temperature of the gases increased because of the absorption. In 1971, Kreuzer applied an He-Ne laser which emits 3.39 μm light to excite a mixture of methane and N₂ to obtain ultra-sensitive (ppb level) spectroscopic measurement [39]. This is the first study to use lasers in PAS setups. Patel et al. showed that PAS is applicable and efficient in trace gas detection in his experiment in the stratosphere layer in the altitude of 28 km [57].

The choice of the laser source to be used in the experiments is crucial to obtain efficient and sensitive measurements. The sensitivity of the system defines how well the trace gases can be detected. UPAC defined the minimum detectable

concentration (MDC) in photoacoustic spectroscopy and Bozoki et al. described the term in their review [7]. The expression is given below:

$$MDC = \frac{\sigma}{m} \quad (12)$$

In Eq. (12), m ($\text{mV}\cdot\text{mol}^{-1}\cdot\text{dm}^{-3}$) is the sensitivity of the photoacoustic system. It is obtained by calculating the slope of the calibration curve of photoacoustic signal with respect to the concentration. σ (mV) is the background noise of the sensor and is the standard deviation of the background signal.

Similarly, the minimum detectable optical absorption coefficient is defined as the product of the laser power and sensitivity of the detector. Taking this into account, we can infer that the limit of detections of diode lasers are in the ppm level whereas gas lasers can reach sub-ppb level since gas lasers (*e.g.*; CO₂ lasers) can reach several Watts of output power [19]. As discussed previously, gas lasers are implemented in the PAS systems using an intensity modulation function (*e.g.*; chopper). One can also modulate the diode lasers with a chopper or an electronic device that directly switches on and off the laser emission.

CO₂ lasers are the sources that provide most sensitive trace gas detection measurements as the sensitivity of PAS systems scales with laser power and these lasers can provide the highest output power in the mid-infrared range. However, they can be tuned to specific lines and are not continuously tunable. Optical parametrical oscillator (OPO) is a highly tunable and high-power laser with Q-switched pulsed output option which makes it preferable for PAS. The range of this laser was first extended to mid-infrared range by Bohren and Sigrist in 1997 to be used in PAS of trace gas mixtures [6]. They measured a mixture of six gases and obtained ppm level sensitivity in the 3–3.5 μm range. Herpen et al. proposed a more developed singly resonant OPO that generates high power idler output (> 1 W) with high tunability (24 GHz) and small linewidth (< 5 kHz) [77]. The source in this study is a CW OPO in contrary to Bohren and Sigrist and Herpen could obtain noise equivalent pressure concentration values in ppb level at 3.34 μm wavelength. The same group also used this source for the detection of CO₂ concentration of small insects [78]. They tuned the laser to the range between 3.9 and 4.8 μm and showed that 20 mW of output power is enough to obtain 7 ppm sensitivity since CO₂ has an intense rotational-vibrational band at 4.23 μm. Sub ppb levels of sensitivity in PAS with OPO lasers were achieved in 2006 for CO₂ and gas mixtures containing methane and ethane [53].

Recently developed quantum cascade lasers bring more tunability in the range of a few hundreds of nanometers to several micrometers. These sources are quite small (*i.e.*; comparable with a pencil) and they reached high powers (>1 W) that enables sensitivity in a wide wavelength range (*e.g.*; 3–13 μm). Sharpe et al. demonstrated the first use of quantum cascade lasers with distributed feedback (QC – DFB) in the application of high resolution NO and NH₃ sensing [69]. A year after this work,

Paldus et al. could acquire signals from ammonia and vapor water using a QC – DFB at 8.5 μm with 16 mW output power. They measured the detection limit of their measurement as 100 ppb. Similarly, Hofstetter and co-authors used QC in a photoacoustic setup with an array of 16 microphones in the measurement cell to increase sensitivity, and they reached 300 ppb [28]. Gagliardi et al. used a single mode CW QCL at 8.1 μm , and they measured several isomers of CH₄ and N₂O. Lima et al. showed that beam quality in PAS crucial [42]. Their experiments proved that with output powers 5–10 times larger than OPO lasers, QCLs could acquire 10–20 times smaller background signals. Spagnolo increased the sensitivity as low as 15 ppb with exposure time as low as 5 s as the power of the QCL reached up to 100 mW [74].

The sensitivity of QCL-based PAS measurements has reached a saturation point by 2010. A new technique called Quartz-Enhanced Photoacoustic Spectroscopy (QEPAS) has already been proposed in 2002 by Kosterev et al. that uses a quartz tuning fork as transducer instead of detecting acoustic energy in a gas-filled photoacoustic chamber. He achieved to obtain the detection limits of conventional PAS systems with a less complicated and compact setup [38]. Using a lock-in amplifier, one can detect the electrical signal at the resonance frequency produced by the piezo-electrically active mode of vibration. PAS can be obtained by scanning the wavelengths of laser since only one wavelength is excited at a time. Since acoustic sources' force direction facing the quartz tuning forks are in the same direction with the sensor, they have no displacement effect on the piezoelectric device. Therefore, the background noise is considerably lower in QEPAS which leads to detect small volumes of gas samples.

It is a frequent need to acquire real-time measurements with trace gas sensors. After Kosterev designed and produced the compact QEPAS sensor, another group [67] performed a small exposure time (0.7 s) measurement that enables real-time investigation of trace gases with a sensitivity level of 4 ppm (at 6177.14 cm^{-1} , 15 mW). Sub-ppm sensitivity with longer exposure times was reported to be available with this experimental setup. Increased sensitivity of QEPAS-based trace gas sensing was observed in 2012 by Spagnolo and co-authors [75]. They chose SF₆ as the target gas trace and obtained 50 ppt (part per trillion) sensitivity in a 1 s measurement with 18 mW of QCL output power. The sensitivity provided by this system corresponds to a noise equivalent absorption of $2.7 \times 10^{-10} \text{ W.cm}^{-1}/\text{Hz}^{1/2}$.

As discussed above, PAS became a compact and sensitive (down to ppt level) method especially after the development of the QCLs. These devices respond to pressure changes from trace gas mixtures in real time. Using photoacoustic spectroscopy technique in stand-off gas detection to reveal the presence of explosive material without any damage (*e.g.*; exploding the bomb, exposure of a light source to eye with an absorbing wavelength) is critical for homeland security. The techniques for remote sensing and our proposal to apply this method is given in the next section.

Laser Doppler Vibrometry for Detecting Photoacoustics

Detection of trace chemicals in gas, liquid and solid form by a photoacoustic effect with the help of laser Doppler vibrometer has recently been shown in different publications [24, 29]. In the standard method, the photoacoustic cell is excited by the laser source and a nearby microphone or transducer record the system response. However, this method requires a laboratory environment to operate and close contact with the examined material [48]. Since having close contact with the material is dangerous in the case of explosives, we have to use another way to retrieve the photoacoustic signal. In this project, it is done by the Laser Doppler Vibrometer (LDV).

The main advantage of LDV is high spatial resolution with low testing time with increased performances. (high-frequency bandwidth up to 20 MHz, velocity range of 730 m/s, resolution of about 8 nm in displacement and 0.5 mm/s in velocity) [10]. The first LDV models were used in 1980s but their low signal to noise ratio made them suitable for very diffusive surfaces only. Through the technological developments in electronic hardware, it has been started to use by many researchers. Compared to traditional accelerometers, LDV does not induce mass loading which ultimately effects the result for the experiment while maintaining at least comparable resolution. Also, LDV is a stand-off sensing technique, and it has been showed that it is able to gather photoacoustic data up to 100 m [24].

The basis for the operation of LDV is the Doppler shift caused by a moving surface. This frequency shift is proportional to the velocity of the surface in the direction of the line of sight for low velocities. Since generally laser has a much higher frequency than Doppler shift (typically 6 or 7) an interferometer like structure should be used to analyze the signal. Scattered light is generally mixed with a mutually coherent beam to produce a beat in the collected light density which has an oscillating frequency of Doppler shift [66]. However, this method does not solve the problem for calculating the total velocity of the surface since the Doppler shift only gives information about velocity in the direction of the line of sight.

In most of today's commercial products Bragg cells are used to create a shift in frequency to learn about the direction of velocity. Also, by changing the frequency shift applied by Bragg cell, we can move to a different region up to 20 dB less noise [24]. By the addition of frequency shift our total signal turns into a standard FM signal whose carrier signal frequency is equal to Bragg cell shift.

To improve SNR, the differential signal coming from two separate beams originating from different spots can be used. This helps us to eliminate common-mode signals resulting from thermal excitations, turbulence in the air or the temperature change in the air which causes a change in the optical path.

One of the most significant problems with the LDV system is the laser speckles which emerges from scattering light from a rough surface. If the surface is uneven in the scale of wavelength, the scattered light which is normally coming from the same wavefront will have a different phase. This generally changes the amplitude of the backscattered signal. In some region, because of the destructive interference, we might have lower signal values on our photodiode. We can try and get rid of this

effect by changing our target position slightly. However, in the case of laser excitation, these speckles might start to move which will create noise on top of our desired signal [47]. The origin of this “speckle-noise” has been explained with the introduction of a more general term “pseudo-vibration” [64, 65].

For better precision in velocity measurement higher carrier frequencies are needed. For better precision in velocity measurement, higher carrier frequencies are needed if we assume the minimum frequency, we can detect in beat signal stays constant. Some commercial products offer up to 600 MHz shift which linearly increases resolution in speed. Also using an all-fiber setup makes it much easier to use LDV outside the lab environment. Dust can damage a non-fiber setup if they get in contact with mirrors which are used in the alignment of the laser, but an all-fiber setup eliminates this problem. It has been shown that all fiber LDV works as good as commercial LDV’s if parameters to signal out the noise is appropriately chosen [88].

In the case of highly refractive surfaces, it has been shown that allowing multiple reflections, between our researched surface and a mirror, significantly decreases noise coming from speckles [87]. However, since this method requires a well-positioned mirror and a surface with good reflectance, it is not viable for our problem of detecting explosives from several hundred meters of distance.

In this project, the output of the detection laser is directed to the target located 1 km away (here we are considering the maximum distance for preliminary signal/noise ratio estimations). The target can be any surface, which scatters the light predominantly equally in all directions (Lambertian reflectance). Assuming 50% of diffuse reflection from the target surface, we expect nearly 10 nW of scattered optical power will be captured by the receiver with 10 cm diameter of the entrance aperture. Independently, 5% of the optical power from the seed source is taken as a heterodyne signal. After the optical attenuator, 30% of this signal is directed into one branch of a balanced detector. The second part of it (70%) is mixed with the signal from the optical receiver by 50/50 coupler (coupler 2 on Fig. 3), and 50% of the combined signal is directed to the second branch of the balanced detector. The first optical attenuator is used to decrease the heterodyne signal below the saturation level of the detector. The second optical attenuator is used to balance the signal level in two arms. Thus, the DC level of the signal will be removed, and the common-noise of the detectors will be effectively reduced (30 dB common mode rejection ratio for PDB210C, Thorlabs Inc.).

To adjust the system and locate the remote target, an electro-optical phase modulator (PhM on Fig. 4) is implemented after the first amplifier of the laser. At the first stage of alignment, the excitation laser will be switched off, and the phase of the detection laser will be modulated with the frequency close to the modulation frequency of the excitation laser (~1 kHz). It will create a heterodyne beating signal on the output of the balanced detector. The signal will be amplified by lock-in-amplifier, which is synchronized with the same frequency. Such a scheme will allow to find the remote target and make the fine adjustment of the receiver direction to obtain the highest signal level from the lock-in amplifier.

Additionally, the scheme allows finding the maximum detectable distance of the system as well as the minimum detectable phase shift of the light scattered from the

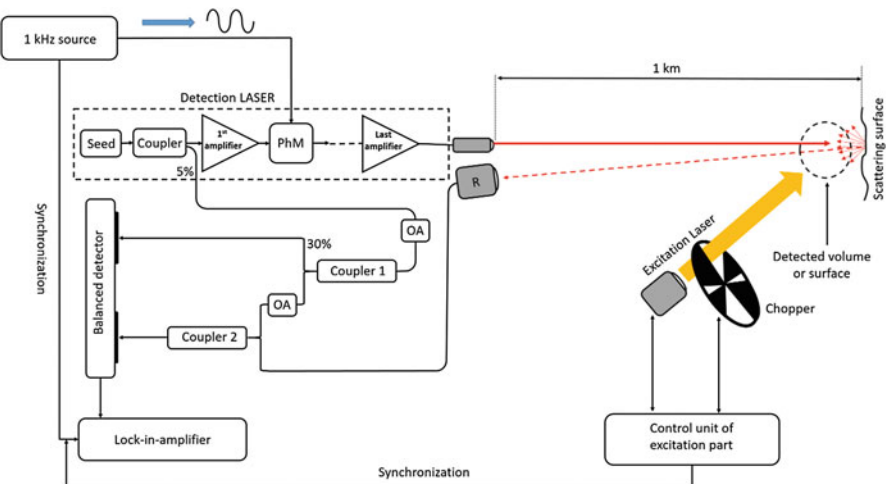
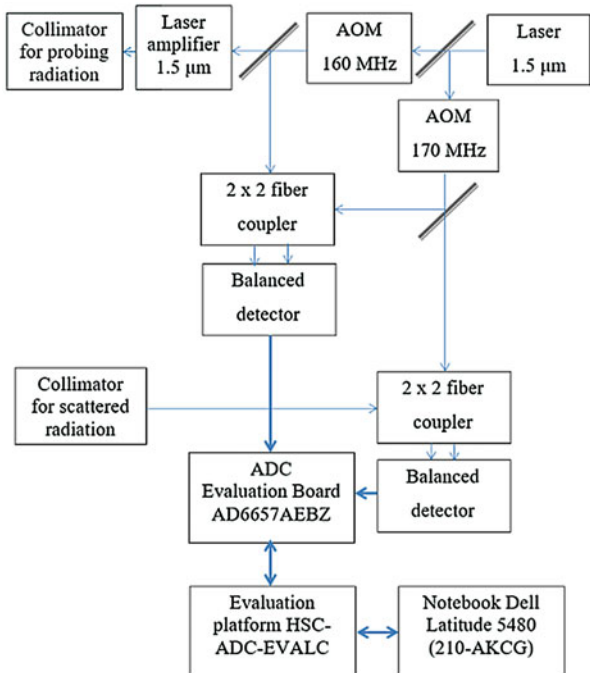


Fig. 3 Proposed LDV based photoacoustic spectroscopy detection system for explosives

Fig. 4 The general scheme of the remote vibrometer setup



target. Independently, the dependency of the detected signal (and signal to noise ratio) on the distance from the target, and the modulation phase shift will also provide the necessary data of applicability and limitations of the proposed laser for

remote vibrometry detection. Thus, the realization of internal heterodyne beating scheme of the laser-detection system by implementation of PhM inside of the laser will provide two essential functions. The first one is an investigation of the limitations of the system for different distances, target types and environmental conditions. The second one is the fine adjustment of the system (if necessary) every time for target identification.

After the preliminary adjustment is made, the PhM will be switched off, and the excitation laser will be turned on to the target, or to any volume on detection laser path, which is going to be investigated. The excitation laser beam is externally modulated, and the synchronization signal at the modulation frequency will be sent to the same Lock-in-Amplifier. If the searched chemical agent which has an absorption at the wavelength of the excitation laser is presented on the target surface or investigated volume, it will create vibration of the surface at modulation frequency, or periodical modulation of the refractive index of the air containing the agent, which finally will be converted to the output signal of lock-in-amplifier. By changing the wavelength of the excitation laser, it will be possible to record the absorption spectra of the investigated area, and identification of harmful or explosive contamination.

Alternatively, if the noise level of the electrical scheme of the PhM will be high, the detection scheme can be built by using two acousto-optical modulators (AOM), working at different frequencies. Because at frequencies higher than 40 MHz noise levels coming from amplification is much lower than the low-frequency regime [88]. In the modified system one of the AOMs will be placed instead of PhM in the signal arm, and the second one will be located in the heterodyne arm. After the mixing these two signals on balanced detector we will amplify the frequency difference signal (around 10 MHz) by lock-in-amplifier. The general scheme of this setup is shown in Fig. 4.

The signal received from the sample and heterodyne reference beams are formed with the acousto-optical shift of laser radiation frequency in the same direction by the frequencies F_s and F_h , respectively. As a result, the information signal, i.e., the photodetector current is a phase-modulated signal with carrier frequency. Digitization of this signal is made with an ADC (AD6657A). Separation of quadrature components, digital heterodyning, decimation and filtration are performed with an evaluation platform HSC-ADC-EVALC. Information on the phase value and rate of change, i.e., on scattering surface shift and velocity, is separated by calculating the modified function atan2 of the ratio between the in-phase and quadrature components of the phase-modulated signal.

Fiber Laser Development for Fiber Based LDV

Contemporary studies on fiber lasers caused a dramatic increase in its usefulness in various fields making the subject one of the most prominent research areas of modern science. In recent years developments lead a significant increase on the output power of fiber lasers, and increased power levels expanded their field of applications ranging from spectroscopy to material processing. Beyond their capacity to achieve high power, fiber lasers draw attention to themselves due to their robust and free of adjustment operation with high beam quality. They also offer high

conversion efficiencies and broad gain linewidths which allow ultrashort pulse operation. Another feature that distinguishes fiber lasers from other types of lasers is that all-fiber lasers are compact systems which have high resistance to variable ambient conditions and they do not require alignment of free-space components.

An important progress in optical fiber technology was the use of rare earth elements, such as Neodymium (Nd^{3+}), Erbium (Er^{3+}) or Ytterbium (Yb^{3+}), as the dopant in the core material. They have received considerable attention for having absorption and fluorescence transition in most of the visible and near-infrared region. Snitzer and Koester did the first experimental investigations of the rare earth doped fiber lasers which enabled high power operation in the early 1960s [36, 72, 73]. Since their first emergence, different active ions used for various applications. As an example, Erbium-doped fiber lasers which have output in the region of 1.5–1.6 μm wavelength, have been used for remote sensing of magnetic fields [37], and they used as the source for all-optical fiber-based communications systems [59].

Until very recently, Er-doped fiber amplifiers have lagged behind Yb-doped fiber amplifier systems in terms of power scaling because Er ions have low absorption cross sections and they have low efficiency at higher concentrations due to their aggregation. This problem was solved using Er-Yb co-doping method [82], in which pump energy is first absorbed by Yb ions and then transferred to Er ions. In 2007, a CW laser was reported in which 297 W optical power could be obtained from an Er-Yb co-doped fiber amplifier [34]. In the following years, other studies also have shown that better beam quality can be maintained [32, 33, 50].

In this project, 30 W detection laser is explicitly chosen to be completely fiber integrated and operating at 1.55 μm . The main reason for this choice is that lasers with 1.55 μm wavelength are at the eye-safe region and they are less sensitive to scattering on small particles in the air like fog or smoke compared to visible or 1 μm wavelength lasers. A general scheme of the designed laser system can be found in Fig. 5. As mentioned above, completely fiber integrated design will provide stable and robust operation, allowing usage of the laser outside of the lab at different environmental conditions, besides, better beam quality will provide the output beam to reach far away from the laser.

Broader Impacts

The results of the project will have a significant impact on two perspectives. Firstly, it will create know-how of really safely, the contact-free remote detection method for potentially dangerous chemicals and explosive materials, which is one of the top priorities for civil security. This know-how will be transferred to defense industry companies. Secondly, we expect the generation of critical scientific data which will result in several high impact publications. The revealed strengths and limitations of the system will create a background for future investigations and international

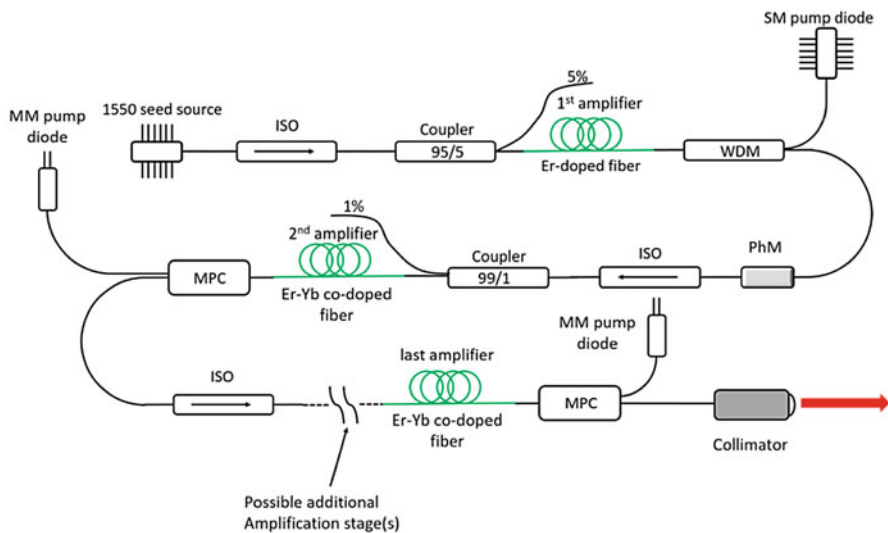


Fig. 5 The eye-safe fiber laser system to be developed for laser doppler vibrometer

project proposals. Besides, the obtained results from the project (including photo and video of real-time measurements) will be demonstrated on multiple international conferences and exhibitions.

Young Researcher Participation

There are currently three graduate students, and one postdoctoral researcher is working in the project, and the project will contribute to the thesis of the graduate students directly. The infrastructure provided by the project will also be useful for many new projects, academic papers and thesis indirectly.

Bibliography

1. Angel S et al. (1992) Remote-Raman spectroscopy at intermediate ranges using low-power cw lasers. *Appl Spectrosc* 46(7):1085–1091
2. Arnold MA, Meyerhoff ME (1988) Recent advances in the development and analytical applications of biosensing probes. *Crit Rev. Anal Chem* 20 (3):149–196
3. Babushok V et al. (2006) Double pulse laser ablation and plasma: Laser induced breakdown spectroscopy signal enhancement. *Spectrochim Acta B At Spectrosc* 61(9):999–1014
4. Bell AG (1880) ART. XXXIV.—On the Production and Reproduction of Sound by Light. *Am J Sci (1880–1910)* 20(118):305

5. Berden G et al. (2000) Cavity ring-down spectroscopy: Experimental schemes and applications. *Int Rev. Phys Chem* 19(4):565–607
6. Bohren A, Sigrist M (1997) Optical parametric oscillator based difference frequency laser source for photoacoustic trace gas spectroscopy in the 3 μm mid-IR range. *Infrared Phys Technol* 38(7):423–435
7. Bozóki Z et al. (2011) Photoacoustic instruments for practical applications: present, potentials, and future challenges. *Appl Spectrosc Rev.* 46(1):1–37
8. Carter JC et al. (2005a) Standoff detection of high explosive materials at 50 meters in ambient light conditions using a small Raman instrument. *Appl Spectrosc* 59(6):769–775
9. Carter JC et al. (2005b) Stand-off Raman detection using dispersive and tunable filter based systems. *Spectrochim Acta A Mol Biomol Spectrosc* 61 (10):2288–2298
10. Castellini P et al. (2006) Laser Doppler Vibrometry: Development of advanced solutions answering to technology's needs. *Mech Syst Signal Process* 20 (6):1265–1285
11. Caygill JS et al. (2012) Current trends in explosive detection techniques. *Talanta* 88:14–29
12. Choi J, Diebold G (1982) Laser schlieren microphone for optoacoustic spectroscopy. *Appl Opt* 21(22):4087–4091
13. Clark LC Jr., Lyons C (1962) Electrode systems for continuous monitoring in cardiovascular surgery. *Ann N Y Acad Sci* 102(1):29–45
14. Cooks RG et al. (2006) Ambient mass spectrometry. *Science* 311 (5767):1566–1570
15. De Lucia FC et al. (2003) Laser-induced breakdown spectroscopy analysis of energetic materials. *Appl Opt* 42(30):6148–6152
16. Dias A et al. (2014) Recent advances in bioprinting and applications for biosensing. *Biosensors* 4(2):111–136
17. Dubroca T et al. (2011) The limit of detection for explosives in spectroscopic differential reflectometry. *Chemical, Biological, Radiological, Nuclear, and Explosives (CBRNE) Sensing XII*, International Society for Optics and Photonics
18. Electronic Nose (2004). Retrieved April 01, 2019, from https://science.nasa.gov/science-news/science-at-nasa/2004/06oct_enose%20.
19. Elia A et al. (2009) Photoacoustic techniques for trace gas sensing based on semiconductor laser sources. *Sensors* 9(12):9616–9628
20. Erkol H et al. (2014) Photoacoustic radiation force on a microbubble. *Phys Rev. E* 90(2):023001
21. Ewing RG et al. (2001) A critical review of ion mobility spectrometry for the detection of explosives and explosive related compounds. *Talanta* 54 (3):515–529
22. Fereja TH et al. (2013) A recent review on chemiluminescence reaction, principle and application on pharmaceutical analysis. *Isrn Spectrosc* 2013

23. Fraga F et al. (2002) CCD readout of GEM-based neutron detectors. *Nucl Instrum Methods Phys Res Sec A: Accelerators, Spectrometers, Detectors and Associated Equipment* 478(1–2):357–361
24. Fu Y, et al. (2016) Standoff photoacoustic sensing of trace chemicals by laser Doppler vibrometer. *Chemical, Biological, Radiological, Nuclear, and Explosives (CBRNE) Sensing XVII*, International Society for Optics and Photonics.
25. Gut K et al. (2010) Sensitivity of Polarimetric Waveguide Interferometer for Different Wavelengths. *Acta Phys Pol A* 118(6)
26. Habib MK (2007) Controlled biological and biomimetic systems for landmine detection. *Biosens Bioelectron* 23(1):1–18
27. Hirschfeld T et al. (1973) Remote spectroscopic analysis of ppm-level air pollutants by Raman spectroscopy. *Appl Phys Lett* 22(1):38–40
28. Hofstetter D et al. (2001) Photoacoustic spectroscopy with quantum cascade distributed-feedback lasers. *Opt Lett* 26(12):887–889
29. Hu Q et al. (2016) Photo-vibrational spectroscopy of solid and liquid chemicals using laser Doppler vibrometer. *Opt Express* 24(17):19148–19,156
30. Hummel RE (2011) Electronic properties of materials, Springer Science & Business Media.
31. Jackson W, Amer NM (1980) Piezoelectric photoacoustic detection: theory and experiment. *J Appl Phys* 51(6):3343–3353
32. Jasapara J et al. (2008) Diffraction limited amplification of picosecond pulses in 1170 μm² effective area erbium fiber. *Opt Express* 16(23):18869–18,874
33. Jasapara JC et al. (2009) Diffraction-limited fundamental mode operation of core-pumped very-large-mode-area Er fiber amplifiers. *IEEE Journal of Selected Topics in Quantum Electronics* 15(1):3–11
34. Jeong Y et al. (2007) Erbium: ytterbium codoped large-core fiber laser with 297-W continuous-wave output power. *IEEE Journal of Selected Topics in Quantum Electronics* 13(3):573–579
35. Kerr EL, Atwood JG (1968) The laser illuminated absorptivity spectrophone: a method for measurement of weak absorptivity in gases at laser wavelengths. *Appl Opt* 7(5):915–921
36. Koester CJ, Snitzer E (1964) Amplification in a fiber laser. *Appl Opt* 3 (10):1182–1186
37. Koo KP et al. (1995) Fiber Bragg grating laser magnetometer. Conference on Lasers and Electro-Optics, Optical Society of America.
38. Kosterev A et al. (2008) Application of quantum cascade lasers to trace gas analysis. *Applied Physics B* 90(2):165–176
39. Kreuzer L (1971) Ultralow gas concentration infrared absorption spectroscopy. *J Appl Phys* 42(7):2934–2943
40. Kurup PU (2008) An electronic nose for detecting hazardous chemicals and explosives. 2008 IEEE Conference on Technologies for Homeland Security, IEEE
41. Kuznitsov A, Osetrov O (2006) Detection of improvised explosives and explosive devices in Detection and disposal improvised explosives. Springer

42. Lima J et al. (2006) Photoacoustic detection of NO₂ and N₂O using quantum cascade lasers. *Appl Phys B Lasers Opt* 85(2–3):279–284
43. Lopez-Moreno C et al. (2006) Test of a stand-off laser-induced breakdown spectroscopy sensor for the detection of explosive residues on solid surfaces. *J Anal Atom Spectrom* 21(1):55–60
44. Luft K (1943) Über eine neue Methode der registrierenden Gasanalyse mit Hilfe der Absorption ultraroter Strahlen ohne spektrale Zerlegung. *Z Tech Phys* 24:97–104
45. Lund N et al. (2003) JEM-X: The X-ray monitor aboard INTEGRAL. *Astron Astrophys* 411(1):L231–L238
46. Marín E (2010) Characteristic dimensions for heat transfer. *Latin-Am J Phys Edu* 4(1):56–60
47. McDevitt T, Vikram C (1997) An investigation of pseudovibration signals in dual beam laser vibrometry. *Rev. Sci Instrum* 68(4):1753–1755
48. McDonald FA, Wetsel GC Jr. (1978) Generalized theory of the photoacoustic effect. *J Appl Phys* 49(4):2313–2322
49. Mokalled L et al. (2014) Sensor review for trace detection of explosives. *Int J Sci Eng Res* 5(6):337–350
50. Morasse B et al. (2007) 10 W ASE-free single-mode high-power double-cladding Er 3+ -Yb 3+ amplifier. *Fiber Lasers IV: Technology, Systems, and Applications, International Society for Optics and Photonics*
51. Murugarajan A, Samuel G (2011) Measurement, modeling and evaluation of surface parameter using capacitive-sensor-based measurement system. *Metrol Measurem Syst* 18(3):403–418
52. Naal Z et al. (2002) Amperometric TNT biosensor based on the oriented immobilization of a nitroreductase maltose binding protein fusion. *Anal Chem* 74(1):140–148
53. Ngai A et al. (2006) Automatically tunable continuous-wave optical parametric oscillator for high-resolution spectroscopy and sensitive trace-gas detection. *Appl Phys B* 85(2–3):173–180
54. Paldus B et al. (1999) Photoacoustic spectroscopy using quantum-cascade lasers. *Opt Lett* 24(3):178–180
55. Patel C, Tam AC (1979) Optoacoustic spectroscopy of liquids. *Appl Phys Lett* 34(7):467–470
56. Patel C, Tam A (1981) Pulsed optoacoustic spectroscopy of condensed matter. *Rev. Mod Phys* 53(3):517
57. Patel C et al. (1974) Spectroscopic measurements of stratospheric nitric oxide and water vapor. *Science* 184(4142):1173–1176
58. Patil SJ et al. (2014) An ultra-sensitive piezoresistive polymer nano-composite microcantilever sensor electronic nose platform for explosive vapor detection. *Sensors Actuators B Chem* 192:444–451
59. Penzkofer A (1988) Solid state lasers. *Prog Quantum Electron* 12(4):291–427
60. Pfund A (1939) Atmospheric contamination. *Science* 90(2336):326–327
61. Preece WH (1881) I. On the conversion of radiant energy into sonorous vibrations. *Proc R Soc Lond* 31(206–211):506–520

62. Rayleigh L (1881) The photophone. *Nature* 23(586):274–275
63. Rosencwaig A, Gersho A (1976) Theory of the photoacoustic effect with solids. *J Appl Phys* 47(1):64–69
64. Rothberg S (2006) Numerical simulation of speckle noise in laser vibrometry. *Appl Opt* 45(19):4523–4533
65. Rothberg S et al. (1989) Laser vibrometry: pseudo-vibrations
66. Rothberg S et al. (2017) An international review of laser Doppler vibrometry: Making light work of vibration measurement. *Opt Lasers Eng* 99:11–22
67. Schilt S et al. (2009) Performance evaluation of a near infrared QEPAS based ethylene sensor. *Applied Physics B* 95(4):813–824
68. Sharma SK et al. (2003) Stand-off Raman spectroscopic detection of minerals on planetary surfaces. *Spectrochim Acta A Mol Biomol Spectrosc* 59 (10):2391–2407
69. Sharpe S et al. (1998) High-resolution (Doppler-limited) spectroscopy using quantum-cascade distributed-feedback lasers. *Opt Lett* 23(17):1396–1398
70. Sharpe SW et al. (2004) Gas-phase databases for quantitative infrared spectroscopy. *Appl Spectrosc* 58(12):1452–1461
71. Shiina T (2011) Optical design and development of near range compact lidar. 2011 Asia Communications and Photonics Conference and Exhibition (ACP), IEEE
72. Snitzer E (1961a) Optical maser action of Nd + 3 in a barium crown glass. *Phys Rev. Lett* 7(12):444
73. Snitzer E (1961b) Proposed fiber cavities for optical masers. *J Appl Phys* 32 (1):36–39
74. Spagnolo V et al. (2010) NO trace gas sensor based on quartz-enhanced photoacoustic spectroscopy and external cavity quantum cascade laser. *Applied Physics B* 100(1):125–130
75. Spagnolo V et al. (2012) Part-per-trillion level SF 6 detection using a quartz enhanced photoacoustic spectroscopy-based sensor with single-mode fiber-coupled quantum cascade laser excitation. *Opt Lett* 37(21):4461–4463
76. Stitzel SE et al. (2001) Array-to-array transfer of an artificial nose classifier. *Anal Chem* 73(21):5266–5271
77. Van Herpen M et al. (2002) Wide single-mode tuning of a 3.0–3.8- μm , 700-mW, continuous-wave Nd: YAG-pumped optical parametric oscillator based on periodically poled lithium niobate. *Opt Lett* 27(8):640–642
78. Van Herpen M et al. (2006) Optical parametric oscillator-based photoacoustic detection of CO 2 at 4.23 μm allows real-time monitoring of the respiration of small insects. *Applied Physics B* 82(4):665–669
79. Vandebaele P et al. (2007) Comparative study of mobile Raman instrumentation for art analysis. *Anal Chim Acta* 588(1):108–116
80. Veingerov M (1938) Eine Methode der Gasanalyse beruhend auf dem optisch-akustischen Tyndall-. Röntgeneffekt. *Dokl. Akad. Nauk SSSR*
81. Veingerov M (1946) Comp. Rend Acad Sci URSS 51:195
82. Vienne GG et al. (1998) Fabrication and characterization of Yb3+: Er3+ phosphosilicate fibers for lasers. *J Lightwave Technol* 16(11):1990

83. Wallin S et al. (2009) Laser-based standoff detection of explosives: a critical review. *Anal Bioanal Chem* 395(2):259–274
84. Wang LV (2008a) Prospects of photoacoustic tomography. *Med Phys* 35 (12):5758–5767
85. Wang LV (2008b) Tutorial on photoacoustic microscopy and computed tomography. *IEEE J Sel Top Quantum Electron* 14(1):171–179
86. Wang LV, Hu S (2012) Photoacoustic tomography: in vivo imaging from organelles to organs. *Science* 335(6075):1458–1462
87. Wang C-C et al. (2009) High sensitivity pulsed laser vibrometer and its application as a laser microphone. *Appl Phys Lett* 94(5):051112
88. Waz A et al. (2009) Laser–fibre vibrometry at 1550 nm. *Meas Sci Technol* 20 (10):105301
89. Wilson R et al. (2003) Paramagnetic bead based enzyme electrochemiluminescence immunoassay for TNT. *J Electroanal Chem* 557:109–118
90. Yang X et al. (2009) Nanoparticles for photoacoustic imaging. *Wiley Interdiscip Rev Nanomed Nanobiotechnol* 1(4):360–368

Multi-Year Project: Project Title

Dušan Gleich (✉)

University of Maribor, Maribor, Slovenia

e-mail: dusan.gleich@um.si

Venceslav Kafedziski

Faculty of Electrical Engineering and Information Technologies, Ss Cyril and Methodius University in Skopje, Skopje, Republic of Macedonia

e-mail: kafedzi@feit.ukim.edu.mk

Emir Skejić

University of Tuzla, Tuzla, Bosnia and Herzegovina

e-mail: Emir.skejic@untz.ba

Project Goals

Explain in Lay-Person Terms the Objectives of the Project

Landmines are made of metal or plastic, and there are many existing detection techniques for landmine detection. Some techniques have a disadvantage in that they cannot detect plastic landmines, but only metal ones. With the use of electromagnetic radiation (EM) and by using appropriate wavelengths, a signal can

penetrate the ground surface and reflect off an item with a different dielectric constant or conductivity. These properties are also valid for explosives inside a plastic housing.

This project deals with methods and strategies for land mine detection using a hexacopter. The goal is to develop a low-cost and light weight ground penetrating radar using standard radio frequency components. There exist two broadly approaches, one in the time domain and one in the frequency domain. The first one requires a pulse with a short duration, typically a few hundred ps. The other approach, which is easier to implement, is to observe the amplitude and phase change between the transmitted and the received signals. The developed radar will be attached to the hexacopter and a graphical user interface will be developed to localize detected landmines in graphical or GPS coordinates. Since the signatures produced in the radar images from reflections off objects usually have hyperbolic shapes, we develop methods for localization based on hyperbola detection and its vertex determination. Also, we use methods based on machine learning using deep neural networks for object detection, localization and classification.

This paper presents radar development principles, the generation and detection of radar signals and radar signal processing, and image processing and pattern recognition of the obtained image scans.

Deliverables

Explain the Tangible Products of the Project – Entire System and Components
The system for landmine detection consists of 4 major components: (a) hexacopter, which is called a small Unmanned Aircraft System (sUAS), or drone, which is used for moving the radar platform over the landmines, (b) a remote controller, which controls the drone and radar system, (c) ground penetrating radar, which consists of microwave circuits for transmitting and receiving electromagnetic waves and (d) batteries, which represent the heaviest part of the system. The weight of the payload drastically influences the drone autonomy; therefore, the goal is to design a light-weight and low-cost system for landmine detection. The data produced by the ground penetrating radar must be analysed to automatically detect landmines. This research is focused on developing new methods for landmine detection using new hardware and software solutions.

The specific deliverables of the project are:

- A ground penetrating radar attached to a hexacopter
- Software for landmine detection, localization, and classification

The scientific approaches to development of the ground penetrating radar are:

- Development of a stepped frequency radar
- Development of an impulse (UWB) radar

- Development of a random frequency stepped frequency radar with compressive sampling

The scientific approaches to landmine detection, localization and classification are

- Hyperbola detection with its vertex determination

Machine learning approaches for detection and classification.

Security Relevance

The topic of the proposal is linked to the “Mine and UXO Detection and Clearance” objective in the SPS Key Priorities. The development of radar-based device for automatic landmine detection addresses directly the SPS Key Priorities. The development of such radar results in the following improvements:

- The objective is to make land mine detection faster, easier, and more efficient. Current systems can move with velocity of 3 km/h. The goal is to develop a platform which can move at a velocity above 15 km/h and cover a 3 m wide area in the range direction
- The use of compressed sensing within the process of radar techniques enables faster data acquisition
- Automatic landmine detection is an objective of this proposal. The development of land mine detection using acquired radar data is based on analysing the radar profiles. These profiles can be analysed after the electromagnetic waves reflect off the buried object, and arrive at the receive antenna. Since the goal is to develop fast detection, in the process of reconstruction compressed sensing techniques will be used to achieve faster reconstructions using only a few samples.

Mine detection is of enormous relevance to protect people and prevent any contact with landmines to prevent injuries. Although numerous techniques for mine detection exist, each of them suffers from some disadvantage. Some of them, such as manual detection, pose a danger to the human operator. Recently, armoured demining vehicles that are remotely controlled have been used for both detection and demining. However, using a drone mounted GPR has advantages over all the other techniques of land mine detection, since it avoids inflicting casualties and/or damage to the vehicle that moves on the ground surface. It also enables access to rough terrain, and terrain covered with vegetation. Mine classification, which we also address in this project, is very important, since knowing the type of mine buried in the ground, could provide information on choosing a suitable method of demining. Using modern methods of machine learning, such as Deep Convolutional Neural Networks, could facilitate landmine detection and classification. The achievements of this project could be used in other areas which require the use of drones, radar design knowledge, and knowledge of machine learning techniques for classification.

Science Relevance

Explain How This Project Advances the “Science Pillar” of NATO SPS

The proposed project is hardware and software oriented. The hardware will be developed using standard components. It is known that a GPR system is very expensive, so our goal is to propose a low-cost solution and make the principles of the solution on a web site, so that the end users can reproduce the experiments.

Besides the hardware development, some new methods for real-time landmine detection are under investigation. Compressed sensing methods, which can recover the original signal using fewer samples than the theoretical bound, are intensively researched. These methods will enable landmine detection using real-time acquisitions.

The project proposes a device which works in 2 modes. The first mode is a classical GPR technique which is widely used in GPR. The second mode, compressed sensing stepped frequency radar, is a novel technique which uses a set of different random generated frequencies. The advantage of this method over the other is that it is able to detect objects using a multi-frequency approach, which differently characterizes targets and helps to make the detection of buried objects more reliable.

The synthetic aperture radar (SAR) technique is a radar-based technique which uses a moving platform in order to simulate a synthetic aperture. This technique introduces three dimensional approaches to monitoring subsurface targets. The advantage of this technique is that it monitors not just a single subsurface point but a wider area. The goal of the project is to capture a 3 m wide area using a flying device, the hexacopter, which will be able to move at a constant velocity. The SAR techniques improve landmine and object visibility within the radargram.

The second part of the project aims to automatically detect buried mines. Mine detection techniques based on radar data analysis will be developed using our proposed radar implementations, where buried objects are detected using hyperbola detection or pattern recognition tools, such as Deep Convolutional Neural Networks (CNN). Hyperbola detection can be done using the Hough transform, after a suitable pre-processing of the obtained images from the GPR. Deep CNN offers additional possibilities to do object classification, i.e. to distinguish between landmines and other objects, or to distinguish between anti-personnel and anti-tank mines, or as a goal of classifying different types of mines in different classes. Classifying the detected landmines would enable us to undertake an appropriate and convenient demining approach.

As can be seen, this project includes many hardware and software-oriented activities which use the most advanced modern scientific achievements, such as advanced hardware implementation techniques, compressive sampling, advanced methods of image processing, and advanced classification techniques using the most recent implementations of deep neural networks.

Partnership Relevance

Explain How This Project Advances the “Partnership Pillar” of NATO SPS

The partnership between Macedonian, Bosnian, and Slovenian universities has intensified in terms of knowledge transfer and enabling performance of real live experiments using developed hardware. All participating universities do not have regular funding for purchasing equipment, so this project provided the necessary infrastructure for radar implementation and enabled knowledge transfer between researchers and institutions using good practices.

The project is multidisciplinary, and included theoretical studies, hardware design aspects, software simulations, and signal processing and pattern recognition techniques. Therefore, the exchange of knowledge and experience in all these fields among the partners is of crucial importance, especially when they have complementary expertise in some areas. Although the partners have sometimes developed their own approaches to some of the problems in their area of expertise, the exchange of the acquired experience during that process is of great benefit to all of them. The integration of all the developed approaches and techniques must be realized during the final year of the project to produce the final deliverables.

End Users

Who Are the End Users for the Project Deliverables, and How Will They Use Them?

End users will be actively involved in the project by providing useful feedback to the developers of the ground penetrating radar. The end users will test the developed device in real environment and provide information about detection accuracy and device handling. The vegetation impact on the detection will also be evaluated by the end users.

The end users will advise developers on how to design the system for landmine detection and they will be actively involved in the device development, providing experience in landmine detection.

The initial hardware will be tested in the HCR Center for testing, development and training (CTRO) in Croatia, where a polygon with real landmines is available. The Bosnian Demining Center will be responsible for hardware testing. The Slovenian ITF Enhancing Human Security has been advising and providing good practices to the project group in terms of knowledge transfer regarding landmine demining.

The hardware platform will be offered to the Bosnia and Herzegovina Mine Action Centre to test, improve and use the proposed system.

Technical Summary

Describe the Scientific or Engineering Approach, Identifying the Main Questions or Problems, and Their Solutions. Please Append Several Graphs or Figures, with Captions

The first part of this section presents two methods for landmine detection. The first one uses properties of the frequency domain and describes the implementation of a Stepped Frequency Continuous Wave (SFCW) radar, while the second method describes the implementation of an impulse radar within the time domain and presents the designs of the transmitter and the receiver. The second part of this section describes the software defined radio (SDR) implementation of the SFCW radar, the compressive sampling version of that radar, and the signal processing approaches to automatic landmine detection.

Stepped Frequency Continuous Wave (SFCW) Radar

Stepped Frequency Continuous Wave (SFCW) radar is a system which transmits electromagnetic radiation by increasing the frequency over a chosen band with fixed steps. SFCW radar systems are based either on the homodyne or super-heterodyne architecture. The homodyne architecture is simpler, with only a single frequency down conversion, while the super-heterodyne performs two frequency down conversions to produce the base-band signal. The super-heterodyne architecture gives better performance. Here we first focus on the homodyne architecture, and then we present the implementation of the super-heterodyne structure.

Landmine detection represents a globally challenging task because of the material mines are made of and because of their small sizes. Landmines are made of metal or plastic, and there are many known detection principles or methods, some of which include the use of animals (e.g. dogs, rats, bees). Many of the methods have the disadvantage that they cannot detect plastic landmines, only metal. With the use of microwave electromagnetic (EM) radiation, this is not the case, because by selecting suitable wavelengths, the signal can penetrate through the ground surface and reflect off items with dielectric constant or conductivity different from those of the ground soil. This also includes the explosive material which is inside the plastic landmines. This method for analysing objects below the ground surface has been used for decades and is known as Ground Penetrating Radar (GPR). However, commercial solutions of GPR radars are large and require contact with the ground surface – ground coupled GPR systems. Using experimental results with Vector Network Analyzer (VNA), the radar parameters can be estimated and then used for implementation on a small sized Printed Circuit Board (PCB) with the use of standard integrated circuits (IC). The purpose of reducing the radar size and non-ground coupled measuring gives us the possibility of mounting the system on a small Unmanned Aircraft System (sUAS), which could be remotely controlled from a safe distance and without direct contact with the investigated surface. Many people are placed at risk and hurt during the landmine detection process, while this solution would avoid this.

There are many kinds of landmines present, but we can broadly divide them into anti-personnel (AP) landmines and anti-tank (AT) landmines. They differ in size and in the amount of explosive inside. Because of their smaller size, the AP landmines are more challenging to detect than the AT landmines. Therefore, in this section the focus is mainly on detecting AP landmines. As mentioned, commercial GPR radars are well known and are based either on the time-domain or the frequency domain architecture. Within the time domain architecture-based radar, the best known is the impulse radar. The basic working principle is very straightforward. Here the time delay between the transmitted and received pulse, which is directly proportional to the target distance, is measured. However, it has many disadvantages that could affect our suggested system. For suitable resolution and penetration depth, the impulse radar must generate pulses of width less than 1 ns and amplitudes of few volts or more to achieve a suitable resolution and penetration depth. Also the receiving part of this kind of radar influences the resolution and has to therefore use an ADC with sample rate of at least few gigasamples per seconds. Therefore, additional hardware is needed to collect the large amount of data, which makes the whole design more complex, large, and expensive. Frequency domain radars do not need high speed analogue to digital converters because the signal is down-converted to a lower Intermediate Frequency (IF), which makes IC design simpler and smaller in size. Therefore, this work proposes using the Stepped Frequency Continuous Wave (SFCW) radar, which is a subcategory of frequency domain radars.

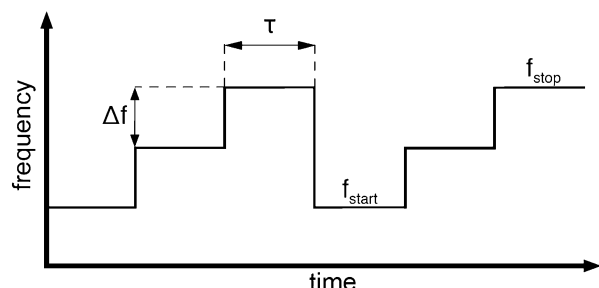
The SFCW radar is a system which transmits electromagnetic radiation with increasing frequency over a chosen band with fixed steps, as is shown in Fig. 1. The frequency at a given step n is switched after time τ and can be expressed as

$$f_n = f_0 + n\Delta f, n = 0, 1, 2, \dots, N - 1 \quad (1)$$

where f_0 is the starting frequency, Δf is the frequency step size, N is the number of steps in one measurement and limits the step number between 0 and $N-1$. The time τN represents one burst and repeats continuously. The SFCW Radar bandwidth is defined as

$$B = N\Delta f \quad (2)$$

Fig. 1 Basic working principle of SFCW Radar



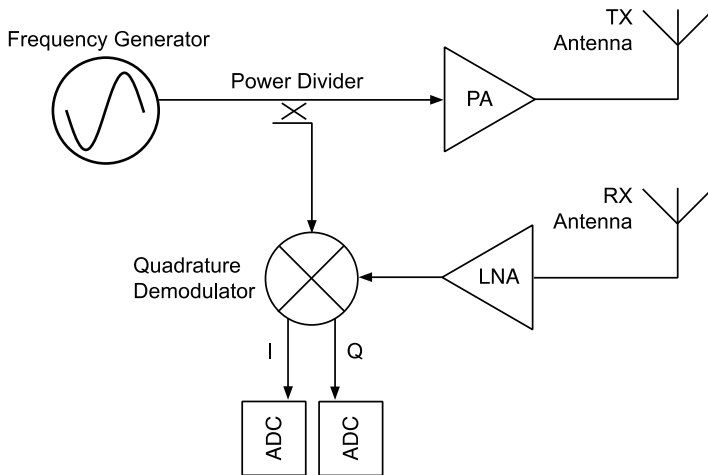


Fig. 2 Basic working principle of VNA

and the range resolution $\Delta R = c/(2B)$ is inversely proportional to B , where c is the speed of light. The maximum radar range is given by $R_{\max} = N\Delta R$, which means that at fixed B , N must be increased to increase the maximum range.

SFCW radar systems are based either on the homodyne or super-heterodyne architecture. The homodyne architecture is simpler, with a single down-conversion, while the super-heterodyne performs two down-conversions to produce the baseband signal. The super-heterodyne architecture gives better performance, but the homodyne architecture is usually integrated within the Vector Network Analysers (VNA). Figure 2 shows the basic block diagram of the VNA.

Frequency hopping is performed in the frequency generator block, which has two outputs. The signal from the first output is amplified through a Power Amplifier (PA) and transmitted through a Tx antenna. If a target is present, the signal will be back-scattered and collected by the Rx antenna, where the signal is then amplified through a Low noise Amplifier (LNA). The output of the LNA is mixed in a Quadrature Mixer with the second output of the RF generator. These two signals are equal in frequency, but the received signal has a different amplitude and phase shift because of the time it has travelled to the target and back. We also get this result from the Quadrature Mixer, where the In-phase (I) and Quadrature (Q) magnitude and phase signals are obtained. To determine the target distance for each transmitted frequency, the quadrature signal must be collected and is called the range bin. The collected bins of magnitude and phase are now represented in the frequency domain with discrete steps. To obtain the target distance, an Inverse Discrete Fourier Transform (IDFT) must be performed to transform the data into the time domain. For the described measurement method, we considered that an A-scan is obtained, and the radar is static. However, this is not useful for practical use where a B-scan GPR image is created. Here the SFCW radar has a disadvantage compared to the

pulse radar because it must be at the same location during the burst duration interval, which lasts $T = N\tau$. Also, other conditions must be considered that can cause aliasing of the target. The pulse width and frequency step must be related according to $\Delta f < 1/\tau$, and the pulse repetition interval must be several times longer than the pulse width.

EM radiation with lower frequencies can reach higher distances and penetrate deeper into the medium. For GPR Radars, the value of f_0 is usually between 100 MHz and 500 MHz, but at the same time the bandwidth B should be large enough to achieve good range resolution. Different scenarios were simulated to prove this concept. The goal was to use parameters which could also be used in real measurements and not be restricted by hardware limitations, which are caused mostly by the antenna and amplifier bandwidth. The simulation scenario has included two close targets, the number of steps does not exceed $N = 100$, and the frequency has been set in the range 400 MHz – 3 GHz, where the bandwidth was not lower than 1.5 GHz. The reason for keeping N low is because the maximal unambiguous range should only be a few meters, thereby keeping the measurement time low. A sine wave signal was generated with fixed steps. Next the original signal was delayed for two targets which differ in range by $\Delta R_{\text{diff}} = 5 \text{ cm}$. The purpose of simulating two targets close to each other is to determine the minimum bandwidth such that they can still be distinguished as separate. In a real scenario this would represent a landmine which is very close to the ground surface. The delayed signal was then multiplied with the original signal to implement quadrature demodulation.

To generate the spatial domain signal for the range profile, IDFT is performed. Figure 3 was obtained using the following parameters: $f_{\text{start}} = 700 \text{ MHz}$, $B = 2 \text{ GHz}$,

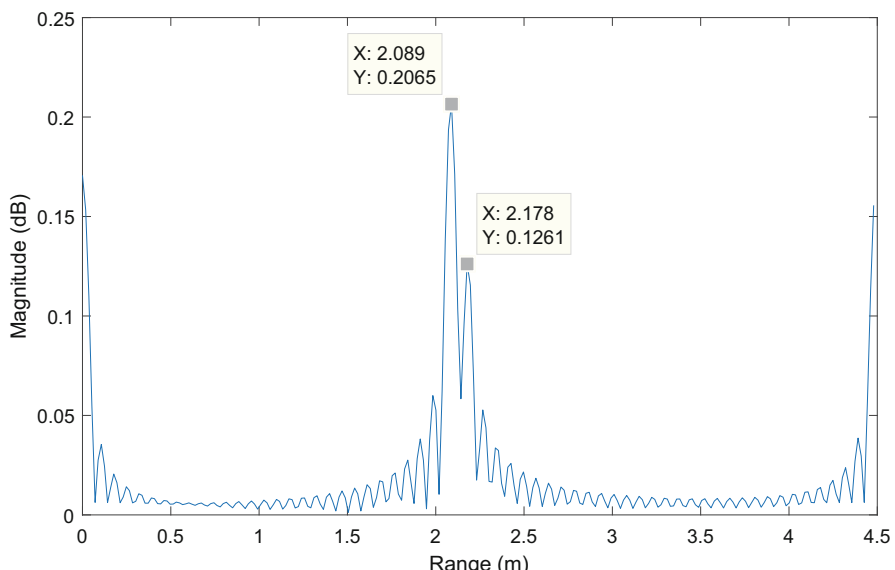


Fig. 3 Simulated SFCW Radar range profile of two targets separated by 5 cm

$N = 60$. The signal was zero-padded with $N_{padd} = 254$ before the IDFT was performed to obtain a longer resulting vector and a smoother range plot. The simulation results show that the two objects can be separated even when they are very close to each other.

The simulations of the SFCW Radar gave us rough information about the parameters and limitations that should be considered. The most critical hardware part is the bandwidth of the antenna and amplifier. It is challenging to design an antenna which has a bandwidth >2 GHz and a low frequency limit below 500 MHz. Amplifiers that must be used on the transmitting and receiving side must be chosen carefully because they are also limited in bandwidth at lower frequencies. The switchable frequency generator can be realized using different multifunctional RF equipment. It is possible to use Software Defined Radios (SDR) as described in [1–2], or a VNA whose basic functionality equals the SFCW method [3–4]. A VNA can usually perform faster frequency switching and has also wider bandwidth, so we have chosen to use the Agilent E5063A ENA VNA as a frequency generator. This equipment can sweep from 100 kHz up to 6.5 GHz, with a maximum of 200 steps and output power of 0 dBm. The output power of the VNA is not enough to penetrate through the ground soil. Therefore, we use a Mini-Circuits ZHL-4240 W+ PA, with an operating frequency from 10 MHz up to 4.2 GHz with 39 dB of gain. This PA has an appropriate bandwidth suitable for a GPR system, with output power up to 37 dBm. The signal is then transmitted over a custom built UWB horn antenna [5], shown in Fig. 4 (left). The proposed SFCW radar system should be air-coupled, meaning that the antenna impedance should be well matched with the air impedance. The radar system impedance is matched to 50Ω , while the impedance of air Z_0 is

$$Z_0 = \sqrt{\mu_0/\epsilon_0} = 377 \Omega \quad (3)$$

Because there is a great difference in the impedance, the antenna must be carefully designed to transmit the EM radiation through the whole frequency band with as little backscattering as possible. The relevant parameters are described as the scattering parameters, or S-parameters, where the S11 parameters are most important

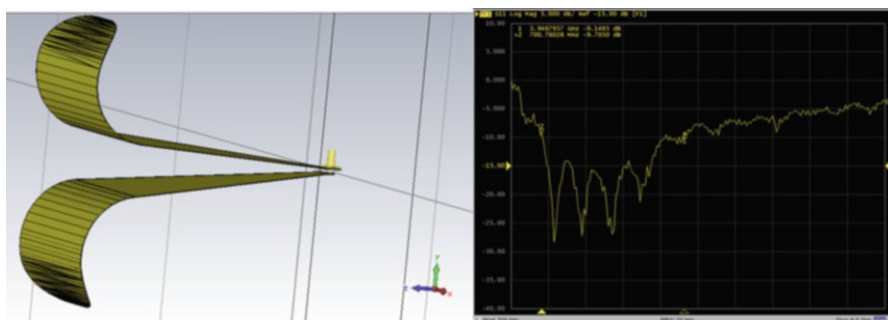


Fig. 4 (Left) UWB horn antenna [5] and (right) the measured magnitude of scattering parameter S11 versus frequency graph. The antenna height was 20 cm

for the antenna. The measured S11 parameter of the developed antenna is shown in Fig. 4 (right). The antenna is suitable for the specific frequency band if the magnitude value is below -10 dB. This confirms that the antenna we built can be used in a frequency range from 700 MHz up to 6 GHz. One critical point occurs at 1.3 GHz, but this should not affect the performance drastically.

The transmitting and receiving antennas were the same. The signal travels through different materials which have different dielectric constants. This means that the signal is highly attenuated and needs to be amplified before the demodulation. A Mini-Circuits Gali-55+ amplifier which operates in the range from DC – 4 GHz with gain of around 20 dB was used for that purpose. The signal is then down-converted in the quadrature demodulator. The output is sampled with a dual ADC to obtain the phase and magnitude. Data are further processed with Matlab Software, where the B-Scan GPR image is also created.

Experimental Results Using Homodyne Realization of GPR with VNA

To obtain experimental results, an AP landmine was buried into a polygon of size $3\text{ m} \times 2\text{ m} \times 1.5\text{ m}$ and filled with mixed soil. The mixed soil contained rocks, and the rock diameter did not exceed 1 cm. The AP landmine size was $5 \times 5\text{ cm}$ and was buried at a fixed position 40 cm from the polygon edge and 25 cm deep. Several B-scans were performed, where the antenna distance from the ground was varied between 5 cm and 1 m. As expected, the best result was achieved with lower antenna distances. The maximum antenna height, where the target was still recognizable, was 20 cm, with more details about the parameters shown in Table 1. Figure 5 shows the processed GPR image where strong reflected signals are of darker colour. The references are marked with lines, where cross-sections of blue lines indicate the actual landmine position and the green line indicates the ground surface. The results show that the surface and the landmine are clearly recognizable. The backscattered signal from the AP landmine is already present before the antenna is above it. This is because the antenna has a wide radiation pattern. This could be resolved with use of additional focusing algorithms.

The simulation and implementation of a SFCW Radar have been presented. The results have shown that an air-coupled GPR system can be implemented with use of a VNA. However, hardware parameters must be chosen carefully. It was shown that with specific parameters a buried AP landmine can be detected. The penetration depth is primarily affected by the frequency range and output power of the radar system. The experimental results have shown that the maximum antenna height is about 20 cm for our system to successfully detect a landmine. This could be improved by choosing a PA with higher gain, with the caveat that this would

Table 1 Experimental parameters

Parameter	Value
f_{start}	700 MHz
B	2.5 GHz
N	100
Antenna height	20 cm

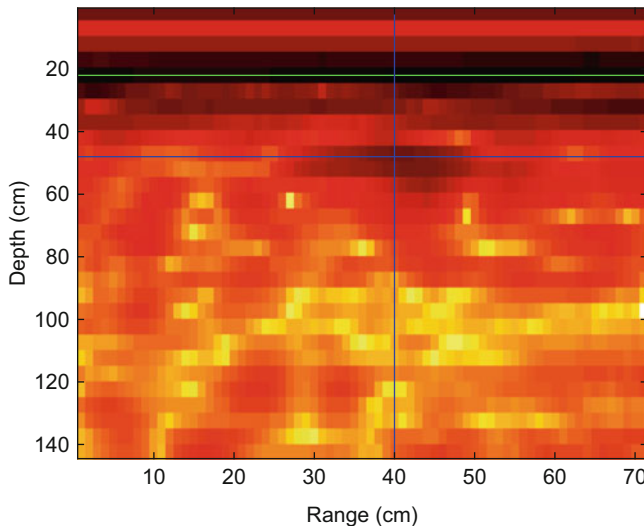


Fig. 5 GPR image obtained from measurement, where cross section of blue lines represents the buried AP landmine, and green line indicates the ground surface

make the radar system heavier and would have a deleterious impact on the size and weight.

Hardware Design of Transmitter and Receiver Using a Super-Heterodyne Structure

We have designed a new platform for CW radar, based on a super-heterodyne structure to reduce target aliasing and quadrature noise. We have used a low noise level amplifier at the receiver side, which has the consequence of SNR improvement with use of an external ADC. Additionally, the FPGA was used for digital quadrature mixing and on-board signal filtering. The results can be stored to an on-board SD card or transferred to a host computer. Figure 2 depicts the homodyne structure of the radar, and Fig. 6 depicts the super-heterodyne structure of the radar. They differ in the receiver part, since different up and down conversion frequencies are used for all generated signals. This structure was implemented, and the details are depicted in Fig. 7. The realization of the hardware is shown in Fig. 8.

Calibration

The designed radar was calibrated using 4 subsequent measurements. The radar responses were captured, and the response was normalized using those measurements. Figure 9 shows the calibration results using a 1 m long wire connected between the Tx output and Rx input of the radar. In Fig. 9 (middle and right) the averages of the amplitudes and phases of the received signals and the standard deviation of 4 subsequent measurements are shown. They confirm that the phase and amplitude are stable.

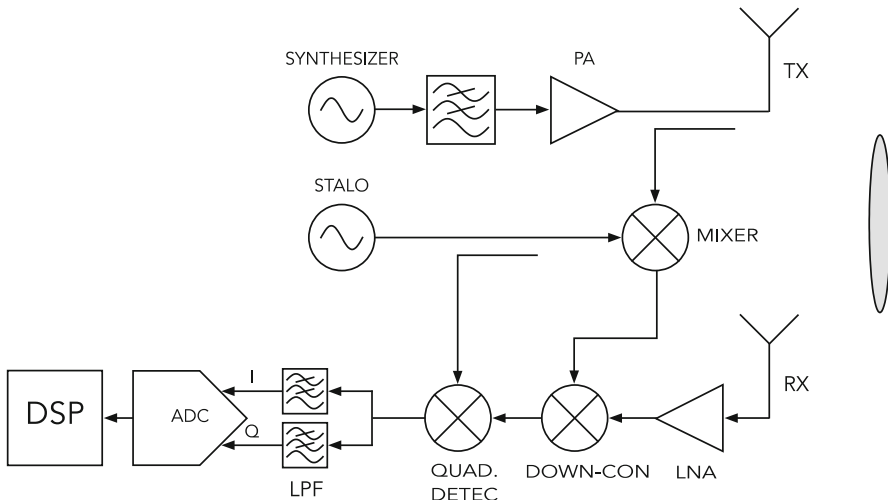


Fig. 6 A block diagram of the super-heterodyne stepped frequency radar

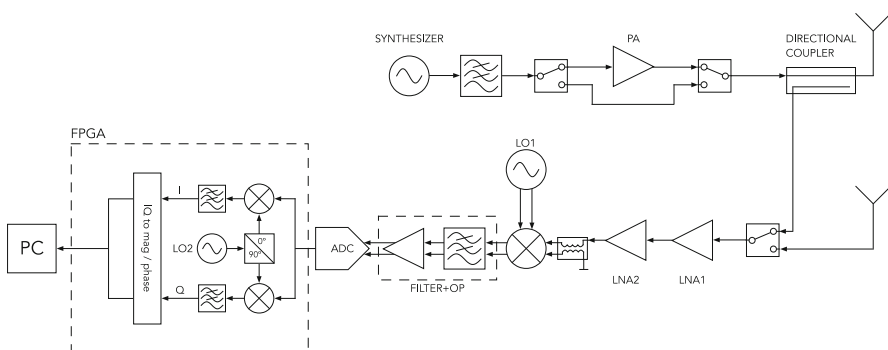


Fig. 7 Block diagram of the custom designed super-heterodyne structure SFCW radar



Fig. 8 Developed SFCW radar system

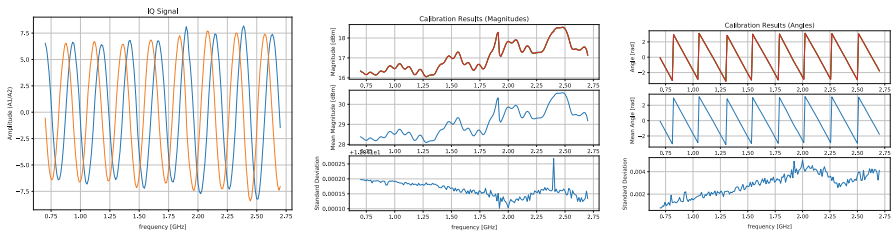


Fig. 9 Calibration. (left) Obtained quadrature data with 1 m long cable connected between Tx and Rx port. (middle) Magnitude variations of the radar system and the standard deviation of 4 subsequent measurements. (right) Phase and standard deviation of 4 subsequent measurements

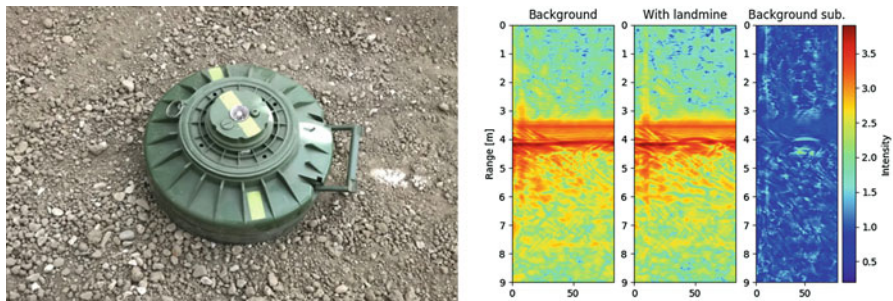


Fig. 10 B-scan of an AT landmine above ground surface. The landmine diameter is 27 cm and the height is 13 cm

Experimental Results

The radar was tested in a laboratory environment. The same laboratory environment was used as in the previous example: a landmine was buried into a polygon of size 3 m x 2 m x 1.5 m, and the AP landmine was buried 25 cm below surface. The radar platform was moved continuously over the polygon. Figures 10 and 11 show landmines and responses of received signals using B-scan. Figures 10 (right) and 6.11 (right) show radargrams without a landmine, with a landmine, and with background removal. The experimental results clearly show that the landmine can be detected.

Time Domain Radar

The Ultra-Wide Band (UWB) radar is based on a picosecond pulse generator. Ultra-short pulses can be achieved with Step-Recovery Diodes (SRD). In the ON state the SRD diode behaves as an ordinary signal diode. A positive signal i_f passes through the diode in the forward regime. When signal changes polarity from positive to negative, an ordinary diode switches off. SRD stores charge in the forward regime, and when signal changes polarity, the SRD does not switch off immediately due to

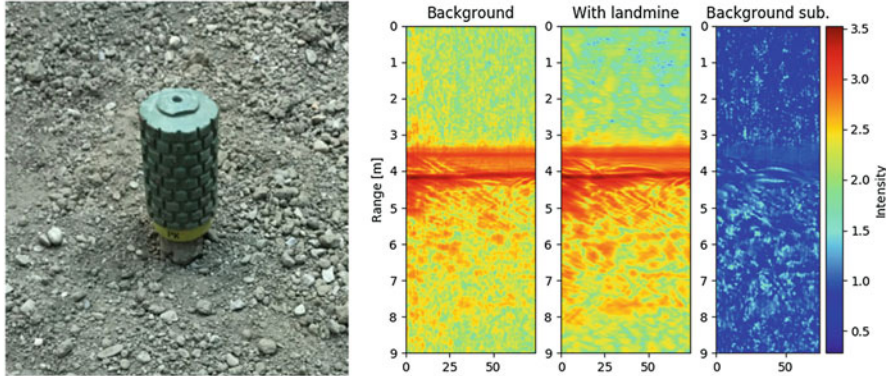
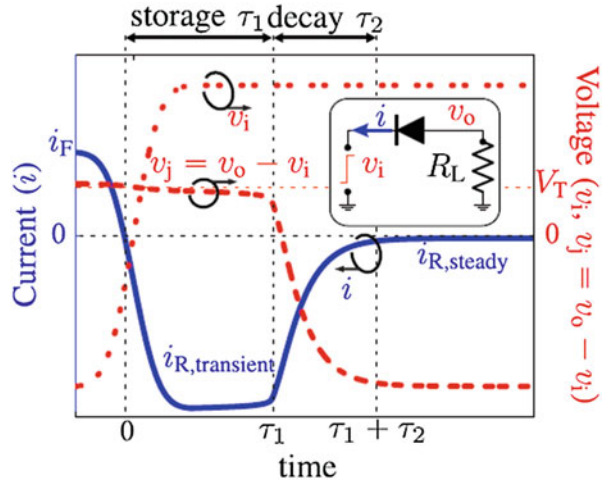


Fig. 11 B-scan of an AP landmine above ground surface. The landmine diameter is 7 cm and the height is 17 cm

Fig. 12 Forward current i_F (blue solid curve) and junction voltage v_j (red dashed curve) in response to a step voltage v_i (red dotted curve) from the forward to the reverse regimes



the stored charge. Near the end of the storage phase, the PN junction increases the resistance and finally switches off the junction during the decay time, which is extremely short. The switch off phase is of the order of picoseconds for an SRD. Fig. 12 shows the SRD in storage, the decay and the off regime when a step excitation signal is applied [9].

Many designs of pulse generator using SRD have been reported in the literature. The most common design is using a single step recovery diode to generate a pulse with a picosecond rising edge which destructively interferes with an opposite-polarity delayed replica of it produced by a short-circuited stub. The pulse width is equal to the round-trip time along the stub. The stub configuration suffers from spurious reflections, which produce ringing tails in the output signal. We designed a

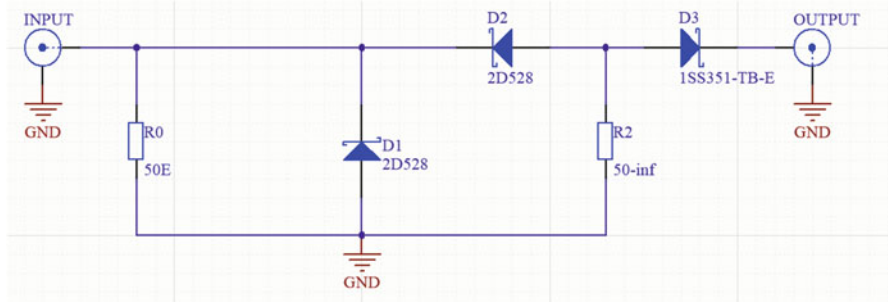
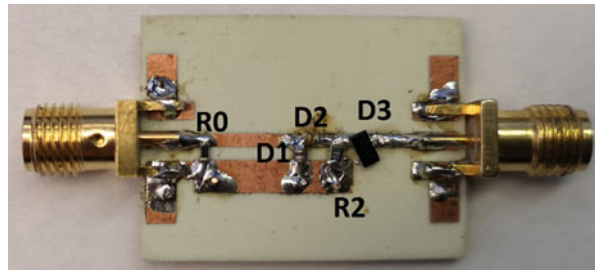


Fig. 13 Schematic of pulse generator: D1 and D2 are Step-Recovery Diodes (SRD) for generating a short pulse; D3 is the Schottky diode for pulse shaping. R_0 is the input matching resistor, and R_2 is the resistor for setting pulse width

Fig. 14 Developed pulse generator



pulse generator based on reference [9]. The authors of [9] used two SRD diodes, one input Schottky diode for blocking input negative voltages, and one output Schottky diode for pulse shaping. The generator is biased with negative DC voltage and is driven by a square-wave from 0 to 2.5 V.

We modified the described design by removing the input diode and the negative DC voltage supply. We used a square-wave input from -1 V to $+1\text{ V}$ generated by the low jitter clock CDCM6208 from Texas Instruments. The used step recovery diodes are 2D528 with a 50 ps decay time and a 0.8 pF capacitance. For pulse shaping at output, the Schottky diode 1SS351-TB-E is used. A schematic diagram of pulse generator is shown in Fig. 13. The PCB was implemented on Rogers, R04350B laminate with $\epsilon_r = 3.66$. Figure 14 shows hardware implementation of the pulse radar. The pulse width and amplitude can be adjusted with R_2 . We used $R_2 = 6.8\text{k}\Omega$ and achieved a pulse width of 116 ps which occupies 9 GHz of bandwidth. Figure 15 shows the amplitude and duration of the pulse in the time domain.

Sampling Mixer for Short Pulses

To detect very short pulses in the range of a hundred picoseconds (about 5 GHz bandwidth), an analog to digital converter (ADC) with at least 10 gigasamples/s is required. ADCs with this performance are very expensive and complex. As an



Fig. 15 Output pulse from generator captured by oscilloscope

alternative to real-time sampling, the so-called signal stretcher is used. The idea is to sample a small fragment of the input RF signal at each time. We assume that the input RF signal is equal over many repetitions. In each subsequent repetition of the RF signal, the sampler takes the next fragment. The output of the sampler is a stretched signal assembled from sampled fragments. With such a sampler, we can stretch the signal from the picosecond range to the microsecond range.

Authors in [10] designed a sampler with two diodes in a bridge configuration. The diodes are opened and closed by narrow strobe pulses, which are triggered by a precise time base. A repetitive sequence of identical input RF pulses with frequency f_0 are required. Strobe pulses are triggered with a slightly offset frequency ($f_0 \pm \Delta f$). The strobe and RF signal are mixed in such a way that the strobe signal slowly scans across the scanned RF signal. The received signal can be reconstructed after a complete scanning cycle with a total time equal to $1/\Delta f$. If f_0 is set to 10 MHz and Δf is set to 1 kHz, then the extending ratio is $f_0/\Delta f = 10,000$. In practice, a 300 ps pulse is extended to 3 μ s. This corresponds to an equivalent sampling rate of 100 gigasamples/s.

We modified the sampler from [10] in such a way that we used fabricated a balun from Mini-Circuits with bandwidth of 8 GHz instead of a microstrip to the slot line balun. As a strobe generator we used the previously described picosecond generator.

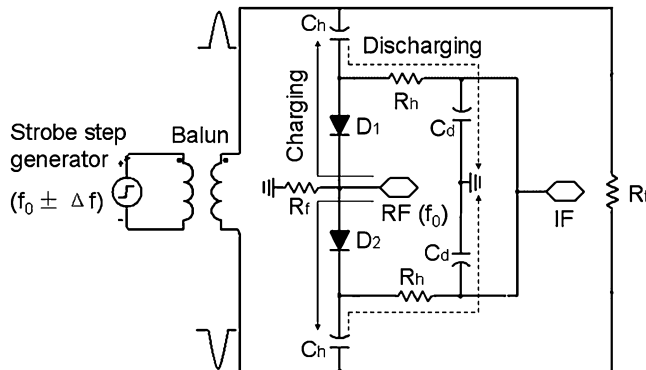


Fig. 16 Schematic of sampler: pulses from balun open the bridge and RF signal charge Ch. When bridge is closed, the signal discharges trough Rh and Cd. The stretched RF signal is on the IF port



Fig. 17 Experimental set-up of generating and sampling UWB signals

The sampler is based on a two-diode bridge configuration. We used fast Schottky mixer diodes (Infineon BAT2402) which have small capacitances and serial resistances and a forward voltage of 0.23 V. The rest of the elements used (resistors and capacitors) are the same as in the original work [10]. Figure 16 shows the schematic of the sampling mixer.

The experimental setup is shown in Fig. 17. The operational amplifier fed with $f_0 \pm \Delta f$ clock is shown on the left. The strobe generator is connected with the amplifier and produces strobe pulses with a repetition frequency $f_0 \pm \Delta f$ at the output. The balun, which divides the input pulse into two opposite pulses, is in the middle. The opposite pulses then open the diodes on the sampler. On the right side of the figure, we can see the pulse generator fed by f_0 clock and attenuator, which attenuates the sampling RF pulse. The sampler stretches the signal from the pulse generator and sends it to the IF port.

Experimental Results

The time domain radar was tested using an educational AT landmine. The landmine was buried into a laboratory polygon of size 3 m x 2 m x 1.5 m, 25 cm below the surface. The radar platform was moved continuously over the polygon. Figure 18 shows that the landmine can be detected efficiently using the laboratory prototype of the radar.

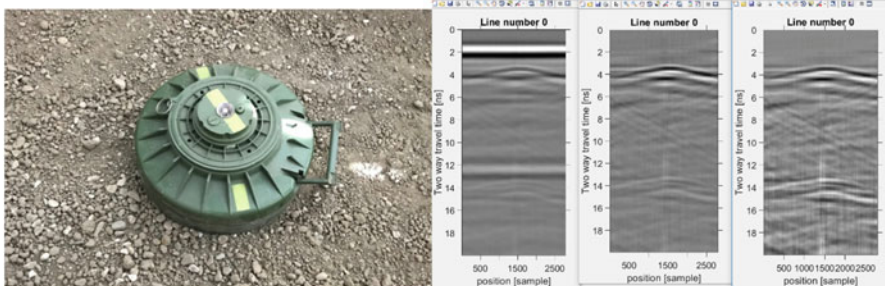


Fig. 18 B-scan of AT landmine above the ground surface. The landmine diameter is 27 cm and height is 13 cm

Overview of the Work Done at University Ss Cyril and Methodius in Skopje

At University Ss Cyril and Methodius (UKIM) in Skopje, we have focused mainly on two activities. The first is the development of a Software Defined Ground Penetrating Radar (GPR), i.e. GPR implemented on a Software Defined Radio (SDR) and its Compressive Sampling version. The second is on the signal processing of the GPR images (B-scans) obtained in order to perform target detection and localization, and, additionally, target classification.

In [11] we presented a practical Software Defined Radio (SDR) stepped frequency radar implementation. It is known that the radar resolution depends on the radar bandwidth. Since the targets in GPR applications can be very small, such as anti-personnel (AP) mines, we need high resolution, which translates to a large radar bandwidth. Since hardware with a wide instantaneous bandwidth is expensive, our radar implementation is based on the Stepped Frequency (SF) radar, which requires much smaller instantaneous bandwidth than the impulse radar. In SF radar, a collection of pulses with increasing frequencies at a fixed frequency step is sent and the response is measured. After down-conversion, in effect, the discrete channel frequency response obtained from the reflections off all the targets is evaluated. By taking the Inverse Discrete Fourier Transform (IDFT), the channel impulse response is obtained, where different delays correspond to the positions of different targets. These delays are transformed into a range profile by using the electromagnetic wave velocity in the respective medium (type of soil). Our approach [11] to the SF radar SDR implementation uses a combination of baseband and RF frequency hopping. The entire RF instantaneous bandwidth at a given carrier frequency is used to accommodate the upconverted baseband signal of N pulses with increasing frequencies (a burst) in that frequency band (which we call a subband). To increase the total bandwidth used M -fold, the RF frequency of the modulated signal is hopped M times. That is, we use M different subbands. The principle is shown in Fig. 19 with $M = 4$.

For the Software Defined Radio (SDR) GPR implementation, we used the NI USRP X310 SDR platform which has a powerful Xilinx Kintex-7 FPGA, combined

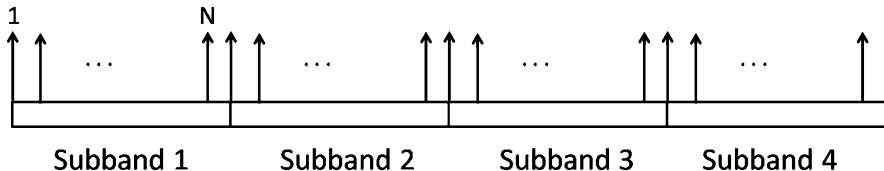


Fig. 19 Our approach to implementation of SDR SF radar

with a UBX-160 radio frequency (RF) daughter-board, which covers the frequency range from 10 MHz to 6 GHz with a bandwidth of 160 MHz [12]. Using the proposed approach, we can increase the radar bandwidth up to the entire frequency range of the USRP of 6 GHz, although our SF radar starting frequency is 500 MHz or 1 GHz, due to the wideband antenna implementation requirements. To design and implement the transmitter and the receiver on the USRP we used the open software radio development environment called GNU Radio with its graphical tool for creating signal flow graphs, GNU Radio Companion (GRC). We tested the implemented radar in a field experiment at the Faculty of Electrical Engineering and Information Technologies (FEEIT) for targets in the air at a distance of 15 m. We used $N = 30$ frequencies in each burst, $M = 4$ subbands to increase the radar bandwidth, and a range resolution comparable to using a single subband. The only limitation is the relatively large RF frequency switching time (settling time), but the entire measurement time is much smaller than when switching all MN frequencies, since the transmission of each burst is instantaneous, i.e. it does not require RF frequency hopping. The details of the implementation and range profile plots are given in [11].

Subsequently, in [13] we developed a Compressive Sampling (CS) version of the same SF radar. Namely, since the targets are sparse, radar signals are sparse in the delay – Doppler domain for moving targets and in the delay domain for stationary targets. The GPR application assumes stationary targets, and, thus, we do not need to treat Doppler shifts. Sparsity is the main signal characteristic for using CS. CS uses a reduced number of measurements (represented by using a proper sensing matrix) which is possible when the signal is sparse in some domain, which does not need to be the original domain. Due to its sparsity, reconstruction of the original signal is possible if the sensing matrix meets certain conditions. There are different reconstruction algorithms, and in [13] we used Basis Pursuit Denoising (BPDN), which is applicable in the presence of noise. It minimizes the L_1 norm of the reconstructed signal vector with a constraint that provides fidelity (i.e. measurement consistency with the reconstructed signal vector) and depends on the noise variance. Our problem is to reconstruct the sparse vector of the reflection coefficients of targets at different ranges on a range grid with J points, i.e. the range profile vector. We implement the CS SF by randomly choosing a subset of L frequencies from the N frequencies in each subband in Fig. 19 and measuring the frequency response at just those L frequencies to obtain the measurement vector of dimension L . The sensing matrix for each subband is a partial DFT matrix of size $L \times J$, i.e. it consists of

complex exponentials that depend on the L randomly chosen frequencies in that subband and all the possible target distances, corresponding to all J points on the range grid. Thus, we get our mathematical model for the reduced number of measurements in each subband, by also adding the noise. We use all the available measurements in all M subbands, by constructing a measurement vector of dimension ML and a tall sensing matrix of dimension $ML \times J$. The reconstruction of the range profile vector of size J is performed by the BPDN. We use cross validation to determine the parameter in the BPDN constraint. The details are given in [13]. The results in [13] are obtained using the same field experiment as in [11] and compare the range profile obtained using all $N = 30$ frequencies in each subband and IDFT with range profiles obtained using CS with $L = 10$ and $L = 5$ randomly chosen frequencies in each subband and BPDN reconstruction of the range profile vector. The main advantage of the CS SF radar is the reduced measurement time. Despite a reduced measurement time, the CS results show improved resolution. Currently we are working on obtaining GPR images with the described SDR SF radar which requires using a much higher bandwidth to obtain high resolution, needed for GPR detection of landmines. We are also working on the CS GPR version, where the number of measurements can be reduced both in the frequency domain (the stepped frequency radar number of frequencies) and in the number of scans used in the cross-range direction (i.e. number of antenna positions used to obtain the GPR image).

We also developed a simulation tool to simulate the GPR radar transmitter, the electromagnetic propagation in different media, and the GPR radar receiver [14]. It uses the Matlab software package and gprMax, which is an open source software that simulates electromagnetic wave propagation in different media using the Finite-Difference Time-Domain (FDTD) method [15]. We implemented the radar transmitter and receiver simulator in Matlab. The tool provides for importing the Matlab generated SF transmit signal into gprMax, simulation of the propagation in the soil using gprMax for each transmit receive antenna position, and for importing the signals from the gprMax receive antenna back to Matlab for demodulation and processing to obtain the B-scan. We used this tool to obtain B-scans of different objects buried in the ground, including anti-personnel (AP) and anti-tank (AT) mines for additional signal processing.

We next describe the signal processing approaches that we used. Part of our investigation included focusing the B-scans and hyperbola detection [14]. For focusing the B-scans, we used f-k migration to obtain more accurate object localization. In [14] we showed the result of f-k migration of a B-scan of a cylinder buried in the ground obtained using our software tool. Smaller objects in the ground produce hyperbolic signatures in the B-scan, due to the longer paths that the signal travels between the transmitter and receiver (which use collocated antennas), when the object in the ground is not exactly below the transmit-receive antennas. Therefore, an object buried in the ground can be detected and localized by detecting its hyperbola signature and hyperbola vertex. For hyperbola detection we used the Hough transform, which is computationally very complex. To reduce the complexity of the Hough transform, and to obtain more distinct hyperbola shapes, we used the Column-Connection Clustering (C3) algorithm on the binarized B-scan image [14].

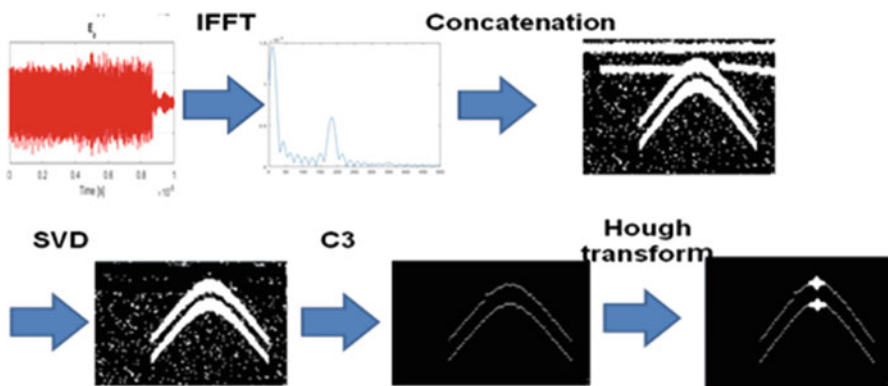


Fig. 20 The proposed signal processing procedure for GPR target detection

C3 algorithm produces single central strings in the place of the hyperbolic shapes, which can be wide and can have irregular edges. It consists of three phases: column segmentation, column-segments connection (clustering) and central string extraction. The block diagram of the procedure is shown in Fig. 20. Note that prior to applying the C3 algorithm, the ground surface reflected wave is removed by using the Singular Value Decomposition (SVD) method, where several leading components of the outer product image SVD expansion, that correspond to the ground surface reflected wave, are removed.

In [14] we presented the results of object detection and localization using the combination of the C3 [17] algorithm and Hough transform [18–19] with both the B-scan of a cylinder buried in the ground obtained using our simulation tool and with B-scans obtained from experimental GPR data available on the Web [16], which contain measured GPR frequency responses from different objects (such as balls, pipes, and other objects of different shapes, including landmines). The results show successful detection of hyperbolas and their vertices.

Additionally, we performed object detection, localization and classification using Faster Region Convolutional Neural Networks (R-CNN) [20]. The objects are detected and localized by the Faster R-CNN which uses Region Proposal Network to predict object bounds. Additionally, we used two classes to perform object classification, the first class being the Object class, and the second class being the AT class, intended for recognition of AT mines. In the object class only objects with hyperbolic signatures were classified. The AT mines have distinctive signatures that are not plain hyperbolas due to their bigger size and the specific shapes they have. We trained the network with the simulated data obtained with our simulation tool and with experimental GPR data provided by other researchers (such as [16]). Additionally, we performed post processing of the Object class to distinguish between AP mines, which also give hyperbolic signatures, and other objects with hyperbolic signatures, based on the object size and location below the ground surface. The results of object detection, localization and classification, are shown in [20]. We used ROC curves and confusion matrices to evaluate the detection and

classification performance of our approach. The results are promising, but they require further investigation and much bigger training sets, which will be provided using field measurements with our own GPR system.

Broader Impacts

Explain How This Project Will Affect People, Ecosystems, the Environment, Industry, Commerce, Transportation, International Relations, or Other Aspects of Life or Society

This project will demonstrate the use of advanced concepts for landmine detection. The deliverables will enable the assembly of small radars and attachment of them to commercially available drone platforms. The time needed for landmine detection will be reduced because the drone platform will be able to automatically scan the area within 20 min, using velocities of up to 15 km per hour.

The proposed method of landmine detection using a drone mounted GPR is ecologically clean, non-hazardous, non-destructive, technologically advanced, efficient, and fast. GPR is a type of radar that can find numerous applications in different sectors, such as utility location, structural assessment, archaeological surveys, environmental applications, geotechnical applications, law enforcement, grave location, and cemetery mapping. Developing a simple and efficient GPR with advanced signal processing and pattern recognition techniques could have an impact on all these areas. Some researchers have used GPR to develop techniques for vehicle localization and autonomous driving, using pre-recorded underground maps obtained by GPR measurements that use stable subsurface features. More generally, developing a light weight radar that can fly on a drone can potentially find many other applications besides its use for detection of underground objects, such as for land remote sensing.

The results pertaining to the radar solution and its hardware development and implementation, developed by the partners, will be publicly available. The potential end-users will be able to build a similar device. We will also provide consulting for hardware development, which will enable sustainable use of the results.

Young Researcher Participation

- **Discuss thesis projects and degrees resulting from the project**
- **Insert number/statistics about the young researchers status and involvement in the project.**

At the moment the following young researchers are involved in the project who are currently working on their PhD and MSc degrees.

1. Danihel Šipoš, Slovenia, PhD Student

2. Blaž Pongrac, Slovenia, PhD Student
3. Siniša Pcov, Macedonia, MSc Student
4. Dimitar Tanevski, Macedonia, Diploma graduate
5. Alen Helać, BiH, Msc Student
6. Dženita Vejsilović, BiH, Msc Student

Contributions

- **Provide citations for conference papers, journal articles, book chapters, etc. arising from the project. See Springer Manuscript Guidelines for format.**
- V. Kafedziski, S. Pcov, “Implementation of a High Resolution Stepped Frequency Radar on a USRP”, Proceedings of 13th International Conference on Advanced Technologies, Systems and Services in Telecommunications TELSIKS 2017, Nish, pp. 236–239.
- V. Kafedziski, “Implementation of a Compressive Sampling Stepped Frequency Radar on a USRP”, Proceedings of 14th Conference ETAI 2018, Struga.
- V. Kafedziski, S. Pcov, D. Tanevski, “Target detection in SFCW ground penetrating radar with C3 algorithm and Hough transform based on gprMax simulation and experimental data”, Proceedings of 25th International Conference on Systems, Signals and Image Processing IWSSIP 2018, Maribor.
- V. Kafedziski, S. Pcov, D. Tanevski, “Detection and Classification of Land Mines from Ground Penetrating Radar Data Using Faster R-CNN”, Proceedings of 26th Telecommunications Forum TELFOR 2018, Belgrade.
- V. Kafedziski, Project presentation at the Workshop organized for the NATO SPS SIARS Project, 24 October 2017, held at the Military Academy in Skopje, with the presence of high NATO representatives and Minister of Defense of Republic of Macedonia.
- V. Kafedziski, Project presentation including an exhibition of the USRP hardware and project brochure dissemination at the first Western Balkans Digital Summit, Skopje, 18–19th April 2018.
- Gleich, V. Kafedziski, Ground Penetrating Radar Attached to a Hexacopter for Automatic Mine Detection, Project presentation at the NATO SPS Advanced Research Workshop on Explosives Detection, Florence, 17–18th October 2018.
- Šipoš, D. Gleich, Blaž Pongrac, Developing of stepped frequency radar for landmine detection, IWSSIP 2018
- D. Šipoš, D. Gleich, Blaž Pongrac, Deep neural networks for classification of SAR data, IGARSS 2018
- DušanGleich, Peter Planinšič, SAR patch categorization using Dual tree oriented wavelet transform and Stacked Autoencoder, on conference IWSSIP 2017 <http://iwssip2017.org/>
- DušanGleich, Peter Planinšič, Danijel Šipoš, Deep Convolutional Neural Networks for SAR Patch Categorization, presented at Elmar 2017, Zadar, Croatia.

- Blaž Pongrac, Deep Convolutional Networks for SAR data categorization, Presented at ERK 2017, Portorož, Slovenia.
- Peter Planinšič, DušanGleich, InSAR Patch Categorization using sparse coding, IEEE Geoscience and remote sensing Letters, June 2017.

References

1. Kafedziski V, Pecov S (2017) Implementation of a high resolution stepped frequency radar on a USRP. In 2017 13th International Conference on Advanced Technologies, Systems and Services in Telecommunications (TELSIKS). pp. 236–239
2. Charisma A, Setiawan A, Rahayu SA, Suksmono A, Munir A (2015) Matlab and gnu radio-based sfcw radar for range detection. 082015
3. Thomas SB, Roy LP (2017) A comparative study on calibration technique for sfcw ground penetrating radar. In 2017 International conference on Microelectronic Devices, Circuits and Systems (ICMDCS). pp. 1–4
4. Fu L, Liu S, Liu L, Lei L (2014) Development of an airborne ground penetrating radar system: Antenna design, laboratory experiment, and numerical simulation. IEEE J Sel Topics Appl Earth Obs Remote Sens 7(3):761–766
5. Ahmed A, Zhang Y, Burns D, Huston D, Xia T (2016) Design of uwb antenna for air-coupled impulse ground-penetrating radar. IEEE Geosci Remote Sens Lett 13(1):92–96
6. Hakim NFA, Chairunnisa, Arifianto MS, Munir A (2017) Accuracy analysis of range detection for sfcw portable through-wall radar. In 2017 third International Conference on Wireless and Telematics (ICWT), pp. 35–38
7. Burki J, Ali T, Arshad S (2013) Vector network analyzer (vna) based synthetic aperture radar (sar) imaging. In INMIC, pp. 207–212
8. Ahmed A (2014) Design and optimization of uwb antenna for air coupled gpr applications. Master's thesis, The University of Vermont, USA, 102014, an optional note
9. Lianfeng Z, Shulabh G, Christophe C (2017) A simple picosecond pulse generator based on a pair of step recovery diodes. IEEE Microwave And Wireless Components Letters 27(5)
10. Zhang C (2008) Hardware development of an ultra-wideband system for high precision localization applications. PhD diss., University of Tennessee.
11. Kafedziski V, Pecov S (2017) Implementation of a high resolution stepped frequency radar on a USRP. Proceedings of 13th International Conference on Advanced Technologies, Systems and Services in Telecommunications TELSIKS, Nish, pp. 236–239
12. <https://www.ettus.com/product/details/X310-KIT>
13. Kafedziski V (2018) Implementation of a compressive sampling stepped frequency radar on a USRP. Proceedings of 14th Conference ETAI 2018, Struga
14. Kafedziski V, Pecov S, Tanevski D (2018) Target detection in SFCW ground penetrating radar with C3 algorithm and Hough transform based on gprMax simulation and experimental data”, Proceedings of 25th International Conference on Systems, Signals and Image Processing IWSSIP 2018, Maribor

15. Warren C, Giannopoulos A, Giannakis I (2016) gprMax: Open source software to simulate electromagnetic wave propagation for Ground Penetrating Radar. *Comput Phys Commun* 209:163–170
16. <http://waymond-scott.ece.gatech.edu/multistaticbeamformingdata/multistaticbeamformingdata/>
17. Dou Q, Wei L, Magee DR, Cohn AG (2017) Real-time hyperbola recognition and fitting in GPR data. *IEEE Trans Geosci Remote Sens* 55(1):51–62
18. Capineri L, Grande P, Temple JAG (1998) An advanced image processing technique for real-time interpretation of ground penetrating radar images. *Int J Imaging Syst Technol*, Ed. Wiley 9/1: 51–59
19. Borgioli G, Capineri L, Falorni P, Matucci S, Windsor CG (2008) The detection of buried pipes from time-of-flight radar data. *IEEE Trans Geosci Remote Sens* 46(N.8):2254–2266
20. Kafedziski V, Pecov S, Tanevski D (2018) Detection and classification of land mines from ground penetrating radar data using Faster R-CNN. *Proceedings of 26th Telecommunications Forum TELFOR 2018*, Belgrade

Multi-Year Project: Biological Method (Bees) for Explosive Detection

Ivan Steker

Croatian mine action centre – Centre for Testing, Development and Training (HCR-CTRO), Sisak, Croatia

Zdenka Babic

University of Banja Luka, Banja Luka, Bosnia and Herzegovina

Graham Turnbull

University of St Andrews, St Andrews, Scotland, UK

Mario Mustra

Faculty of Transport and Traffic Sciences, University of Zagreb, Zagreb, Croatia

Project Goals

Explain in lay-person terms the objectives of the project.

The problem of legacy landmines in post-conflict areas still carries a huge cost in terms of injury to civilians, unfarmed land, and loss of trade and communication, and there is the potential security threat of the availability of explosive materials being scavenged by terrorist organisations for homemade explosive devices. The Bee4Exp

project aims to develop a tool allowing the detection of landmines in contaminated areas using a multidisciplinary, innovative approach.

Three different techniques (training honeybees for explosive detection, polymer films as an explosive sensor, and honeybee imaging over the landmines) which have shown positive results in the past, will be integrated to provide a flexible, sensitive, and robust technology. The interconnecting component of Bee4Exp is trained honeybee colonies. Honeybees are known for their ability to “sniff” a variety of compounds from drugs to pesticides to CBRN materials; explosives have also been shown to be detectable by honeybees. Two main methods will be used with the trained honeybee colonies: the passive and the active method. In the passive method, bees are allowed to fly freely around a particular area, and when they return to the hive, the hive environment can be sampled for any explosive materials picked up by the bees. To detect these molecules from the hive, conjugated polymer films are used as sensors – these materials strongly emit light in the visible wavelength when excited by a laser or LED. These materials are highly sensitive to nitroaromatic molecules like TNT, so when the explosive molecules come into contact with the polymer film, the light level decreases. This can be monitored using standard photodiode and microprocessor technology to provide a robust, portable and reliable instrument. In this project we aim to advance our existing sensor through integration with the beehive, and using multiple sensor pixels to discriminate explosives from other nitroaromatics like pesticides to help avoid false positive detections.

The second, active method mode involves using trained bees that fly towards a specific odour in a contaminated area. This is achieved by exposing the bees to, for instance, TNT when given syrup. The bees associate the smell of TNT with sugar syrup, and so when released into the field they hover above a landmine. This method, while proven and reliable, can be difficult to monitor in the field: using drones and cameras has so far run into problems with resolution due to the relative size of a single bee compared to the environment. In Bee4Exp we aim to mitigate this by utilising high-definition cameras alongside thermal cameras. By using three drones simultaneously equipped with high-definition cameras, the area can be overlaid for higher reliability. Methods for automatic (computer) video analysis that will be developed in this project will enable tracking of bees above areas suspected to be contaminated with explosives. From georeferenced high-resolution video, a map of the space-time density of trained bees over the suspected area will be generated, which should allow the determination of the precise location of an explosive device. In summary, Bee4Exp aims to develop two methods for the detection of legacy landmines in an ambitious, multidisciplinary, and novel project. A particular area is scanned to detect the presence of explosives when applying a passive method. In a suspected hazardous area, the proposed active method can be used to identify the location of an explosive device.

Deliverables

Explain the tangible products of the project – entire system and components.

The deliverables of the project will be a series of reports that document the development of new hardware and methodologies for trace explosives detection using colonies of honeybees.

The outputs of the project on the Active Method side include development of image acquisition equipment achieving sufficient resolution to detect honey bees in flight; achievement of formation flight with a UAV to take multiple images with geo-location data; a video database built for bee flight recordings; a method for automatic identification of bees in the video; and an approach for honeybee quantification. For the Passive Method, the outputs include the development and operation of prototype vapour sensors successfully integrated with the beehive for the passive detection method and an assessment of a novel approach for selective detection of vapours.

For both Active and Passive methods, field trials will be undertaken with conditioned colonies of honey bees for the active detection method, and with explosive vapour sensors for the passive detection method; and finally performance assessment of passive and active methods in laboratory and test minefield conditions. Additionally, a pathway will be identified to future implementation of the technologies, and scientific advances will be continually disseminated to the academic community and to end user groups.

Security Relevance

Explain how this project advances the “security pillar” of NATO SPS.

Bee4Exp addresses the security pillar of NATO SPS by focusing on the SPS key priorities of (1) Security-related Advanced Technology, through the development and application of emerging optical and nanotechnologies and Unmanned Aerial Vehicle (UAV) platforms; and (2) Mine and Unexploded Ordnance Detection and Clearance’ through development of advanced technologies and new methodologies. By combining the area survey of foraging honeybees with advanced imaging techniques on UAVs and novel chemical sensors, it is anticipated that large areas can be assessed for landmine contamination on terrain not easily accessed by typical vehicles and used as Quality Assurance post-clearance. This enhances human security by removing direct non-discriminatory explosive devices from the ground, opening that land for farming or other use, which improves social security, and removing available explosive material that may be harvested by malicious actors.

Science Relevance

Explain how this project advances the “science pillar” of NATO SPS.

The innovative research conducted in Bee4Exp combines cutting-edge scientific knowledge that spans organic semiconductor sensor physics, apiological science, UAV/flight engineering and signal processing, to develop advanced explosives detection methods. This multidisciplinary project is the first to approach the landmine problem in this way, and early results indicate that this has potential to be a high-impact solution to aid humanitarian demining. One publication in a high-impact scientific journal (*Science of the Total Environment*) on the Passive Method has recently been published from work undertaken in the first year of the project. Project aims and results have also been disseminated in a number of international conferences, with audiences of both scientists and the humanitarian demining end-user community.

Partnership Relevance

Explain how this project advances the “partnership pillar” of NATO SPS.

The multidisciplinary nature of the project has created a new partnership of scientists and engineers from quite disparate backgrounds and expertise, across three countries and five institutions. The groups are coordinated by the Croatian mine Action Centre’s Centre for Testing, Development and Training, and they have a close working relationship, with weekly Skype meetings for the whole group, and smaller face-to-face meetings among partners happening frequently. At least twice a year the whole group meets for conferences and/or field trials, with the next meeting due in April 2019 at the Mine Action conference in Slano, Croatia.

End Users

Who are the end users for the project deliverables, and how will they use them?

The end users of this technology will chiefly be humanitarian deminers who can use all or part of the Bee4Exp outputs to assess or conduct quality assurance on a suspected site. As part of a wider toolbox including existing technologies like metal detectors or vehicles, this project is envisaged to help with demining efforts by making it more efficient, cheaper, and robust.

Technical Summary

Mine clearance, and the occurrence of civil mine casualties, is a pressing problem in many countries. The experience in Croatia of civil demining over the last 20 years is mainly in using conventional methods including metal detectors and sniffer dogs. The main activity of CTDT and the Scientific Council for Demining is developing, testing, and introducing new methods to make demining safer, faster and more reliable. Part of this activity is developing biological methods, mainly with bees. In the FP7 project TIRAMISU methods were developed for training bees to detect and search for raw military explosives. The main objective of Bee4Exp is to develop new complementary methods to the standard methods.

Bees can passively collect particles from air from the flying and foraging area and can be trained to actively search for smell of TNT and DNT.

Branched hairs of the bee developed for collecting pollen can collect other molecules from the surroundings [25], and the electrostatic charge of hair increases the possibilities of collecting particles [5, 15, 31]. In a honey bee colony there are up to 40,000 bees going for food on average 15 times a day. Food availability can increase the number of foraging flights up to 100 times [28].

Bees can be applied to mine fields to passively collect TNT particles and introduce them to the hive, which, when the hive environment is subsequently analysed, can indicate the presence/absence of landmines and unexploded ordinance in the surrounding area. By training with a food reward, the bees can be oriented to fly above a defined area of interest.

A major advantage of the passive method is that bees can be used in hard-to-reach terrains and with significant vegetation for surveying a suspected area prior to demining, or for Quality Assurance after demining activity.

The active method is oriented to apply on demined fields as an internal and/or external additional method for safety and quality control, and generally for mine fields without a lot of vegetation. Honeybee colonies can be trained to actively search for TNT and DNT odours. With a few days training in a mesh tent with a sugar solution, bees associate the scent of TNT and DNT with the availability of food. The conditioned honeybee colony is then transferred to the mine field to search for TNT and DNT odours. To prolong and increase interest in the odour, free flying bees need to be briefly re-trained with TNT and DNT each day early in the morning. To be able to use honeybees for explosive detection, they should be monitored over a minefield and the most frequently visited places identified could be suspected areas. Our solution is based on using Unmanned Aerial Vehicles (UAVs), high definition georeferenced video capturing in visible and infrared spectrums, and sophisticated video analysis algorithms.

One of the chief advantages of using bees includes the short period required for conditioning, the day-long sampling, and the ability to cover a wide area in large numbers.

Restrictions in the use of bees occurs when the natural pasture in the area is present and temperature is below 15 °C. Wind and rain can also interfere with the activity of bees generally, and high vegetation can obstruct their monitoring.

The in-field testing methods for the Bee4Exp project are on Croatian test mine fields in Benkovac and Cerovac. The Benkovac test site, inaugurated in 2000, has 1000 buried mine targets in a Mediterranean climate spanning over 10,000 m². There are 39 blind test lanes, each of which is 47 m long and 1 m wide, and various mines are buried at 5–27 cm depths. The distance between the lanes is 3 m. The lanes are divided into 1 × 1 m squares. The Cerovac test site, inaugurated in 2004, is in a continental climate, on 55,000 m² for testing of demining machines, mine detection dogs, metal detectors, PPE, and new technologies.

Testing of bee activity is performed on this site for testing and certification of mine detection dogs and handlers. The test site is divided in 66 testing boxes of size 10 × 10 m, with a 3 m distance between the boxes.

The basic foraging behaviour and anatomy of honeybees as groundwork for research of using honeybees for explosive detection.

For centuries bees have been known and used for commercial pollination. However, not all plants are equally attractive to the bees. In order to orient bees for pollination of less attractive crops, conditioning with flowers and a sugar solution is used. Flower (smell) fidelity is well expressed in honeybees, which means that bees will pollinate the same plant species as long as the source of food is present [1, 8]. To attract pollinators, plants have developed smell as a cue as a result of coevolution between plants and bees. Bees learn very quickly, and they can remember smell for a long time [14]. Bees have been shown to connect the smell of TNT and DNT with the source of food [13, 16, 18]. To combine the smell of TNT or DNT with the food, bees need to be conditioned in a closed environment for 4 days. After conditioning, the honeybee colony is transferred to a test mine field for an active method of explosive detection. To prolong the interest for TNT and DNT odours early in the morning before foraging activities, bees need to be reconditioned with feeders containing TNT and DNT odour and a source of food like a sugar solution.

During foraging activities, particles from the environment collect on the body hair of honeybees. To fulfil the task of pollination and to collect the pollen as food, bees are well covered with hairs [12]. The design of the hair and electrostatic charges retain the pollen grains on the honeybee body [24]. Besides the pollen grains, particles from the environment (smell, molecules) are attracted to the body hairs. Bees are known to forage up to 3 km from the hive to find food [28], and they cover a wide area. With an artificial food source bees can be kept within an area of interest. One colony can have up to 40,000 foraging bees, depending on the size of the total population. Bees returning from foraging bring particles back to the hive; in the hive bees are electrostatically discharged and the particles are subsequently released inside the hive. With several foraging flights, bioaccumulation of the particles in the hive occurs. In that sense, bees bring molecules of TNT and DNT to the hive. By sampling the hive interior, with the passive method we can detect the presence of explosives in the foraging area. Passive collection of particles from the environment has been shown in the literature for monitoring pollutants and radionuclides [3, 11, 32].

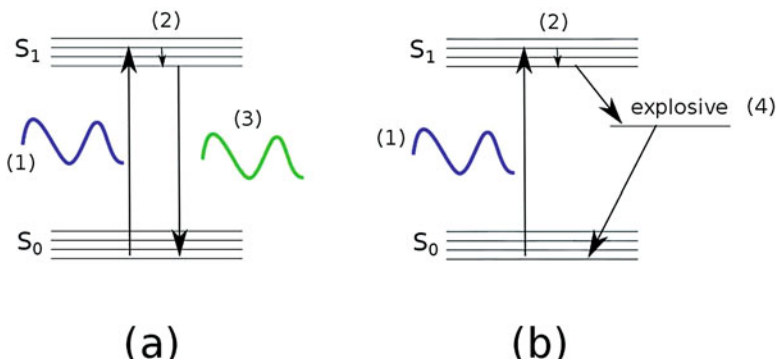


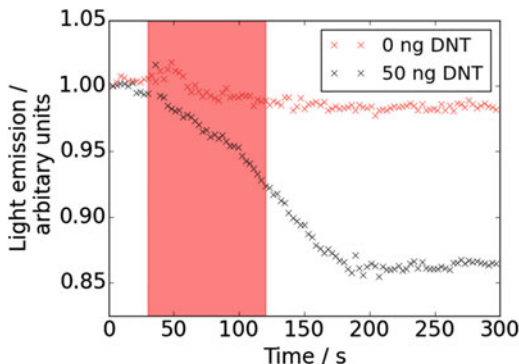
Fig. 1 Jablonski diagram of fluorescence quenched by explosives: **(a)** absorption of light produces luminescence; **(b)** The introduction of an explosive molecule causes non-radiative decay and loss of luminescence

Optical chemical sensing is an attractive method for the detection of a wide range of analytes since it can offer advantages including low-cost, portable instrumentation, rapid response, and high sensitivity [29]. Organic semiconductor materials, like those found in the displays of many consumer electronics, are suitable for optical chemical sensing of explosives due to their high brightness, relatively simple processing, and sensitivity to nitroaromatics like TNT [21, 22, 30], where the light emission decreases when explosive molecules come into contact with the polymer surface. This is due to a transfer of energy from the light-emitting polymer to the explosive and is known as “quenching.” By exciting the polymer with an LED or laser, the material absorbs the excitation light to produce luminescence at a red-shifted wavelength (Fig. 1a). When the electron-deficient explosive molecule is introduced to the polymer surface, the explosive causes non-radiative decay and thus a loss of fluorescence intensity from the polymer (Fig. 1b). The strong quenching effect of the explosive molecules can be monitored by a photodiode, allowing a portable, inexpensive instrument based on this measurement technique to be developed using largely off-the-shelf components [10].

In a typical lab-based experimental set-up, a light-emitting polymer such as Merck Super Yellow, polyfluorene (PFO) or F8BT is dissolved in a co-solvent like toluene and spin-coated onto a cleaned glass slide. The sensing film is placed in an air-tight chamber and exposed to explosive vapours while being photoexcited by an LED or laser, and the resulting emission spectrum monitored by a fibre optic attached to a spectrometer.

The luminescence quenching process in this set-up can detect trace amounts of vapour, typically down to a few parts per billion (ppb) [20, 21]. However, difficulties arise in field environments since trace vapours are easily dispersed by wind. To mitigate this, a technique adapted from REST (Remote Explosive Scent Tracing) [7] has been developed. REST involves sampling the air above suspected landmine-contaminated areas onto plastic netting which is then interrogated by dogs to identify mined locations. The drawback with this method includes the timescale and often the

Fig. 2 Response of luminescent film Super Yellow to 50 ng of 2,4-DNT on an Aflas preconcentrator (black line) versus an uncontaminated Aflas preconcentrator



distance between the sampled site and the sniffer dogs, the temperament of the dogs, and the sorbing capability of the plastic netting. Preconcentration is a method commonly used in analytical chemistry to increase the amount of target analyte by sorbing the analyte over time onto a host material [6, 19, 23, 26]. The target analyte, in this case explosives, is then thermally desorbed, allowing delivery of an increased amount of the target to the sensing element. However, a material able to sorb explosives more efficiently than paper or cotton swabs should be used to increase preconcentration ability.

The commercial fluoropolymer Aflas has been shown to sorb Volatile Organic Compounds (VOCs) [27]. Aflas was first tested for affinity to DNT by dissolving the polymer in tetrahydrofuran (THF) and spot-cast onto filter paper prior to dropping DNT dissolved in acetonitrile at various concentrations onto the surface, and allowing the solvent to evaporate. The Aflas-coated substrate was then heated to approximately 100 °C for 1 min and a Super Yellow film was excited by a laser at 305 nm. Figure 2 shows the quenching response of the 2,4-DNT on the Super Yellow film, where almost 20% of the light emission is lost over 300 seconds.

This indicates that Aflas is a suitable sorbing material for DNT down to nanogram-levels, and can be successfully thermally desorbed for subsequent optical detection by a fluorescent polymer.

To assess the material for preconcentration capabilities in the field, it was dissolved in THF and either blade-coated on canvas substrates to be inserted in 1 cm² tubes in the hive entrance and exit (Fig. 3), or spot-cast onto circular filter paper for placement in the air sampler (Fig. 4).

The field trial to determine efficacy of Aflas as a preconcentrator for the Bee4Exp project was to sorb explosive materials initially through air sampling via a specialized cupola on the colony, then by inserting preconcentrator substrates into the entrance of the colony for bees to deposit explosives as they return to the hive after foraging. The air samples were taken for 10 min at the end of every 24-h period, and the entrance samples removed after 24-h on-site prior to testing with an organic semiconductor sensor. The sampling and sensing procedure is illustrated in Fig. 5.

Figure 6 shows results from the field where the quenching response from preconcentrators in the hive entrance are compared against a clean control sample



Fig. 3 Preconcentrators in the hive entrance



Fig. 4 Air sampling with specialized cupola

from a non-contaminated site. It can be seen from the “One Day In” bar, that is, the return of bees from free-flying foraging and passing through the entrance preconcentrator, leads to a drop in emission of approximately 10%, while the control samples show no decrease in emission.

The promising early results from the passive method of detecting landmine-contaminated areas indicate that free-flying honeybees can electrostatically collect enough explosive materials from the environment to be concentrated onto a fluoropolymer substrate and be detected by optical sensors [9]. It is hoped that this method can aid in humanitarian demining efforts in future in both area surveying and post-clearance quality assurance.

The Active Method developed in this project aims to find a suitable solution for determining the activity of honeybees on minefields, and based on that, for determining the location of legacy landmines. Bearing in mind the aforementioned advantages and limitations of honeybees, the method is primarily intended for safety and quality control.

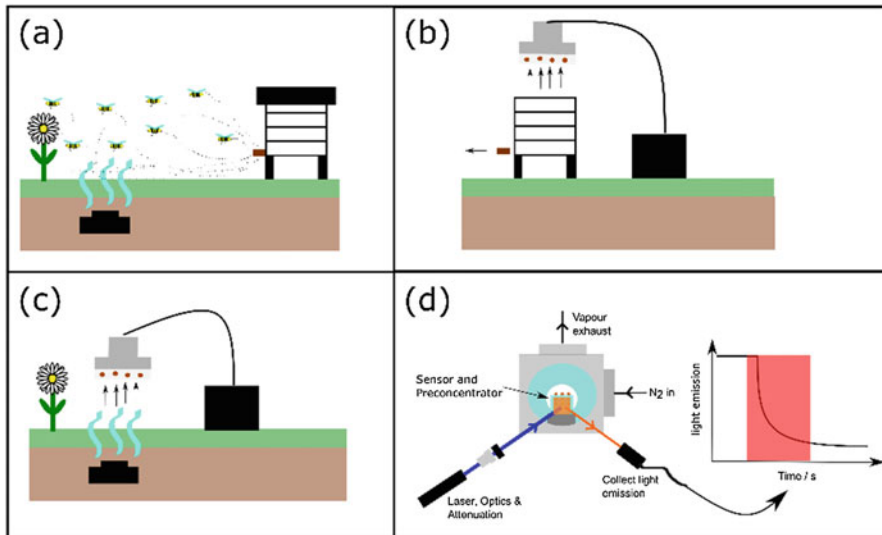


Fig. 5 Passive Sampling and Detection Procedure using organic semiconductor thin films. (a) Free-flying bees above contaminated land; (b) hive air and entrances are sampled by the preconcentrators; (c) air above landmines are sampled; (d) the preconcentrator is heated and exposed to a luminescent thin film, where the drop in light emission is monitored over time

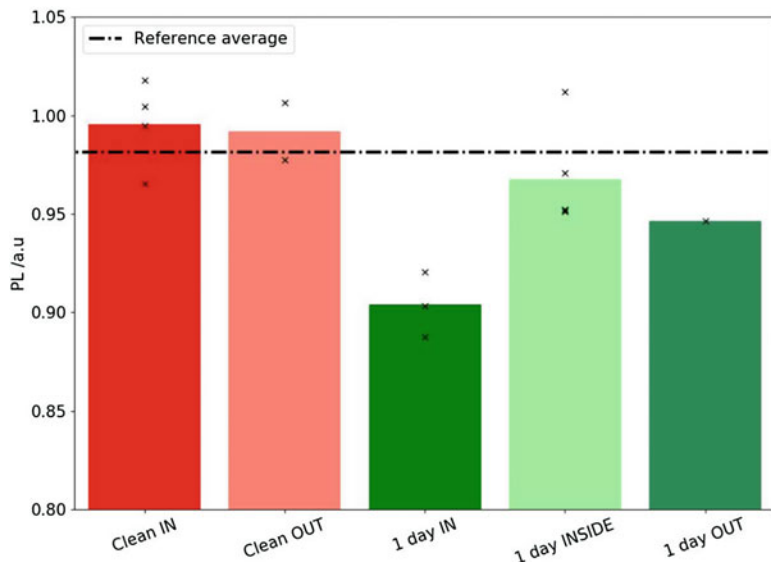


Fig. 6 Results from honeybee colony entrance after one day foraging

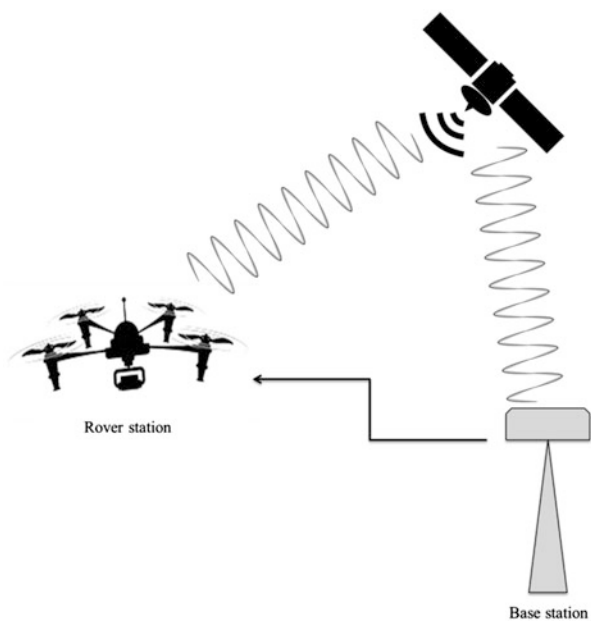
The proposed method relies on accurate capture and detection of honeybees flying outside a hive and over a terrain which contains mines. For that purpose, it is necessary to have honeybees specially prepared to carry on the task of detecting explosive vapours (scent) of explosive substances contained in landmines. Honeybees are trained to associate scent of explosive with the food belonging to a certain area where the desired minefield is located. This gives us a possibility of marking the most frequently visited places as suspicious areas. To detect honeybees flying or hovering over a patch of the field, it is necessary to have a high-resolution video or some other spatio-temporal marker providing a good detection possibility. The first step is to get all the acquisition parameters correct. These parameters include tuning of capturing equipment as well as choosing the appropriate platforms for carrying the capturing equipment. The acquisition part, which should provide enough information for the automatic detection method, consists of video capture using a UAV equipped with an ultra-high definition video (UHD) and a thermal camera (TC). To cover the largest possible ground in one frame, we have decided to use UHD video resolution, meaning that each frame contains more than eight million pixels. Bearing in mind that the UAV hovers at around 8 to 10 meters and camera is equipped with a 50 mm lens (equivalent to a 35 mm system), each honeybee covers the area of around 20 pixels. Translated to the dimensions of the ground covered by this kind of setup, this means that each frame covers around 7 meters in width and 4 meters in height. Choosing these parameters is very sensitive to the type of UAV used and amount of wind it generates, because the wind from the rotors makes the ground, covered in grass or small plants, rather unsteady and therefore difficult to isolate in the process of detection of honeybees. Another good marker for detection of honeybees is their temperature, which is usually different from the ground. To harvest that property, it is possible to use a TC. Currently available TCs are rather low-resolution in comparison to standard UHD camera and expensive but offer a good (thermal) information, which can be used to enhance UHD video. Trying to manually detect honeybees in a still image is rather difficult, if not impossible, because of the masking effect. On the other hand, in a thermal still image is this detection much easier when there is substantial difference in the temperature of bees and their surroundings, as shown in Fig. 7.

The combination of these two detectors should provide better automatic detection results and easier elimination of grass and plants, which are of low interest in the detection of honeybee flight. Another important aspect of this system is navigation and the possibility of the system to map actual coordinates to the captured video. This is important due to post-processing and the ability to place results of the detection back onto the field. For that purpose, we require using a more precise navigation than standard satellite navigation, which offers accuracy of a couple of meters and varies in precision because of obstacles and the satellite constellation at the moment of usage. To cope with that challenge, we have decided to use Real-Time Kinematic GPS (RTK), which provides much greater accuracy than standard GPS and an overall accuracy of under 2 cm. This system is much more complex than the standard GPS because it uses phase-detection of the carrier signal, instead of detection through code correlation. Because of that, it is necessary to have more than

Fig. 7 Thermal image of grassy terrain with several honeybees which appear as bright (white) spots



Fig. 8 RTK GPS system used to provide highly accurate mapping of the terrain



one receiver to detect this highly accurate position. One receiver is usually named Base Station and the other, which actually moves, the Rover Station. Both of these receivers have to be on a relatively small area and have to “see” the same satellites in the constellation, as depicted in Fig. 8.

The described system, which contains a UAV with a UHD camera, TC, and RTK, should be a good platform for data acquisition in the Active Method and give an acceptable amount and accuracy of data for the automatic detection of honeybees from video. This system is, however, rather complicated to assemble because it requires a lot of calculation and testing in order to make all the components suitable

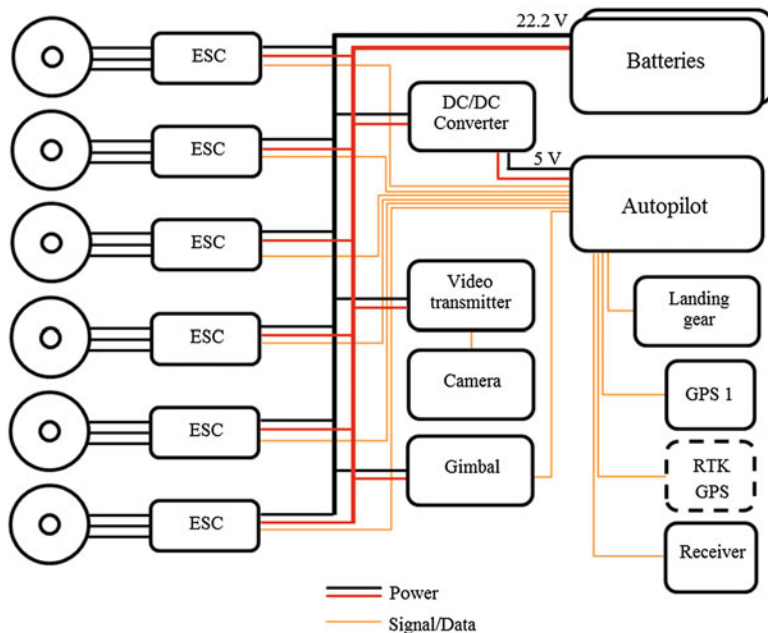


Fig. 9 Scheme of the assembled UAV with power and signal wiring

to work together as a system. Figure 9 shows the basic schematic of the assembled UAV with the most important components.

As mentioned above, honeybees are rather small insects in comparison with the examined area. They are usually 15 mm long, representing around 10–20 pixels in a video. Moreover, honeybees are coloured in a way as to be well concealed when flying above grass- or dirt- terrain. These properties make them difficult to detect and track during free flight over a field. Figure 10 shows images (three frames of videos) containing honey bees. Without the artificially added yellow circles it is almost impossible to visually find bees in these images. An appropriate solution is still missing, although several systems using video imaging, radar taggants and LIDAR have been proposed in the last few decades [2, 4, 17].

After observing huge numbers of videos, and knowing about honeybee biology, we concluded that the most descriptive feature that can separate honeybees from the background is their style of movements. Therefore, we base our research on small moving object detection in a video, using state-of-the-art algorithms like the Gaussian mixture model and Convolutional Neural Networks. We also employ several preprocessing and postprocessing methods like filtering, video stabilization, morphological operation, and data and information fusion. To make the system as robust as possible, the UAV video analysis method takes into account imaging conditions, and many sources of degradation, like random movements caused by wind and UAV turbulence; as an example, the obtained results are marked in Fig. 10 with the yellow circles. As the result of several overflights, a space-time density map



Fig. 10 Images of honeybees during a free flight. The yellow circles marked automatically detected honeybees

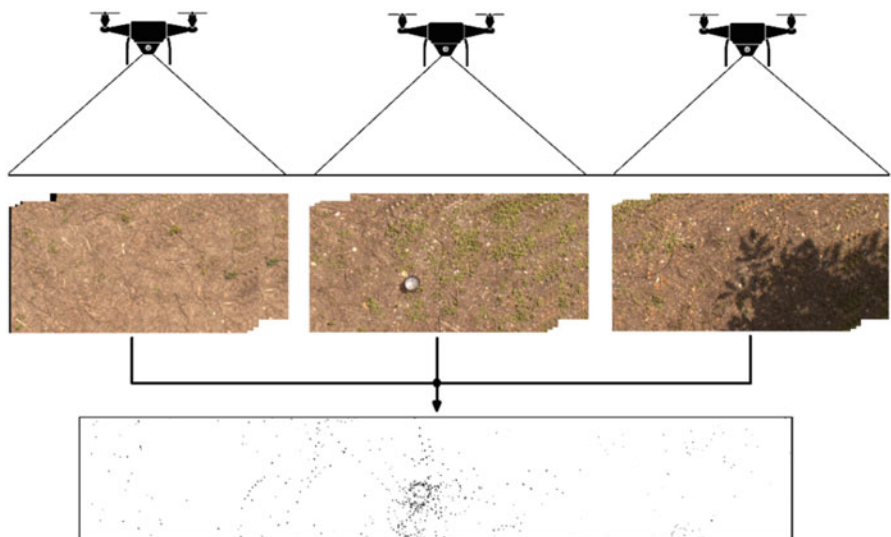


Fig. 11 Schematic representation of the active method

(Fig. 11) of trained honeybees is generated that shows the most frequently visited places, indicating the possible locations of legacy landmines.

In conclusion, the Active Method is a promising tool for real-time detection of landmines across a wide range of terrains.

Wind, rain, and low temperatures are well known factors which can interfere with the activity of bees. Investigation of the influence of environmental parameters is very important for understanding bee behaviour in the field. Therefore, a component of this research is the development of an electronic system for bee activity monitoring as well. Such a system should provide information about environmental parameters paired with detected activity of bees at the entrance and at the exit of the beehive. Monitoring over longer periods of time during changes of environmental parameters can be very useful in planning testing activities and interpreting data within our active and passive methods, as it can determine the optimal periods of the day or ambient parameters in which bees are most active.

Fig. 12 Schematic overview of the proposed system for monitoring of bees' activities

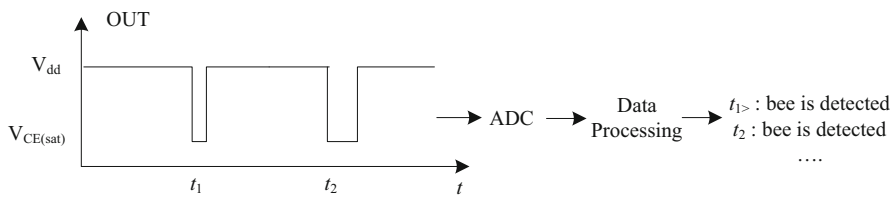
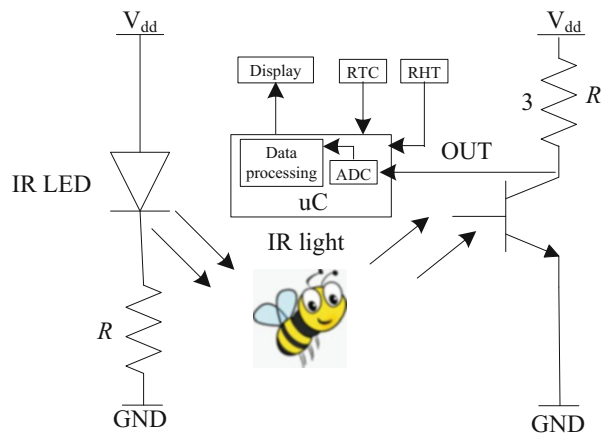


Fig. 13 Detection of bee activity with voltage measurement

The schematic overview of the proposed structure of the electronic system for bee activity monitoring is shown in Fig. 12.

An infrared (IR) LED is used as the source and a phototransistor in switching mode as the detector. The IR LED emits a light beam and if there is no bee in the input channel the phototransistor will be off, which can be detected by a voltage measurement between the OUT pin and the ground (GND). If the phototransistor is off, the expected value of voltage at the OUT pin is equal to the V_{dd} . However, if a bee is present in the input channel it will reflect light towards the phototransistor which will go to the on state, and voltage at the OUT pin will drop to the collector-emitter saturation voltage as shown in Fig. 13.

A microcontroller (uC) with an embedded analog-to-digital converter (ADC) can be used for voltage measurement and data processing. Monitoring the daily activities of bees should be registered with information regarding time and date collected with a real time clock (RTC), as well as ambient temperature and relative humidity (RHT sensor).

- The hardware realization of the electronic system for bee activity monitoring (Fig. 14a) is based on an ATmega2560 microcontroller, 6 QTR Pololu pairs of IR LEDs and phototransistors, a DS3231 RTC and a Sensirion SHT11 RHT sensor. Tubes used for placement of the canvas substrates were used for the Pololu sensors as well (Fig. 14b).

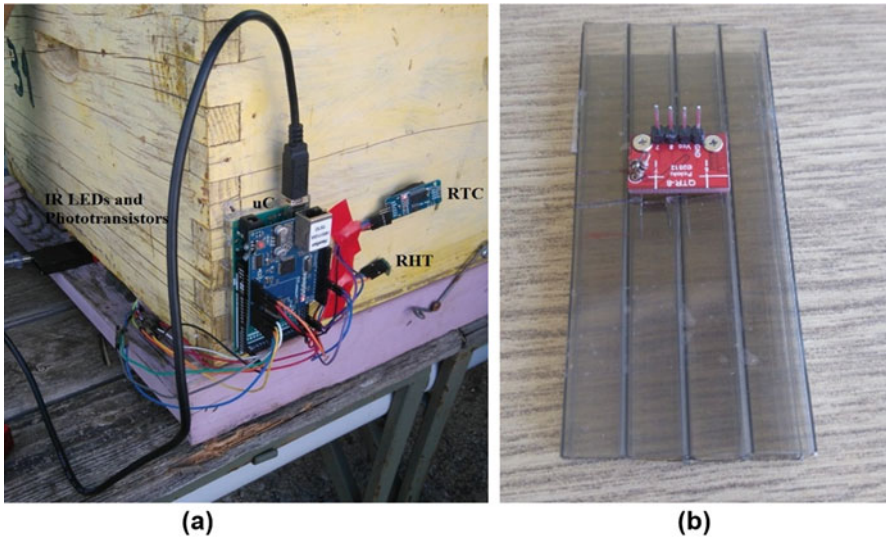


Fig. 14 (a) Hardware realization of the electronic system for bee activity monitoring. (b) Placement of the Pololu sensors on entrance and exit tubes

The electronic system for bee activity monitoring was tested at the Benkovac test site during September 2018. A selection of the obtained results from the monitoring of ambient air temperature ($^{\circ}\text{C}$), relative humidity (%RH) and percentage of input voltage compared to the Vdd are shown in Figs. 15 and 16. Results are presented starting from 5 am, with samples obtained every second. As shown in Fig. 15, it can be noticed that around 6:30 am bees started leaving the beehive along with an increase of temperature and a decrease in relative humidity.

However, channels at the entrance of the beehive (Fig. 16) registered lower level of activities, which was expected as bees start going out to look for food early in the morning.

The Bee4Exp project combines free-flying honeybees for passively sampling explosives materials, and actively trained bees to detect buried explosives with UAV-assisted monitoring. Passive sampling allows for explosives to be collected by foraging honeybees which then deposit the explosives on the surface of a preconcentrator which can then be introduced to an optical sensor for detection; this method is anticipated to be useful for area surveying and Quality Assurance post-clearing. The active method is intended to be able to pinpoint individual land mines in an area, with bee swarming over a suspected mine being followed and recorded by a camera mounted to an UAV, while an electronic system for monitoring of bee activity provides kinetic and environmental information. Both methods together may provide a robust beginning-to-end procedure for humanitarian demining.

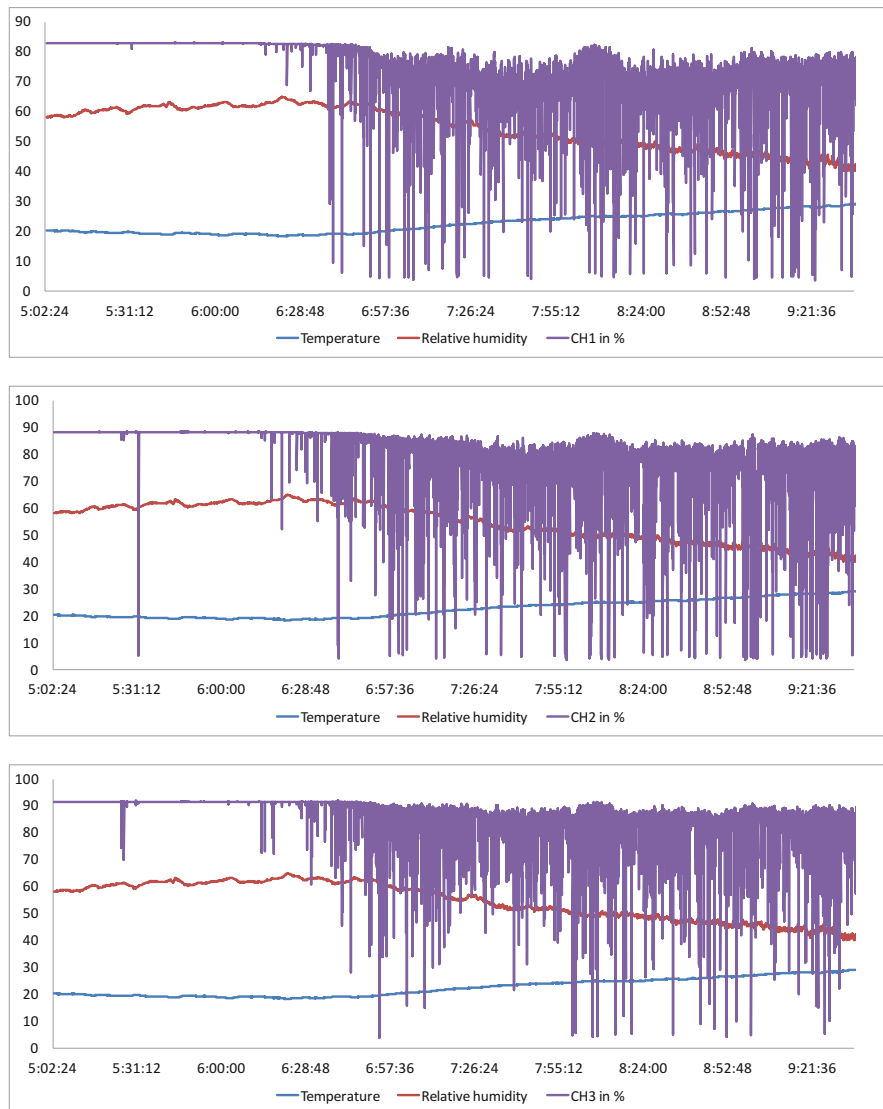


Fig. 15 Obtained results for channels at the exit of the hive

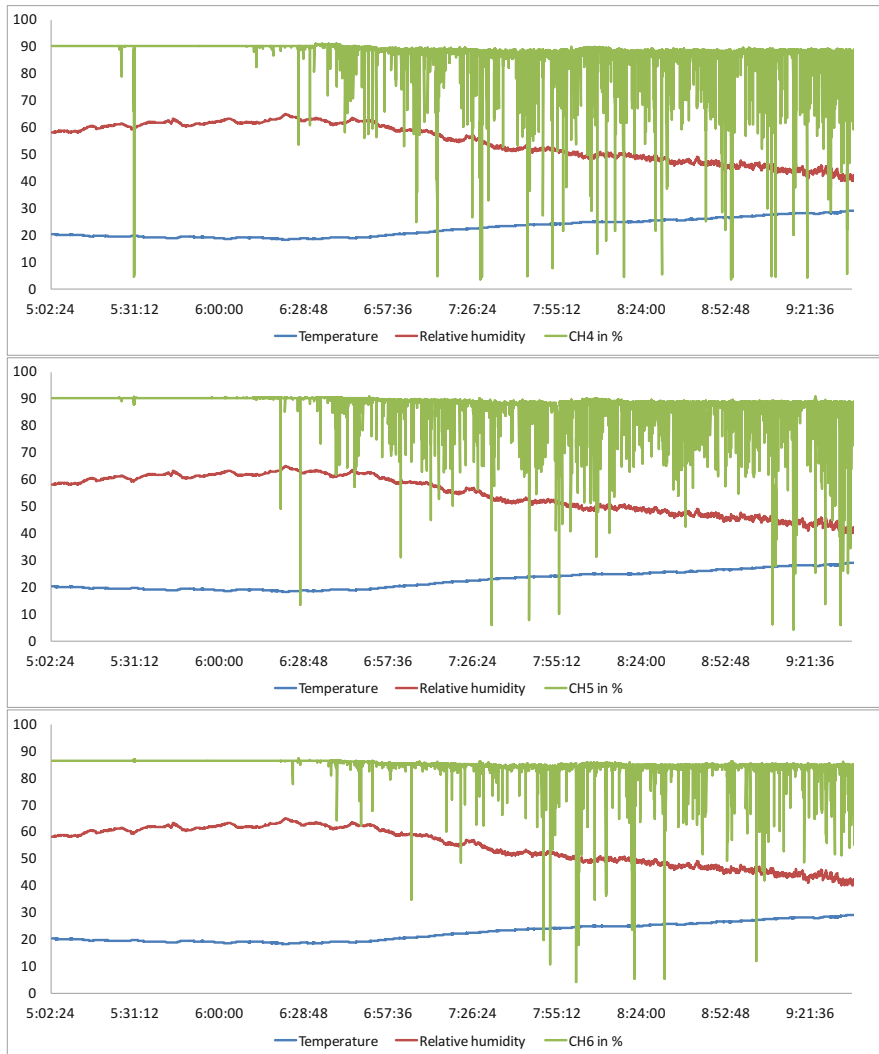


Fig. 16 Obtained results for channels at the entrance to the hive

Broader Impacts

Explain how this project will affect people, ecosystems, the environment, industry, commerce, transportation, international relations, or other aspects of life or society.

The impact of the project will be to provide new tools and methodologies for stand-off detection of minefields and individual landmines. The methods may be applied to suspected minefield area reduction and to confirm completion of the demining process in internal and external quality control. Current Remote Explosive

Scent Tracing techniques for technical surveys of minefields can suffer from delays of days to weeks when air/dust samples are transported to detection dogs in centralised facilities. By combining the search/collection of explosives by honeybees with imaging and sensing technologies the outcome of the detection process can be made in the same day in the minefield. These new tools should in the future help to reduce the time (and hence the cost) of detection and help mine action centres release land to civilian use. While these new tools will be tested in Croatia, they are low-cost technologies appropriate for use in many countries around the world.

Young Researcher Participation

- Discuss thesis projects and degrees resulting from the project
- Insert number / statistics about the young researchers status and involvement in the project.
- USTAN
- James ME Glackin, PhD, 2019, “Hybrid and organic semiconductor explosive sensors”
- UNIZG
- Dario Petrec, Masters thesis, 2019, “Improvements in GNSS location estimation using additional terrestrial station”
- UNIBL

Contributions

- Provide citations for conference papers, journal articles, book chapters, etc. arising from the project. See Springer Manuscript Guidelines for format.
- Preconcentration Techniques for Trace Explosive Sensing, Ross N Gillanders, James ME Glackin, Janja Filipi, Nikola Kezic, Ifor DW Samuel, Graham A Turnbull, *Science of the Total Environment* 658 (2019) 650–658
- Honeybee Activity Monitoring in a Biohybrid System for Explosives Detection, Mitar Simić, Ross Gillanders, Aleksej Avramović, Slavica Gajić, Vedran Jovanov-ić, Vladan Stojnić, Vladimir Risojević, James Glackin, Graham Turnbull, Janja Filipi, Nikola Kezić, and Zdenka Babić, International Conference on Medical and Biological Engineering (2019), Banja Luka
- Advances in Optical Sensing of Explosive Vapours, Ross N. Gillanders, James M.E. Glackin, Iain A. Campbell, Ifor D.W. Samuel, and Graham A. Turnbull, Photoptics 6 (2018) 323–327
- Bees for Explosive Detection, Nikola Kezić, Zdenka Babić, Janja Filipi, Graham Turnbull, Ross Gillanders, James Glackin, Goran Mirjanić, Mario Muštra and Nikola Pavković – Book of papers, The 15th International Symposium Mine Action 2018

- Improved organic semiconductor explosive sensors for application on minefields, authors: J.M.E Glackin, R.N. Gillanders, N.Kezić, J.Filipi, G.A.Turnbull – Book of papers, The 15th International Symposium Mine Action 2018

References

1. Abrol DP (2012) Pollination biology. Springer
2. Avramović A, Pilipović R, Stojnić V et al. (2018) Honeybee video-tracking for explosive detection. In: Proceedings of the International Symposium Mine Action 2018. pp. 44–48
3. Barisic D, Bromenshenk JJ, Kezic N et al. (2002) The role of honey bees in environmental monitoring in Croatia. In: Devillers J, Pham-Delegue M (eds) Honey Bees: estimating the environmental impact of chemicals. Taylor & Francis, New York, pp. 160–185
4. Bromenshenk JJ, Henderson CB, Seccomb RA et al. (2015) Bees as biosensors: chemosensory ability, honey bee monitoring systems, and emergent sensor technologies derived from the pollinator syndrome. Biosensors-Basel 5:678–711
5. Corbet SA, Beament J, Eisikowitch D (1982) Are electrostatic forces involved in pollen transfer? Plant Cell Environ 5:125–129
6. Egorov OB, O'hara MJ, Grate JW (2006) Equilibration-based preconcentrating minicolumn sensors for trace level monitoring of radionuclides and metal ions in water without consumable reagents. Ana Chem 78:5480–5490
7. Fjellanger R (2004) Remote explosive scent tracing – a method for detection of explosive and chemical substances
8. Free JB (1993) Insect pollination of crops. Academic Press Inc.
9. Gillanders RN, Glackin JME, Filipi J et al. (2019) Preconcentration techniques for trace explosive sensing. Sci Total Environ 658:650–658
10. Gillanders RN, Samuel IDW, Turnbull GA (2017) A low-cost, portable optical explosive-vapour sensor. Sens Actuators B-Chem 245:334–340
11. Girotti S, Ghini S, Maiolini E et al. (2013) Trace analysis of pollutants by use of honeybees, immunoassays, and chemiluminescence detection. Anal Bioanal Chem 405:555–571
12. Goodman L (2003) Form and function in the honey bee. International Bee Research Association
13. Hadagali MD, Suan CL (2017) Advancement of sensitive sniffer bee technology. Trac-Trends Anal Chem 97:153–158
14. Hammer M, Menzel R (1995) Learning and Memory in the Honeybee. J Neurosci 15:1617–1630
15. Heuschmann O (1929) Über die elektrischen Eigenschaften der Insekten Haare. Z Vgl Physiol 10:594–664
16. Kerk WC, Chua LS (2016) Sniffer bees as a good alternative for the current sniffing technology. Biointerface Res Appl Chem 6:1391–1400
17. Kezić N, Babić Z, Filipi J et al. (2018) Bees for explosive detection. In: Proceedings of the International Symposium Mine Action 2018. pp. 42–44

18. Leitch O, Anderson A, Kirkbride KP et al. (2013) Biological organisms as volatile compound detectors: a review. *Forensic Science International* 232:92–103
19. Martin M, Crain M, Walsh K et al. (2007) Microfabricated vapor preconcentrator for portable ion mobility spectroscopy. *Sens Actuators B-Chem* 126:447–454
20. Shoaei S, Chen SSY, Cavaye H et al. (2017) Assessing the sensing limits of fluorescent dendrimer thin films for the detection of explosive vapors. *Sens Actuators B-Chem* 239:727–733
21. Thomas SW, Amara JP, Bjork RE et al. (2005) Amplifying fluorescent polymer sensors for the explosives taggant 2,3-dimethyl-2,3-dinitrobutane (DMNB). *Chem Commun*:4572–4574
22. Thomas SW, Iii, Joly GD, Swager TM (2007) Chemical sensors based on amplifying fluorescent conjugated polymers. *Chem Rev.* 107:1339–1386
23. Tiwary N, Vinchurkar M, Patel M et al. (2016) Fabrication, characterization and application of ZnO nanostructure-based micro-preconcentrator for TNT sensing. *J Microelectromechanical Syst* 25:968–975
24. Vaknin Y, Gan-Mor S, Bechar A et al. (2000) The role of electrostatic forces in pollination. *Plant systematics and evolution* 222:133–142
25. Van Der Steen JJM, Bergsma-Vlami M, Wenneker M (2018) The Perfect Match: Simultaneous Strawberry Pollination and Bio-Sampling of the Plant Pathogenic Bacterium *Erwinia Pyrifoliae* by Honey Bees *Apis Mellifera*. *Sustain Agric Res* 7:25–32
26. Voiculescu I, McGill RA, Zaghloul ME et al. (2006) Micropreconcentrator for enhanced trace detection of explosives and chemical agents. *IEEE Sens J* 6:1094–1104
27. Wang P, Schneider NS, Sung NH (1999) Sorption and diffusion of organic vapors in two fluoroelastomers. *J Appl Polymer Sci* 71:1525–1535
28. Wilson ML (1987) The biology of the Honey Bee. Harvard University Press
29. Wolfbeis OS (2008) Fiber-optic chemical sensors and biosensors. *Anal Chem* 80:4269–4283
30. Yang JS, Swager TM (1998) Porous shape persistent fluorescent polymer films: An approach to TNT sensory materials. *J Am Chem Soc* 120:5321–5322
31. Zakon HH (2016) Electric fields of flowers stimulate the sensory hairs of bumble bees. *Proc Nat Acad Sci* 113:7020–7021
32. Zarić NM, Deljanin I, Ilijević K et al. (2018) Honeybees as sentinels of lead pollution: Spatio-temporal variations and source appointment using stable isotopes and Kohonen self-organizing maps. *Sci Total Environ* 642:56–62

Magnetic Resonance & Microwave Detection of Improvised Explosives and Illicit Materials

Bulat Rameev (✉)

Gebze Technical University, Gebze, Turkey

e-mail: rameev@gyte.edu.tr

Georgy Mozzhukhin

Gebze Technical University, Gebze, Turkey

Sergey Tarapov

O. Ya. Usikov Institute for Radiophysics and Electronics of NAS of Ukraine,
Kharkiv, Ukraine

İlhami Ünal

TUBITAK, Marmara Research Center, MILTAL Lab, Gebze, Turkey

Introduction

The detection of explosive and dangerous liquids is a very important issue in both airborne and critical infrastructure security [1, 2]. The techniques that provide the possibility of low-cost and reliable discrimination in a large group of various materials are especially interesting with respect their practical implementation in security scanners. In this chapter, we describe novel technology based on the application of two techniques of explosive detection: time-domain nuclear magnetic resonance (NMR) and micro/mm-wave dielectric spectroscopy. The main goal of our studies was to develop an effective and fast method of identification of explosive and illicit substances by the combined use of these techniques.

The first work on the application of NMR for the detection of dangerous liquids was published by L. J. Burnett [1] and his colleagues [3]. In this work, the parameters obtainable using low-field or time-domain (TD) NMR for scanning liquid substances in security checkpoints were defined as follows: the signal amplitude (A_0); the spin-lattice relaxation time (T_1); the spin-spin relaxation time (T_2); the diffusion constant (self-diffusion coefficient – SDC) (D); and the spin-spin coupling constant (J). In principle, the measurement of signal amplitude is easy to realize in NMR measurements with a calibrated container, as in the case of invasive (type A) NMR scanners. However, measuring the signal amplitude is typically more difficult in the situation of a universal bottle scanner of type B, because the quantity of liquid in a container (bottle, small glass or plastic container, etc.) is different and the mass of the container can vary as well. In addition, the NMR signal amplitude depends on a number of experimental parameters. These should all be taken into account using very careful calibration, but this is hardly possible in practical situations. On the other hand, measurements of the spin-spin coupling constant require a magnetic field

with homogeneity of about 1 ppm, while typical *low-cost* permanent magnet systems have homogeneity at the level of 100 ppm at best. Therefore, in most cases only three parameters: the spin-lattice relaxation time (T_1), the spin-spin relaxation time (T_2), and the diffusion constant (D) (the so-called self-diffusion coefficient, SDC) can be exploited to identify liquid substances using time-domain NMR (TD-NMR). The most technically simple solution is to apply the TD NMR (or NMR relaxometry) to measure only the spin-lattice relaxation time (T_1) and the spin-spin relaxation time (T_2), since for the detection of D, additional hardware should be used to apply the pulse gradient of the magnetic field to the sample [1–4]. Unfortunately, there is no obvious law for the T_1 and T_2 value distributions in various groups of liquids [3, 5, 6, 7]. Therefore, the use of ^1H NMR relaxometry alone does not provide enough discrimination among a large group of substances (i.e. in the typical airport situation). For that reason, additional parameters for discrimination (e.g., real and imaginary permittivity, ^{14}N NMR signal, and D constant) need to be obtained in parallel to ^1H TD NMR. Thus, effective approaches based on the acquisition of additional NMR or other information should be developed. In our study, in addition to standard ^1H TD NMR, we apply ^{14}N TD NMR as well as a MW/mm-wave technique, which probes the complex dielectric permittivity and has the potential advantage of easy integration with the time-domain NMR in a single detection device.

In this chapter, we first present ^1H TD NMR approaches which may be applicable for the fast scanning of liquids. We then present the results of time-domain ^{14}N NMR measurements of nitrogen-containing substances that have been analyzed with a view toward their use in discrimination in a broad class of nitrogen-containing energetic materials. Thirdly, we discuss the MW detection technique applied in a broad range of frequencies with the use of various sensors that have been explored.

NMR Sequences for T_1 and T_2 Relaxation Measurements

The most important problem of ^1H TD NMR is developing a method which allows for *fast* detection measurements of the relaxation (T_1 , T_2) and, if possible, diffusion (D) parameters. It is clear that classical NMR methods, e.g., T_1 measurements, cannot be directly applied because of the very long measurement times (several minutes at least). Therefore, special attention should be given to the NMR measurement methods that last at most several seconds.

We first review both the classical methods and the recently proposed approaches of fast measurements of T_1 and T_2 below. We then demonstrate an application of prospective sequences in ^1H TD NMR measurements for detection of some flammable liquids and hydrogen peroxide (an explosive precursor).

There exist a vast number of different methods for measurements of T_1 and T_2 . Below we briefly mention the following methods: the Carr-Purcell-Meiboom-Gill sequence (CPMG), saturation recovery sequence, superfast inversion recovery (SURFIR), correlation function of T_1 - T_2 , drive equilibrium CPMG, CRELAX for combined T_1/T_2 measurements, T_2 -Filtered T_2 - T_2 Exchange NMR, and the Csaki-

Bene sequence. Unfortunately, it is not possible to consider all of the possible sequences due to space limitations.

The Carr-Purcell-Meiboom-Gill Sequence (CPMG)

Similar to the simple but time-consuming Hann-spin echo, the GPMG sequence is very often used in TD-NMR devices to measure the relaxation time T_2 . The advantage of the CPMG sequence is the relatively short time needed for accurate T_2 measurements. In laboratory NMR measurements, the total time of “single shot” measurements (i.e., a single CPMG series without averaging repetitions to increase the SNR of the NMR signal) is about $5*T_2$. Taking into account that the T_2 time constant for most liquids does not exceed 3 seconds, it implies that the time for T_2 measurements of an unknown liquid by CPMG is at most 15 s. The signal amplitude is defined by the following formula:

$$M(t) = M_0 \exp \left(-\left(\frac{1}{3} \gamma^2 g^2 D \tau^2 + \frac{1}{T_2} \right) t \right)$$

where M_0 is the initial amplitude of the signal, T_2 is the time of spin-spin relaxation, D is the diffusion coefficient, γ is the gyromagnetic ratio, and g is the gradient (or non-uniformity) of the static magnetic field. Here, we see that diffusion may affect the T_2 measurements in the case of long τ times and *non-uniform magnetic fields*. Therefore, in the TD NMR experiment with a magnet system having an inhomogeneous magnetic field, it is important to set a short time τ to exclude the influence of diffusion in the experimental value of T_2 . On the other hand, if the static magnetic field gradient is applied, it is possible to obtain both T_2 and D if *at least two CPMG measurements* with different values of “echo” times (τ) are used [8] (Fig. 1).

Saturation Recovery Sequence

There are two basic sequences to measure the time T_1 : inversion recovery and the *saturation recovery sequence* (Fig. 2). They are similar to each other, with the only difference being an initial state formed by the first pulse. In inversion recovery, inversion of the magnetization with a 180° degree pulse is used to trace the signal decay with time, while in the *saturation recovery sequence* the first pulse is the “saturating” 90° pulse. Although they are similar, the latter technique is preferred because the total time needed for the measurements is smaller.

In the experiment the signal is first saturated by a 90 degree pulse, and after waiting a variable time τ_n , the restoration of the magnetization from zero to equilibrium value M_∞ is probed with another short 90 degree pulse to measure the FID signal. In this manner, one can see how much the magnetization is restored towards

Fig. 1 The CPMG sequence: the diagram above shows the sequence of RF excitation pulses, while the diagram below demonstrates the first FID signal with following echo signals centered at the time points of 2τ , 4τ , ..

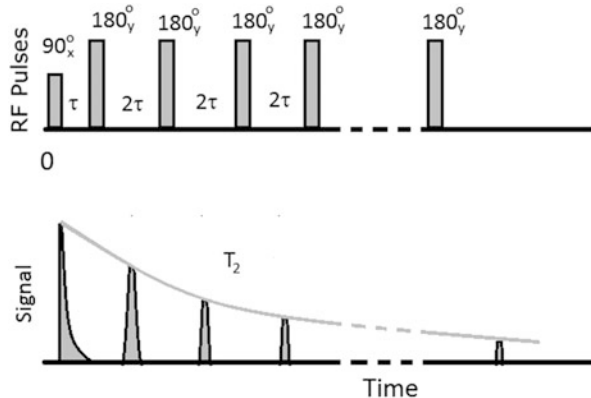
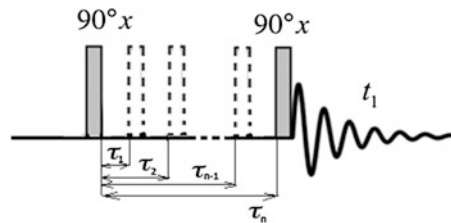


Fig. 2 Saturation recovery sequence for the detection of T_1



equilibrium after waiting the time τ_n . The decay of the signal amplitude is defined as follows:

$$M_z(\tau) = M_0 \left[1 - \exp \left(-\frac{\tau}{T_1} \right) \right]$$

However, the fact that a second “measurement” pulse has been applied means that the magnetization recovery process is broken by this measurement, therefore the cycle of application of saturation 90° pulse and measurement 90° pulse should be repeated again using another evolution (“recovery”) τ_n . It is clear that between each repetition a nuclear system should relax again to equilibrium (at least $2.5 \cdot T_1$). Although this time is half as long as $5 \cdot T_1$ in the case of inversion recovery (which is also often used to measure T_1), the total time of all measurement cycles is unacceptably high due to the repetition of N changes to τ_n (e.g., for inversion recovery: $T_{IR} = N \cdot 5 \cdot T_1 + T_{aq} + T_1$, where T_{aq} is the acquisition [or measurement] time [9]).

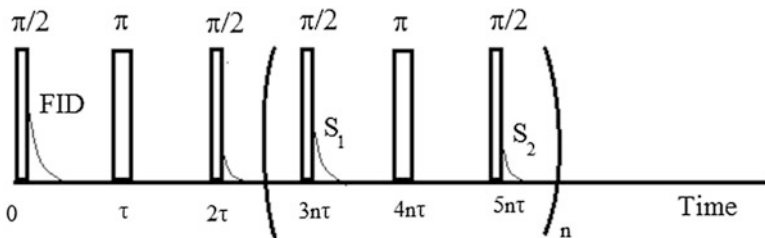


Fig. 3 The superfast inversion recovery (SURFIR) sequence

Superfast Inversion Recovery (SUFIR)

The superfast inversion recovery (SUFIR) sequence is one of the sequences proposed for fast determination of T_1 [10]. This sequence is shown in Fig. 3.

The value of T_1 is determined by Free Induction Decay (FID) amplitudes according to the following formula:

$$T_1 = -\tau / \ln \left(1 - \frac{S_2}{S_1} \right)$$

The SUFIR has an important advantage that it enables the detection of T_1 for a “single shot” cycle of observation with the provision that time T_2 is shorter than T_1 . In this case, the detection time is comparable to T_1 (in the range of $0.5T_1 \leq \tau \leq 3T_1$). However, if the T_2 and T_1 values of relaxation parameters are very close to each other, then the transverse magnetization is maintained until the beginning of each RF pulse. This in turn produces undesirable spin-echo contributions to S_1 and S_2 signals. In this case, up to eight SUFIR sequences with phase cycling of RF pulses are needed to filter out this spurious contribution to S_1 and S_2 . This in turn leads to an increase in the total measurement time to at least several factors of T_1 . Another disadvantage is that this sequence is appropriate for determining the time constant T_1 of substances characterized by a *mono-exponential T_1 recovery process*.

T_1 - T_2 Correlation Sequence

Multidimensional correlation is a well known and broadly used concept in modern NMR spectroscopy, for studies of both molecular structures and dynamics [11]. In the case of TD NMR, the measurements of the so-called T_1 - T_2 correlation function have been known for years. An algorithm for fast, two-dimensional inverse Laplace transformation to obtain T_1 - T_2 correlation functions may also be used for substance analysis [12] (Fig. 4).

The data obtained are presented as a two dimensional array $M(\tau_1, \tau_2)$, where τ_1 is the recovery time and τ_2 is the echo time.

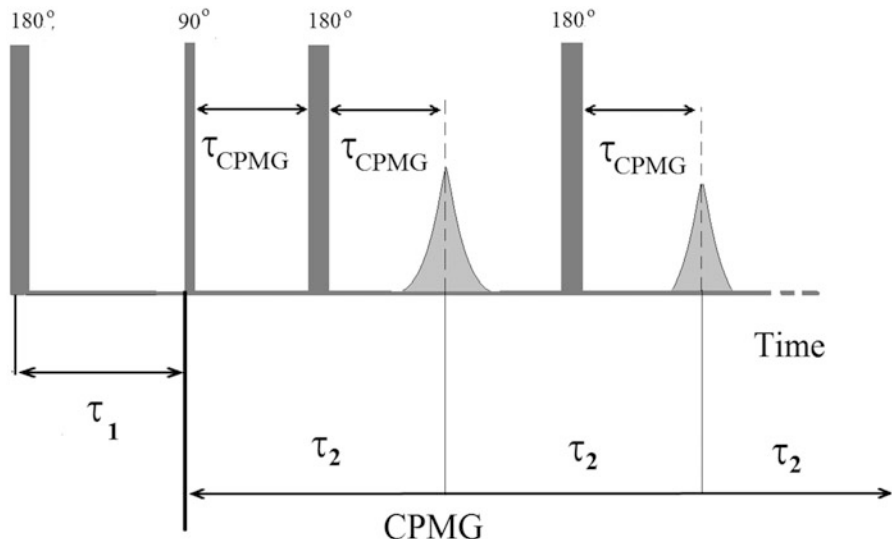


Fig. 4 The inversion recovery sequence detected by CPMG is used for the T_1-T_2 correlation experiments. CPMG signals were collected for typically 30 values of τ [14]

$$M(\tau_1, \tau_2) = \iint \left(1 - 2e^{-\frac{\tau_1}{T_1}}\right) e^{-\frac{\tau_2}{T_2}} F(T_1, T_2) dT_1 dT_2 + E(\tau_1, \tau_2),$$

Here $E(\tau_1, \tau_2)$ is the experimental noise and the function $F(T_1, T_2)$ corresponds to the probability density of molecules with relaxation times of T_1 and T_2 .

In the above-mentioned work, a new algorithm for the two-dimensional Laplace transform was proposed for the correlation function of T_1-T_2 . However, the time needed for 2D experiments is nearly 2–3 h. Therefore, although this technique provides very rich information, it cannot be used for fast scanning of substances in our case.

CRELAX Sequence for Combined T1/T2 Measurements

In this method (see also [13, 14]), the magnetization of the sample is initially saturated, so that the recovery of the magnetization is observed. Recording of NMR signals, which start out with completely saturated magnetization (in fact, apart from the fully saturated state, the substantially saturated state of initial magnetization is also possible), has the advantage that the repetition time between the individual measurements can be selected to be short. CRELAX starts with a saturation pulse sequence, consisting of a $\pi/2$ pulse followed by a series of $i \pi$ pulses. After some delay D , the duration of which is gradually increasing in successive recordings, a CPMG sequence is applied with a number $n(m)$ of repetitions of π pulses to record the decaying echo signals. The free induction decay (FID), shown by dashed lines in

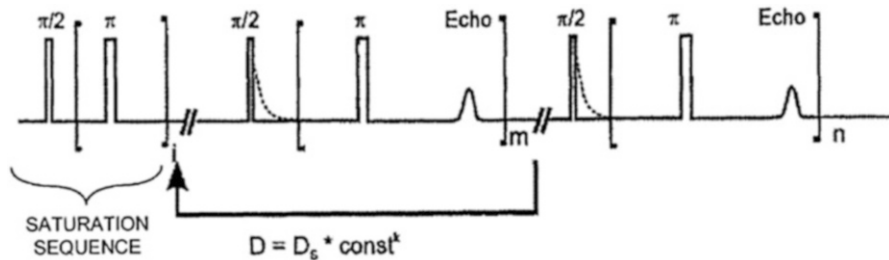


Fig. 5 CRELAX pulse sequence according to the Ref. [16]

Fig. 5, can be acquired as well in order to quickly record relaxing components of the sample to be measured. The delay time of this sequence is cycled as $D = D_s \cdot (\text{const})^k$, where const is dependent on the substance, and a power k equals to a successive index of the probing CPMG sub-sequence. Thus the time D is gradually increasing evolution delay before the next CPMG sub-sequence begins. The duration of the experiment depends on the relaxation parameters of substances. For instance, a single CRelax series, used for the quantification of oil and protein in cottonseeds, lasted near 40 seconds [15]. In fact, this sequence, which looks very promising for a number industrial applications (including the detection of counterfeit food products), may be modified to work even faster for use in bottle scanners. In principle, this is possible by using not a full but a reduced pulse train. However, in this case instead of measurements of the true T_1 and T_2 relaxation times, some effective (apparent) characteristic relaxation times (which depend on the real values of T_1 and T_2) are used for discrimination.

Csaki –Bene Sequence for Measurements of T_1

The Csaki-Bene sequence was proposed for acceleration of the process of T_1 measurements as early as 1960 [16]. In this sequence, the first pulse rotates the vector of nuclear magnetization at angle 180° , then the evolution of the component M_z will be defined by an exponential dependence on spin-lattice relaxation time (T_1). Csaki and Bene proposed to add after the first pulse a group of three pulses, $90^\circ - t_2 - 180^\circ - t_2 - 90^\circ$, separated by time t_s from the first pulse. The pulse group is repeated periodically. Within the sequence the nuclear magnetization is observed after second 180° pulse. The last 90° pulse in a group returns the magnetization to initial state, because the total effect of the three pulses is rotation of 360° . An important condition for the sequence is $2t_2 < T_2$ (Fig. 6).

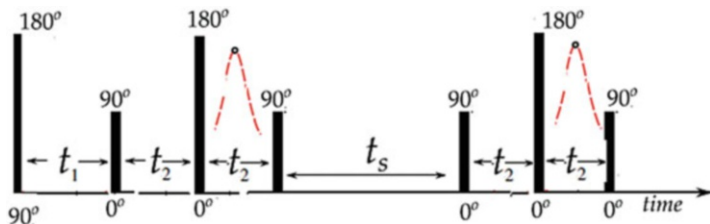


Fig. 6 Csaki-Bene sequence [18]

The behavior of nuclear magnetization can be given by following formula:

$$A(t) = A_0 \left| 1 - 2e^{-\frac{t}{T_1}} \right|,$$

Here $t = t_1 + [t_2 + t_2(\text{acquisition time}) + t_s]n$, where n is number of cycles, related to T_1 value as follows:

$$n \sim 3T_1 / \{ t_1 + [t_2 + t_2(\text{acquisition time}) + t_s] \}$$

Thus, a minimally possible time of measurements is defined by a single sequence duration. For protons we need only a single scan (may be as small as 5 seconds), while for nitrogen we usually need to average a signal for the better detection (because the SNR of ^{14}N is only 0.02 of the SNR of protons). In our experiments for 1 ml we need approximately 50 seconds to obtain the $\text{SNR} > 10$ and 15 seconds for $\text{SNR} > 5$.

Conclusions on the Practical Use of the Above NMR Sequences

The discrimination based on two parameters (T_1 and T_2) may be optimized using fast measurement sequences (e.g. the Csaki –Bene sequence). In any case, for shortening the time of detection by ^1H TD NMR, a two-mode regime can be implemented in the bottle scanner: a “quick scan” and a “full scan” as proposed in Ref. [5]. For instance, in the “quick scan” mode, only the parameter T_2 is measured and is compared with the database. Depending on the results (whether the value for the time T_2 is within the range for dangerous liquids), the “full scan” mode can be applied sequentially. For the first mode, the time for detection is expected to be below 15 s, while for the second mode it may be in the range of 25–90 seconds. Taking into account that apparent T_1 and T_2 values depend on the details of the experimental setup as well as on the value of magnetic field of the bottle scanner, a special “learning mode” for adding NMR data to the database as well as “diagnostic mode” for self-testing of the device should be also be available in the prototype of the bottle scanner.

¹H TD NMR Measurements for Detection of Liquids

General Consideration and References to Previous Work

During our studies on development of a NMR detection technique a large number of various dangerous liquids have been measured (the authors from GTU had already started the studies in this direction during the NATO SfP project No. 982836, 2010–2013). The results of these studies have been published in the papers [7,8,9]. The measurements have been done for approximately 70 beverages. All of them were divided to 5 groups of liquids: water, soft drinks, juices, milk & dairy produce, and alcoholic drinks. Approximately 10 potentially dangerous liquids have been measured as well: liquids that can be used as a precursor for explosives and flammable solvents and are potentially dangerous liquids that are banned for public transportation. Based on those measurements we concluded that NMR measurements of three parameters ($T_1 - T_2 - D$) instead only one or two parameters significantly increases the reliability of liquid discrimination in security scans. Furthermore, if pre-known information on a scanned bottle is used from the database (using, e.g., a barcode label), the measurement of all three parameters can be excluded in great number of typical liquid scans. Thus, the measurement of a number of parameters to increase identification accuracy is needed only in limited number of cases. It is also clear a smart protocol of identification should start from measuring of only one (T_2) or two parameters (e.g. T_1-T_2 or T_2 – dielectric permittivity) and should proceed only as needed with measurements of the third (the diffusion constant or dielectric permittivity).

It is obvious from the previous discussion above that the main issue in classical NMR sequences is the long time needed to measure relaxation parameters (especially T_1). Unfortunately, the same issue appears in the case of traditionally used NMR sequences to obtain the diffusion parameter D. The experiment time is as long as 30 min for variants of the classical Pulsed Field Gradient Stimulate [Spin] Echo sequence (PFG STE or PFG SSE), and it can be shortened to less 1 min in the case of so-called one-shot pulse sequence. Thus, it is clear that shortening the total NMR measurement time is critical issue in the case of NMR detection based on multi-dimensional ¹H TD NMR. Therefore, the feasibility of ¹⁴N NMR detection (see the next section) has been explored as an alternative approach to make NMR detection faster, because it is known that the relaxation times of ¹⁴N usually are very short. The fast ¹⁴N relaxation results in much broader and consequently weaker ¹⁴N NMR signals. Of course, this presents a technical challenge, but, at the same time, *it becomes an advantage because the acquisition times of ¹⁴N NMR measurements are much shorter.*

It is clear that in any case that the ¹H TD NMR technique could be used to detect some flammable liquids or hydrogen peroxide (a precursor for TATP explosive). A very detailed database of ¹H NMR relaxation parameters (T_1 and T_2) at a broad range of magnetic fields and for very different dangerous and benign liquids should be built to help in development of a security-scanning device. However, in our opinion,

the first task of the work on ^1H TD NMR should be related to the development of smart (fast) protocols for ^1H TD NMR.

A Few Examples of Typical ^1H TD NMR Measurements

Below are a few examples of typical ^1H NMR experimental signals of distilled water (H_2O) and peroxide (H_2O_2) measured on an Apollo console using both “one shot” sequences (Figs. 7, 8, 9 and 10).

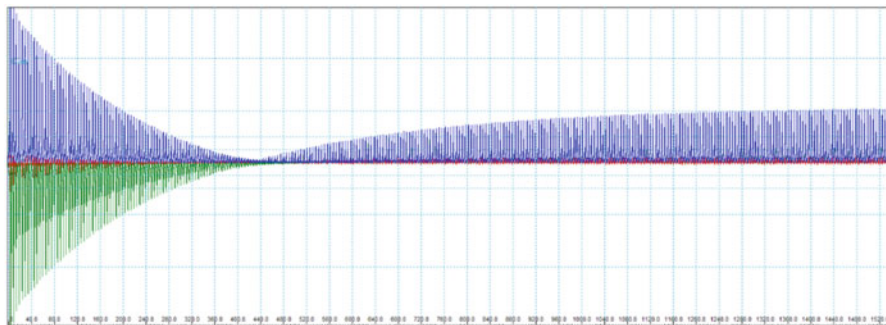


Fig. 7 ^1H TD NMR signal of distilled water (H_2O) on an *Apollo Tecmag* NMR Console by application of the Csaki-Bene sequence with the following parameters $t_1 = 50$ ms, $t_2 = 5$ ms, $t_s = 15$ ms. The spin-lattice relaxation time is $T_1 = 3300 \pm 35$ ms. The measurement frequency is 24.5 MHz. The total time for the measurements is 8 s

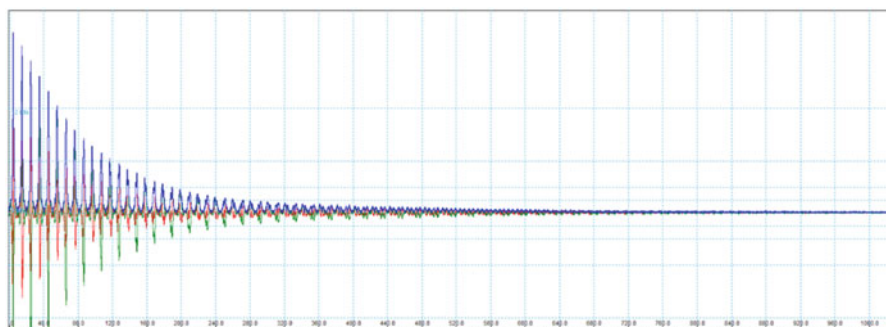


Fig. 8 ^1H TD NMR signal of distilled water (H_2O) on an *Apollo Tecmag* NMR Console obtained by the CPMG sequence with the following parameters ($\tau = 20$ ms, $t_{\text{pulse}} = 50$ μs). The spin-spin relaxation time is $T_2 = 2900 \pm 80$ ms. The measurement frequency is 24.5 MHz. The total time for the measurements is 5 s

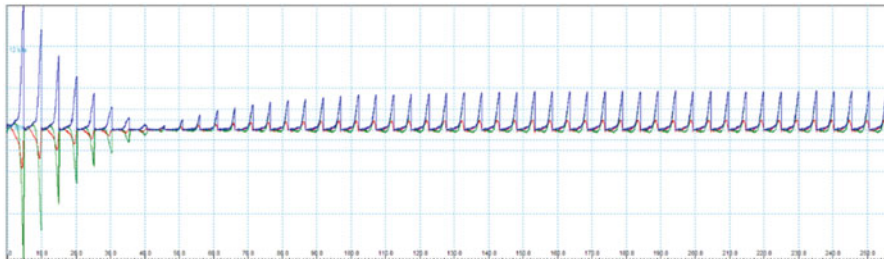


Fig. 9 ^1H TD NMR signal of hydrogen peroxide (H_2O_2) on an *Apollo Tecmag* NMR Console by application of the Csaki-Bene sequence with the following parameters $t_1 = 5$ ms, $t_2 = 5$ ms, $ts = 15$ ms. The spin-lattice relaxation time is $T_1 = 1239 \pm 150$ ms. The measurement frequency is 24.5 MHz. The total time for the measurements is 5 s

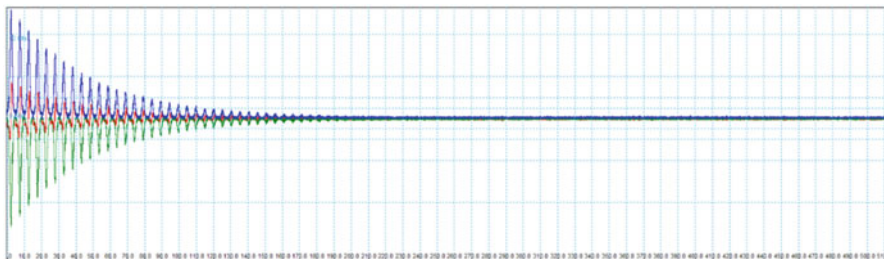


Fig. 10 ^1H TD NMR signal of hydrogen peroxide (H_2O_2) on an *Apollo Tecmag* NMR Console obtained by the CPMG sequence with the following parameters ($\tau = 20$ ms, $t_{pulse} = 50 \mu\text{s}$). The spin-spin relaxation time is $T_2 = 250 \pm 20$ ms. The measurement frequency is 24.5 MHz. The total time for the measurements is 5 s

Low Field ^{14}N NMR for Detection of Nitrogen-Containing Energetic and Dangerous Liquids

It is well known that most **solid** energetic and explosive materials include nitrogen nuclei of ^{14}N . However, the situation is similar in the case of **liquids**: a number of energetic and explosive liquid substances contain nitrogen in their structure. For that reason, the detection of the ^{14}N NMR signal as secondary parameter for more reliable detection of dangerous substances has been proposed by P. Prado et al. [17].

In this section, we first present the T_1 and T_2 parameters for NMR of ^1H nuclei in some nitrogen-containing liquids. We then proceed with ^{14}N TD NMR measurements of various nitrogen-based liquids, including dangerous and energetic materials.

The list of the most common explosive liquids containing nitrogen in their structure has been given in the patent [19] (see the Table 1). There is, however, an issue in the detection of ^{14}N NMR because the gyromagnetic ratio of ^{14}N nuclei is rather small in comparison to the ^1H signal. Therefore, the nitrogen NMR signal has a very small SNR.

Table 1 The list of the most common explosive liquids containing nitrogen in their structure

Material	Tested by ^{14}N NMR in our work, (Yes or No)*
Nitromethan	Yes
Nitroethan	Yes
Nitrobenzene	Yes
Nitric acid (HNO_3)	Yes
Ammonium nitrate NH_4NO_3	Yes
Hydrazine N_2H_4	No
Ethylene glycol Dinitrate, Nitroglycerol ($\text{C}_2\text{H}_4\text{N}_2\text{O}_6$)	No
Nitroglycerin ($\text{C}_3\text{H}_5\text{N}_3\text{O}_9$)	No
Picatinny liquid explosive (CH_3NO_2 , $\text{C}_2\text{H}_8\text{N}_2$)	No
Propylene glycol Dinitrate ($\text{C}_3\text{H}_6\text{N}_2\text{O}_6$)	No
Tetranitromethane CN_4O_8	No
Dinitrogen tetroxide N_2O_4	No

aSome of dangerous substances were unavailable to our laboratory because of their toxicity or self-detonation risk

The NMR nitrogen detection of energetic substances is characterized by the following features:

- The relative sensitivity of ^{14}N NMR is close to 0.018 of the sensitivity of NMR of ^1H .
- A number of liquid explosives containing ^{14}N has an NO_2 group.
- The number of illicit and explosive liquids containing nitrogen in their structure is rather limited. Therefore, in the fast scanning protocol the presence of a ^{14}N NMR signal already indicates a threat. However, because ^{14}N measurements are quite fast, it is possible to probe one or two relaxation parameters to identify a liquid explosive material. On the other hand, two relaxation constants, T_1 and T_2 , are not enough in the case ^1H TD NMR, which needs to use an additional parameter for discrimination due to very large group of hydrogen-containing liquids.

Experimental Details A special setup to check the feasibility of ^{14}N NMR detection has been assembled. In the setup, a homemade permanent magnet system with a magnetic field of 0.475 T and a homemade RF probe with resonance frequency of 1.775 MHz have been used. A *Tecmag Apollo* NMR console and 500 W *Tomco* power amplifier have been used in the NMR experiments.

Experimental Results and their Discussion

^1H TD NMR of Nitrogen-Containing Liquids

Firs the T_1 and T_2 parameters for NMR of ^1H nuclei in some nitrogen-containing liquids were measured (see Table 2).

Table 2 The results of the measurements of NMR ^1H (1 ml, temperature of 40 °C, 24.69 MHz)

Name	T_1 , s ^1H	T_2 , s ^1H	T_1/T_2 ^1H
Nitromethan	3.56 ± 0.02	3.43 ± 0.2	1.03
Nitroethan	3.4 ± 0.08	3.3 ± 0.12	1.03
Nitrobenzene	2.70 ± 0.1	2.7 ± 0.1	1
Nitric acid (HNO_3)	2.57 ± 0.02	2.55 ± 0.02	1.007
Ammonium nitrate	3.34 ± 0.2	1.33 ± 0.2	2.5
Peroxide (H_2O_2)	1.55 ± 0.2	0.276 ± 0.02	5.61
$\text{Mg}(\text{NO}_3)_2 \cdot 6\text{H}_2\text{O}$	1.86 ± 0.2	1.84 ± 0.2	1.01

aIn this table, T_1 parameters were measured by the Csaki-Bene method (Fig. 9), T_2 parameters were measured by CPMG. We used an *Apollo Tecmag* NMR Console with the *Spincore* permanent magnet (about 0.575 T) and *Chromatek Proton-20 M TD-NMR* spectrometer with a working frequency of 22.9 MHz ($B_0 = 0.538$ T) at 40 °C

^{14}N NMR of Nitrogen-Containing Liquids

The time domain ^{14}N NMR signal has been successfully detected in all nitrogen liquids included in the test set. The results of ^{14}N NMR relaxation measurements of the nitrogen-containing liquids are summarized in Table 3 below. We used the CPMG sequence for measurements of T_2 and the inversion recovery sequence for measurements of T_1 . The measurements were done at room temperature with a resonance frequency of 1.777 MHz and a sample volume of 1 mL.

A very interesting result has been achieved in the NMR measurements of a water solution of ammonium nitrate (AN). The NMR of AN is characterized by rather narrow ^{14}N lines due to smaller contribution of quadrupole channel of relaxation. It is a result of highly symmetric coordination of nitrogen, especially for ammonium cation. We have observed that the frequency (Fourier Transform) spectrum of this compound contains two lines in accordance with typical chemical shift values of nitrogen for nitrate anion and ammonium cation coordinations.

The T_1 relaxation times are presented below in Fig. 11 shown as the bar plot with a logarithmic scale. For all liquids, excepting the NH_4^+ line in ammonium nitrate, the T_2 times are very close to the T_1 relaxation time. For the NH_4^+ line in ammonium nitrate, the value of T_2 is also given in Fig. 11.

The relaxation parameters (except for the NH_4^+ of AN) have been calculated using *Tools capture* of the *NTNMR* software package. The parameters for the NH_4^+ of AN have been calculated using the *Origin* program to exclude the influence of the magnet temperature shift during the long experiment time.

All the results presented above have been obtained by the standard NMR protocols usually applied to measure T_1 and T_2 relaxation times: *inversion recovery* and *CPMG* sequences, respectively. The CPMG sequence is quite a fast protocol, while the inversion recovery sequence is not. Therefore, at the next step we have first analyzed what is the most promising sequence to obtain the relaxation constant T_1 . Based on our total time calculations (see the results in Table 4) and the possibility of

Table 3 ^{14}N NMR relaxation parameters of the measured liquids

Material	T_2 , ms	T_1 , ms
Nitromethane CH ₃ NO ₂	17.83 ± 0.6	18.38 ± 0.5
Nitroethane C ₂ H ₅ NO ₂	12.9 ± 0.9	12.6 ± 0.5
Nitrobenzene C ₆ H ₅ NO ₂	2.44 ± 0.3	2.85 ± 0.5
Nitric acid (HNO ₃)	25.38 ± 1.6	27.9 ± 0.5
Ammonium nitrate NH ₄ NO ₃		
NO ₃ - 1	43.9 ± 3.5	49.4 ± 2.0
NH ₄ + 2	78.62 ± 16.51	1325 ± 220
Potassium nitrate KNO ₃	60.09 ± 4.5	59.8 ± 1.0
Sodium nitrite NaNO ₂	~ T_1	≤ 0.4
Lead nitrate Pb(NO ₃) ₂	19.04 ± 2.1	19.24 ± 1.0
Magnesium nitrate hexahydrate mg(NO ₃) ₂ 6H ₂ O	38.09 ± 2.6	39.54 ± 1.0
Dimethylformamide C ₃ H ₇ NO	~ T_1	1.07 ± 0.1
Dimethylacetamide CH ₃ C(O)N(CH ₃) ₂ .	~ T_1	0.67 ± 0.1
Acetonitrile CH ₃ CN	3.8 ± 0.2	3.77 ± 0.15

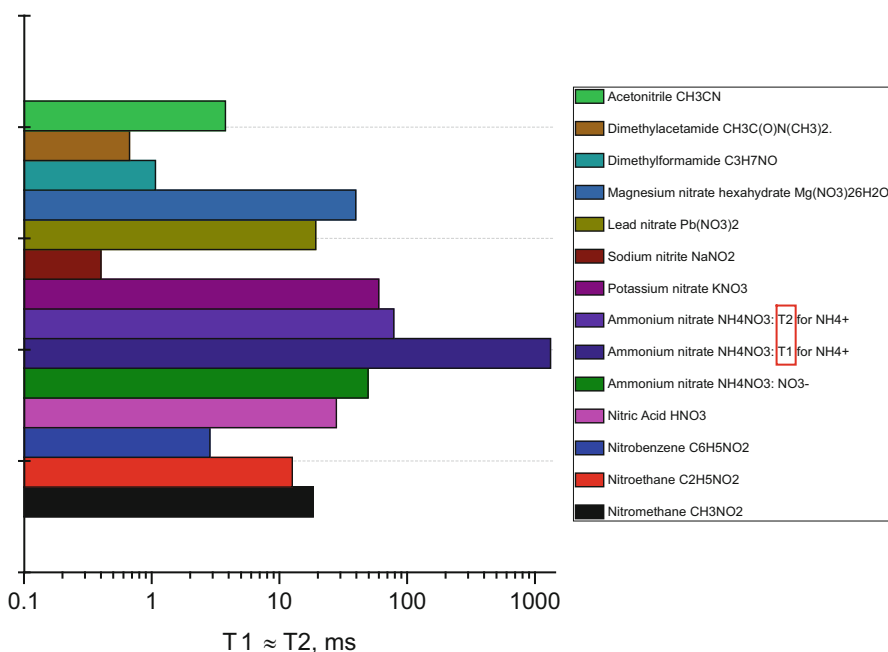


Fig. 11 T_1 relaxation times are shown in the bar plot with the logarithmic scale. For all liquids, except the NH₄⁺ line in ammonium nitrate, the values of the relaxation time T_2 are very close to T_1 . The only exception is the NH₄⁺ line in ammonium nitrate solution in water; the value of T_2 for this material is given as separate bar in Fig. 3

Table 4 Estimated time for measurements of T_1 and T_2 for nitromethane at room temperature by various experimental protocols. NMR frequency is near 1770 kHz, **100 averages**

Sequence	Common time of measurement, s
Free induction decay (FID)	50
Inversion recovery	500
Saturation recovery	500
Echo T2 measurements	240
CPMG	50
Csaki -Bene	50

realizing them effectively using our experimental equipment (the Apollo and KEA-2 NMR consoles), we came to the conclusion that the Csaki-Bene sequence looks more promising.

Both the CPMG and Csaki-Bene sequences allow recording of the experimental curves by “one shot” measurements. Due to the low SNR of ^{14}N NMR in comparison with ^1H NMR as well as due to the small volume of the sample (**1 mL**), we applied 100 averages to detect of the nitromethane signal with SNR ~ 10 (Table 4).

The representative NMR curves for nitromethane and ammonium nitrate samples obtained with the Csaki-Bene sequence are presented in Figs. 12 and 13, respectively.

It should be noted that the accuracy of the measurements is defined by spacing in time between radiofrequency pulses in CPMG and the Csaki-Bene sequence. One should also take into account the effect of inhomogeneities in radiofrequency and magnetic fields, and deviations of RF pulse durations (amplitudes) from an ideal 90° and 180° pulse condition are expected to affect measurement accuracy. The development of the most effective measurement protocol is a very important task and we plan to work toward its effective implementation in both ^{14}N and ^1H TD-NMR in the next project period.

Conclusion We have studied an approach based on the detection of ^{14}N NMR signal as an additional parameter to discriminate between various liquids. The feasibility of ^{14}N NMR detection of various energetic and illicit liquids has been demonstrated. ^{14}N NMR signals of various nitrogen-based substances have been successfully detected, and the relaxation parameters of the ^{14}N signals have been obtained. We also show that due to large chemical shift values of ^{14}N NMR signal, it is possible to observe splitting of FT NMR spectra of nitrogen-based compounds even by low field NMR devices (in our case, at 0.475 T that corresponds to a frequency of ^{14}N NMR of 1.775 MHz). It is possible to identify liquid explosives on the basis of two parameters ($T_1 - T_2$) in the case of a small group of substances. The time of measurements is small (≤ 50 s) because values of $T_1 - T_2$ are typically short for ^{14}N nuclei. In these experiments, the samples of very *small volume* (only 1 mL) have been measured, and therefore a set of 100 of averages has been used to detect the signal. Therefore, a fast liquid scanning protocol (with a **duration below a few seconds**) is feasible for larger scanning volumes and/or more sensitive detection probes. Some technical challenges

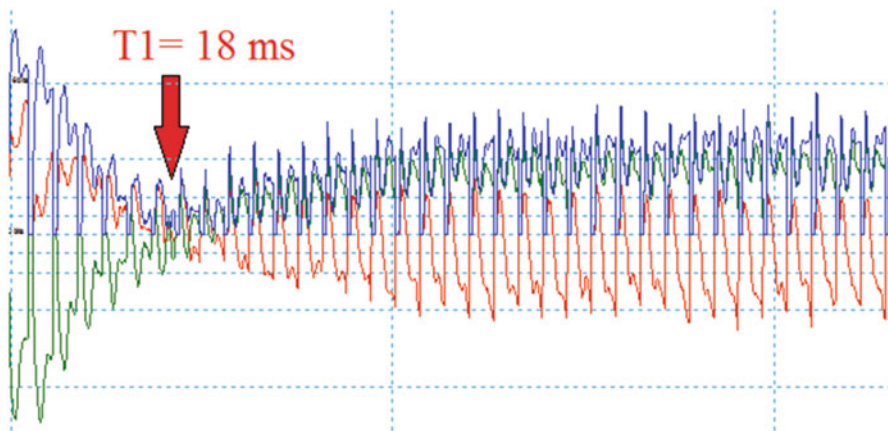


Fig. 12 The Csaki-Bene sequence in nitromethane (an interval between RF pulses is about 1 ms). The minimum point of the signal approximately corresponds to the relaxation time T_1 ($\sim 18 \text{ ms}$)

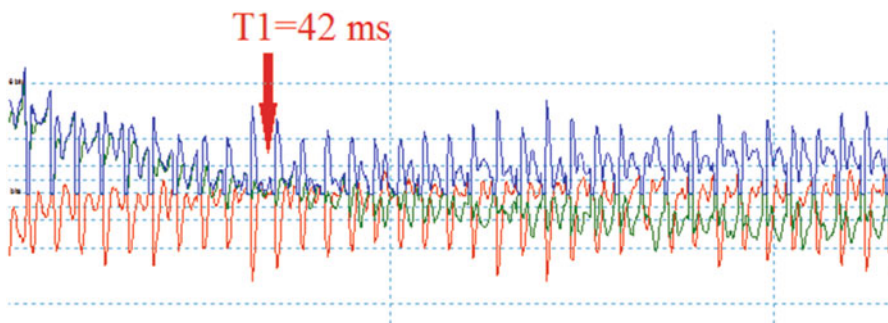


Fig. 13 The Csaki-Bene sequence in ammonium nitrate (an interval between RF pulses is about 1.24 ms). The point of minimum of the signal approximately corresponds to the relaxation time T_1 ($\sim 42 \text{ ms} \pm 2.5 \text{ ms}$)

related to the low resonance frequency, broad linewidths, and low SNR of ^{14}N NMR in comparison to ^1H NMR have been identified and resolved.

Planar Photonic Crystal (PPC) Based Microwave Technique

Physical Background of the Method

Structures based on Planar Photonic Crystals (PPC) approach looks very promising for designing microwave sensors for identification of liquids. PPC-sensors provide a predictable and controllable spatial concentration of electromagnetic (EM) energy in

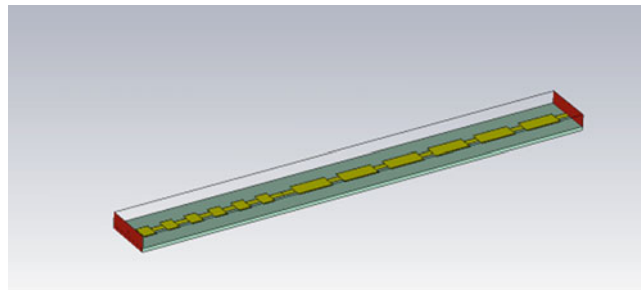


Fig. 14 A metamaterial consisting of two PPC in microstrip design – the detection cell model to measure the permittivity [20] (the PPC-sensor)

the close proximity to the sensor. The PPC technique can be used to probe the liquid content inside a bottle located at a distance of about 30–80 mm from the sensor (the distance depends on the operating frequency range of the PPC sensor). A laboratory setup for the liquid identification based on such a sensor for operation at GHz band has been designed and tested.

In a number of methods for detecting the complex permittivity ϵ of liquids to obtain an effective measurement, it is necessary to have direct contact with the liquid under study using special calibrated liquid containers or probes immersible in liquid. However, in many practical cases this is unacceptable, for example, if we need to scan liquids placed in a closed container (bottle). In such situations, it is particularly important to develop fast methods of non-destructive (remote, non-contact) measurements of the complex permittivity.

For attaining this goal, we employed a special design of the microstrip line, which forms a kind of planar metamaterial. The measuring element (i.e. permittivity sensor) is formed by combination of two Planar Photonic Crystals (PPC) in form of microstrips of various size (Fig. 14) [18].

Elements of PPC are realized as segments of ***spatially modulated microstrip*** lines of various widths (with various impedances). Such a structure demonstrates a maximum transmission coefficient, corresponding to an electrodynamical analog of the “Tamm state” [20] at a certain frequency in the band gap of transmission spectra of the PPC. This band gap is formed by the coincidence of band gaps of each of two photonic crystals. As a result of electromagnetic excitation of the sensor with frequency corresponding to the “Tamm state”, a peak of concentrated EM field is formed in the middle between these two PPC. The container with liquid under study is placed close to this region.

Detecting the Real and Imaginary Parts of Permittivity Using the PPC-Technique for Fast Identification of Liquids

The operating principle of our device for detecting the real and imaginary parts of the permittivity is based on a known technique described, for instance, in [19]. However, instead of the set of cylindrical resonators (a hollow one and dielectric one) we

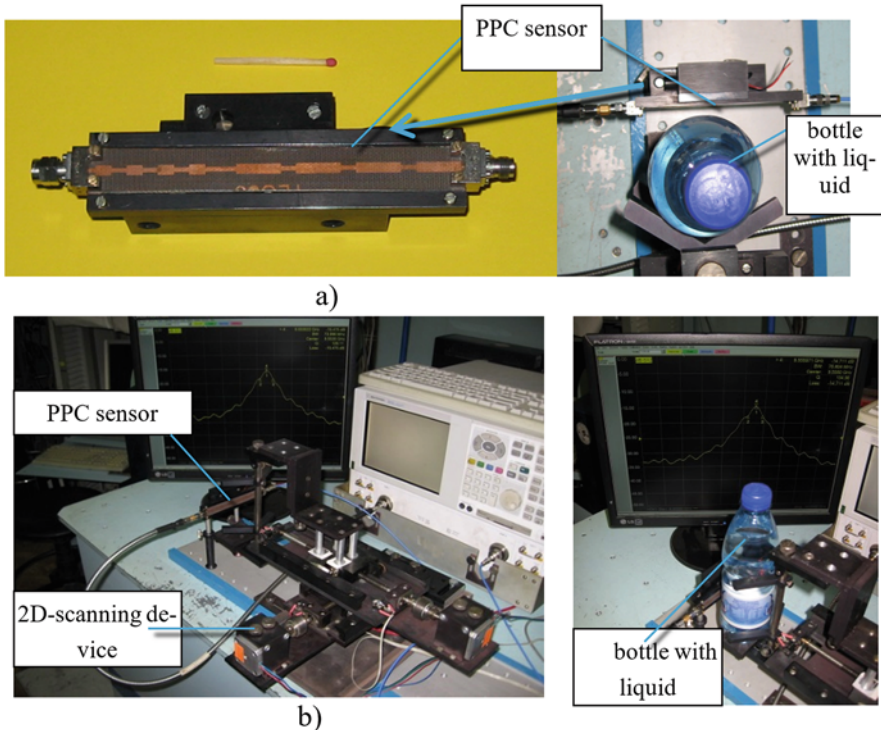


Fig. 15 The experimental setup: (a) metamaterial based on two planar photonic crystals (PPC-sensor); (b) the layout of the measurement test bench

applied the PPC-sensor [20] described in previous part. An important advantage of the PPC sensor is related to its planar geometry [20]. It is easy to bend such a resonator without deterioration of its electrodynamical properties. Besides the PPC-sensor has the simplicity of technological implementation that is very attractive. At the frequency of the “Tamm state”, a peak in the electromagnetic energy concentration occurs on the interface of two photonic crystals with the EM field which is partially extended in the ambient space over of PPC [20,22].

The experimental setup for the liquids analysis using planar metamaterials [22] is shown in Fig. 15. It consists of the PPC-sensor connected by a coaxial-microstrip adaptors and cables with a Vector Network Analyzer N5230A for measuring the transmission coefficient of electromagnetic waves in the frequency range 1–12 GHz. A two-coordinate scanning device is used for precise positioning of the measured liquid container relative to the PPC sensor [22, 23]. The positioner is controlled by a computer which allows setting the coordinates of the container with a precision less than 0.1 mm.

The resonance peak frequency and its *Q*-factor are determined by the measured frequency dependence of the transmission coefficient (*T*) of the electromagnetic wave as follows. First, the least-squares method of approximation of the

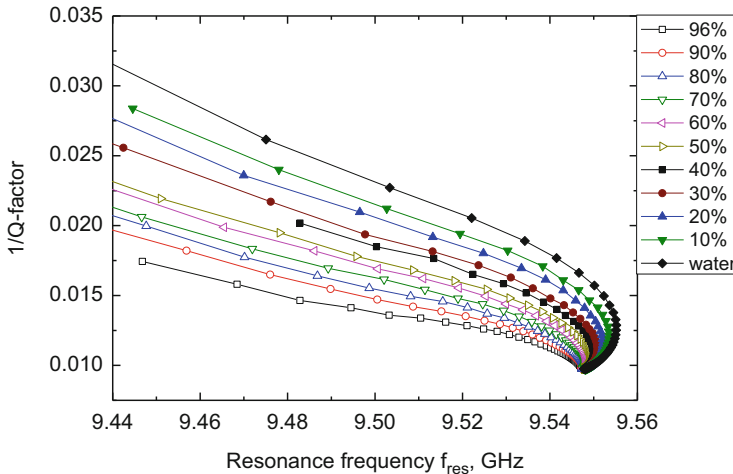


Fig. 16 The typical dependences of $Q^{-1} = f(f_{\text{res}})$ for various liquids analysed

transmission coefficient spectrum by Lorenz curve shape is carried out, which is described by the formula $T = c + a/(1 + b \cdot (f - f_{\text{res}})^2)$ [22]. Here a , b , c , f_{res} are adjustable parameters. The parameters of the resonance peak are defined from the approximation dependence: the resonant frequency f_{res} is defined just as the peak value of the curve, while the Q -factor $Q = f_{\text{res}} \sqrt{b \cdot (1 + \sqrt{2})}/2$.

When the distance between PPC and the bottle (δh_{var}) is changed, we obtain a set of experimental parameters. It is suitable to present them as curve on a.

$$Q^{-1} = f(f_{\text{res}}) - \text{graph} (\text{Fig. 16}).$$

We note that each material demonstrates its own unique curve that can be used for identification of liquids. In this figure we used the coordinates $Q^{-1}(f_{\text{res}})$ following to [21]. Note that Q^{-1} is directly related to the imaginary part of the liquid permittivity, while shift of f_{res} is defined by its real part. This dependence is unique for each material (liquid) because the real and imaginary parts of the liquid permittivity are both unique features of a particular material.

Influence of Technological Parameters on Complex Permittivity Detection

The Wall Thickness Affect

It is a very important to consider as accurately as possible the impact of various technological/external parameters on liquids measurement. Among the most important ones are the bottle thickness and the incline angles of the bottle relative to the PPC-sensor symmetry axes.

Fig. 17 The $Q^{-1} = f(f_{\text{res}})$ dependences for polystyrene containers with pure water and different wall thicknesses (t)

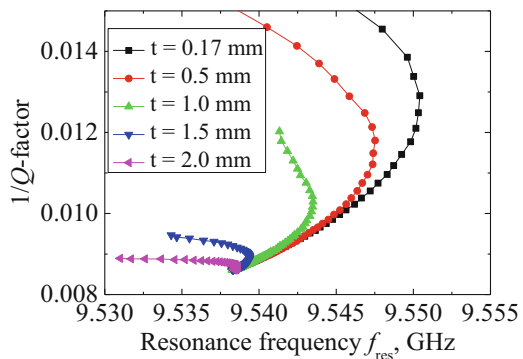
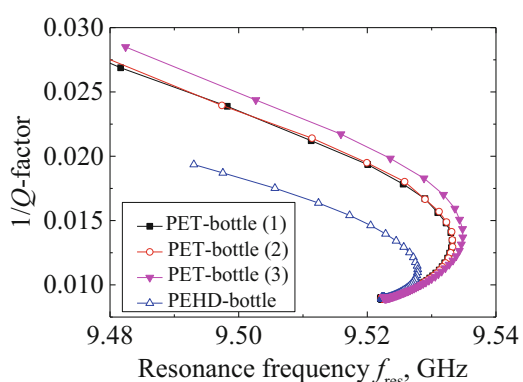


Fig. 18 The $Q^{-1} = f(f_{\text{res}})$ dependences for the different plastic containers with pure water



The influence of the wall thickness (t) of the polystyrene container with water on the shape of the dependence Q^{-1} and f_{res} on the distance δh_{var} is shown in Fig. 17.

It is easy to see that increasing losses in the liquid lead to a decrease in the peak Q -factor, and the above-described curve is shifted up. Note that the thickness of the container walls with liquid has a significant impact on the shape of the dependence of the inverse Q -factor and on the resonant frequency on the distance δh_{var} . Starting with a thickness of $t = 1.0$ mm, a decrease in the sensitivity of the setup to the container content is observed (Fig. 17). The reason of this is the fact that at $t > 1.0$ mm the penetration depth of the EM field into liquid under test becomes too small.

Effect of Container Material

The influence of the material of various plastic containers filled by the water on the shape of the inverse Q -factor and the effect of the resonant frequency of the peak on the distance of δh_{var} was investigated [21] (Fig. 18).

We demonstrated that the effect of the high-pressure polyethylene (PEHD-bottle) container is larger than that of a series of polyethylene terephthalate containers (PET-bottles) of the same thickness approximately. However, we note that this difference can be easily taken into account for removing its effect from the experimental data.

Another Possible Application of the PPC Detection Technique

The Ethanol Concentration in Water

We have also measured the influence of the ethanol concentration in water on the shape of dependence of the inverse Q -factor and the resonance frequency on the distance (Fig. 19). It is obvious that an increase in the alcohol concentration results in smaller values of the inverse Q -factor (due to the decrease in the imaginary part of the permittivity).

It can be seen that dependences in Fig. 19 are clearly distinguishable. The accuracy of the measurements makes it possible to estimate the alcohol concentration to within 1% in various liquid mixtures during the analysis of liquids.

Determination of the Ethanol and Methanol Concentration in Water

One of the actual tasks for controlling of the quality of alcohol drinks without opening the bottle is measuring the ethyl and methyl concentration in their water solutions.

We applied PPC-sensor at frequencies and $f_1 = 9.5$ GHz and $f_2 = 3.2$ GHz which have been investigated in [22] (Fig. 20). The measurements were carried out for three water solutions with 40% ethanol; 20% ethanol +20% methanol; and 40% methanol. As can be seen in Fig. 20, the difference between the measured values for

Fig. 19 The $Q^{-1} = f(f_{\text{res}})$ dependences for the different concentrations of alcohol in water

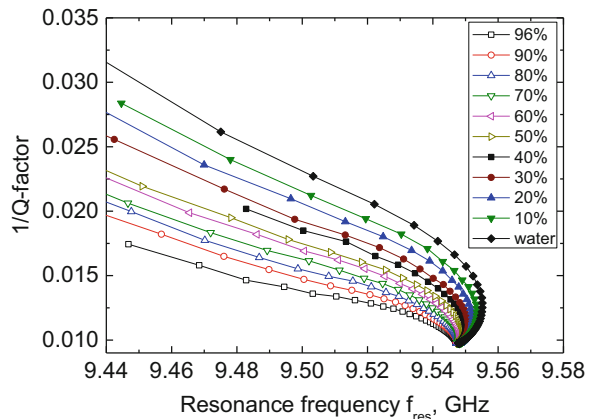
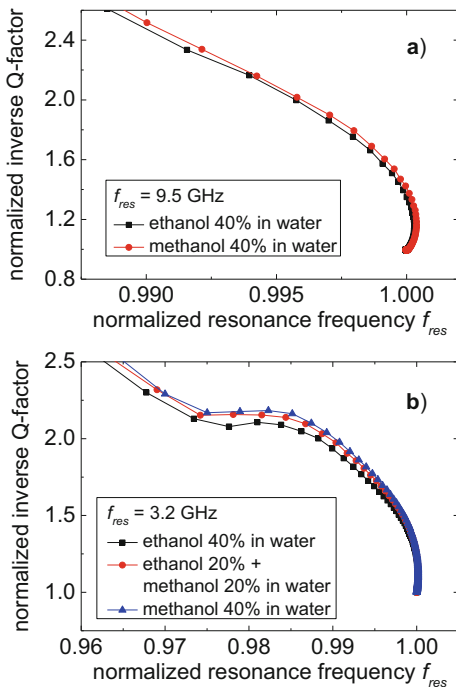


Fig. 20 The $Q^{-1} = f(f_{\text{res}})$ dependences [24] for ethyl and methyl alcohol solutions in water placed into PET-bottles containers at: (a) $f_1 = 9.5$ GHz and (b) $f_2 = 3.2$ GHz



the $Q^{-1} = f(f_{\text{res}})$ is much larger at $f_2 = 3.2$ GHz, than at $f_1 = 9.5$ GHz. It is easy to explain this by the significant difference between the characteristic (eigen) resonance frequencies for molecules of these two alcohols and for water.

For water, one of the main eigen frequencies is at about 19 GHz, for ethanol this value is about 1 GHz, and for methanol it is about 3 GHz. At the same time, the water absorption significantly exceeds the absorption of alcohols at a frequency $f_1 = 9.5$ GHz. However, at frequency $f_2 = 3.2$ GHz, a significant contribution to the total absorption takes place due to methanol since its resonant absorption frequency is close to 3 GHz, whereas the contribution of the absorption in ethanol and water is much lower at this frequency. This leads to a larger shift of Q^{-1} in the curve (Fig. 20b) in comparison with that observed in Fig. 20a. Therefore, the frequency $f_2 = 3.2$ GHz is the more preferable operating frequency for distinguishing these two alcohols in water.

Summary of the PPC-Based MW Sensor

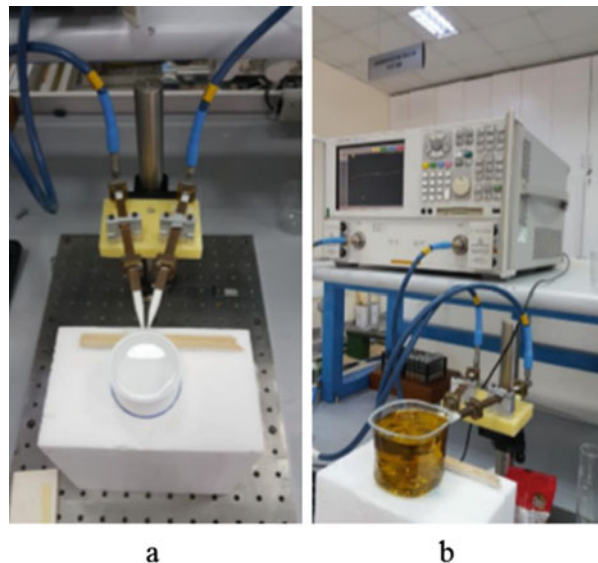
- The concept of the Tamm state was formulated for a periodic chain consisting of two periodic subsystems with different constitutive parameters. The experimental sensor based on Planar Photonic Crystal (PPC) has been designed for liquid identification using measurement data of the complex permittivity.

- It is possible to count the influence of technological parameters on the liquid identification data using PC-software. This leads to the possibility of reducing the measurement errors from 10–15% to 1–3%;
- The possibility of non-contact discrimination between pure ethyl and pure methyl alcohol solutions in water, as well as also mixed solutions, has been demonstrated.

Reflection Mode Method (26.5–40 GHz) and Application of Clustering/Classification Algorithms

One of possible approaches for identification of liquid materials is to implement free space measurements of reflection of EM energy by a container with a liquid. In these measurements the magnitude and phase of S_{21} parameter is measured simultaneously. The schematic view of the free space reflection microwave setup (installed in MILTAL, TUBITAK) is shown in Fig. 21. This measurement system consists of two dielectric rod antennas, a sample holder, and a VNA. The receiving and transmitter antennas are set around the sample holder with different angles [23]. Three different containers were used as sample holders in which the determined liquids were put (Fig. 22). The incident wave is sent by a transmitter antenna, while the reflection signal is received by a receiver antenna after interaction of the emitted radiation with the material. Using this setup, the S_{21} parameter in the frequency range of 26.5–40 GHz for a number of different liquid materials has been measured.

Fig. 21 Measurement setup for reflection measurements



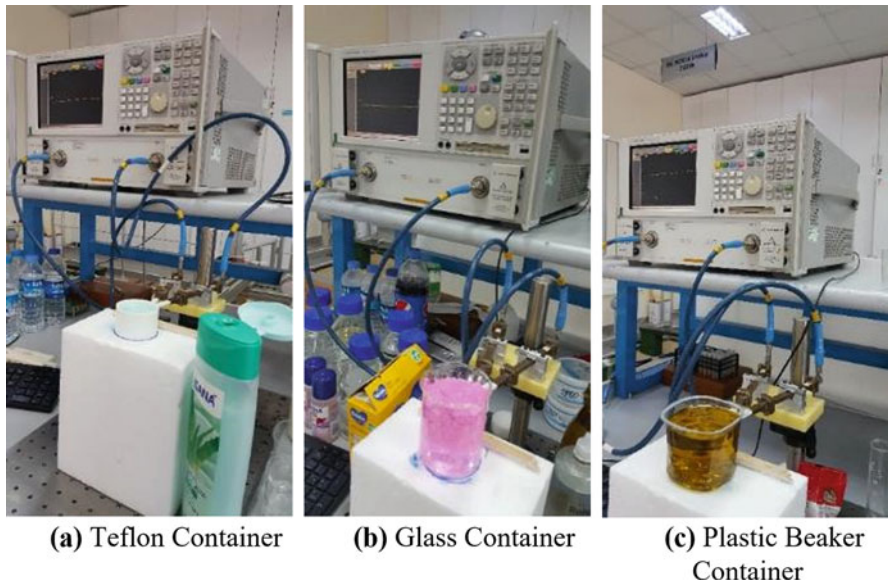


Fig. 22 Measurement system with different liquid containers

It should be noted that the position of the antennas should be determined carefully to obtain the reflected signal at different angles, which is the transmission parameter for the receiving path [24]. A spherical wave is considered instead of a plane wave. Moreover, the antennas should be placed very close to a probed container to reduce diffraction effects. All measurements have been implemented at room temperature.

Measurements of a set of liquids, consisting of four alcohols, five spring waters, and three salt solutions, were performed using the free space reflection method between 26.5–40 GHz (Ka-band). Prior to the application of various clustering algorithms, it is useful to make a qualitative evaluation of the received results. As seen in Fig. 23, this frequency range provides a very good possibility for classification by comparing the differences in the S_{21} parameter for different substances. In the group consisting of solutions of salt in water, the S_{21} parameter reveals a relatively slight change (between -5 and -10 dB) with frequency, while in the group consisting of three various alcohols (i.e. threat liquids) the S_{21} parameter changes are all between -10 and -20 dB. The third group, consisting of various brands of drink (spring) water reveals a pronounced minimum between 36 and 37 GHz. Thus, qualitative evaluation of the received results immediately reveals “fingerprint” features which could be used in automated algorithms for discrimination between benign and threat liquids in the Ka-band.

The classification and clustering algorithms demonstrated in Fig. 24 were also applied also to other containers with similar results. For all three containers (glass beaker, plastic [PET] glass, and Teflon), different data clustering techniques can be

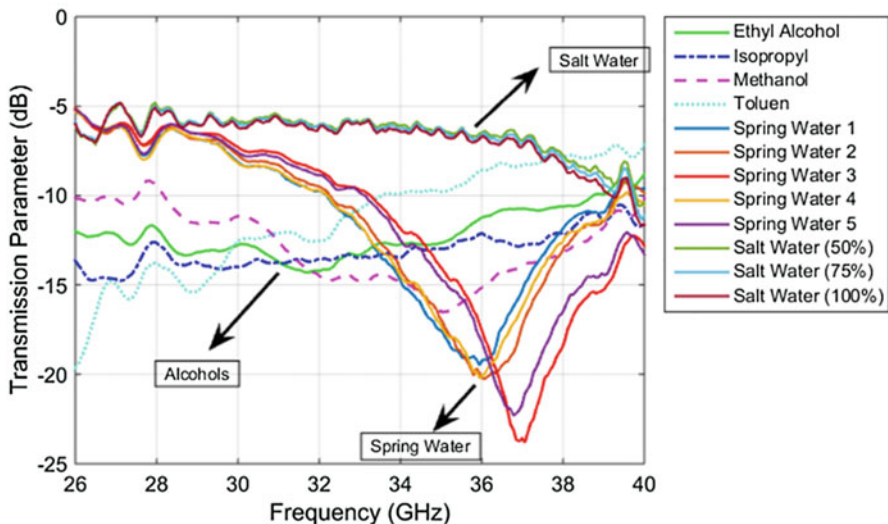


Fig. 23 S_{21} parameters for various liquid in the tested set between 26.5–40 GHz using the free space reflection setup

used. However, when using three different containers in a single data set, it has been established that the K-means technique provides better results. Another possible technique, which may be used for data discrimination is the Self-Organizing Map (SOM). It is an alternative technique for the clustering and data analysis processes and is a type of artificial neural network technique. It is trained using unsupervised learning to produce a low-dimensional (typically two-dimensional) map, discretized representation of the input space of the training samples. The SOM model depends on nonlinear generalization of principal components as a nonlinearly projection mapping. The SOM technique is applied in many applications such as reduction of dimension, vector quantization, and data visualization. [25, 26]. We tested the SOM algorithm and found that it provides results comparable to and in some cases even better than the K-means technique. As an example, we gave the result of the application of the SOM technique to the case of using three different containers in a single data set in Fig. 25. The data for ethyl alcohol, isopropyl, methanol, and toluene (the data for three different containers are shown by green symbols) have been discriminated inside a blue-colored circle automatically by application of the SOM technique.

Thus, we demonstrated that the threat group (alcohols in our case) can be successfully separated from the group of benign liquids (various brands of the drinking water and water solutions of salt with various concentration).

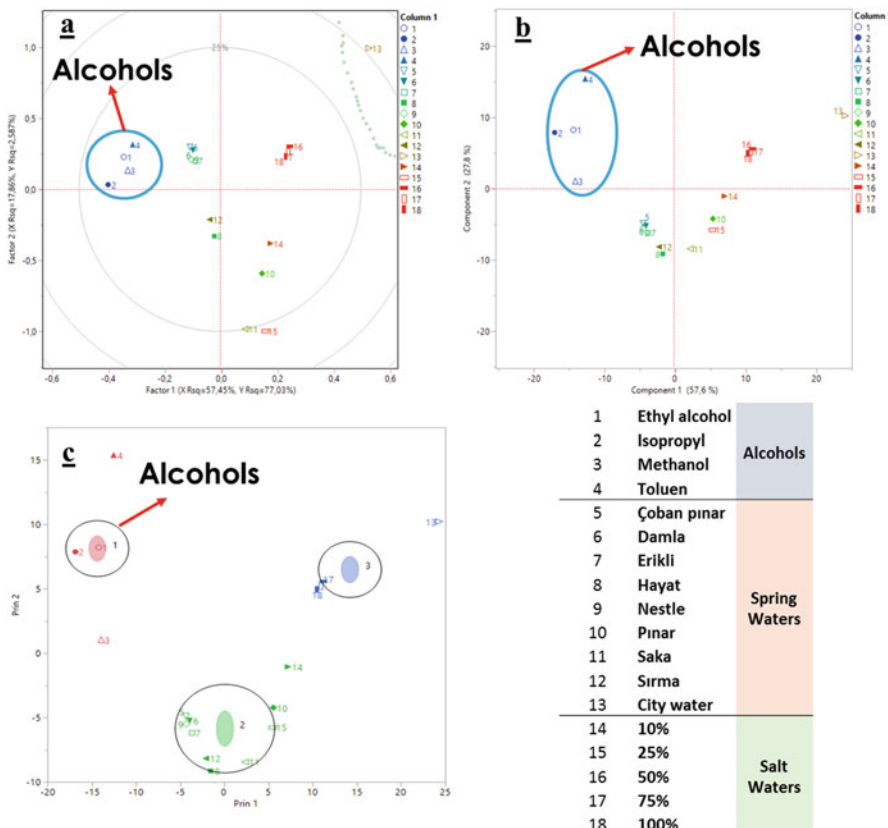


Fig. 24 Classification of liquids measured by free space reflection in a beaker container **(a:** PLS, **b:** PCA, **c:** K-means)

Conclusions

An issue of critical importance is developing effective methods for the detection of explosive and other dangerous substances at entrance points to various transport means as well as to objects of critical infrastructure. To address this issue with respect to liquid threats, we proposed the combined use of two complementary methods of explosive detection: (1) a time-domain (TD) nuclear magnetic resonance (NMR) technique; (2) MW & sub-THz dielectric spectroscopy. A combined use of ^1H and ^{14}N non-invasive TD-NMR techniques for detection of energetic liquids has been shown to be promising for security applications. A system based on use of Planar Photonic Crystal (PPC) structures (or patterned microstrip lines) as sensors for MW detection of liquids in containers has been developed and implemented in a model device for the identification of liquids at various frequency bands. We have

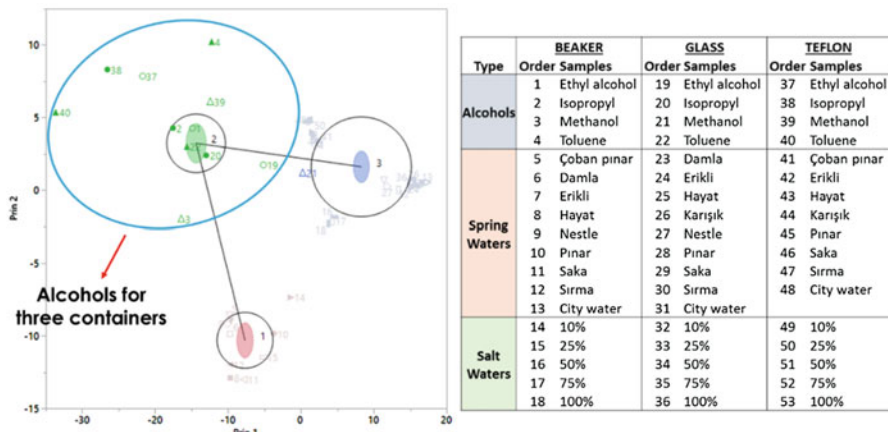


Fig. 25 Classification of liquids for all three containers by the SOM technique

also developed and tested different clustering/classification algorithms for implementation in the signal processing as well as threat detection techniques using MW measurements.

The follow-on work that is planned in this research direction includes the practical realization of the prototype of the device, which will use both TD NMR and MW spectroscopy. Unfortunately, due to space limitations, we have not presented here our studies on the development of novel methods of NQR detection of explosives and their practical implementation (these results have been published in part in the works [27, 28]). We have also not addressed the issue of detection of liquids in metallic containers (it is possible to use TD NMR in a very low or Earth's magnetic field for scanning their content; see, e.g. Ref. [29]).

The authors acknowledge support of NATO SPS Programme by ongoing project No. 985005 (G5005). B. Rameev and G. Mozzhukhin also acknowledge the support of the previous NATO SfP project No. 982836 (2010–2013).

References

- Burnett LJ (1993) Liquid explosives detection, SPIE Vol. 2092 Substance Detection Systems, pp. 208–216
- Apikh T, Rameev B, Mozzhukhin G, Barras J (eds) (2014) Explosives detection using magnetic and nuclear resonance techniques, NATO science for peace and security series B: physics and biophysics. Springer, Dordrecht
- Kumar S, McMichael WC, Kim Y-W, Sheldon AG, Magnuson EE, Ficke L, Chhoa TK, Moeller CR, Barrall GA, Burnett LJ, Czipott PV, Pence JS, Skvoretz DC (1997) Screening sealed bottles for liquid explosives. Proc SPIE 2934:126–137

4. Mauler J, Danieli E, Casanova F, Blimich B (2009) In: Fraissard J, Lapina O (Eds) Explosives detection using magnetic and nuclear resonance techniques. NATO Science for Peace and Security Series B: Physics and Biophysics, pp. 193–203
5. Rameev B, Mozhukhin GV, Khusnutdinov R, Aktas B, Konov A, Krylatykh NA, Fattakhov YV, Gabidullin DD, Salikhov KM (2012) SPIE Proceeding DSS12 – SPIE Defense, Security, and Sensing, 8357 – 33 V. 1, 83570Z
6. Konov AB, Salikhov KM, Vavilova EL, Rameev BZ (2013) Multiparameter NMR Identification of Liquid Substances. In: Apih T, Rameev B, Mozhukhin G, Barras J (Eds) NATO book “Magnetic Resonance Detection of Explosives and Illicit Materials”, NATO Science for Peace and Security Series – B: Physics and Biophysics. Springer, pp. 111–122
7. Krylatykh NA, Fattakhov YV, Fakhrutdinov AR, Anashkin VN, Shagalov VA, Khabipov RS (2016) Detection of Explosive Precursors Using Low-Field Magnetic Resonance Imaging. *Appl Magn Reson* 47(8):915–924
8. Gradišek A, Apih T (2010) NMR-Based liquid explosives detector. *Appl Magn Reson* 38:485–493. <https://doi.org/10.1007/s00723-010-0145-9>
9. Bhattacharyya R, Kumar A (2004) A fast method for the measurement of long spin-lattice relaxation times by single scan inversion recovery experiment. *Chem Phys Lett* 383:99–103
10. Canet D, Brondeau J, Elbayed K (1988) Superfast T1 determination by inversion, recovery. *J Magn Reson* 77(3):483–490
11. Ernst RR, Bodenhausen G, Wokaun A (1994) Principles of nuclear magnetic resonance in one and two dimensions. Oxford University Press, New York
12. Song Y-Q, Venkataraman L, Hurlimann MD, Flaum M, Frulla P, Straley C (2002) T1-T2 Correlation spectra obtained using a fast two-dimensional laplace inversion. *J Magn Reson* 154:261–268
13. Gauthausen G, KamloWski A, Schmalbein D (2008) Method for determining the content of at least one component of a sample by means of nuclear magnetic resonance spectrometer, Patent No.: US 7397241 B2, Jul. 8, 2008.
14. Kamar H, Gnosh S, Paproski RE, Krygsman P, Bhalia B (2011) Simultaneous determination of bitumen and water content in oil sand and oil sand extraction process samples using low field time domain NMR, US 2011/0316534 A1, Dec. 29, 2011.
15. Horn PJ, Neogi P, Campbell T, Chapman K (2011) Simultaneous quantification of oil and protein in cottonseed by low field time domain nuclear magnetic resonance. *J Oil Fat Ind.* <https://doi.org/10.1007/s11746-011-1829-5>
16. Csaki A, Bene G (1960) Use method de mesure de T1 par echos de spin, *Cop. Rend* 251:228–233
17. Prado P, Detecting Hazardous materials in containers utilizing nuclear magnetic resonance based measurements. Patent US 2014/0225614 A1, Aug.14, 2014
18. Belozorov DP, Girich AA, Tarapov SI (2013) Analogue of surface Tamm states in periodic structures on the base of microstrip waveguides. *Radio Sci Bull* 345:64–72

19. Klein N, Krause H-J, Vitusevich S, Rongen H, Kurakin A, Shaforost ON (2011) Dual-mode microwave cavity for fast identification of liquids in bottles, *Microwave Symposium Digest (MTT)*, 2011 IEEE MTT-S International, pp. 1–4
20. Polevoy SY, Vakula AS, Nedukh SV, Tarapov SI (2017) Fast identification of liquids using planar metamaterial. *Telecommun Radio Eng* 76(3):237–243
21. Nedukh SV, Polevoy SY, Tarapov SI, Vakula AS (2017) Identification of liquids in different containers a using microwave planar meta,material. *Radiophys Electron* 22(4):69–74
22. Polevoy SY, Michaylichenko VA, Vakula AS, Nedukh SV, Tarapov SI (2018) Principal parameters for optimization of experimental technique for fast remote identification of liquids at microwaves. *Telecommun Radio Eng* 77 (18):1639–1648
23. Li C, Han B, Zhang T (2015) Free-space reflection method for measuring moisture content and bulk density of particulate materials at microwave frequency. *Rev. Sci Instrum* 86:034712
24. Haddadi K, Lasri T (2014) Geometrical optics-based model for dielectric constant and loss tangent free-space measurement. *IEEE T Instrum Meas* 63 (7):1818–1823
25. Akinduko AA, Mirkes EM. Initialization of self-organizing maps: principal components versus random initialization. A Case Study, pp. 1–18. <https://arxiv.org/pdf/1210.5873.pdf>
26. Kohonen T (2013) Essentials of the self-organizing map. *Neural Netw* 37:52–65. <https://doi.org/10.1016/j.neunet.2012.09.018>
27. Mozzhukhin GV, Rameev BZ, Doğan N, Aktaş B (2008) Secondary signals in two frequency nuclear quadrupole resonance on ^{14}N nuclei with $I = 1$. *J Magn Reson* 193(1):49–53
28. Mozzhukhin GV, Kupriyanova GS, Mamadazizov S, Rameev BZ (2018) ^{14}N NQR and ^{14}N NMR detection of explosive and dangerous compositions. In: Karpov IV, Borchevskina OP (Eds) *Proceedings of VI International Conference. Atmosphere, ionosphere, safety (AIS-2018, June 03–09, 2018, Kaliningrad, Russia)*, Pt. 2, 259p. Kaliningrad, pp. 217–222. ISBN 978-5-9971-0492-4(Pt. 2)
29. Balçıcı E, Rameev B, Acar H, Mozzhukhin GV, Aktaş B, Çolak B, Kupriyanov PA, Ievlev AV, Chernyshev YS, Chizhik VI (2016) Development of Earth's Field Nuclear Magnetic Resonance (EFNMR) Technique for Applications in Security Scanning Devices. *Appl Magn Reson* 47(1):87–99. <https://doi.org/10.1007/s00723-015-0730-z>

Comprehensive Package for Strengthening Jordanian C-IED Defence Capabilities

Levente Tábi (✉) 

National University of Public Service, Doctoral School of Military Sciences, The theory of military art 2017-2021, Budapest, Hungary

Abbreviations

AtN	Attack the Networks
BIFEC	Basic Field Exploitation Course
BSC&T3	IED Basic Search and Clearance & Train the Trainer Course
BSCC	IED Basic Search and Clearance Course
CIAC	C-IED Awareness Course
C-IED COE	Counter Improvised Explosive Devices Centre of Excellence
C-IED	Countering Improvised Explosive Devices
DCB	Defence Capability Building
DtD	Defeat the Device
ESCD	Emerging Security Challenges Division
HQ	Headquarters
IED	Improvised Explosive Device
JAF	Jordanian Armed Forces
MAT	Mobil Advisory Team
NATO	North Atlantic Treaty Organization
PtF	Prepare the Force
SLE	Senior Leadership Engagement
SPS	Science for Peace and Security
TTP	Technics, Tactics and Procedures
WIT	Weapon Intelligence Team

“If your vision is one year, plant crops

If your vision is ten years, plant trees

If your vision is one hundred years, teach people”

(African ancient sayings).¹

¹Nieves, Marisol: *Understanding the Adult Learner*, C-IED COE internal Train the Trainer training, C-IED COE, 2016. Slide #2.

L. TÁBI

National University of Public Service, Doctoral School of Military Sciences, The theory of military art 2017-2021, Budapest, Hungary

e-mail: ltabi@ciedcoe.org

Introduction

According to the Counter Improvised Explosive Devices Centre of Excellence (C-IED COE) policy, one of the most important issues for fighting against the Improvised Explosive Device (IED) threat is to continuously develop, maintain and improve the Countering Improvised Explosive Devices (C-IED) capabilities. In order to achieve this goal the C-IED COE builds, sustains and uses its relationship for supporting any nation, organization, entity all over the word which has mission for fighting against the IED system.

Since 2015 the C-IED COE has actively taken part in NATO's Defence Capability Building (DCB) initiatives and has supported much of NATO's DCB initiatives in the field of C-IED. The most recent projects led by the C-IED COE are the support to the Jordanian C-IED capability development.

With this article, I would like to give you some insight into how the C-IED COE works, what the Center's concerns under in providing support for the DCB initiative and what Lessons Learnt the COE has gained in the project for Jordan.

I am Lieutenant Colonel Levente Tábi (HUN A). I have been working in the C-IED COE since 2015 and I am the NATO Project Director of the Jordanian C-IED DCB project.

C-IED COE Introduction

The C-IED COE was established in 2010 and during its 8 years existence the C-IED COE has developed and supported the development and improvement of NATO, Allied and also partner nation's C-IED capabilities. The mission of the C-IED COE is (*„... to provide subject matter expertise in order to support the Alliance, its Partners, and the International Community in the fight against IED and co-operate to increase security of Allied Nations and also all the troops deployed in theatres of operations, reducing or eliminating the threats from improvised explosive devices used or for use....”*).²

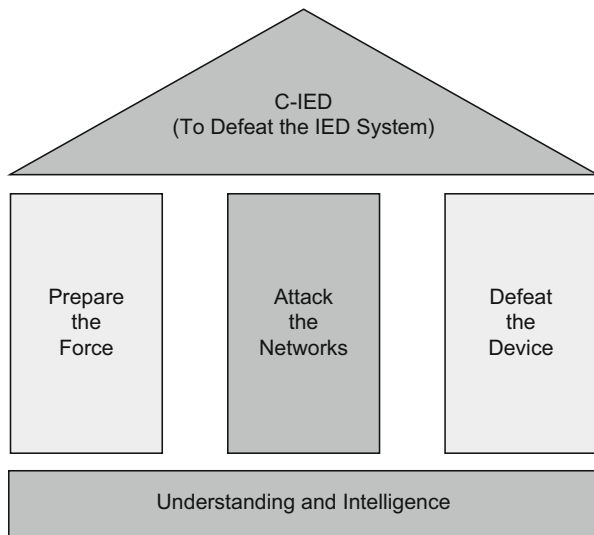
Supporting this idea the C-IED COE is structured according to the “Allied Joint Doctrine for Countering Improvised Explosive Devices” (Allied Joint Publication – AJP 3.15 (C)).³ It has three main pillars, and each pillar has significant roles for supporting the fight against the IED system, as you can see in the Fig. 1.

- The **Prepare the Force** (PtF) branch is responsible for analyzing the friendly and adversary forces C-IED/IED related Technics, Tactics and Procedures (TTP) and

²C-IED COE: Status, Mission & Concept, Source: <https://ciedcoe.org/index.php/about-c-ied-coe/status-mission-concept>

³AJP 3.15 (C), Allied Joint Doctrine for Countering Improvised Explosive Devices, Edition C Version 1, February 2018, Source: https://nsd.nato.int/protected/nsdd/_CommonList.html, page 1-6

Fig. 1 The C-IED Approach with Supporting Activity Pillars. (ACIEDP-01, *Counter-Improvised Explosive Device (C-IED) Training Requirements*, Edition B, Version 1, November 2018, Source: file:///C:/Users/ltabi/Downloads/ACIEDP-01%20EDB%20V1%20E.pdf, page 1–2)



providing training solutions for the friendly forces in case of identified gaps or NATO requirements.

- The **Attack the Networks** (AtN) branch is responsible for engaging the IED system by analyzing the IED events, the adversary, friendly and neutral networks; and then providing targeting solution, recommending how to influence or engage the different systems.
- The **Defeat the Device** (DtD) branch is responsible for identifying the trend of the IED events, analyzing technically the adversary TTP, and taking part in the research and development projects, initiatives for supporting the friendly forces C-IED capabilities.

The C-IED COE contains these three pillars (PtF, AtN, DtD) and does its best to support these goals on daily basis. To achieve the above mentioned COE mission one of our main tasks is to build worldwide relationships. As it can be seen in the Fig. 2 the C-IED COE has real worldwide relationships. The COE is not exclusively supporting NATO organizations and NATO allied nations, but also has close cooperation with other national, international organizations (i.e.: INTERPOL, EUROPOL, UN entities, other Centres of Excellence, etc.). Furthermore, the C-IED COE has actively cooperates with many universities and collaborates with NATO partner nations, as well.

The relationship with the partner nations is obviously quite different than with NATO and the Allied nations. A small number of those partner nations are the ones who can support the COE's C-IED activities; on the other hand, the majority of them are the receiver of the C-IED COE support.



Fig. 2 The C-IED COE worldwide relationships

C-IED COE DCB Supports

Since 2014 the C-IED COE receives requests for support to assist or deliver DCB related activities in different countries. The first request actually came from the United Nations (UN) in 2014 requesting delivery of a kind of staff course for UN staff personnel in Mali. The first real NATO DCB request came in 2015 to support the Ukrainian defense and security forces C-IED capability development (Fig. 3).

Beside these two milestone events – in Mali and in Ukraine – multiple other visits took place in North-African and Middle Eastern countries in this period, mainly for mapping the current IED threat of the region and those countries' C-IED capabilities. Based on those official visits, the C-IED COE staff has a clear picture about those nations' needs and what support is necessary for their C-IED improvements.

C-IED DCB Egypt & Jordan

C-IED DCB for Egypt

Because of the experience gained, it is quite obvious why NATO would ask the C-IED COE for C-IED support to those NATO partner nations which are selected with high priority by NATO. In 2017–2018 this picture has been clear because in the C-IED field for NATO there are only a couple of important nations to be focused on: Egypt and Jordan.

Fig. 3 Nations, where the C-IED COE conducted C-IED DCB activities



The Egypt C-IED DCB project was a “simple” mission for whom the C-IED COE had to deliver two separate “*Basic Field Exploitation Course*”-s (BIFEC) to improve the Egyptian defense forces post blast and identified IED event on scene first responders’ reaction and exploitation capabilities. With these two training events the C-IED COE was able to train all together 30 Egyptian military personnel. Along with the training, based on the project funding organization (NATO Emerging Security Challenges Division (ESCD), Science for Peace and Security (SPS)) request, the C-IED COE is to manage several kits of Weapon Intelligence Team (WIT) equipment. With those kits the Egyptian defense forces will be able to set up their first C-IED teams with which they can start developing their own improved C-IED capabilities.

C-IED DCB for Jordan

The C-IED DCB project for Jordan is a significantly unique and totally different project in the C-IED COE’s life. The collaboration between the Jordanian Armed Forces (JAF) and the C-IED COE started in 2015 when the COE delivered the first BIFEC for JAF personnel and also paid a few visits in Jordan to examine and discover the real IED threat in the country and the JAF C-IED capabilities. Then, in 2016 NATO SPS officially requested the C-IED COE to prepare a C-IED project plan for the Jordanian C-IED capability development.

During the planning and preparation phase the COE staff analyzed the Jordan related NATO partner nations program goals documents, the different COE internal reports, the documents prepared after each visit in Jordan and obviously the JAF’s

requests. After the COE “mission analysis” process, and the coordination with JAF and NATO SPS, the following multi-year project was created, approved and endorsed:

- Title of the project:
 - Comprehensive Package for Strengthening Jordanian C-IED Capabilities
- Execution timeframe:
 - 3 June 2017 – 31 December 2018
- Leading organization:
 - NATO C-IED COE
- Project goals:
 - “The primary goal of the project is to bolster Jordan’s C-IED capabilities and assists in developing a more robust national and operational level program capable of addressing the IED threat during a period of sustained violence. This will be achieved through provision of comprehensive training package, Train the Trainer and assistance in the development and implementation of national interagency C-IED policy and programs (C-IED curriculum and Lessons Learned programs)⁴”.
- Designated end-user:
 - The end-users of this project is the Jordanian defense and security forces; and primary JAF.
- Desired end-state:
 - Jordan will have a national C-IED policy, and other supporting national documents and programs that enable the Jordanian defense and security forces to cooperate more formally and coherently.
 - The JAF will be able to sustain its training capability with a stand-alone Jordanian program.
 - Jordan C-IED capabilities will be strengthened, allowing the country to better cope with future security challenges.

The best way to understand this project you have a look at Fig. 4.

You can see in this figure that in 2017 the project focused on the Jordanian national C-IED Policy development and in 2018 the tactical units’ C-IED capability

⁴NATO ESCD, SPS Programme, Multi-Year Project Application: “*Comprehensive Package for strengthening Jordanian C-IED defence capabilities*” Source: <https://www.nato.int/science/country-fliers/Jordan.pdf>, page 1

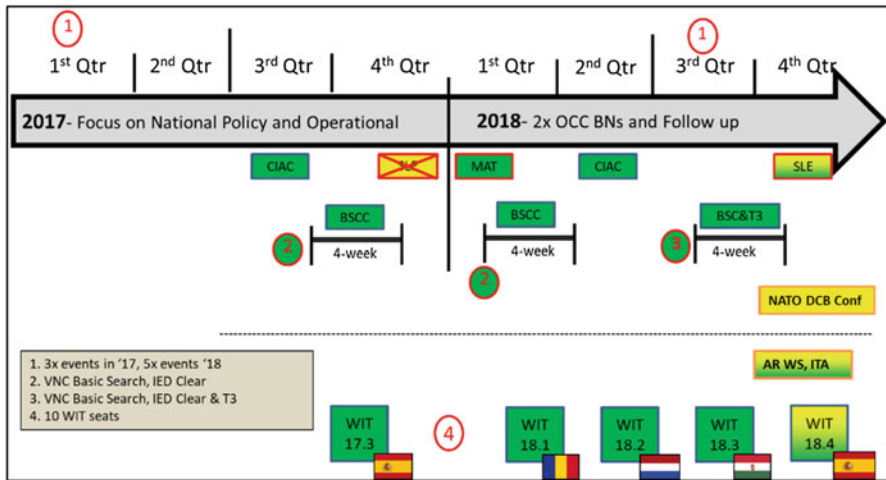


Fig. 4 The Jordan C-IED project plan and execution

improvement. In the upper part of the picture the events which can be seen were conducted in Jordan and the bottom part those activities were delivered outside of Jordan.

The *C-IED Awareness Course* (CIAC) is a staff course where the C-IED COE trained the Jordanian armed forces, gendarmeries, law enforcement, security service and the national crisis management center representatives about the basic understanding of the C-IED approach. *IED Basic Search and Clearance Course* (BSCC) and *IED Basic Search and Clearance & Train the Trainer Course* (BSC&T3) are tactical level courses and they were delivered to train JAF EOD and Military Engineer personnel responsible for dealing with the threat coming from the improvised explosive devices. During these courses the Mobile Training Team composed the C-IED COE staff members and several external Subject Matter Experts (SMEs) from the following voluntary contributing nations:

- Greece
- Hungary
- Ireland
- Romania
- Spain
- United States of America

The BSC&T3 was the pace of the training events because the training audience was selected from those JAF personnel who already attended several international courses before and their performance convinced their JAF superiors that they could become instructor in the future. With this course for the C-IED COE the aim was that the selected 15 JAF personnel could gain information and practice the IED search

and clearance tactics and technics at advanced level and they could also started learning how to become an instructor.

The *Weapon Intelligence Team* (WIT) course is a NATO certified course. Every year, usually, four iterations of WIT courses are carried out on a rotation basis in different European countries. In this project there are five iterations of WIT course and in each course Jordan has 2 seats. With those trained JAF personnel the JAF C-IED capability significantly improved.

During the project a *Mobil Advisory Team* (MAT) and a *Senior Leadership Engagement* (SLE) type of visits were also planned and conducted. Each time the MAT/SLE pays visits to multiple Jordanian organizations (i.e.: JAF General Staff HQ, JAF Royal Engineer Corps, Jordanian Public Security Directorate, Bomb Disposal Unit HQ, Jordanian Public Security Directorate, National Crime Laboratory, National Center for Security and Crises Management). The aim of these visits is to provide assistance for developing the national C-IED policy and other related documents, to strengthen their cross-governmental, interagency collaboration, cooperation and to institutionalize their informal relationships.

In total, as it is stated in the project goals, this project is a real “robust” program because it not only has training events but also key leader engagement activities and meetings; plus the consulted authorities are from the tactical, operational and strategic levels; and not only the JAF but also the Jordanian law enforcement, security and public safety sectors are involved. All together 104 Jordanians took part in the different courses. To understand the meaning of this number, we should see for instance that during the last 5 WIT courses the C-IED COE has 100 attendees, from different NATO, allied and partner nations, 10% of those attendees came from Jordan. There is no any other nation with such a number of WIT trained personnel in this period.

So if we are looking at the foreseeable outcome of the project, we can declare that this is a well-designed, well-accomplished DCB project. Of course, we cannot say the success comes from only one single organization’s contribution. The reason for the success comes from the fact that the objectives were identified and coordinated among the respective entities, comes because the receiver/end-user was able to recognize that they have a key active role in this project, and comes from the voluntary contributing nations and their SMEs who carried out an exemplary job during the delivery of the courses.

This project plan is also a good product that we should follow in future in C-IED DCB projects. The project line of efforts are of a complex variety of different courses, that target all levels in the army structure and the interagency approach, with not only the representatives from the defense area but also the security and public safety sectors were involved, brought them around the table.

Contributors from each side of the project identified challenges that we could solve together or we would need to work on to avoid those difficulties in the future. One of the biggest challenging issues is the language barrier. When the attendees cannot speak in English, but the delivered course is in English, immediately the instructors should count on extended time of lectures. On the other hand, the translation should utilize the proper terminology, and the interpreters should have

education about the C-IED subject matter otherwise the planned message of the class will not reach to the audience properly. Other lessons learnt include better coordination between other nations and organizations, entities that are providing similar training, in order to avoid redundancies or duplications regarding the C-IED content and try to avoid not having two or more training teams in the same period at the same training venue.

Another outcome of this project is that for Jordan, even though this project is going to be closed soon, their progress continues. When they officially release their newly developed national C-IED policy document they should start developing and updating their existing laws and regulations, and they should start to institutionalize the relationship among different national bodies, organizations, etc. Beside the C-IED policy document there is another objective of this project, to assist to JAF for revising and improving its national C-IED training curriculum and landscape, with which JAF can train and educate respective personnel not only at tactical level, but also at operational, strategic and even at political level, if it is needed.

Summary

The NATO accredited C-IED Center of Excellence is a multinational organization whose role and responsibility is to provide support for NATO, Allied and partner nations, and organizations whose mission is to fight against the existing IED threat all over the world. For this reason the COE continuously analyzes the IED threat and provides recommendations, suggestions and solutions for its partners. Being the hub among the multiple international organizations, entities, bodies within the C-IED Community of Interest has benefited for sharing and pulling information with the C-IED COE.

One of the supports the C-IED COE provides is education and training solutions and NATO partners' C-IED Defence Capability Building. In recent years the COE has gained much experience and proved its ability to prepare, coordinate or conduct such initiatives on behalf of NATO.

The recent C-IED DCB projects in Egypt and Jordan significantly improved their C-IED capabilities and supported those nations' development. The Jordan C-IED DCB project plan can be a good tool for the future because this plan engages each national defense and security sector and also supports the Jordanian national C-IED capability development.

References

1. ACIEDP-01, *Counter-Improvised Explosive Device (C-IED) Training Requirements*, Edition B, Version 1, November 2018, Source: https://nso.nato.int/protected/nsdd/_CommonList.html (date of downloading: 22 November 2018)
2. AJP 3.15 (C), *Allied Joint Doctrine for Countering Improvised Explosive Devices*, Edition C Version 1, February 2018, Source: https://nso.nato.int/protected/nsdd/_CommonList.html (date of downloading: 04 March 2018).

3. C-IED COE homepage, Source: <https://ciedcoe.org/> (date of downloading: 04 March 2018)
4. C-IED COE “Comprehensive Package for strengthening Jordanian C-IED defence capabilities 2017–2018” presentation by LTC TÁBI at the NATO SPS Advanced Research Workshop on Explosive Detection event
5. Horváth, Tibor (2016) *Az IED hálózat, mint korunk egyik aszimmetrikus kihívása*, Source: In: Csengeri János, Krajnc Zoltán (szerk.) Humánvédelem – békeműveleti és veszélyhelyzet-kezelési eljárások fejlesztése. 791 p. Budapest: Nemzeti Köszolgálati Egyetem, Hadtudományi és Honvédtisztképző Kar, pp. 275–298. (ISBN: 978-615-5305-35-1)
6. NATO Emerging Security Challenges Division, Science for Peace and Security Programme, Multi-Year Project Application: “Comprehensive Package for strengthening Jordanian C-IED defence capabilities”, Source: <https://www.nato.int/science/country-fliers/Jordan.pdf> (date of downloading: 22 November 2018)
7. NATO Standardization Office, The Official NATO Terminology Database, Source: <https://nso.nato.int/natoterm/Web.mvc> (date of downloading: 17 February 2018)
8. Tábi, Levente: *Távoktatás a C-IED területén*, Source: Hadtudományi Szemle, 2018. XI. évfolyam 2. szám, Source: http://archiv.uni-nke.hu/downloads/kutatas/folyoiratok/hadtudomanyi_szemle/szamok/2018/2018_2/18_2_forum_tabil.pdf (date of downloading: 11 November 2018)

Bibliography

- Lieutenant Colonel TÁBI, Levente is (Hungarian Defence Forces – HDF, A), currently has been assigned at the NATO accredited C-IED Center of Excellence, Madrid Spain.
- He started his military carrier in 1992 when he graduated as Military Engineer Officer. During his professional military life he has had multiple military engineer assignments from platoon leader up to senior Military Engineer (MILENG) desk officer (MILENG advisor) at Hungarian Defence Forces Joint Force Command.
- Beside his MILENG education and experiences, he graduated as Civilian Engineer Teacher and in 2006 he also attended the Zrínyi Miklós Defence University and got university degree of military leader. His operational assignments include Afghanistan, in 2007.
- Currently he is working as Military Engineer Analyst at Prepare the Force branch, Training section, NATO C-IED COE; deals with course development, to be the custodian of the ACIEDP-01, leads NATO C-IED DCB project for the Jordanian C-IED development and supports the C-IED revision of the NATO Defence Planning Process.

Multi-Year Project: Development of New Chemical Sensors and Optical Technologies for Fast and Sensitive Detection of Improvised Explosives

Tomás Torroba (✉)

University of Burgos, Burgos, Spain

e-mail: totorroba@ubu.es

Israel Schechter

TECHNION, Haifa, Israel

e-mail: israel@technion.ac.il

José García-Calvo

University of Burgos, Burgos, Spain

e-mail: jgcalvo@ubu.es

Andrea Revilla-Cuesta

University of Burgos, Burgos, Spain

e-mail: arc0060@alu.ubu.es

Project Goals

Over the past decade, the use of improvised explosive devices has increased, highlighting a growing need for a method to quickly and reliably detect explosive devices in both military and civilian environments before the explosive can cause damage. Conventional techniques have been successful in explosive detection, however they typically suffer from enormous costs in capital equipment and maintenance, costs in energy consumption, sampling, operational related expenses, and lack of continuous and real-time monitoring. The goal of this project is to produce portable sensors that continuously monitor the environment, detect the presence of explosive compounds and alert the user. It will facilitate mutual beneficial cooperation on issues of common interest, including international efforts to meet emerging security challenges in counter-terrorism by the implementation of detection technologies against the terrorist threat for explosive devices and other illicit activities. The specific objective of this work will be to use chemical sensors combined with multiphoton electron extraction spectroscopy (MEES) in a platform that will consist of two independent sensing mechanisms, by chemical sensing and spectroscopy, which will take measurements from the same sample simultaneously and will

provide a redundancy in response for positive explosive identification. By the system, TATP, HMDT and conventional explosives will be reliably detected. Each analyte will display a unique signature and the results will indicate a detection limit at the ppb level. By the accomplishment of the project we will generate new knowledge and technology in counter-terrorism by generating new detection technologies against the terrorist threat for explosive devices and other illicit activities.

Deliverables

- 1 – Development of a portable fluorescent device for the detection of gaseous traces of triacetone triperoxide and hexamethylene triperoxide diamine.
- 2 – Construction of a dedicated and optimized MEES setup.
- 3 – Production of MEES spectra and LOD of the target materials in relation to conventional explosives.
- 4 – Validation Progress and Technical meetings to assess the validation progress at every work package.
- 5 – Validation of the optical devices, recommendations to the end-users regarding the system, final validation report of the developed system and report with recommendations on how to use the system.
- 6 – Presentation of international patents of the project work packages results.
- 7 – Publication of the project work packages results in high impact journals.

Security Relevance

The society exhibits several vulnerable points in which terrorist groups may launch an attack utilizing improvised explosive devices that would culminate in a widespread panic situation and casualties. There is a need in increasing in security, as well as significantly increase the level of expertise in security against deliberate attacks that have increased over these last years. There is urgency in rendering the society more secure and diminish the values of victims of the past years. If successful, this project will improve the security against any major deliberate use of improvised explosive devices. The project will achieve this by providing specific outcomes and achievements identified below:

1. New sensors with a faster detection time, and improved re-usability
2. Combination of MEES with fluorogenic probes to reduce false positive rates and improve sensor robustness
3. Capability to network different sensors at different stages/locations of (vertical and horizontal dimensions)
4. Capability to improve the quality of detection through combination of results
5. Set of scenarios specifically adapted to the validation methodology.

These achievements will impact in rendering the society more secure eventually leading to the anticipation of attacks employing improvised explosive devices.

Science Relevance

Terrorism involving the use of improvised explosive devices (IEDs) has become all too common in today's society, often with high numbers of fatalities. IEDs using explosives such as triacetone triperoxide (TATP) as the detonator for higher energy explosives or as the energetic material itself still go largely undetected in densely populated venues such as airports and subway stations. TATP has been used in a number of recent terror attacks including the 2015 Paris attack, the 2016 Brussels Airport bombing and the 2017 concert bombing in Manchester, UK. More than ever, there is a need for a continuous explosive monitoring system that can compete with a dog's nose to sniff out explosives vapors. Ideally, such an autonomous trace detection system would be able to warn the public of a potential attack or be used to screen for potential threats. Triacetone triperoxide (TATP) is a powerful explosive without military use because it is very sensitive to mechanical shock and so very difficult to safely handling, a reason for which terrorists dubbed TATP "the Mother of Satan". TATP is easily prepared from acetone and hydrogen peroxide under acidic catalysis, being a home-made explosive almost undetectable by dogs or sniffer devices usually trained for nitrogen-containing explosives. The possibility of being prepared on board gave rise to restrictions on carrying liquids in hand luggage at airports, and the careful monitoring of luggage and people, so TATP is presently one of the substances with more impact in the everyday life of millions of people who probably never heard about its existence. TATP is frequently used in suicide terrorist attacks, therefore constitutes a threat in public transport or mass events where prevention of indiscriminate attacks with explosives is a major concern. Manufacturers of explosive detectors tend to concentrate on X-rays for bulk materials, but the signature of TATP is not clearly visible except by bulky mass spectrometers. A consequence of this is that better systems still need to be developed. Looking for much simpler technologies, optical portable methods have been developed on the basis of colorimetric or fluorimetric sensor arrays for detection of TATP vapor, by detecting hydrogen peroxide from TATP decomposition, because TATP itself did not react with the probes. So the search for fluorogenic probes that are specific for TATP is still an unresolved problem required for the easy and portable detection of peroxide explosives in checking of unknown materials at police controls. The ideal probe should have a strongly fluorescent reporter and a quenching group easily oxidizable by a mild oxidizing reagent in the absence of any solvent. Perylenediimides (PDIs) are strongly fluorescent compounds of known stability under light and air, suitable for high value dendrimeric materials in bioimaging and gene delivery applications, therefore they are appropriate candidates for the reporter unit. Our approach consisted of a modification of a fluorescent perylenediimide core with one electron donor aryl group by the classic carbon-

carbon coupling chemistry. From the study of its physicochemical characteristics, its sensitivity to oxidants and its covalent anchoring to a polymer we have developed a fluorogenic material that was able to generate fluorescence in the presence of triacetone triperoxide, TATP, under solvent-free, solid state conditions. The material, a perylenediimide functionalized polyacrylate, worked by accumulating vapors of TATP, giving a colorimetric and strongly fluorescent response. The fluorescent response given by the material to the presence of TATP was permanent so it could be checked at any time after the TATP exposition. With the membrane we developed an easy “white powder test” to detect solid TATP from suspect packages containing ‘white powder’ that could be involved in unidentified threats. In a typical experiment, a polymer piece from a vial with TATP acquired a strong orange fluorescence and pink color whilst an unreacted piece was non fluorescent and purple colored, indicating the unequivocal presence of TATP in the white powder. Building on this technique, we have developed new surface functionalized silica nanoparticles for the off-on fluorogenic detection of the improvised explosive triacetone triperoxide TATP in a vapor flow, so the system will expand the applications to a wider scope. Along the accomplishment of the project we will develop new detection technologies against the terrorist threat that will help in countering improvised explosive devices and we will extend the research to the detection of hexamethylene triperoxide diamine (HMTD), another important explosive used in improvised explosive devices. The need of reliable analytical methods for TATP and HMTD is due to several different scenarios that could be found in their use:

- (a) Unknown materials confiscated by the police need to be unambiguously identified as containing these substances in order to allow suspects to be prosecuted and to estimate the measures that are immediately required for public safety. The analytical method used in this case needs to be selective for the peroxides, suitable for on-site analysis and should permit safe sampling by the operator. However, very low limits of detection are not required.
- (b) Debris at post-explosion sites needs to be analyzed in order to identify the explosive material used. The analytical method used here needs to have low limits of detection and high selectivity so that it can detect small residues of explosives in complex matrices.
- (c) Air samples at airports, governmental buildings, etc. need to be checked for the peroxides in order to prevent terrorist acts. An extremely low limit of detection is required in this case, which may be easier to achieve with the highly volatile TATP than with the less volatile HMTD.

It is obvious that these requirements cannot be fulfilled by a single analytical method. Although the investigation of endangered sites, e.g. public buildings, by means of tracker dogs is a favorable option for rapidly screening a suspicious area, the unambiguous identification of either TATP or HMTD is not currently possible if these kinds of biological detection systems are used. Not surprisingly, most physicochemical analytical methods for peroxide-based explosives, like those described in the introduction, focus on the easier tasks (a and b) mentioned above, while only a few preliminary approaches that can be used for task (c) have been published. Vapor

detection is a practical, non-invasive method suitable for explosive detection among current explosive detection technologies. Optical methods (especially colorimetric and fluorescence spectral methods) are low in cost, provide simple instrumentation alignment, while still maintaining high sensitivity and selectivity, these factors combined facilitate broad field applications. Trace vapor detection of the highly volatile TATP and the less volatile HMTD represents an effective approach to noninvasive detection of peroxide-based explosives, though development of such a sensor system with high reliability and sufficient sensitivity (reactivity) still remains challenging. As example, TATP, the most commonly used explosive by terrorists in improvised explosive devices, (IEDs) is still going largely undetected in many densely-populated venues. No electronic trace detection system currently exists that is capable of continuously monitoring TATP vapors or its precursors. In this project we will establish new methods for the determination of TATP and HMTD targeted to the requirements stated above with the aim to give a broad approach to the resolution of the problem. Then, a portable testing setup will be developed which will allow for field-testing and generation of real-time results. By reducing the sensor footprint and reconfiguring the apparatus until it will fit into a carrying case, we will be able to test for explosives in a number of different environments. We will also extend the newly developed methods to the more conventional explosives with the aim to generate an integral system of larger scope in the detection of explosives. While our fluorescent methodology has a tendency to be very selective, it will need pre-concentration of the samples in suitable portable devices to give reliable results. The use of pre-concentration in addition to the sensing mechanism will allow for a controlled and highly concentrated burst of analyte to be delivered to the chemical sensor. To complement the methods based on fluorescence, a more general approach is required, therefore we will use the multiphoton electron extraction spectroscopy and its comparison with other spectroscopies for direct detection of solid explosives under ambient conditions. Multiphoton electron extraction spectroscopy (MEES) is an analytical method in which UV laser pulses are utilized for extracting electrons from solid surfaces in multiphoton processes under ambient conditions. Counting the emitted electrons as a function of laser wavelength results in detailed spectral features, which can be used for material identification. The method has been applied to detection of trace explosives on a variety of surfaces. Detection was possible on dusty swabs spiked with explosives and also in the standard dry-transfer contamination procedure. Plastic explosives could also be detected. The analytical limits of detection (LODs) are in the sub-pmole range, which indicates that MEES is one of the most sensitive detection methods for solid surface under ambient conditions. Scanning the surface with the laser allows for its imaging, such that explosives (as well as other materials) can be located. The imaging mode is also useful in forensic applications, such as detection of explosives in human finger-prints. In more detail, multiphoton electron extraction spectroscopy (MEES) is an analytical method for direct analysis of solids under ambient conditions in which the samples are irradiated by short UV laser pulses and the photo-charges emitted are recorded as a function of the laser wavelength. By this method, many peaks are observed at wavelengths that are in

resonance with the surface molecules. The analytical capabilities of MEES have recently been demonstrated, including conventional as well as peroxide explosives. By performing a systematic comparison with some traditional spectroscopies that are commonly applied to material analysis such as absorption, reflection, excitation and emission fluorescence, Raman, Fourier transform IR, and Fourier transform near-IR spectrometries, conducted for powders and for thin films of compounds that are active in all spectroscopies tested, for most parameters MEES has been shown to be a superior analytical tool to the other methods tested for both sample morphologies. Besides the obvious spectral parameters (signal-to-noise ratio, peak density, and resulting limits of detection), we introduce two additional variables- the spectral quality and the spectral quality density- that represent our intuitive perception of the analytical value of a spectrum. Along the accomplishment of the project we will develop new detection technologies against the terrorist threat that will help in countering improvised explosive devices and we will extend the current research to the detection of TATP and HMTD, the most important explosives used in improvised explosive devices, and compare to the conventional explosives. Then, a portable testing setup will be developed which will allow for field-testing and generation of real-time results. By reducing the sensor footprint and reconfiguring the apparatus until it will fit into a convenient carrying case, we will be able to test for explosives in a number of different environments. We will test the method with conventional and peroxide explosives with the aim to produce an integral system of large scope in the detection of explosives used in improvised explosive devices.

Partnership Relevance

The University of Burgos currently has almost 10,000 students studying at the Faculties of Science, Economics and Business Studies, Humanities and Education, Law, and the Higher Polytechnic School. It currently offers over 30 different undergraduate degrees, over 20 PhD Programmes, as well as several Official Masters and other graduate courses. It is located at the North of Spain, in the region of Castilla and León. The Faculty of Science offers the European degrees, official masters and doctorates of Excellence in Chemistry and Food Technology. Research in the Faculty is performed by the departments of Chemistry and Biotechnology-Food Science and the technical support of a fully equipped technological and scientific park. The Research Strategy and Doctoral Training of the University of Burgos, approved by the Council of Government of the University of Burgos on 20th July 2012, establishes the Applied Chemistry as the foundation of the joint research line in the Department of Chemistry and one of the main research pillars of the University of Burgos. Therefore, the Advanced Chemistry PhD Program and its associated research lines are integrated in the strategy of research, transfer and PhD training of the University of Burgos. The Faculty of Science is currently involved in several regional, national and European research projects, including some Excellence research projects. The Supramolecular Chemistry Group, involved in the

NATO SPS project, is integrated in the Chemistry Department and is currently working in the development of new selective fluorogenic probes for bio-metabolites, a field in which the group of research has got some successful achievements. Through the consolidation and integration of competences, the interdisciplinary nature of the members can better address research questions in the complex field of sensor design. Although the size of the unit is not excessively large, the training and recruiting capacity is really high, showing that the staff of the unit is able to conduct high level research. The strengths of this unit are related to the high quality of the research carried out for the different investigators in the research lines currently active and productive. In the last years the interaction with the private sectors has been reinforced, in part thanks to the regional projects achieved because all of them are directly linked with a company that favours and simplifies the transference of the research outputs of our research groups to the society in general and to the industrial sector in particular. The strengths of the unit have also relationship with the research outcomes related to quality and quantity of research articles published and transference of knowledge got during the last years.

Technion – Israel Institute of Technology is a public research university in Haifa, Israel. Founded in 1912, it is the oldest university in Israel. The Technion offers degrees in science and engineering, and related fields such as architecture, medicine, industrial management, and education. It has 18 academic faculties and 52 research centers. Since its founding, it has awarded 95,821 degrees, and its graduates are cited for providing the skills and education behind the creation and defence of the State of Israel. The Technion's 616 Faculty members currently include three Nobel Laureates in chemistry. In 2012, the magazine Business Insider ranked the Technion among the World's top 25 engineering schools. In 2011, the Technion partnered with Cornell University to submit a winning proposal to New York City to set up the Jacobs Technion Cornell Institute of Innovation (JTCII) on Roosevelt Island. In 2013, the Technion embarked on establishing the Technion Guangdong Institute of Technology (TGIT) in Shantou, Guangdong Province, China. In 2013, Technion was ranked in sixth place in the world for entrepreneurship and innovation, in the first comprehensive survey conducted by the MIT. In 2013, the Center for World University Rankings ranked the Technion 66th in the World. In 2013, the Shanghai Academic Ranking rated the Technion as 77th in its list of the World's top 100 universities. In 2013, the Technion was the only school outside of the United States to make it into the top 10 on a new Bloomberg Rankings list of schools whose graduates are CEOs of top US technical companies. Technion graduate Arieh Warshel, Distinguished Professor of Chemistry and Biochemistry at the University of Southern California won the 2013 Nobel Prize in Chemistry, together with Michael Levitt and Martin Karplus for "the development of multiscale models for complex chemical systems". Martin Karplus, Michael Levitt and Arieh Warshel pioneered the use of computer models that mirror chemical reactions. The work also has applications in the use of complex processes in the development of drugs. In 2011, Prof. Dan Shechtman, a Technion professor, won the Nobel Prize in Chemistry for his discovery of quasi-crystals, a new form of matter. The Nobel Prize in Chemistry 2004 was awarded jointly to Aaron Ciechanover, Avram Hershko,

Technion professors, and Irwin Rose “for the discovery of ubiquitin-mediated protein degradation”. The Technion is the premier technological university in Israel – in fact, it is one of the top institutions of scientific and engineering learning and research in the world. Chemistry lies at the very center of research and study in the Technion, and the Schulich Faculty of Chemistry leads the way in both of these endeavours. Scientists and engineers in the Technion are moving more and more into the realm of the smallest devices possible – molecular devices. And for this reason the Faculty of Chemistry is central for all of the research and studies at the Technion. The Schulich Faculty of Chemistry at Technion is a vibrant academic unit, with dynamic research and teaching programs, active faculty members and modern research laboratories and facilities. It spans the full spectrum of disciplines within chemistry – physical, analytical, inorganic, organic, biochemical and theoretical – and overlaps the associated fields of physics, materials sciences, biology, medicine and electronics and nanotechnology. The Schulich Faculty of Chemistry at the Technion is ranked eighth in Europe, 38th in the world according to Shanghai Rankings ARWU 2013. At the forefront of the Faculty’s interests is the evolution of chemical research towards molecular materials engineering and life sciences, and many of the Faculty’s research projects, particularly the most exciting recent discoveries, are characterized by a highly multidisciplinary nature. Faculty members are cooperating with the local industry on various levels. This cooperation can take different forms, such as direct funding of research by partners in the industry, government funding of joint projects between academic researchers and industry, start-up companies in which academic staff are involved, consulting services provided to industry, patent applications and commercialization, and service work provided to industry by our service research laboratories. Some faculty members’ research projects are directly funded by Israeli companies. In these cases, very focused applied research is carried out in collaboration with industrial programs with financial support provided from the industrial side. Some of the faculty (i.e. I. Shechter) take part in joint academic-industrial research programs funded by government foundations. In these cases, several industrial partners and academic groups join a large project that includes research and development in several directions. Therefore the collaboration between both groups will bring the best success to the development of the project.

End Users

The Technology Center Foundation of Miranda de Ebro (Fundación Centro Tecnológico de Miranda de Ebro), is a part of the Castilla y León Innovation and Entrepreneurship Network, and includes Industry activities, innovation in product/services design and processes, internationalization of R&D and technology-based entrepreneurship support of the latest advances in technologies, including sensor technology, as applied to the industrial and entrepreneurial sector. The Technology Center Foundation Miranda de Ebro (CTME), as a benchmark on environmental

issues, has a specialized staff and equipment and facilities perfectly adapted to support and advise their lines of the projected work. Their mission is to respond responsibly and sustainably to the competitive needs of the environment through the R & D and innovation, developing new lines of research aimed at supporting businesses in the region, mainly small and medium enterprises (SMEs). D. Raúl de Saja González, Team Leader and Technology Transfer, will be the representative of the CTME.

The Centro de Investigação da Academia Militar (CINAMIL) is the structure responsible for the scientific research and technological development in the Portuguese Army, and is framed in the chain of command of the Military Academy, being responsible for the coordination of the R&D in the Portuguese Army. The Military Academy Research Center (CINAMIL), promotes and conducts research and development (R&D) projects, in cooperation with other national and international relevant scientific and academic institutions, producing and sharing scientific knowledge, specifically in the defence and security area of interest. The Military Academy International Program aims to enhance cultural, scientific and technical cooperation, through international exchange with similar academic institutions, in order to deepen bilateral and multilateral relationships, mainly directed to the Euro-Atlantic area of interest. In this project, Mr. Wilson Antunes, from the Laboratório de Bromatologia e de Defesa Biológica (LBDB) will be the representative of the CINAMIL in this project.

Both end-users will be involved in the creation of an Advisory Board with the aim of exchange of information with specialists on the area of sensors and sensor networks and with every end-user. The Advisory Board will be implemented and supported along the development of the project. An advisory board comprising experts on the domains considered in the project will be set up. Members of identified projects as well as researchers will be invited to this group. A collaborative workspace will be created within the website for the workgroup members and both end-users for exchange of opinions and consultation. From the end-users, D. Raúl de Saja González, Team Leader and Technology Transfer of CTME, will provide advice in defining an exploitation strategy for project outcomes and pursuing exploitation activities, managing IPR in an adequate way, interfacing and providing contributions to standardisation groups (including standards for platform interoperability, performance metrics, safety of operations and regulatory matters), analysis of potential markets for future based products, preparation for project exploitation and technology use plans, establishing an exploitation strategy to maximize the opportunities for the results market adoption, define future steps including market analyses, manufacturing cost estimations, business models, etc. and examine project outcomes' exploitation possibilities from different stakeholders' viewpoints in order to stimulate market awareness about the value of the results of the project. From the end-users, Mr. Wilson Antunes, as the representative of the CINAMIL, will be involved in the definition of the operational requirements for the system, especially under the scope of end user. It will advise in the supervision, testing and validation of the sensors, together with the partners of this project.

Technical Summary

Over the past decade, the use of improvised explosive devices (IEDs) has increased, domestically and internationally, highlighting a growing need for a method to quickly and reliably detect explosive devices in both military and civilian environments before the explosive can cause damage. Conventional techniques have been successful in explosive detection, however they typically suffer from enormous costs in capital equipment and maintenance, costs in energy consumption, sampling, operational related expenses, and lack of continuous and real-time monitoring. Triacetone triperoxide (TATP),[1] prepared from acetone, hydrogen peroxide and an acid,[2] constitutes an improvised explosive of very difficult detection,[3] for this reason has been frequently used in suicide terrorist attacks.[4] The lack of nitro groups or aromatic moieties makes the detection of this improvised explosive a difficult task.[5] TATP is usually detected by mass spectrometry,[6] ion mobility spectrometry,[7] multiphoton spectroscopy,[8] or MS spectrometry.[9] Therefore, portable and selective systems still need to be developed. Good alternatives are chemically modified nanosensor arrays,[10] or optical portable methods based on colorimetric sensor arrays that detect hydrogen peroxide (H_2O_2) from TATP decomposition.[11] Indirect detection of H_2O_2 from TATP, linked to oxidative processes, [12] was successfully used for colorimetric[13] or fluorimetric[12b,14] sensing. TATP direct detection has been achieved by fluorescence quenching[15] or quartz crystal microbalances.[16] Turn-on fluorogenic chemosensing systems are a good alternative for many analytes,[17] therefore fluorogenic probes that are specific for TATP are valuable methods for the detection of peroxide explosives. Perylenemonoimides (PMIs)[18] as well as perylenediimides (PDIs)[19] are strongly fluorescent compounds, stable under light and air, so they are good candidates for the search of new fluorogenic reporters. PMIs/PDIs bear an electron poor π -conjugated aromatic core, suitable for multiple chemical modifications and optical sensing,[20] that could be appropriate for the selective detection of pristine TATP in the vapour phase, a major as yet unresolved issue.[21] Our approach consisted of modifying the fluorescent PMI and PDI core with donor groups by established Suzuki coupling[22] to obtain compounds suitable for anchoring to silica surfaces, on the way to solid fluorogenic sensors for the sensitive and selective detection of TATP in the vapour phase. From the initial tests, we discovered that a modification of the PMI and PDI core with a substituted pyridyl group was able to modulate the electron donor-acceptor effect on the fluorescent core, giving products with an outstanding performance in terms of selectivity and sensitivity to TATP, that were suitable for their covalent anchoring to silica matrixes. For this reason, we are studying the preparation of new surface modified fluorogenic silica materials for the selective detection of TATP in a vapour flow (Fig. 1).

For the anchoring of silylated peryleneimides we used commercial silica nanoparticles, 10–20 nm, and TLC plates (silicagel 60, aluminium sheets 5 × 10 cm). Functionalized silica nanoparticles were prepared from 500 mg of pristine silica nanoparticles and 4 mg of the triethoxysilyl perylene derivatives **JG131** and **JG135**.

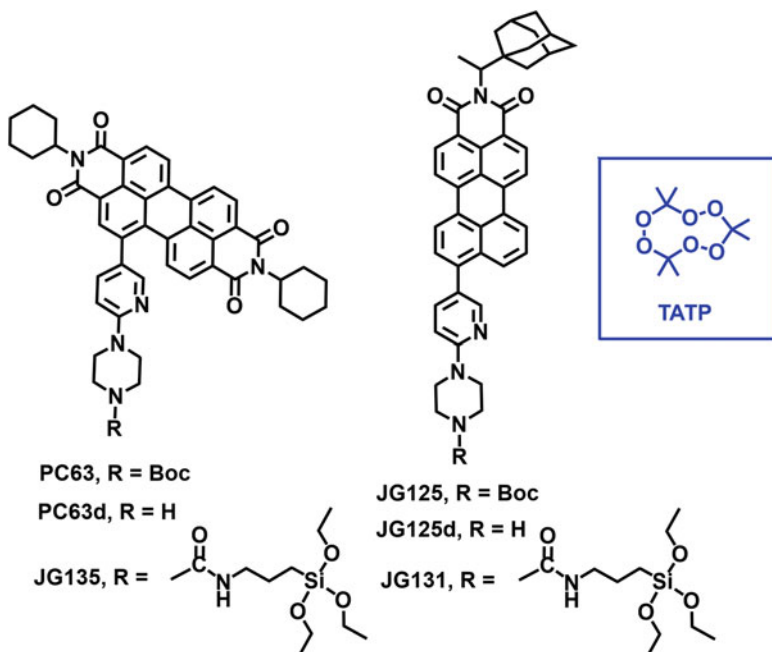


Fig. 1 PMI/PDI derivatives used for TATP detection

The mixtures were refluxed at 112 °C in a mixture of toluene:water (500:10 µL) for 24 h, finally, the nanoparticles were washed with toluene, DCM and Et₂O. The materials obtained were labelled **nJG131** and **nJG135** (Fig. 2). By the same way, the silane derivatives were bonded to silica TLC plates, 0.5 mg of **JG131** or **JG135** for every 5 × 10 cm plate. Instead of reflux, the plates were heated at 60 °C for 48 h, until the solutions had neither colour nor fluorescence. Then, the TLC plates were cleaned by the same procedure used in previous case. The materials obtained were labelled **pJG131** and **pJG135** (Fig. 3). With the purpose of comparison to purely adsorbed materials, **JG125** and **PC63** were mixed with TLC plates under similar conditions to get the products adsorbed on silica, labelled **aJG125** and **aPC63**. We then checked colour and fluorescence qualitative and quantitative changes of all solid materials in the presence of TATP in the gas phase.

We started by checking colour and fluorescence qualitative and quantitative changes of solid materials **nJG131** and **nJG135** in the presence of TATP in a vapour flow. Silica nanoparticles were fixed to borosilicate glass coverslips 18 mm × 18 mm by spray adhesive and placed in a glassware system schematized in Fig. 4. Every experiment employed 2 mg TATP and a dry nitrogen gas flow adjusted to 100 cm³/min in a round bottom flask, gently warmed below 50 °C with an external air flow heating (a laboratory hot air gun) for 10 min. The gas flow having an average concentration of 0.2 mg/L of evaporated TATP was conducted through a glassware tube to another similar flask at room temperature containing the

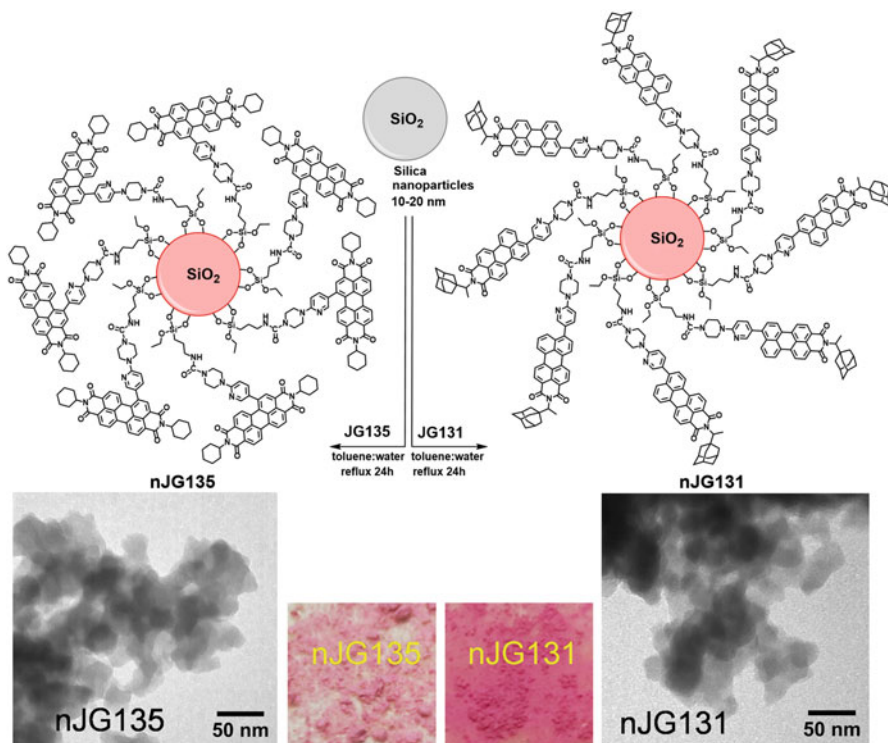


Fig. 2 Preparation of nJG131 and nJG135, TEM and day-light images of nJG131 and nJG135

solid sensor. Then the gas flow was finally vented through a glassware tube to exhaust (Fig. 4) and the sensor material checked for changes in colour and fluorescence. We also checked the action of hydrochloric acid vapour (1 mL, 35% aqueous HCl, 30 seconds), acetic acid vapour (glacial AcOH vapour, 1 mL, 30 seconds), triethylamine vapour (neat NEt₃ vapour, 1 mL, 30 seconds) and hydrogen peroxide vapour (5 mL, 30% aqueous H₂O₂ for 10 min) under related conditions in order to assess the selectivity of the detection system (Fig. 5).

Except for a slight sensitivity to strong acid vapour, seen as a small increase in fluorescence emission, the most remarkable finding was a dramatic increase in the fluorescence emission of nJG131 and nJG135 in the presence of TATP vapour in a very selective fashion. Acetic acid, triethylamine or hydrogen peroxide vapours did not show noticeable fluorescence changes under the same conditions, even more, NEt₃ or AcOH reversed the action of HCl on the materials. Therefore, both materials were best suited for the detection of TATP vapour in a stream flow at one third of the maximum saturation equilibrium concentration of TATP (reported as 600 $\mu\text{g L}^{-1}$).^{1a} Steady state spectra in Fig. 6 showed a clear increase in the emission intensity in both cases, nJG131/nJG135 in the presence of TATP, very little increase of intensity in the presence of HCl and no change in the presence of H₂O₂. The quantitative

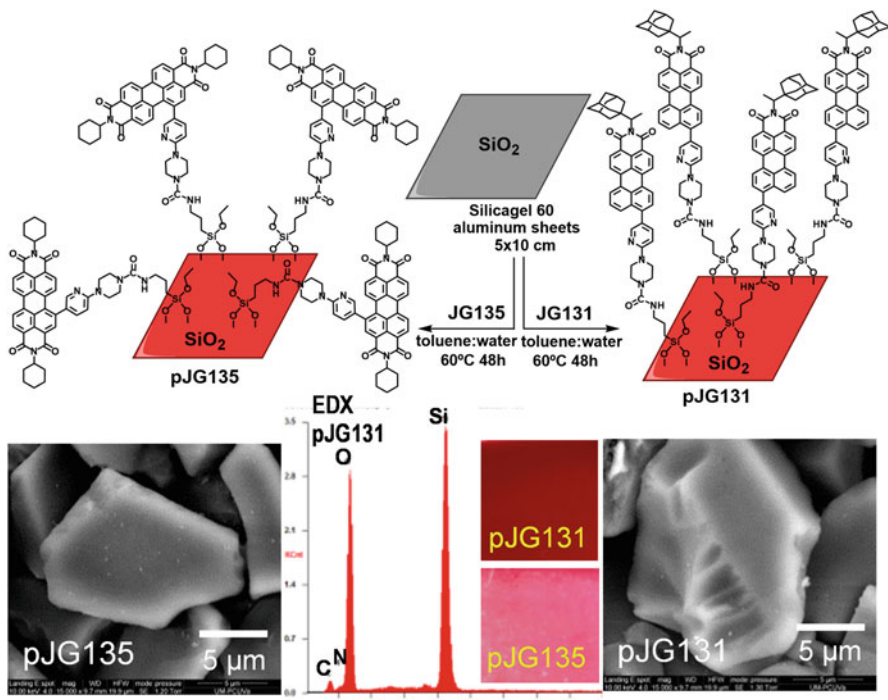


Fig. 3 Preparation of pJG131 and pJG135. SEM and day-light images of pJG131 and pJG135. Inset: EDX profile of pJG131

increase in fluorescence with the solid materials was performed by measurement of quantum yield differences between samples, by repeating three times each sample until the error was lower to 2%. Consequently, for nJG131 the overall increase of the quantum yield in the presence of TATP vapour was $\Phi_{n\text{JG131} + \text{TATP}}/\Phi_{n\text{JG131}} = 3.5$; for nJG135 the overall increase of the quantum yield in the presence of TATP vapour was $\Phi_{n\text{JG135} + \text{TATP}}/\Phi_{n\text{JG135}} = 3.1$; for comparison, the overall increase of the quantum yield in the presence of HCl vapour was much lower, $\Phi_{n\text{JG131} + \text{HCl}}/\Phi_{n\text{JG131}} = \Phi_{n\text{JG135} + \text{HCl}}/\Phi_{n\text{JG135}} = 1.6$. In all cases, the increase in fluorescence in the presence of TATP vapour was sufficient for reliable measurements.

Similarly, we tested colour and fluorescence qualitative and quantitative changes of solid plates pJG131 and pJG135 in the presence of TATP in the gas phase and compared them to the changes in the presence of HCl and H_2O_2 vapour. Albeit the shape of the particles moved from roughly 20 nm to 20 μm , the homogeneity of the plates could lead to an easier managing of the samples. The conditions were as in previous experiments, this time with 20 mm x 20 mm plates, the results are shown in Fig. 7. We compared the results with the adsorbed colorants in plates, aJG125 and aPC63, in the same conditions, also shown in Fig. 7. Again the main features are a dramatic increase in the fluorescence emission of pJG131 and pJG135 in the

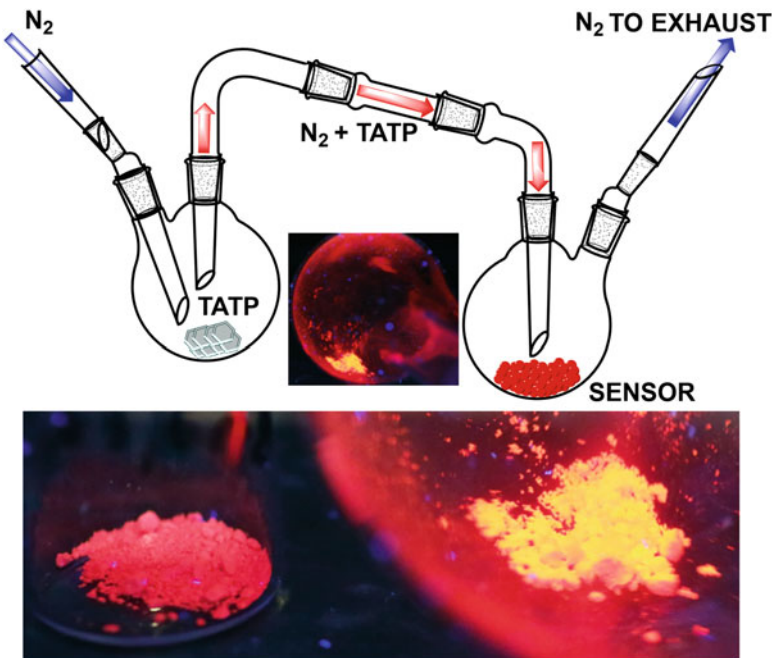


Fig. 4 Upper: Glassware system design for the detection of TATP in the gas phase with **nJG131/pJG131** and **nJG135/pJG135**. Inset: Image of the right flask under UV light, 366 nm, after TATP experiment. Lower: **JG131** nanoparticles (left) as prepared and (right) after treatment with TATP vapour, both under UV light, 366 nm

presence of TATP vapour in a very selective fashion and a slight sensitivity to strong acid vapour, seen as a small increase in fluorescence emission. Acetic acid or triethylamine vapours did not show noticeable fluorescence changes (not shown). On the other hand, hydrogen peroxide vapour, under the same conditions, showed a remarkable decrease in the initial fluorescence of the materials. The adsorbed colorants **aJG125** and **aPC63** showed similar features, albeit the initial colours of plates were less pronounced. Therefore both types of materials were suited for the detection of TATP vapour but the functionalized silica samples had better performance. Steady state spectra in Fig. 8 showed the increase in the emission intensity of **pJG131/pJG135/aJG125/aPC63** in the presence of TATP or HCl. The quantitative increase in fluorescence with the solid materials was performed by measurement of quantum yield differences between samples, by repeating three times each sample until error was lower to 2%. Consequently, for **pJG131** the overall increase of the quantum yield in the presence of TATP vapour was $\Phi_{\text{pJG131} + \text{TATP}}/\Phi_{\text{pJG131}} = 3.4$; for **pJG135** the overall increase of the quantum yield in the presence of TATP vapour was $\Phi_{\text{pJG135} + \text{TATP}}/\Phi_{\text{pJG131}} = 3.5$; for comparison, the overall increase of the quantum yield in the presence of HCl vapour was much lower, $\Phi_{\text{pJG131} + \text{HCl}}/\Phi_{\text{pJG131}} = 1.0$; $\Phi_{\text{pJG135} + \text{HCl}}/\Phi_{\text{pJG131}} = 1.6$. The adsorbed colorants on silica gave

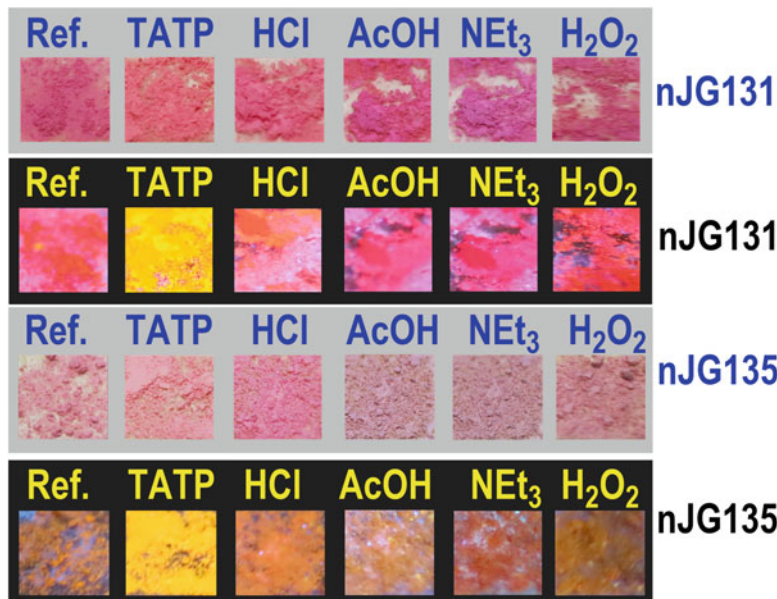


Fig. 5 Detection of TATP in the gas phase by the colour and fluorescence changes of modified silica nanoparticles **nJG131/nJG135** with vapours of TATP, acids, amine and hydrogen peroxide. *First row:* **Ref.**: pristine **nJG131**; **TATP**: **nJG131** in the presence of the vapours of TATP; **HCl**: **nJG131** in the presence of the vapours of HCl 35% w/v; **AcOH**: **nJG131** in the presence of the vapours of glacial acetic acid; **NEt₃**: **nJG131** in the presence of the vapours of triethylamine; **H₂O₂**: **nJG131** in the presence of the vapours of H₂O₂, all under white light; *Second row*: same experimental conditions than in the first row, but under a UV lamp, 366 nm. *Third row:* **Ref.**: pristine **nJG135**; **TATP**: **nJG135** in the presence of the vapours of TATP; **HCl**: **nJG135** in the presence of the vapours of HCl 35% w/v; **AcOH**: **nJG135** in the presence of the vapours of glacial acetic acid; **NEt₃**: **nJG135** in the presence of the vapours of triethylamine; **H₂O₂**: **nJG135** in the presence of the vapours of H₂O₂, all under white light. *Fourth row*: same experimental conditions than in the third row, but under a UV lamp, 366 nm

similar results. In all cases, the increase in fluorescence in the presence of TATP vapour was sufficient for reliable measurements. To understand the observed luminescent behaviour we performed quantitative fluorescence titration experiments of **JG125** (2.5·μM solution in CHCl₃:MeOH 9:1, $\lambda_{\text{exc}} = 500$ nm) by adding increasing concentrations of TATP in the same solvent mixture (Fig. 9) and compared the results to a similar titration with a common organic oxidant, *m*-chloroperbenzoic acid (MCPBA) (Fig. 10). TATP titration of a **JG125** solution showed the appearance of an emission in fluorescence at 556 nm and the decrease of the initial band at 665 nm after addition of excess TATP (Fig. 9). The titration plot could be fitted to a sigmoidal curve with an asymptotic maximum after addition of a large excess of TATP (Fig. 9). MCPBA titration of a **JG125** solution showed the appearance of an emission in fluorescence at 556 nm and the decrease of the initial band at 665 nm

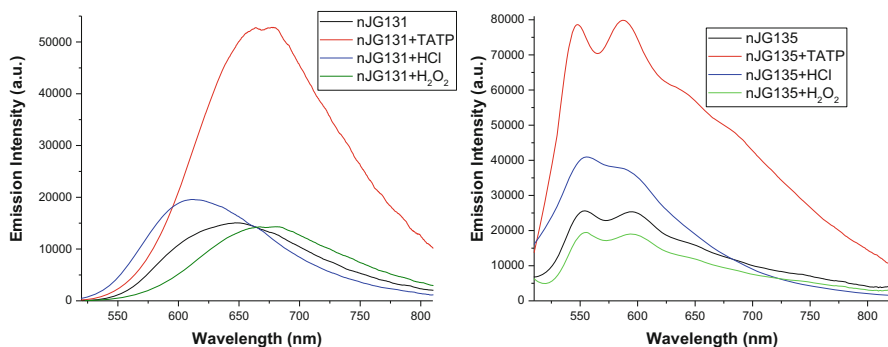


Fig. 6 Response in fluorescence of nJG131/nJG135 and TATP, HCl or H_2O_2 . nJG131: $\lambda_{\text{exc}} = 492 \text{ nm}$. nJG135: $\lambda_{\text{exc}} = 495 \text{ nm}$

after addition of excess MCPBA (Fig. 10). The titration plot could be fitted to an asymptotic curve by addition of excess of MCPBA (Fig. 10).

The main differences between both fluorescence titration corrected spectra were the presence of an isosbestic point for the TATP titration, which is not evident in the case of the MCPBA titration, and the steepest titration profile in the case of MCPBA acid (that afforded a limit of detection of $7.4 \mu\text{M}$ or $1.3 \mu\text{g/mL}$) that reached the asymptotic maximum at a much lower concentration of oxidant. In conclusion, we have developed fluorogenic materials that were able to generate fluorescence in the presence of vapours of triacetone triperoxide, TATP, an improvised explosive used in terrorist attacks. The materials worked in a stream of vapours of TATP, giving a strongly fluorescent response. The fluorescent response given by the materials to the presence of TATP was permanent so it could be checked at any time after the TATP exposition. The mechanism consisted in the oxidation of an amino-substituted pyridine side group that quenched the fluorescence of the conjugated fluorophore by an intramolecular charge-transfer effect until it was oxidized with subsequent release of the original fluorescence of the perylenemonoimide/perylenediiimide fluorophores. The materials are insensitive to hydrogen peroxide, the decomposition product of TATP, which is the common analyte used to detect TATP, but in itself it is not a threat. Therefore the reported materials detect TATP solely by the interaction with the vapours of the intact explosive, minimizing the risk of a false positive detection.

Detection of Trace Explosives under Ambient Conditions Using Multiphoton Electron Extraction Spectroscopy (MEES) Numerous analytical approaches have been applied to detection of trace explosives [22, 23]. Since the vapor pressure of many of these compounds is very low, most of the used methods are based on detection of trace solids, such as aerosols or residues adsorbed to surfaces. The detection limits should be as low as possible, but definitely lower than 1 ng. In most field security applications many samples must be examined in a short time, so the detection must be accomplished within seconds. Also the detection reliability is very

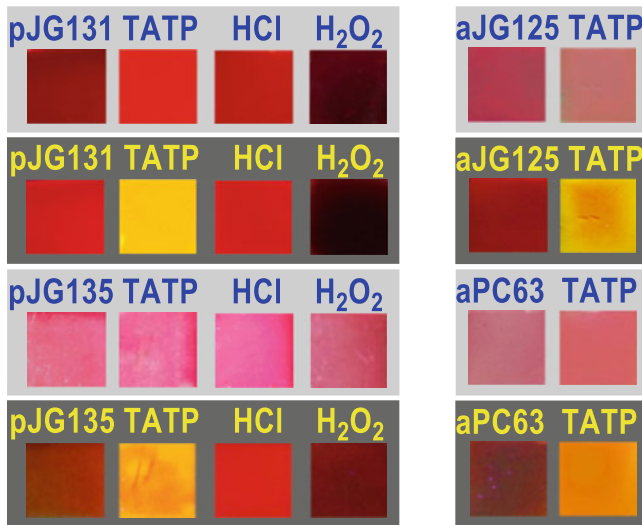


Fig. 7 Detection of TATP in the gas phase by the colour and fluorescence changes of silica plates with vapours of TATP, HCl and hydrogen peroxide: *Left column:* pJG131/pJG135. *Right column:* aJG125/aPC63. *First row:* pristine pJG131; TATP: pJG131 in the presence of the vapours of TATP; HCl: pJG131 in the presence of the vapours of HCl 35%; H₂O₂: pJG131 in the presence of the vapours of H₂O₂; pristine aJG125; TATP: aJG125 in the presence of the vapours of TATP, all under white light; *Second row:* same experimental conditions than in the first row, but under a UV lamp, 366 nm. *Third row:* pristine pJG135; TATP: pJG135 in the presence of the vapours of TATP; HCl: pJG135 in the presence of the vapours of HCl 35%; H₂O₂: pJG135 in the presence of the vapours of H₂O₂; pristine aPC63; TATP: aPC63 in the presence of the vapours of TATP, all under white light. *Fourth row:* same experimental conditions than in the third row, but under a UV lamp, 366 nm

important, therefore, only a few analytical technologies are adequate for such applications. The most commonly used technique is the Ion Mobility Spectrometry (IMS) [23, 24]. It is considered a successful technology, however, it suffers of some known drawbacks. These are related to matrix effects, which prevent detection in some cases. Also, since IMS detection is based on physical molecular properties, false positive alarms may occur. Therefore, new analytical methods that are directly related to the molecular identity (such as energy levels), and are sensitive enough and can provide fast results, are of considerable interest. Many laser based analytical technologies have been considered for detection of trace explosives [25, 26]. These include Raman spectroscopy methods [E.g., 27], cavity ring-down spectroscopy [E.g., 28, 29], laser induced breakdown spectroscopy [E.g., 30, 31], photo-dissociation followed by laser induced fluorescence [E.g., 32] and LIDAR [E.g., 33]. Each of these methods has specific advantages and drawbacks, however, only a few methods were applied for field applications and for standoff detection of explosives [26]. In many cases their sensitivity is not good enough under such conditions. [30]. Laser induced multiphoton ionization has been developed in mass spectrometry under

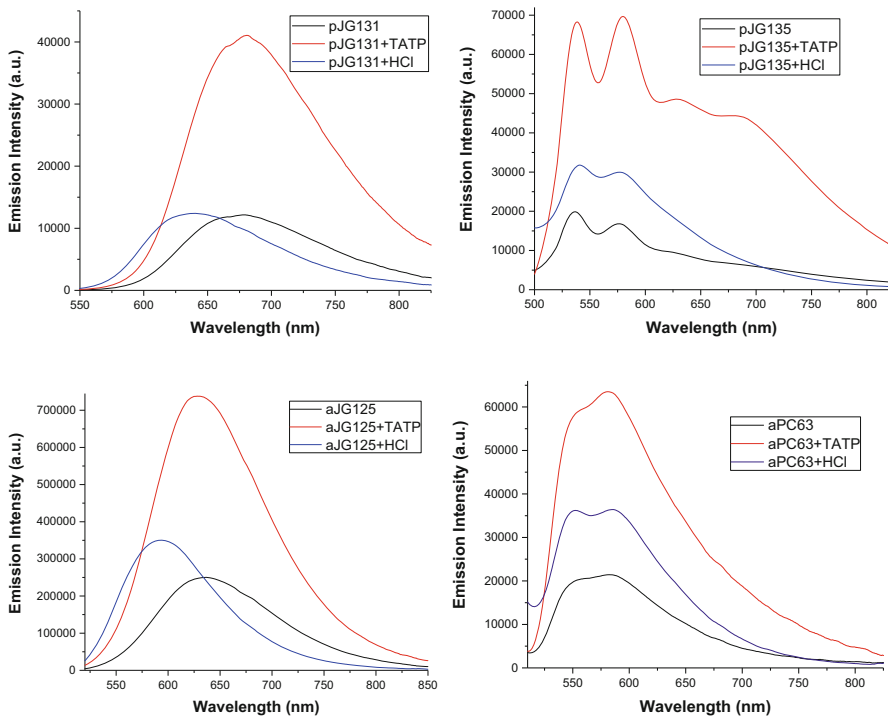


Fig. 8 Response in fluorescence of **pJG131/pJG135** and TATP or HCl. **nJG131:** $\lambda_{\text{exc}} = 438 \text{ nm}$. **nJG135:** $\lambda_{\text{exc}} = 487 \text{ nm}$

vacuum conditions. This ionization method yields a large percentage of the parent molecular ions [34] and is considered a very effective and sensitive technique [35]. Addition of wavelength-dependent ionization, known as Resonance Enhanced Multiphoton Ionization (REMPI), has considerably improved its selectivity and specificity [36, 37]. The main drawbacks of this technology for field applications are its high cost and the high vacuum requirement. Moreover, the huge dilution factor when moving from ambient conditions to the required high vacuum, restricts its practical sensitivity. Multiphoton ionization under moderate pressure conditions has also been suggested [38–41]. Under such conditions, improved detection limits were achieved, however, at the price of losing the mass spectrometry detection and the selectivity. Analytical applications of multiphoton ionization under ambient conditions were developed as well. Since no mass information is possible under such conditions, the measurements were based solely on conductivity. A UV laser beam ionized the substrate and the released charges were collected and counted. This method was applied to solids [42–46], to liquids [47, 48] and to aerosols [49–52]. Since only a single laser wavelength was applied, no molecular identification was possible and the only discrimination between the analyte and its matrix was based on differences in their ionization potentials. Some early attempts of ionizing analytes in

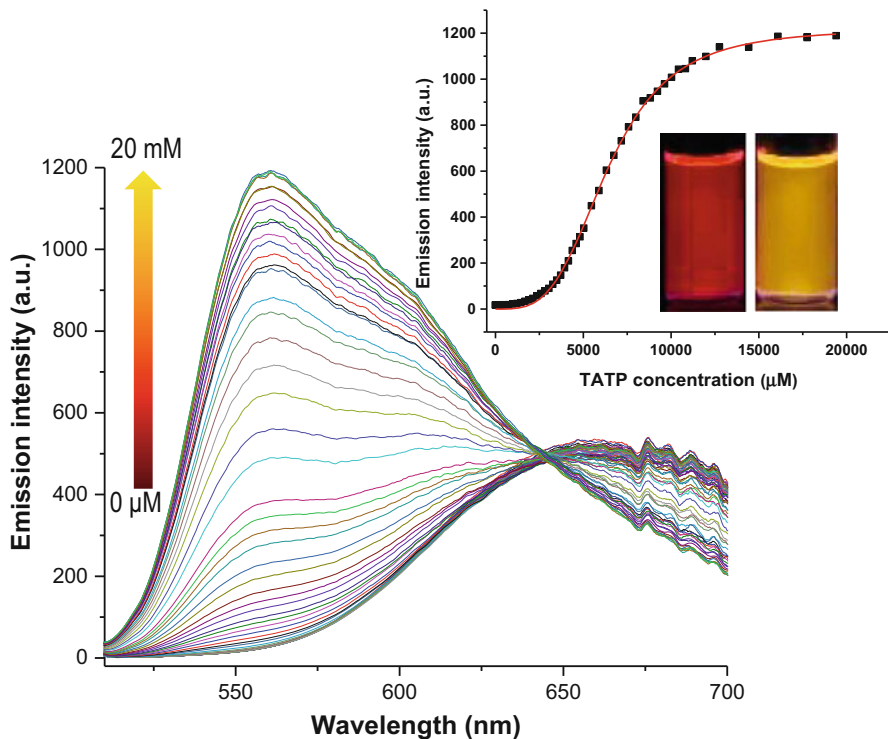


Fig. 9 Fluorescent titration and titration profile at 556 nm of **JG125** (2.5 μ M solution in CHCl_3 : MeOH 9:1) under increasing concentrations of TATP. Inset pictures: Initial fluorescence of **JG125** (left) and after addition of 20 mM TATP (right)

the gas phase [53] and in liquid solutions [54, 55] at a series of wavelengths were performed using dye lasers. Very limited information could be obtained, because of the narrow tuning capability of these lasers and due to other technical issues [51]. Recently, a new approach to multiphoton ionization spectroscopy has been suggested [56, 57]. It was based on direct induction of multiphoton processes and it was named Multiphoton Electron Extraction Spectroscopy (MEES). It has been shown that this method provides detailed spectral features, as well as excellent sensitivity. The first generation experimental setup has been described and the physical basis of the method has been discussed [56–58].

In this project we will address the potential application of MEES to analysis of trace improvised and traditional explosives under field conditions. In preliminary work, a variety of energetic materials have been tested, including military grade explosives and home-made explosives (HME). The method can provide imaging of explosives on surfaces and this feature, which has promising forensic applications, will also be investigated. In our preliminary work we have tested explosives including 2,4,6-trinitrotoluene (TNT), 2,4-dinitrotoluene (DNT), 1,3,5-trinitro-

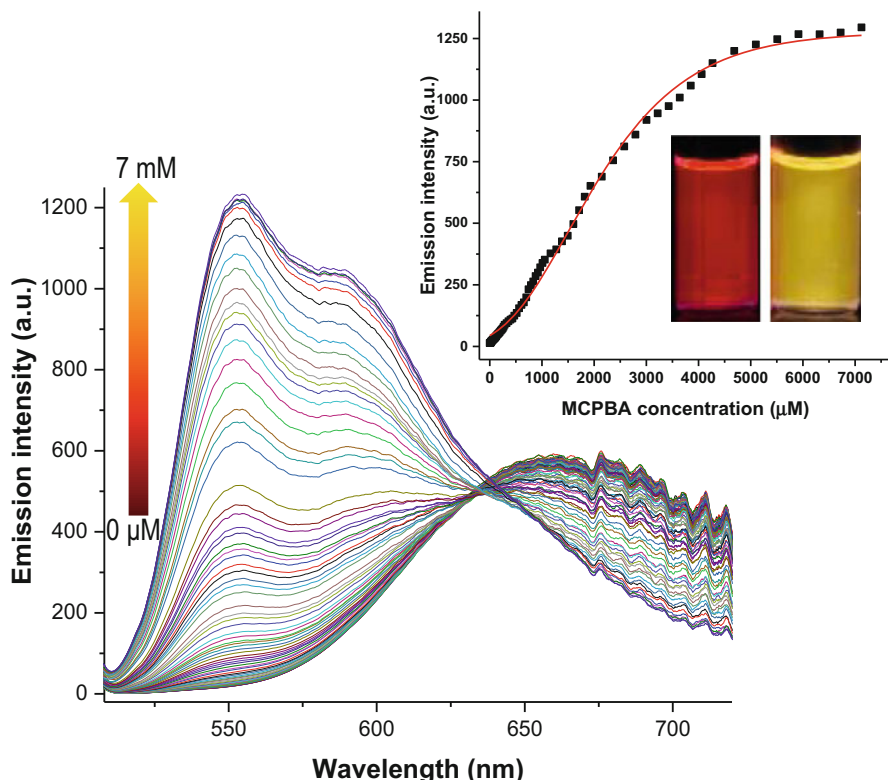


Fig. 10 Fluorescent titration and titration profile at 556 nm of **JG125** (2.5 μM solution in CHCl_3 ; MeOH 9:1) under increasing concentrations of MCPBA. Inset pictures: Initial fluorescence of JG25 (left) and after addition of 20 mM MCPBA (right)

1,3,5-triazacyclohexane, (RDX), sodium salt of 1-nitroso-2-hydroxynaphthalene-3,6-disulfonic acid (Nitroso-R salt), Pentaerythritol tetranitrate (PETN), Octahydro-1,3,5,7-tetranitro-1,3,5,7-tetrazocine (HMX), picric acid, nitrocellulose and triacetone triperoxide (TATP). All explosive compounds were of military grade and used without further purification. Small quantity (less than 1 mg) of TATP was synthesized and used without purification. The sampling materials included swabs commonly used for explosives (Smiths 15883E) and glass microfiber filters (Wattman GF/A). For controlled measurements, the sampling materials were spiked with known quantities of the tested explosives.

Quantification was performed using thin films of the examined compound. The surface concentration was varied for the quantification plots. The standard protocol for detection of explosives is the so called “dry transfer” test [59]. It includes the following steps: (a) application of a well-defined quantity (in the ng range) of explosive solution to a Teflon plate, (b) full evaporation of the solvent, (c) bringing the Teflon plate in contact with a target object (E.g., suitcase), such

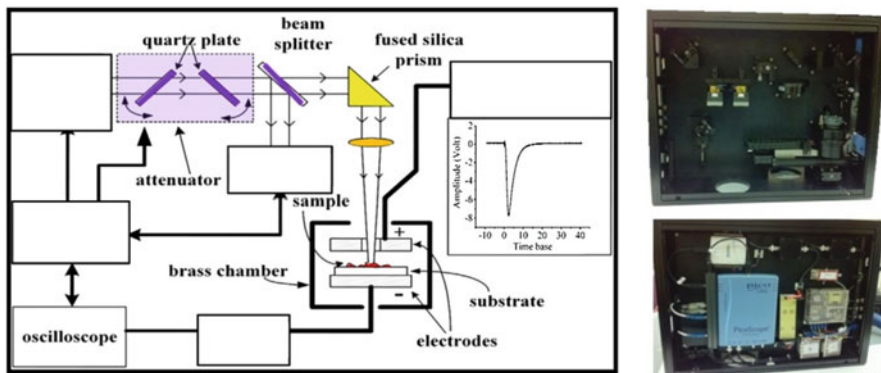
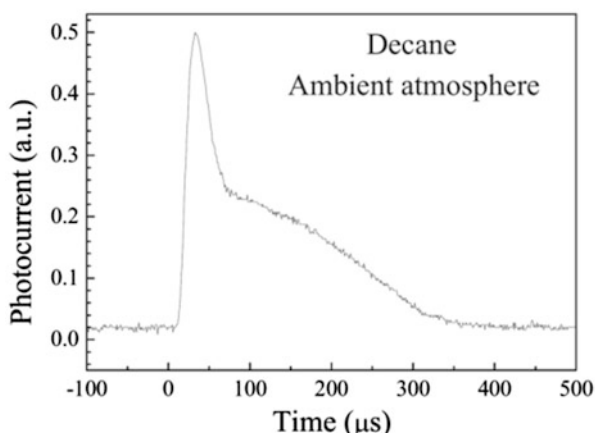


Fig. 11 The MEES experimental setup scheme (left) and its packing (right)

that the explosive (or some of it) is transferred, (d) collecting material from the target object using a swab, (e) transferring the swab to the detection instrument.

The current setup of the home-made MEES spectrometer is schematically shown in Fig. 11. Its components include a pump laser (Nd:YAG, 5 ns, running up to 10 Hz repetition rate), equipped with second and third harmonic generators. The third harmonic generation (130 mJ per pulse) was transferred to an optical parametric oscillator (OPO) laser (NT342/3/UVE EKSPLA, Vilnius, Lithuania), emitting pulsed radiation in the wavelength range of 210–410 nm. The laser tuning maximum wavelength resolution was 0.1 nm. The OPO output power at each wavelength was measured using a pyroelectric power meter (Ophir Laserstar PE-10-sh-v2, Israel). It was passed through a computerized optical attenuator, which was pre-calibrated. The attenuator was readjusted for each wavelength, such that the output power was almost constant and wavelength independent. The average energy applied to the samples was about 40 μ J per pulse. The dependence of the MEES signals on irradiation power is described in the following. The laser spot was of ca. 20 μ m, and this particular power density was selected in order to avoid plasma formation. The thus attenuated laser light was guided through an optical setup to the sample, where it was slightly focused using a quartz lens of $f = 180$ mm. The stainless steel sample holder and the anode were placed in a Faraday cage. It was attached to a motorized tray, which pushed it out of the cage for loading and pulled in for analysis. Although the attenuator compensated for wavelength dependent power changes, pulse-to-pulse fluctuations could not be avoided (of the order of 10%). In order to partially compensate for these fluctuations the photo-charge yield was divided by the energy of each individual pulse. The result is the normalized photo-charge, which is presented as a function of laser wavelength. For obtaining the spectra, the samples were placed on the stage and irradiated by the pulsed OPO laser. They were contacted with a cathode and an anode was placed above it, at a distance of ca. 1 cm. The voltage drop between the electrodes was varied using a variable high voltage power supply (Keithley – model 2290), in the range of 500 V to

Fig. 12 Photo-current as a function of time, resulted from a single laser pulse hitting a surface in ambient air



2000 V. The time-dependent current, which resulted from each laser pulse, was amplified (Keithley current amplifier Model-428, typical gain: 106 V/A) and monitored using a digital oscilloscope (PicoScope, 3206 A). A sensitive microphone was positioned close to the irradiated spot, to alert in case of optical breakdown. The whole setup was automated using LabVIEW™ software. The oscilloscope waveforms were integrated for obtaining the total photo-charges released by the laser pulses. The experimental setup was packed in a portable box, of the size of a typical desktop PC (Fig. 11). The measurement time depends on the specific program selected. Measurement at only a few wavelengths takes a few seconds, including data analysis steps. Acquisition of full MEES spectrum at the best resolution of 0.1 nm, over a range of 50 nm, takes a few minutes.

The sample molecules placed on the stage are ionized in a multiphoton process and the released electrons are collected by the positive electrode placed above the sample. The thus produced current is amplified and recorded as a function of time. A typical photoelectron current as a function of time, measured under ambient conditions, is shown in Fig. 12. The current starts just after the laser pulse (of a few ns) and lasts ca. 300 μs. It results from photoelectrons moving towards the anode, while colliding with air molecules. The longer tail is attributed to electrons entrapped by oxygen molecules, which migrate to the anode at a slower velocity (it disappears under nitrogen environment, but the total charges reaching the anode is unchanged). The integration of the current over time provides the total emitted photo-charges. When the laser wavelength is scanned (in the UV range), the photo-charges are recorded and this makes the multiphoton electron extracted spectrum. Irradiation of most materials by short UV laser pulses almost always results in a certain level of ionization, regardless of the laser wavelength. This is the so called “non-resonant multiphoton ionization”, which takes place via virtual states [60–62]. Since these are forbidden transitions of very low probability, the resulting non-resonant currents are very low. However, if one of the photons (or a combination of photons) exactly

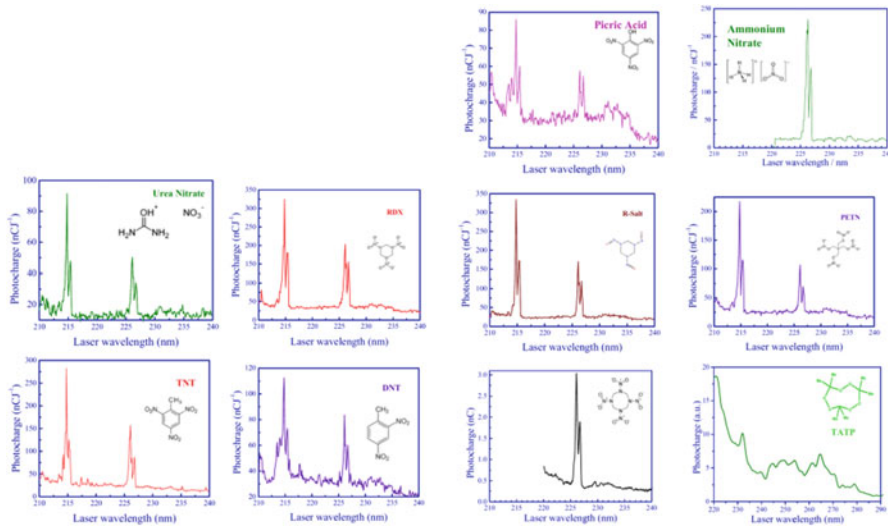


Fig. 13 Multiphoton electron extraction spectra of explosives. The photo-charges are presented as a function of laser wavelength

matches a transition to a real molecular energy level, the transition becomes an allowed one, and its probability dramatically increases. This kind of ionization is called “resonant ionization” and at such a wavelength a peak in the current is observed. The principle of MEES is that by scanning the laser wavelength we scan the various molecular energy levels and detect resonant transitions. In contrast to single photon spectroscopies, MEES is characterized by many peaks, all of them resulting from scanning in a small wavelength range. Due to the following reasons, MEES is usually more informative than the corresponding single photon spectroscopies: MEES is governed by different selection rules, depending on the number of photons involved. For example, some transitions, which are dipole moment forbidden, can be achieved by 2 photon absorption [63]. While single photon absorption are only sensitive to the energy gap between the ground electronic energy level and some excited states, in MEES transitions between excited states also take place. Moreover, while only low energy levels are usually sampled using UV light, in MEES also high energy levels are sampled.

Multiphoton electron extraction spectra of common solid explosives are provided in Fig. 13. One can observe that the spectra of all explosive molecules possessing nitro/nitrate/nitroso-groups show similar features, while the TATP spectrum is completely different. At least 10 significant peaks are observed in the spectra of the nitro-based compounds in the examined laser-wavelength range. One group is close to 215 nm and another group is close to 226 nm. Note that the noise level in these measurements is very small and most of the observed spectral features are significant. Many small peaks are observed in this spectral range and their origin will be discussed in the following.

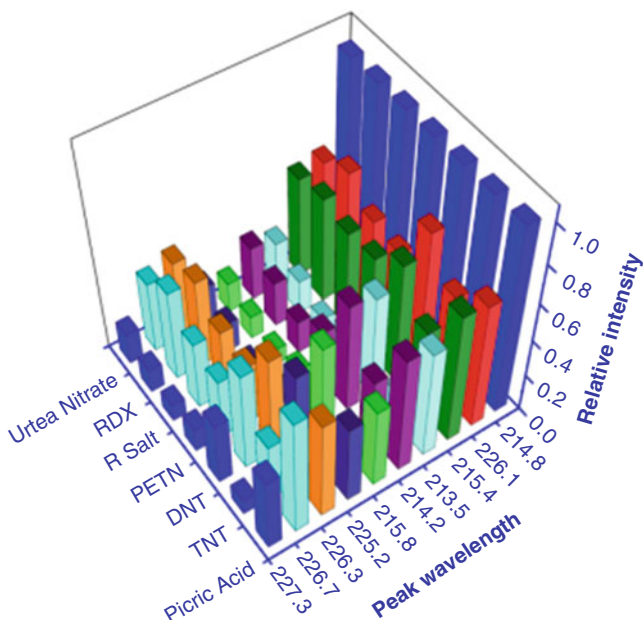


Fig. 14 The relative intensities (normalized at 214.8 nm) of the 10 most significant peaks in the MEES of some explosives containing nitro/nitrate/nitroso groups

The relative intensities of the 10 most significant peaks are presented in Fig. 14. The variations in the relative intensities are higher than the signal standard deviations, which imply that differentiation between the various molecules might be possible. However, the current quality of the spectra is not adequate for drawing a solid conclusion on this issue. In the MEES setup the laser beam excites NO_2 into a dissociative energy region and ionizes secondary fragment NO (as well as primary NO molecules, if available). Moreover, the NO/NO_2 ratio could be determined from the changes in ion peak shapes. (These changes are due to the release of kinetic energy from NO fragment ions formed by the dissociation of NO_2 .) Actually, full understanding of the photo-dissociation of nitro-compounds has not been yet achieved, and some interesting new aspects have recently been disclosed [43]. These results are not surprising since old studies on photolysis of nitro-compounds, also have shown that NO/NO_2 are produced [64–67]. The above studies reveal some of the processes that might take place in our MEES measurements of explosives. They certainly explain the major peaks at around 215 nm and 226 nm. However, one cannot exclude the possibility that other processes, besides photo-dissociation and ionization of NO, do take place. The energetic schemes and the interactions in the condensed phase are more complicated and still unknown. Most probably, the laser ablates some of the surface molecules, so the gas-phase processes do contribute to the spectra in MEES. However, we believe that additional processes take place directly in the surface molecules. Some evidences supporting the molecular surface

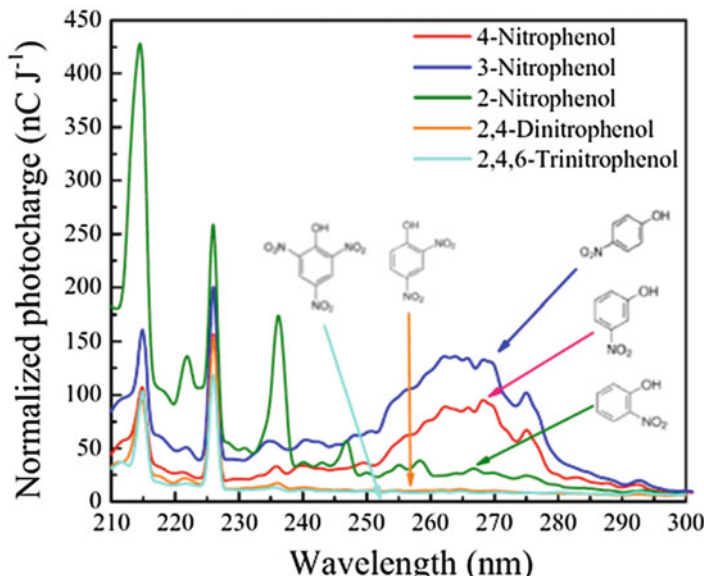


Fig. 15 MEES spectra of nitrophenol isomers between 210 and 300 nm

processes in MEES are shown in Fig. 15, where the MEES spectra of several nitrophenol isomers are presented. One can see that besides the peaks traditionally attributed to NO species, additional spectral features appear in the range 250 nm to 280 nm. These features are related to the aromatic ring and can be explained in terms of the electron induction by the attached NO_2 and OH groups. These evidences strongly support the hypothesis that molecular ionization takes place in MEES and the ionization of NO fragments is only partially responsible for the emitted photoelectrons. These spectra might indicate that MEES signals cannot be attributed solely to NO or other molecular fragments in the gas phase, but might be directly related to the molecules in the solid phase. This statement is based on the differences in MEES results. Most probably, the laser induces some fragmentation and NO species are responsible for the peaks at around 215 nm and 226 nm, but molecular information is also available in MEES. Another interesting question is whether most of the ionization processes take place in the solid phase or in the ablated gas phase. So far we do not have enough evidences to answer this question.

Dependence of MEES signals on laser pulse energy: According to theory [37, 68], the logarithm of the MEES signal should be a linear function of the logarithm of the laser power. The slope is called ionization order and it should be equal to the number of absorbed photons. The effect of the laser power on the MEES signals of TNT was tested at the two observed peaks, at 215 nm and 226 nm. TNT solution (in ethanol) was placed on a glass fiber filter, dried and irradiated under soft focusing conditions (using a focusing lens of $f = 180$ mm and placing the sample at a distance

of 150 nm). The maximum pulse energy was $48 \pm 2 \mu\text{J}$ at 215 nm and $65 \pm 2 \mu\text{J}$ at 226 nm. This is a rather small range, however, it ensures that no plasma is formed on one side, and the signals are far from the noise level, of the other side. Variation of the pulse energy was achieved using a number of calibrated quartz plates, which attenuated the laser beam. The MEES signals were calculated by averaging the corresponding peak area over 10 independent measurements. The ionization order was 1.39 ± 0.10 at 215 nm and 1.13 ± 0.06 at 226 nm. The ionization order is close to 1, indicating a strong resonant process, via a real state. The non-integer order is well known in multiphoton processes where the laser is focused [62]. It results from a mixture of orders, originating from the variety of energy densities that are present in the focal region. In addition, the ionization might be a result of photo-dissociation and fragmentation steps, in which case integer numbers are not expected.

Analytical quantification: In most applications only reliable detection of explosives is needed and the value of interest is the practical LOD. It is defined experimentally, in relation to the specific application of interest and it will be discussed in a following session. However, the analytical LOD, which is based on 95% confidence intervals and obtained from linear calibration plots, is also important, especially for allowing comparison to other methods. Analytical quantification of TNT was performed by preparing well defined thin films, at a series of surface concentrations. For each surface concentration, 10 film replicates were prepared and measurements were averaged over all replicates, in order to reduce errors due to sample preparation fluctuations. The resulted calibration plot and its 95% confidence intervals indicate an LOD of 0.15 pmole. This result suggests that MEES is one of the most sensitive methods for direct detection of solids.

Security applications:

Standard swab sampling: Security checks in most airports include collecting residues from suspected items (luggage, electronic devices, shoes and hands) using a swab, and transferring it to an IMS explosive detector. The swabs used in airports are optimized for collection of residues and for their introduction into IMS instruments. They are often made of a cotton fabric, with large holes between its fibers. Such swabs are un-favorite for MEES analysis, since the laser passes through the holes and samples the holder. Moreover, their background signal is not negligible. A dense matrix, such as a glass filter, performs much better for MEES analysis. However, in order to test the MEES system under the same conditions as used in airports, we obtained standard swabs, contaminated with dust collected from suitcases (using a commercial wiping wand), and spiked with several explosives. Scanning was performed at 226 nm, so the signal alarmed the presence of TNT. Although the swab itself and the dust cause many peaks, the characteristic signals of TNT at 215 and at 226 nm are clearly observed. These results imply that MEES is a candidate for detecting explosives in airports.

Standard dry transfer protocol: The standard protocol for detection of explosives, as described in our report of the methodology [69] by using MEES in comparison to other techniques [70], was applied and tested. This protocol is well defined, however, the quantity of the explosive sampled and introduced into the measuring instrument is not known. Nevertheless, this test is practically useful for comparing

various sampling and detection methods. The dry transfer test was applied to MEES method, using 3 ng TNT. Thus, some of this quantity of explosive was transferred to a suitcase and the sampling step was done using a glass fiber swab. The swab was introduced into the MEES instrument and scanned at 226 nm. The results indicate that MEES can be used for detection of dry transferred traces of explosives.

Detection of plastic explosives: Some explosives, such as the plastic explosives, are composed of a mixture of materials, including binders and plasticizers, which make their traditional detection more difficult. One of these explosives is Semtex H, which consists of 41.2% RDX, 40.9% PETN, 9.0% binder, 7.9% plasticizer, 0.5% antioxidant and 0.5% dye. A swab spiked with Semtex H was scanned by MEES and the results are shown in Fig. 16. The spectrum at a suspected spots is shown in Fig. 17. The signals due to the additives are much lower than those due to the explosives. Again, the ability of MEES to detect Semtex H implies its potential in security applications.

In summary, the optical technique named Multiphoton Electron Extraction Spectroscopy (MEES) allows for direct analysis of solid surfaces under ambient conditions. The method is fast (a few seconds) and does not require pre-treatment of the examined materials. When scanning the surface, the method provides chemical imaging, namely, 2D chemical morphology. The potential of this method was exemplified for detection of trace nitro/nitrate/nitroso-bearing explosives (including plastic explosives). The analytical LODs are in the sub-pmol range. The method was tested for practical security (E.g., swab sampling and dry transferring) and the conclusion is that it is a good candidate for such applications.

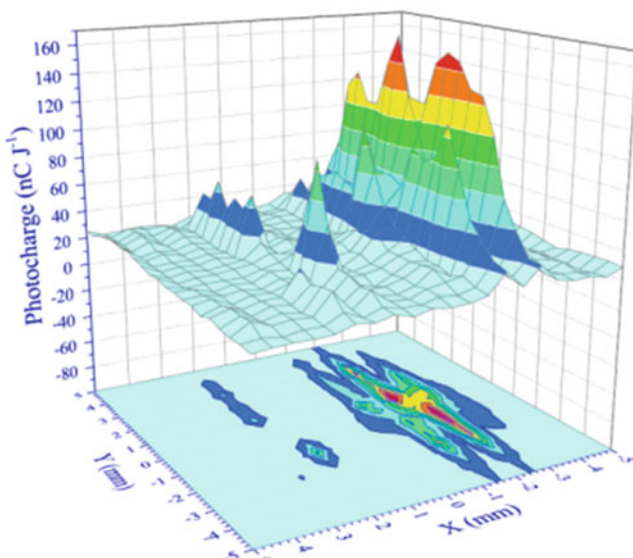
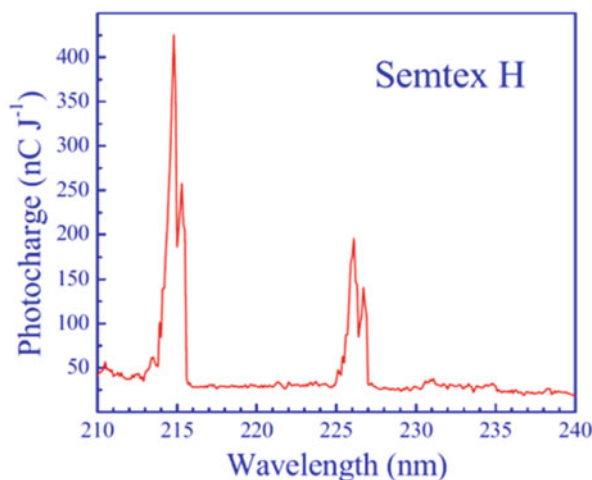


Fig. 16 MEES imaging of a swab spiked with Semtex H

Fig. 17 The spectrum at a suspected point



Broader Impacts

The expected impact is the production of faster and more efficient detection and monitoring technologies and improved detection and monitoring capabilities of improvised explosive devices and conventional explosives used for terrorist attack. The research to be performed is potentially highly relevant to the establishment of advanced detection systems and countermeasures against potential explosive threats, which is a worldwide security priority. The project will be focused on cutting edge ideas and approaches to mitigate the effects of improvised explosive devices on society. The project will focus on the fundamental chemistry underlying the mode of action of explosive agents as well as methods for real-time and high-sensitivity detection of explosive vapours, and translation research into the development of countermeasures.

Young Researcher Participation

The project SPS G5536 started 01/09/2018 and will finish 01/09/2021, currently two young researchers are receiving stipends from the project, Dr. José García-Calvo, under a post-doc contract, and Andrea Revilla-Cuesta, under a young-researcher contract. By the time their contributions are being successful and the project is progressing fast. They have made advances in the Work Package 2: Design and synthesis of fluorogenic probes for the detection of home-made explosives: Task 1. Synthesis of perylenemonoimides bearing donor groups: The synthesis have been

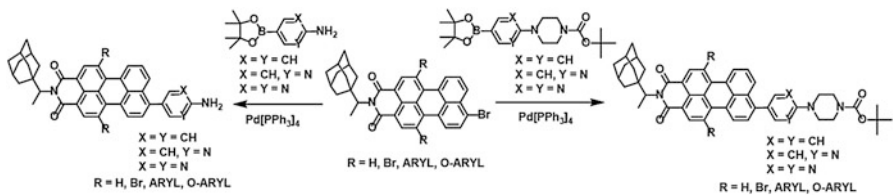


Fig. 18 Synthesis of perylenemonoimides bearing donor groups

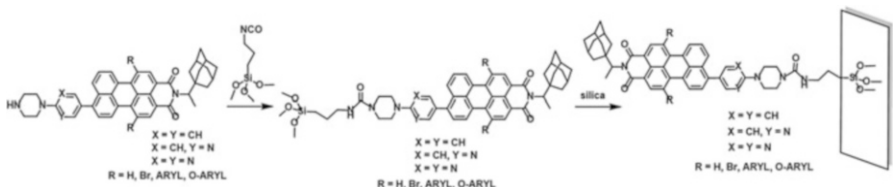


Fig. 19 Anchoring to solid silica substrates of perylenemonoimides bearing donor groups

performed by using Suzuki reactions with arylboronic esters having amine groups. Some of the obtained structures are shown in the Fig. 18 for R = H.

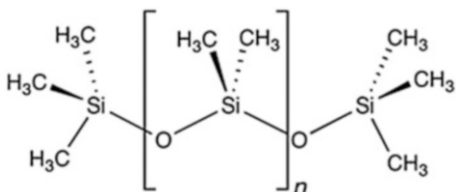
Task 4. Preparation of silica supported perylenemonoimides bearing donor groups: This task implied the preparation of fluorogenic materials by the chemical modification of reactive solid silica substrates by their reaction with the previously prepared perylenemonoimides bearing donor groups and anchoring moieties such as the represented in the Fig. 18, conveniently functionalized for their anchoring to solid silica substrates shown in Fig. 19 for R = H.

Task 5. Checking the sensitivity of silica supported perylenemonoimides to gaseous traces of home-made explosives: In this task, the sensitivity of the solid supported perylenemonoimides with donor groups was studied in the presence of gaseous traces of home-made explosive triacetone triperoxide and the fluorogenic materials were capable of discriminate the presence and the nature of the most important oxygen based home-made explosive TATP.

Task 6. Preparation of solid polydimethylsiloxane (PDMS) supported perylenemonoimides bearing donor groups: This task implied the preparation of new fluorogenic materials by the chemical modification of polydimethylsiloxane (PDMS) substrates by their reaction with the previously prepared perylenemonoimides bearing donor groups and anchoring moieties such as the represented in the Fig. 18, conveniently functionalized for their anchoring to solid silica substrates as described in the Fig. 19. Anchoring in PDMS expanded the possibilities of sensing TATP, at the moment, to perform practical applications.

Polydimethylsiloxane (PDMS) is a polymer widely used for the fabrication and prototyping of microfluidic chips. It is a mineral-organic polymer of the siloxane family and a hydrophobic elastomer (Fig. 20). Polar solvents, such as water, struggle to wet the PDMS (water beads and does not spread) and this leads to the adsorption

Fig. 20 Structure of polydimethylsiloxane (PDMS)



of hydrophobic contaminants from water on PDMS, which will help detection schemes. PDMS oxidation using plasma changes the PDMS surface chemistry and produces silanol terminations (SiOH) on its surface. This helps making the PDMS hydrophilic for 30 min or so. In addition, PDMS plasma oxidation is used to functionalize the PDMS surface with trichlorosilane derivatives or to covalently bond PDMS (at the atomic scale) with dyes or on an oxidized glass surface by the creation of $\text{Si}-\text{O}-\text{Si}$ bonds. The fabrication of a chip by soft-lithography methods is performed as follows: A mixture of PDMS (liquid) and crosslinking agent (to cure the PDMS) is poured into the mold and heated at high temperature. Once the PDMS is hardened, it can be taken off the mold. Then, the face of the block of PDMS is treated with plasma. The plasma treatment allows PDMS to be functionalized by siloxane derivatives and also permits glass bonding to close in case it is necessary to construct a microfluidic chip. PDMS was chosen primarily for those reasons: It is transparent at optical frequencies (240 nm – 1100 nm), which facilitates the observation of fluorescence through a fluorometer. It has a low auto-fluorescence. It is considered as bio-compatible (with some restrictions). The PDMS bonds tightly to glass or another PDMS layer with a simple plasma treatment. This allows the production of multilayers PDMS devices to take advantage of the technological possibilities offered by glass substrates, such as the use of metal deposition, oxide deposition or surface functionalization to make sensor arrays. PDMS, during cross-linking, can be coated with a controlled thickness on a substrate using a simple spin-coat. It is inexpensive compared to previously used materials (e.g. silica). The PDMS is also easy to mold, because, even when mixed with the cross-linking agent, it remains liquid at room temperature for many hours. The PDMS can mold structures at high resolutions. With some optimization, it is possible to mold structures of a few nanometers. It is gas permeable. It adsorbs hydrophobic molecules and can release some molecules from a bad cross-linking into the liquid and this can be a problem for some studies in PDMS microfluidic devices. Two types of PDMS are commonly used for these applications: PDMS RTV-615 and PDMS Sylgard 184. PDMS RTV-615 is the most robust and convenient to bond bilayer microfluidic devices but there are variabilities in plasma bond strength between different batches. PDMS Sylgard 184 (Dow Corning) is the cleaner PDMS although this PDMS is less often used for multilayers chip. With the projected PDMS materials we have prepared functionalized-PDMS as shown in Fig. 21. Optimization of the technique and the preparation of fluorogenic sensing materials is now being performed in the University of Burgos.

Fig. 21 Structure of a functionalized polydimethylsiloxane (PDMS)

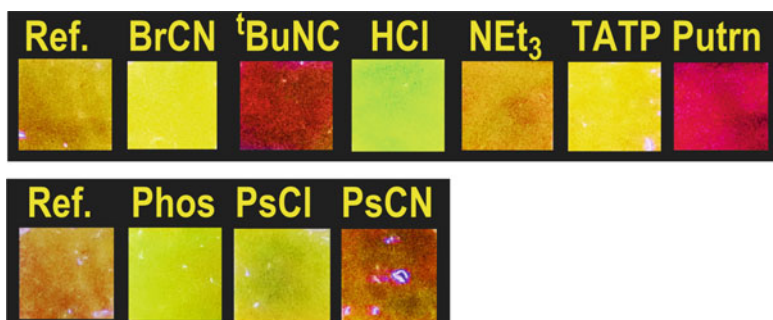
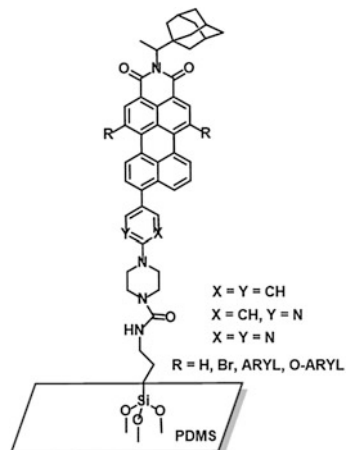


Fig. 22 Preliminary results of the polydimethylsiloxane (PDMS) based material and diverse toxic or explosive vapors: BrCN: cyanogen bromide, ^tBuNC: tertbutylisocyanide, HCl: hydrogen chloride, NEt₃: triethylamine, TATP: triacetone triperoxide, Putrn: putrescine, Phos: phosgene, PsCl: diethylchlorophosphate, PsCN: diethylcyanophosphonate

Task 7. Checking the sensitivity of PDMS supported perylenemonoimides to gaseous traces of home-made explosives: In this task, the sensitivity of the PDMS supported perylenemonoimides with donor groups are being studied in the presence of gaseous traces of home-made explosives, triacetone triperoxide at the moment and hexamethylene triperoxide diamine in the near future, on the way to the preparation of an array of fluorogenic materials capable of discriminate the presence and the nature of the most important oxygen based home-made explosives (Fig. 22).

Contributions

By the time the chapter was written the project has only recently started, first September 2018. The project was presented at a conference paper: Tomás Torroba, Israel Schechter: Development of new chemical sensors and optical technologies for fast and sensitive detection of improvised explosives. Short talk 20 min. T. Torroba at the Advanced Research Workshop on Explosives Detection, Florence, Italy, 17–18th October 2018.

The scientific grounds of the project have been described in a PhD Thesis and a paper:

PhD Thesis: José García-Calvo: Fluorescent probes and nanostructured materials for the detection of environmental toxins and catalysts development. University of Burgos, Faculty of Science, Department of Chemistry, 21st September 2018, Outstanding “Cum Laude”.

José García-Calvo, Patricia Calvo-Gredilla, Marcos Ibáñez-Llorente, Daisy C. Romero, José V. Cuevas, Gabriel García-Herbosa, Manuel Avella, Tomás Torroba: Surface functionalized silica nanoparticles for the off-on fluorogenic detection of an improvised explosive, TATP, in a vapour flow. *Journal of Materials Chemistry A*, **2018**, 6, 4416–4423.

References

1. (a) Härtel MAC, Klapötke TM, Stiasny B, Stierstorfer J 2017 Gas-phase concentration of Triacetone Triperoxide (TATP) and Diacetone Diperoxide (DADP), *Propellants Explos Pyrotech* 42: 623–634; (b) Homemade explosives, Indiana Intelligence Fusion Center, 2015, 302 W. Washington St., Indianapolis, IN 46204, http://www.arkiaai.com/files/handouts/2016/Spring/homemade_explodes.pdf. Accessed 23 Aug 2017
2. Dubnikova F, Kosloff R, Almog J, Zeiri Y, Boese R, Itzhaky H, Alt A, Keinan E (2005) Decomposition of Triacetone Triperoxide Is an Entropic Explosion. *J Am Chem Soc* 127:1146–1159
3. (a) Yeager K (2007) In: Woodfin RL (Ed) Trace chemical sensing of explosives. Wiley, New Jersey, Ch. 3, pp. 43–67; (b) Ong T-H, Mendum T, Geurtsen G, Kelley J, Ostrinskaya A, Kunz R (2017) *Anal Chem* 89:6482 – 6490; (c) Sheykhi S, Mosca L, Anzenbacher P Jr. (2017) *Chem Commun* 53:5196–5199
4. Ranstorp M, Normark M (eds) (2015) Understanding Terrorism Innovation and Learning: Al-Qaeda and Beyond, Routledge, Taylor & Francis Group LLC, 7625 Empire Drive, Florence, Kentucky 41042-2919, USA, Chapt. 1, pp. 1–15
5. (a) R. Schulte-Ladbeck, M. Vogel, U. Karst, Recent methods for the determination of peroxide-based explosives, *Anal Bioanal Chem* 2006, 386, 559–565; (b) Kangas MJ, Burks RM, Atwater J, Lukowicz RM, Williams P, Holmes AE (2017) Colorimetric sensor arrays for the detection and identification of chemical weapons and explosives. *Crit Rev. Anal Chem* 47: 138–153; (c) Girotti S, Ferri E, Maiolini E, Bolelli L, D’Elia M, Coppe D, Romolo FS (2011) A

- quantitative chemiluminescent assay for analysis of peroxide-based explosives. *Anal Bioanal Chem* 400: 313–320; (d) Collins GE, Malito MP, Tamanaha CR, Hammond MH, Giordano BC, Lubrano AL, Field CR, Rogers DA, Jeffries RA, Colton RJ, Rose-Pehrsson SL (2017) Trace explosives sensor testbed (TESTbed). *Rev. Sci Instrum* 88: 034104(1–9)
6. Makinen M, Nousiainen M, Sillanpaa M (2011) Ion spectrometric detection technologies for ultra-traces of explosives: a review. *Mass Spectrom Rev.* 30: 940–973. (b) Kangas MJ, Burks RM, Atwater J, Lukowicz RM, Williams P, Holmes AE (2017) Colorimetric sensor arrays for the detection and identification of chemical weapons and explosives. *Crit Rev. Anal Chem* 47: 138–153; (c) Girotti S, Ferri E, Maiolini E, Bolelli L, D'Elia M, Coppe D, Romolo FS (2011) A quantitative chemiluminescent assay for analysis of peroxide-based explosives. *Anal Bioanal Chem* 400: 313–320; (d) Collins GE, Malito MP, Tamanaha CR, Hammond MH, Giordano BC, Lubrano AL, Field CR, Rogers DA, Jeffries RA, Colton RJ, Rose-Pehrsson SL (2017) Trace explosives sensor testbed (TESTbed). *Rev. Sci Instrum* 88: 034104(1–9).
7. Jiang D, Peng L, Wen M, Zhou Q, Chen C, Wang X, Chen W, Li H (2016) Dopant-Assisted Positive Photoionization Ion Mobility Spectrometry Coupled with Time-Resolved Thermal Desorption for On-Site Detection of Triacetone Triperoxide and Hexamethylene Trioxide Diamine in Complex Matrices. *Anal Chem* 88:4391–4399
8. Tang S, Vinerot N, Fisher D, Bulatov V, Yavetz-Chen Y, Schechter I (2016) Detection and mapping of trace explosives on surfaces under ambient conditions using multiphoton electron extraction spectroscopy (MEES). *Talanta* 155:235–244
9. (a) Tomlinson-Phillips J, Wooten A, Kozole J, Deline J, Beresford P, Stairs J (2014) Characterization of TATP gas phase product ion chemistry via isotope labeling experiments using ion mobility spectrometry interfaced with a triple quadrupole mass spectrometer, *Talanta* 127, 152–162; (b) Correa DN, Melendez-Perez JJ, Zacca JJ, Borges R, Schmidt EM, Eberlin MN, Meurer EC (2017) Direct Detection of Triacetone Triperoxide (TATP) in real banknotes from ATM Explosion by EASI-MS, *Propellants Explos Pyrotech* 42: 370–375; (c) Hagenhoff S, Franzke S, Hayen H (2017) Determination of Peroxide Explosive TATP and Related Compounds by Dielectric Barrier Discharge Ionization-Mass Spectrometry (DBDI-MS), *Anal Chem* 89:4210 – 4215
10. Lichtenstein A, Havivi E, Shacham R, Hahamy E, Leibovich R, Pevzner A, Krivitsky V, Davivi G, Presman I, Elnathan R, Engel Y, Flaxer E, Patolsky F (2014) Supersensitive fingerprinting of explosives by chemically modified nanosensors arrays. *Nature Commun* 5:4195. <https://doi.org/10.1038/ncomms5195>
11. (a) Lin H, Suslick KS (2010) A colorimetric sensor array for detection of triacetone triperoxide vapor. *J Am Chem Soc* 132: 15519–15,521; (b) Li Z, Bassett WP, Askim JR, Suslick KS (2015) Differentiation among peroxide explosives with an optoelectronic nose. *Chem Commun* 51: 15312–15,315; (c) Askim JR, Li Z, LaGasse MK, Rankin JM, Suslick KS (2016) An

- optoelectronic nose for identification of explosives. *Chem Sci* 7: 199–206; (d) Kumar V, Kim K-H, Kumar P, Jeon B-H, Kim J-C (2017) Functional hybrid nanostructure materials: advanced strategies for sensing applications toward volatile organic compounds. *Coord Chem Rev.* 342: 80–105
12. (a) Parajuli S, Miao W (2013) Sensitive determination of triacetone triperoxide explosives using electrogenerated chemiluminescence. *Anal Chem* 85: 8008 – 8015; (b) Malashikhin S, Finney NS (2008) Fluorescent signaling based on sulfoxide profluorophores: application to the visual detection of the explosive TATP. *J Am Chem Soc* 130: 12846–12,847
13. (a) Üzer A, Durmazel S, Ercag E, Apak R (2017) Determination of hydrogen peroxide and triacetone triperoxide (TATP) with a silver nanoparticles-based turn-on colorimetric sensor. *Sens Actuators B* 247: 98–107; (b) Can Z, Uzer A, Turkekul K, Ercag E, Apak R (2015) Determination of triacetone triperoxide with a N,N-Dimethyl-p-phenylenediamine sensor on Nafion using Fe₃O₄ magnetic nanoparticles. *Anal Chem* 87: 9589 – 9594; (c) Xu M, Han J-M, Wang C, Yang X, Pei J, Zang L (2014) Fluorescence ratiometric sensor for trace vapor detection of hydrogen peroxide. *ACS Appl Mater Interfaces* 6: 8708–8714
14. (a) Sella E, Shabat D (2008) Self-immolative dendritic probe for direct detection of triacetone triperoxide. *Chem Commun*: 5701–5703; (b) Xu W, Fu Y, Gao Y, Yao J, Fan T, Zhu D, He Q, Cao H, Cheng J (2015) A simple but highly efficient multi-formyl phenol–amine system for fluorescence detection of peroxide explosive vapour. *Chem Commun* 51: 10868–10,870; (c) Chen J, Wu W, McNeil AJ (2012) Detecting a peroxide-based explosive via molecular gelation. *Chem Commun* 48: 7310–7312; (d) Salinas Y, Martínez-Máñez R, Marcos MD, Sancenón F, Costero AM, Parra M, Gil S (2012) Optical chemosensors and reagents to detect explosives. *Chem Soc Rev.* 41: 1261–1296
15. (a) Rao MR, Fang Y, De Feyter S, Perepichka DF (2017) Conjugated covalent organic frameworks via michael addition–elimination. *J Am Chem Soc* 139: 2421 – 2427; (b) Zhang HQ, Euler WB (2016) Detection of gas-phase explosive analytes using fluorescent spectroscopy of thin films of xanthene dyes. *Sens Actuators B* 225: 553–562
16. (a) Lubczyk D, Siering C, Lörgen J, Shifrina ZB, Müllen K, Waldvogel SR (2010) Simple and sensitive online detection of triacetone triperoxide explosive. *Sens Actuators B* 143: 561–566; (b) Lubczyk D, Grill M, Baumgarten M, Waldvogel SR, Müllen K (2012) Scaffold-optimized dendrimers for the detection of the triacetone triperoxide explosive using quartz crystal microbalances. *Chem Plus Chem* 77: 102 – 105; (c) Hammer BAG, Müllen K (2016) Dimensional evolution of polyphenylenes: expanding in all directions. *Chem Rev.* 116: 2103 – 2140
17. (a) Wu J, Kwon B, Liu W, Anslyn EV, Wang P, Kim JS (2015) Chromogenic/fluorogenic ensemble chemosensing systems. *Chem Rev.* 115: 7893 – 7943; (b) Yang Z, Cao J, He Y, Yang JH, Kim T, Peng X, Kim JS (2014) Macro-/micro-environment-sensitive chemosensing and biological imaging. *Chem Soc*

- Rev. 43: 4563 – 4601; (c) Köstereli Z, Scopelliti R, Severin K (2014) Pattern-based sensing of aminoglycosides with fluorescent amphiphiles. *Chem Sci* 5: 2456–2460; (d) Hof F (2016) Host–guest chemistry that directly targets lysine methylation: synthetic host molecules as alternatives to bio-reagents. *Chem Commun* 52: 10093 – 10,108; (e) Wu D, Sedgwick AC, Gunnlaugsson T, Akkaya EU, Yoon J, James TD (2017) Fluorescent chemosensors: the past, present and future. *Chem Soc Rev.* <https://doi.org/10.1039/c7cs00240h>
18. (a) Kaloyanova S, Zagranyarski Y, Ritz S, Hanulová M, Koynov K, Vonderheit A, Müllen K, Peneva K (2016) Water-soluble NIR-Absorbing rylene chromophores for selective staining of cellular organelles. *J Am Chem Soc* 138: 2881–2884; (b) Lewandowska U, Zajaczkowski W, Chen L, Bouilliére F, Wang D, Koynov K, Pisula W, Müllen K, Wennemers H (2014) Hierarchical supramolecular assembly of sterically demanding π-Systems by conjugation with oligoprolines. *Angew Chem Int Ed* 53: 12537–12,541; (c) Bolag A, Sakai N, Matile S (2016) Dipolar photosystems: engineering oriented push–pull components into double- and triple-channel surface architectures. *Chem Eur J* 22: 9006–9014; (d) Hutchison JA, Uji-i H, Deres A, Vosch T, Rocha S, Müller S, Bastian AA, Enderlein J, Nourouzi H, Li C, Herrmann A, Müllen K, De Schryver F, Hofkens J (2014) A surface-bound molecule that undergoes optically biased Brownian rotation. *Nature Nanotech* 9: 131–136; (e) Lewandowska U, Zajaczkowski W, Pisula W, Ma Y, Li C, Müllen K, Wennemers H (2016) Effect of structural modifications on the self-assembly of oligoprolines conjugated with sterically demanding chromophores. *Chem Eur J* 22: 3804–3809
19. (a) Liu K, Xu Z, Yin M (2015) Perylenediimide-cored dendrimers and their bioimaging and gene delivery applications. *Prog Polym Sci* 46: 25–54; (b) Würthner F, Saha-Möller CR, Fimmel B, Ogi S, Leowanawat P, Schmidt D (2016) Perylene bisimide dye assemblies as archetype functional supramolecular materials, *Chem Rev.* 116: 962 – 1052; (c) Sun M, Müllen K, Yin M (2016) Water-soluble perylenediimides: design concepts and biological applications. *Chem Soc Rev.* 45: 1513 – 1528; (d) Fernández-Lázaro F, Zink-Lorre N, Sastre-Santos A (2016) Perylenediimides as non-fullerene acceptors in bulk-heterojunction solar cells (BHJSCs). *J Mater Chem A* 4: 9336 – 9346; (e) Guo Y, Li Y, Awartani O, Han H, Zhao J, Ade H, Yan H, Zhao D (2017) Improved performance of all-polymer solar cells enabled by naphthodiperylenetetraimide-based polymer acceptor. *Adv Mater* 29: 1700309.
20. PDIs: (a) Seifert S, Schmidt D, Würthner F (2015) An ambient stable core-substituted perylene bisimide dianion: isolation and single crystal structure analysis. *Chem Sci* 6: 1663–1667; (b) Jänsch D, Li C, Chen L, Wagner M, Müllen K (2015) Versatile colorant syntheses by multiple condensations of acetyl anilines with perylene anhydrides. *Angew Chem Int Ed* 54: 2285–2289;

- (c) You L, Zha D, Anslyn EV (2015) Recent advances in supramolecular analytical chemistry using optical sensing. *Chem Rev.* 115: 7840–7892; (d) Ma W, Qin L, Gao Y, Zhang W, Xie Z, Yang B, Liua L, Ma Y (2016) A perylene bisimide network for high-performance n-type electrochromism. *Chem Commun* 52: 13600–13,603; PMIs: (e) Vagnini MT, Mara MW, Harpham MR, Huang J, Shelby ML, Chen LX, Wasielewski MR (2013) Interrogating the photogenerated Ir(IV) state of a water oxidation catalyst using ultrafast optical and X-ray absorption spectroscopy. *Chem Sci* 4: 3863–3873; (f) Liu Z, Tonnellé C, Battagliarin G, Li C, Gropeanu RA, Weil T, Surin M, Beljonne D, Lazzaroni R, Deblliquy M, Renoirt J-M, Müllen K (2014) Functional layers for ZnII ion detection: from molecular design to optical fiber sensors. *J Phys Chem B* 118: 309 – 314; (g) Sanguineti A, Sassi M, Turrisi R, Ruffo R, Vaccaro G, Meinardi F, Beverina L (2013) High Stokes shift perylene dyes for luminescent solar concentrators. *Chem Commun* 49: 1618–1620; (h) Shao P, Jia N, Zhang S, Bai M (2014) Synthesis and optical properties of water-soluble biperylene-based dendrimers. *Chem Commun* 50: 5648 – 5651
21. Gomes N (2017) Trace detection of TATP vapors using a low-mass thermodynamic sensor. Open Access Master's Theses, 1067. <http://digitalcommons.uri.edu/theses/1067>
22. (a) Díaz de Greñu B, Moreno D, Torroba T, Berg A, Gunnars J, Nilsson T, Nyman R, Persson M, Pettersson J, Eklind I, Wästerby P (2014) Fluorescent discrimination between traces of chemical warfare agents and their mimics. *J Am Chem Soc* 136: 4125–4128; (b) Díaz de Greñu B, García-Calvo J, Cuevas J, García-Herbosa G, García B, Busto N, Ibeas S, Torroba T, Torroba B, Herrera A, Pons S (2015), Chemical speciation of MeHg+ and Hg2+ in aqueous solution and HEK cells nuclei by means of DNA interacting fluorogenic probes. *Chem Sci* 6: 3757–3764; (c) Calvo-Gredilla P, García-Calvo J, Cuevas JV, Torroba T, Pablos J-L, García FC, García J-M, Zink-Lorre N, Font-Sanchis E, Sastre-Santos A, Fernández-Lázaro F (2017) Solvent-free off-on detection of the improvised explosive triacetone triperoxide (TATP) with fluorogenic materials. *Chem Eur J* 23: 13973–13,979; (d) García-Calvo J, Ibeas S, Antón-García E-C, Torroba T, González-Aguilar G, Antunes W, González-Lavado E, Fanarraga ML (2017) Potassium-ion-selective fluorescent sensors to detect cereulide, the emetic toxin of *B. cereus*, in Food Samples and HeLa Cells. *ChemistryOpen* 6: 562 – 570
23. Caygill JS, Davis F, Higson SPJ (2012) Current trends in explosive detection techniques. *Talanta* 88:14–29
24. Technology Assessment (2010) Explosives Detection Technologies. Report to Congressional Committees, GOA-10–898
25. Eiceman GA, Karpas Z, Hill HH Jr. (2013) Ion mobility spectrometry, third edn. CRC Press, Boca Raton

26. Skvortsov LA (2012) Laser methods for detecting explosive residues on surfaces of distant objects. *Quantum Electron.* 42(1):1–11
27. Pellegrino PM, Holthoff EL, Farrell ME (2015) Laser-based optical detection of explosives. CRC Press, Boca Raton. (ISBN 9781482233285)
28. Tuschel DD, Mikhonin AV, Lemoff BE, Asher SA (2010) Deep ultraviolet resonance Raman excitation enables explosives detection. *Appl Spectrosc* 64 (4):425–432
29. Ramos CI, Dagdigian PJ (2007) Detection of vapors of explosives and explosive-related compounds by ultraviolet cavity ringdown spectroscopy. *Appl Opt* 45(4):620–627
34. Boyson TK, Rittman DR, Spence TG, Kirkbride KP, Moore DS, Harb CC (2014) Rapid, wideband cavity ringdown spectroscopy for the detection of explosives, Lasers and Electro-Optics (CLEO). IEEE, San Jose
30. Gottfried JL, De Lucia Jr. FC, Munson CA, Mizolek AW (2008) Strategies for residue explosives detection using laser-induced breakdown spectroscopy. *J Anal At Spectrom* 23:205–216
31. Gottfried JL, De Lucia Jr. FC, Munson CA, Mizolek AW (2009) Laser-Induced Breakdown Spectroscopy for detection of explosives residues: a review of recent advances, challenges, and future prospects. *Anal Bioanal Chem* 395:283–300
32. Wynn CM, Palmacci S, Kunz RR, Aernecke M (2011) Noncontact optical detection of explosive particles via photodissociation followed by laser-induced fluorescence, *Opt. Express* 19:18671–18,677
33. Forest R, Babin F, Gay D, Hô N, Pancratii O, Deblois S, Désilets S, Maheux J (2012) Use of a spectroscopic LIDAR for standoff explosives detection through Raman spectra. *Proc. SPIE 8358, Chemical, Biological, Radiological, Nuclear, and Explosives (CBRNE) Sensing XIII*, 83580 M
34. Boesl U, Neusser HJ, Schlag EW (1981) Multi-photon ionization in the mass-spectrometry of polyatomic-molecules – cross-sections. *Chem Phys* 55:193–204
35. Hahn JH, Zenobi R, Zare RN (1987) Subfemtomole quantitation of molecular adsorbates by two-step laser mass spectrometry. *J Am Chem Soc* 109:2842–2843
36. Lubman DM, Kronick MN (1982) Mass spectrometry of aromatic molecules with resonance enhanced multiphoton ionization. *Anal Chem* 54:660–665
37. Tembreull R, Sin CH, Pang HM, Lubman DM (1985) Resonance enhanced multiphoton ionization spectroscopy for detection of azabenzenes in supersonic beam mass spectrometry. *Anal Chem* 57:2911–2917
38. Schechter I, Schröder H, Kompa KL (1992) A simplified method for absolute MPI cross-section measurements. Application to three photon non-resonant ionization of Xe at 266 nm. *Chem Phys Lett* 194:128–134

39. Schechter I, Schröder H, Kompa KL (1992) Quantitative laser mass-analyzer by time resolution of the ion-induced voltage in multi-photon-ionization processes. *Anal Chem* 64:2787–2796
40. Schechter I, Schröder H, Kompa KL (1993) A new sensor for ecological determinations of benzene in ambient air. *Anal Chem* 65:1928–1931
41. Litani-Barzilai I, Bulatov V, Gridin VV, Schechter I (2004) A detector based on time resolved ion-induced voltages in laser multiphoton ionization and laser induced fluorescence. *Anal Chim Acta* 501:151–156
42. Gridin VV, Korol A, Bulatov V, Schechter I (1996) Laser two-photon ionization of pyrene on contaminated soils. *Anal Chem* 68:3359–3363
43. Gridin VV, Bulatov V, Korol A, Schechter I (1997) Particulate material analysis by a laser ionization fast-conductivity method – water content effects. *Anal Chem* 69:478–484
44. Gridin VV, Bulatov V, Korol A, Schechter I (1997) Photoionization Fast-Conductivity Technique for Analysis of Traffic Contaminated Soils. *Instrum Sci Technol* 25:321–333
45. Gridin VV, Litani-Barzilai I, Kadosh M, Schechter I (1998) Determination of aqueous solubility and surface adsorption of polycyclic aromatic hydrocarbons by laser multiphoton ionization. *Anal Chem* 70:2685–2692
46. Kadosh M, Gridin VV, Schechter I (2001) Detection of time-resolved photoionization currents from pesticide contaminated vegetation. *Israel J Chem* 41:99–104
47. Yamada S, Sato N, Kawazumi H, Ogawa T (1987) Laser two-photon ionization spectrometry of perylene and naphthacene in hexane. *Anal Chem* 59:2719–2721
48. Inoue T, Gridin VV, Ogawa T, Schechter I (1998) Simultaneous laser induced multiphoton ionization and fluorescence for analysis of polycyclic aromatic hydrocarbons. *Anal Chem* 70:4333–4338
49. Gridin VV, Litani-Barzilai I, Kadosh M, Schechter I (1997) A renewable liquid droplet method for on-line pollution analysis by multi-photon ionization. *Anal Chem* 69:2098–2102
50. Bulatov V, Gridin VV, Polyak F, Schechter I (1997) Application of pulsed laser methods to in-situ probing of highway originated pollutants. *Anal Chim Acta* 343:93–99
51. Gridin VV, Inoue T, Ogawa T, Schechter I (2000) On-line screening of airborne PAH contamination by simultaneous multiphoton ionization and laser induced fluorescence. *Instrum Sci Technol* 28:131–141
52. Litani-Barzilai I, Fisher M, Gridin VV, Schechter I (2001) Fast filter-sampling and analysis of PAH aerosols by laser multiphoton ionization. *Anal Chim Acta* 439:1–8
53. Johnson PM (1980) Molecular multiphoton ionization. *Acc Chem Res* 13:20–26
54. Siomos K, Kourouklis G, Christophorou LG (1981) Laser two photon ionization of organic molecules in dielectric liquids. *Chem Phys Lett* 80:504–511
55. Siomos K, Christophorou LG (1980) Laser two photon ionization spectroscopy of molecules in liquids. *Chem Phys Lett* 72:43–48

56. Chen Y, Bulatov V, Vinerot N, Schechter I (2010) Multiphoton ionization spectroscopy as a diagnostic technique of surfaces under ambient conditions. *Anal Chem* 82:3454–3456
57. Vinerot N, Chen Y, Bulatov V, Gridin VV, Fun-Young V, Schechter I (2011) Spectral characterization of surfaces using laser multi-photon ionization. *Opt Mater* 34:329–335
58. Schechter I, Bulatov V (2013) Multiphoton Ionization Spectrometer. Patent US 8455813B2
59. Chamberlain RT (2002) Dry transfer method for the preparation of explosives test samples. Patent US 6470730 B1.
60. Hamachi A, Okuno T, Imasaka T, Kida Y, Imasaka T (2015) Resonant and non-resonant multiphoton ionization processes in the mass spectrometry of explosives. *Anal Chem* 87(5):3027–3031
61. Aicher KP, Wilhelm U, Grottemeyer J (1995) Multiphoton ionization of molecules: a comparison between femtosecond and nanosecond laser pulse ionization efficiency. *J Am Soc Mass Spectrom* 6(11):1059–1068
62. Chin SL, Lambropoulos P (1984) Multiphoton ionization of atoms. Academic Press. ISBN: 978-0-12-172780-2
63. McClain WM (1974) Two-photon molecular spectroscopy. *Acc Chem Res* 7:129–135
64. Bornschlegl A, Weishaeupl R, Boesl U (2006) A new approach for fast, simultaneous NO/NO₂ analysis: application of basic features of multiphoton-induced ionization and dissociation of NO_x. *Anal Bioanal Chem* 384:161–168
65. Hause ML, Herath N, Zhu R, Lin MC, Suits AG (2011) Roaming-mediated isomerization in the Photodissociation of Nitrobenzene. *Nat Chem* 3:932–937
66. Chen B, Yang C, Goh NK (2006) Photolysis pathway of nitroaromatic compounds in aqueous solutions in the UV/H₂O₂ process. *J Environ Sci (China)* 18 (6):1061–1064
67. Compton RG, Bamford CH, Tipper CFH (ed) (1972) Decomposition and Isomerization of Organic Compounds, Elsevier Science. ISBN 978-0-444-40861-7
68. Mainfray G, Manus C (1991) Multiphoton ionization of atoms. *Rep Prog Phys* 54:1333–1372
69. Tang S, Vinerot N, Fisher D, Bulatov V, Yavetz-Chen Y, Schechter I (2016) Detection and mapping of trace explosives on surfaces under ambient conditions using multiphoton electron extraction spectroscopy (MEES). *Talanta* 155:235–244
70. Tang S, Vinerot N, Bulatov V, Yavetz-Chen Y, Schechter I (2016) Multiphoton electron extraction spectroscopy and its comparison with other spectroscopies for direct detection of solids under ambient conditions. *Anal Bioanal Chem* 408:8037–8051

Terahertz Imaging and Spectroscopy for Security and Defense Applications

Mohamed Lazoul

Ecole Militaire Polytechnique, Bordj-El-Bahri, Algeria

Noureddine Maamar

Ecole Militaire Polytechnique, Bordj-El-Bahri, Algeria

Bellada Amel

Ecole Militaire Polytechnique, Bordj-El-Bahri, Algeria

Fredrik Laurell

Department of Applied Physics, Royal Institute of Technology, Stockholm, Sweden

Jean-Louis Coutaz (✉)

IMEP-LAHC, University Savoie Mont Blanc, Le Bourget du Lac, France

e-mail: Jean-Louis.Coutaz@univ-smb.fr

Introduction

The far-infrared region (FIR) of the electromagnetic spectrum, also named the terahertz domain ($1 \text{ THz} = 10^{12} \text{ Hz}$), is located between the infrared and the microwaves. It is generally admitted that it includes waves of frequencies ranging from $\sim 0.1 \text{ THz}$ up to $\sim 10 \text{ THz}$, i.e. wavelengths from $\sim 30 \mu\text{m}$ up to $\sim 3 \text{ mm}$. It has been investigated since the end of the nineteenth century by researchers, like pioneers J. Bose [1], Rubens [2], or Nichols and Tear [3]. Subsequently, amazing techniques were developed, such as the Fourier-transform infrared spectroscopy (FTIR) [4]. However, FIR studies and related development of applications were strongly limited by the lack of efficient, compact, reliable and cheap sources and detectors. The situation changed at the end of the 1980's, when commercial femtosecond lasers became commercially available. These new lasers have stimulated the emergence of original optoelectronic techniques to explore the THz region, such as the wildly spread time-domain spectroscopy (TDS). Simultaneously, other THz technologies have been greatly improved, like high-frequency electronic components, micro-bolometers, or even video-rate cameras. It has to be noted that the present expansion of application-oriented THz activities would not have been possible without the availability of sufficiently sensitive detectors and powerful radiation sources, all at affordable costs.

Even if the THz technology still merits improvements, foreseen and promising applications of the THz waves are nowadays under development, and their transfer

to the industry has started and will be more and more effective in the coming years. These applications address medicine and biology, telecommunications, environment and so on. In this chapter, we are interested in the use of THz-waves technology for security and defense issues. The present intense worldwide activities on this topic are justified by two main properties of the interaction between THz and matter. First, many materials, mainly dielectrics, are transparent in the THz range, while they are opaque in other electromagnetic regions, like visible or infrared. These materials include clothes, paper and plastic sheets, and most packaging films. Therefore, a THz camera can “see” items hidden by such covering materials. This is also possible with radar and millimeter-wave cameras, which exhibit an even better sensitivity, but at the expense of a lower spatial resolution and much larger optics. The second main application of THz technology to security and defense is linked to the unique spectral signature of molecules in the THz range. These signatures originate in the vibrations of the whole molecular skeleton, which occur in the FIR for many common molecules, including explosive ones. Therefore, recording the spectrum reflected or radiated by a material may allow one to chemically identify it. Let us recall the reader that, as compared to the THz, spectroscopy in the infrared gives informations on the chemical links, while spectroscopy in the visible supplies data on the atoms. The ultimate dream of security specialists would be to employ hyperspectral video-rate THz cameras, i.e. cameras that are able to record images at different frequencies, which would permit to image the shape of an item and to identify its chemical composition.

In this chapter, we will present the basic principles of THz imaging and spectroscopy. Then we will review the main achievement in imaging for security and defense applications, and finally we will give trends for future developments.

Physics of THz Electromagnetic Waves

The Far-Infrared Domain

As written above, THz frequencies lie between ~ 0.1 and ~ 10 THz. Thus, the period of the THz waves is $0.1\sim 10$ ps. This is the order of magnitude of the fastest chemical reactions, for example the formation of a water molecule when hydrogen and oxygen atoms are in contact. This is also the order of magnitude of the fastest non-subatomic events in matter, like energy relaxation through phonons, electron scattering time in conductors, etc. The corresponding limit wavelengths are 3 mm and 30 μ m, i.e. photon energies from 0.41 up to 41.2 meV, and equivalent temperatures from 4.8 to 478 K. Therefore, the THz photon energy is extremely weak. Consequently, photonics at THz will not be efficient. Moreover, if performed at room temperature, thermal noise will strongly perturb the THz signal records.

Electromagnetic Response of Matter at THz Frequencies

Non-resonant Response of Matter to an Electromagnetic Excitation

The interaction of an exciting light beam and dielectric matter is generally not resonant, i.e. the incident light does not induce transition between the different discrete energy states of the atoms or molecules, or does not involve collective excitation in the matter. In this case, the electrical field \vec{E} of the light beam produces a deformation of the electronic cloud of the atoms/molecules, and thus creates a dipole $\vec{p} = \alpha\vec{E}$, where α is the polarizability of the atoms/molecules. The resulting polarization of matter is $\vec{P} = N\vec{p} = N\alpha\vec{E}$, with N is the density of atoms/molecules. The classical Lorentz model of polarizability leads to $\alpha \propto (\omega_o^2 - \omega^2)^{-1}$, where ω_o belongs to the visible or UV domain. Therefore, in the FIR, the dielectric constant of matter is larger than in the visible/IR. In addition to the electronic origin of the polarizability, ionic or dipolar contributions may even increase the polarization. In the case of conducting materials like metals, which obey the Drude model, the dielectric constant is much more negative than in the visible/IR.

Molecules

It is known from quantum mechanics that the rotation energy states of diatomic molecules vary as $E_J = BJ(J + 1)$, where B is the rotation constant that depends on the inertia moment of the molecule, and J the quantum number (here we neglect centrifugal distortion). The transition between two levels J and $J + \Delta J$ must fulfil the selection rule $\Delta J = \pm 1$ and it occurs in the THz range for relatively light molecules (typically <300 umu). For poly-atomic molecules, the preceding expression of the energy state is generalized. One must also take into account the vibration states of the molecules given by $E_N = hf(N + 1/2)$, where f is the proper vibration frequency of the molecule and N the quantum number (there is no transition rule on N , but the transitions $\Delta N = \pm 1$ are the most intense). Finally, the energy of the molecules is the sum of both rotation and vibration energies: $E = E_J + E_N$.

Molecule made of n atoms exhibits $3n$ degrees of freedom: 3 translations, 3 rotations and $3n - 6$ vibrations. The absorption or emission spectra in the THz range of molecules in the gaseous phase is thus complex. Let us notice that they are observed only from molecules that exhibit a dipolar momentum (thus, for example, CO_2 and Cl_2 do not present absorption lines in the THz range). In the case of low pressure gases, THz spectroscopy shows better spectral resolution and selectivity than visible or infrared spectroscopies, thanks to a weaker Doppler broadening.

The different movements of the atoms in the molecule and/or the molecule skeleton are sketched in Fig. 1, together with the range of frequencies in which these movements are resonant. Table 1 gives the dipolar moment of selected molecules: the absorption is more intense for molecules with a higher dipolar moment.

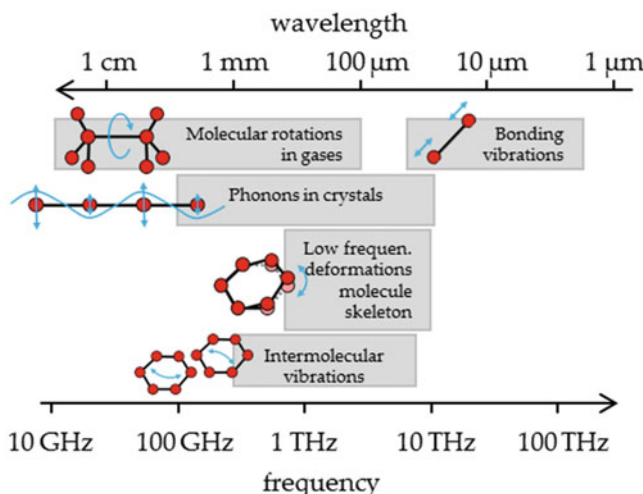


Fig. 1 Transparency spectrum (tendency) for common materials

Table 1 Dipole moment (given in Debye) of selected molecules that exhibit THz absorption lines. The higher the moment, the stronger the absorption

Molecule	HCN	H	CO	NH ₃	HF	H ₂ S	HCl	CCl ₂ O	H ₂ O	OCS
Dip. Moment	2.98	2.00	2.33	1.47	1.83	0.97	1.11	1.17	1.86	0.71

In conclusion, THz spectroscopy is an exclusive tool to address inter- and intramolecular vibrational modes of gases, which constitute a unique fingerprint that permits the identification of numerous molecules.

Solids

In solids, atoms or molecules are linked together, which limits the electronic cloud deformation under electromagnetic excitation. Therefore, molecular peaks are strongly attenuated as compared to those in the gas phase. Collective excitations of atoms or molecules, like optical phonons, are likely located in the THz range, and appear at room temperature as bumps in the absorption spectra of the solids. Therefore, in addition to intramolecular vibrations, intermolecular collective vibrations are also addressed by THz spectroscopy. This gives THz spectroscopy the potential to provide both chemical and structural information. Indeed, THz-TDS has been shown to be a particularly sensitive technique for studying the structural dynamics of crystal forms, providing additional information for sample analysis. In amorphous solids, localized vibrations of molecules lead to an increase absorption in the THz range, known as the boson peak. Generally, as these phonon lines are situated over several THz, they induce a monotonous increase of the absorption in

the range from sub-THz up to several THz. Many materials exhibit characteristic spectral features in the THz frequency range (particularly over 1 THz), enabling THz spectroscopy to be used as a tool to uniquely identify chemical species.

Liquids

Polar liquids, like water or given oils, strongly interact with the incoming THz beam, through a dipolar interaction. In fact, the energy of hydrogen bonds are comparable with the one of THz photons and are responsible for the strong interaction of water at THz frequencies [5]. Excited water molecules in the liquid phase show two relaxation times, respectively of the order of 10's of ps and sub-ps. They are related to the reorientation of the dipole moment and the damping of the vibration modes. All these effects make the absorption of water at THz frequencies larger than 100 cm^{-1} . On the contrary, non-polar liquids are very transparent at THz frequencies [6].

Summary

Figure 2 shows the tendencies of the transparency spectra of bulk materials (here bulk means thicknesses of the order of millimeter or thicker). Apart from resonances due to molecular vibrations or phonons, sample transmission decreases monotonously with frequency. Pure crystals like quartz, organic materials or intrinsic semiconductors are rather transparent in the THz range. On the other hand, moistened or electrically-conductive materials are quite or totally opaque.

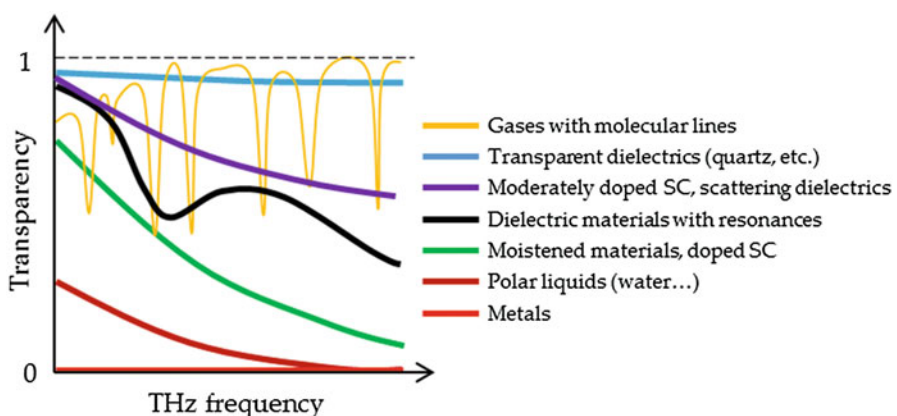


Fig. 2 Transparency spectrum (tendency) for common materials

THz Technology: Sources, Detectors and Components

Sources

The THz gap

Because the THz domain ranges between the infrared and microwaves, one would adapt either optical or electronic techniques to produce or detect THz waves. Unfortunately, optical techniques become less efficient because of the thermal noise that is bigger than the photon energy. Similarly, electronics reaches hardly the high frequency regime because of the RC constant time of circuits and of the transit time in most of active components. However, since the 80's, impressive progress has been made, based initially on laser-driven sources, and then on the improvement of electronic components.

Electronic Sources

Electronic sources delivering THz signals involve high frequency components whose operation is mostly based on ultra-short transit times and negative differential resistance, like resonant tunneling, IMPATT, Gunn diodes. MMIC circuits, built with FET transistors, also reach the THz region. The performance of such devices is progressing rapidly. For example, generation of signals up to 2 THz has been reported with RTD diodes, while the upper limit of these diodes was 0.1~0.2 THz about 15 years ago. Therefore, electronic components constitute the best choice of sources for THz systems up to 0.5~0.7 THz, but they deliver a too weak power over 1 THz (see Fig. 3).

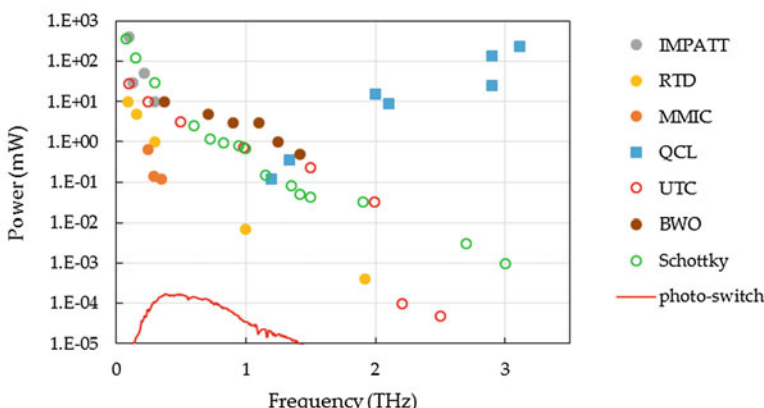


Fig. 3 THz power delivered by diodes (IMPATT, RTD), MMIC high frequency circuits, QCL lasers, BWO, and optical mixing in UTC and Schottky diodes. The continuous line corresponds a 2- μ W THz pulsed signal from a LTG-GaAs photo-conducting antenna (integrated over 50 GHz). Data collected by the authors from the literature on Jan. 2019

Optoelectronic Sources

They include two types of devices. First, one of the most popular components is the ultrafast photoconductive switch that is excited by a femtosecond laser pulse, delivering electromagnetic burst of sub-picosecond duration. Switches made from low-temperature grown GaAs, GaBiAs and multi-layered InGaAs could be excited by 0.8, 1 and 1.5- μ m lasers. CW generation is also possible through the mixing of two laser beams at different wavelengths. Similar signals are delivered by nonlinear dielectric crystals through femtosecond optical rectification. In these crystals, other ways of generating a THz beam through optical excitation are efficient, like difference frequency generation, THz parametric generation, oscillation and amplification. Higher pulse power are generated from photo-induced plasmas in air or liquids at the expense of employing amplified laser systems. Typically, the spectrum of these sub-picosecond pulse spread from 0.1 up to several THz, and even some tens of THz from plasmas, and their averaged power is of the order of μ W or less.

The second family of devices includes electronic components, like UTC or Schottky diodes, that are excited by CW laser beams and thus are used as a nonlinear optical component to produce THz waves through optical mixing. Even if photomixing produces more THz power, its efficiency is very weak over 1 THz.

Other Sources

Quantum cascade lasers (QCL) are made of a multi-layered semiconductor quantum well structure. Under a bias, free electrons may tunnel-transit from the lowest quantum level of one well to an excited one in the neighbor well, and then they return to the lowest energy level by emitting a THz photon. The advantages of QCL is that the THz wavelength depends on their geometry and not on their material, and that the radiated power is rather high due to the simultaneous emission of several wells. However, the population inversion in each well is affected by thermal effect, even at cryogenic temperatures, which makes the QCL THz power strongly decreasing below 2 THz. To our knowledge, no QCL laser is commercially available below 1.3 THz.

Vacuum tubes in which free electrons move in a periodic field, like backward oscillators (BWO), deliver huge power up to the THz over a rather wide bandwidth (0.1~0.2 THz). However, they are bulky and their uneven spectrum makes them impracticable to employ in many applications.

A list of the main THz sources with their characteristics is given in Table 2.

Table 2 Main THz sources and their characteristics

	sources	bandwidth (THz)	power	pros	cons
Thermal	Blackbody	Entire THz band	~ pW	Simple, broadband	Low power incoherent
Solid state electronics	GUNN	0.1 → 1	100 mW	Compact high power	Limited band
	IMPATT	→ 0.4	100 mW	Compact high power	Limited band
	TUNETT, RTD	→ 0.4	1~10 mW	Compact	Limited band
Vacuum electronics	Klystron	→ 0.3	0.3~50 mW	Tunable	No commercial THz klystron
	BWO	→ 1.2	10 mW	Tunable	Uneven spect. Bulky
	Gyrotron	→ 0.5	100 W	Powerful	High magnetic field, bulky
Large instruments	FEL	Entire THz band	100 W average	Powerful broadband	Huge
Lasers	Molecular lasers	Spectral lines	100 mW	Spectral purity high CW power	Low stability bulky
	QCL	1.3 ←	0.1~100 mW	Compact, efficiency	Cryogenic low power

Detectors

Basics of Detection Physics

Receivers transform the incoming THz beam field or power into another physical value that can be easily measured. In the case of power detectors, an electrical current I or voltage U is delivered, which varies linearly with the THz beam strength. The responsivity R of the receivers is defined by:

$$R = \frac{U}{P} \text{ (unit = V/W)}, \quad R = \frac{I}{P} \text{ (unit = A/W)}. \quad (1)$$

The minimum power that could be recorded is equal to the noise of the receiver (either intrinsic or due to the environment). Thus one defines the noise equivalent power (NEP), which is the incoming power that will correspond to a detection signal equal to the noise power. In the FIR, NEP is proportional to the square root of the size of the detector and of its bandwidth. To compare different detectors, one defines their NEP in a 1-Hz bandwidth, and thus NEP is given in $\text{W}/\sqrt{\text{Hz}}$. Generally speaking, power detectors integrate the beam energy and are slow, while field detectors are ultrafast but less sensitive and require time-equivalent techniques to retrieve the temporal shape of the THz signal.

Electronic Detectors [7]

Today, the most promising electronic detectors are field-effect transistors (FET), with a nanometric channel that allows for high frequency operation, or CMOS receivers in which a second order nonlinearity (provided for example by a Schottky barrier) rectifies the THz signal. The state-of-the-art devices show a *NEP* varying from $8.4 \text{ pW}/\sqrt{\text{Hz}}$ at 0.26 THz to $100 \text{ pW}/\sqrt{\text{Hz}}$ at 0.9 THz. Heterodyne detection, in which the signal is mixed with the one from a local oscillator, permits to strongly reduce the minimum detected power level, down to $0.1 \text{ pW}/\sqrt{\text{Hz}}$ at 0.9 THz [7].

Optoelectronic Antennas

Optoelectronic antennas are used either in emission or receiving mode, and they include photo-conducting switches and electro-optic sensors. In switches, a gap in a coplanar or micro-strip waveguide, deposited over an ultrafast intrinsic semiconductor (like low-temperature grown GaAs), is made conducting by excitation with a femtosecond laser pulse. In the detection scheme, the photo-generated free carriers are accelerated by the THz pulsed field that impinges simultaneously the device. The resulting current is proportional to the electrical field of the THz wave, and it is read by highly-sensitive electronics. Electro-optic sensors take benefit of the Pockels effect, i.e. the index ellipsoid of a crystal is modified by the incoming THz field, and this modification is read by looking at the polarization change of a transmitted optical probe beam. Both types of antennas, either switches or the electro-optics ones, require time-equivalent sampling technique to retrieve the THz waveform, and consequently a repetitive pulsed THz source is compulsory.

Bolometers

In bolometers, a material absorbs the incoming THz beam and its temperature increases. The resistance of a thermo-resistive material in contact with the heated material varies proportionally to the THz power. This change of resistance is read by electronics, and thus the incoming THz power is determined. Bolometers in which the sensitive material is a superconductor are among the most sensitive FIR receivers, with a *NEP* as low as $10^{-19} \text{ W}/\sqrt{\text{Hz}}$ for kinetic inductance detectors (KID), transition edged sensors (TES) or hot-electron bolometers (HEB) devices, and they are used in astrophysics. Unfortunately, most of them operate at very low cryogenic temperatures (below 1 K). In room-temperature bolometers, the absorber and thermistor are usually made of the same material, the best one being Vox (oxides of vanadium). They show a *NEP* of the order of $20\text{--}50 \text{ pW}/\sqrt{\text{Hz}}$ and are sensitive in the range over 1.5~2 THz. Thanks to microelectronics processing, large scale fabrication is possible as well as manufacturing of arrays that serve as focal plane sensors for video-rate cameras.

THz Absorption Spectrum of Molecules of Interest

Introduction

This paragraph deals only with the THz spectral signature of the materials of interest, either lethal gases, explosives, or drugs. The difficult issue of recording at a remote distance the signal requested for the identification will be addressed in the last part of this paragraph.

Molecules of interest in the domains of security and defense include dangerous molecules (explosives, lethal gases...), prohibited substances (drugs, flammable liquids...), or substances that are inert by their own, but may serve as basic components of dangerous compounds. For example, powder of aluminum is one of the constituents of thermite, which is a well-known pyrotechnic material that can produce short bursts of high temperature. Additionally, regular sugar powder reacts violently with molten potassium chlorate when the reaction is initiated with a drop of sulfuric acid, which releases amount of smoke, flame and high temperature.

When the molecules or materials are dangerous, like explosives, remote THz sensing presents a clear advantage. However, as any method based on electromagnetic waves (IR or visible spectroscopies, Raman sensing, etc.), their sensitivity is much weaker than what can be achieved with a direct chemical analysis of a sample taken at the scene.

An additional challenge facing explosive detection is the improvised explosive device (IED). This type of unconventional threat has existed since the invention of gunpowder. IEDs can take any form and the activation is enabled in a variety of ways. Nowadays, it is the preferred tool of terrorists because of its low cost and its relatively simple manufacturing methods, shared through modern means of communication, especially from the Internet.

Depending on the context and usage, it is important to point out that remote and real-time THz detection and identification is not currently available for security applications. Providing a preliminary alert before any spectrometry measurement is done, is certainly an efficient way to reduce the risk of explosion.

Explosives

The THz response of most explosive materials has been studied in the past, including, for example, ammonium nitrate, TNT 2,4-dinitrotoluene, HMX, PBX, RDX, PETN, Metabel, Semtex, etc. [10–15]. Even if all of the studies are not published for evident reasons of security, the related literature is quite huge. The specific signatures of explosive materials in the THz range are related to the vibration of the molecules (for example ring torsion or bend in molecules that include a phenyl or benzene ring like 2,4-DNT, TNT, RDX, etc.; chemical bond wagging, etc.). Also intermolecular modes, which could be coupled to phonons when the material is crystalline (even at a short scale), contribute to THz absorption lines. The position of

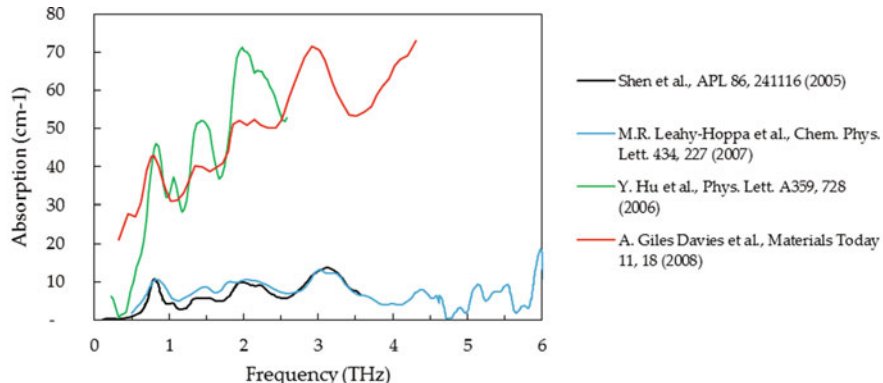


Fig. 4 Absorption of RDX in the THz range extracted from the papers listed on the right side [11, 13–15]. The 2 upper curves are obtained with a pure material, while the lower ones are measured with RDX diluted in a PTFE powder

the related spectral lines can be calculated using the differential functional theory with dedicated codes like Gaussian®. Let us notice that the spectroscopy of explosive materials is most of the time performed with pellets of compressed powder, which can be pure or a mixture of explosive and ligand (HDPE, Teflon...) powders.

Typically, the interesting absorption lines of explosives are situated in the range over 1 THz. The spectral position of these lines as well as their strength may differ from one sample to another, depending on the material purity and fabrication process. This is clearly shown in Fig. 4, where different data for the RDX explosive taken from the literature [11, 13–15] are plotted. Nevertheless, the more intense lines are clearly identified.

Drugs-of-Abuse

Drugs-of-abuse exhibit THz absorption features for the same reason as explosives (see above). Most of the drugs have been characterized in the THz range, like cocaine, ecstasy, amphetamine (MDMA), heroin, morphine, ephedrine, and so on [11–12, 16]. Usually, the samples are pellets of compressed powders, and very often, the drug powder is diluted in a transparent matrix (powder of HDPE or Teflon). The resonances in the THz absorption spectra appear as bumps of rather large width (typically 100 GHz or more), most often at higher frequencies (generally over 1.5 THz). For some illicit drugs like MDMA or heroine, the resonances are not well contrasted, while in some others like cocaine, the resonance peak arises well over the spectral baseline. But the main technical difficulty in identification originates in the impure drug samples that are available in the “real-world”. Many of them are diluted with adulterants (lactose, caffeine, lidocaine, etc.): this adds absorption features in the THz spectrum. Moreover, the drug itself varies in composition from one street-sample to another, leading to a distribution of the spectra around a mean value.

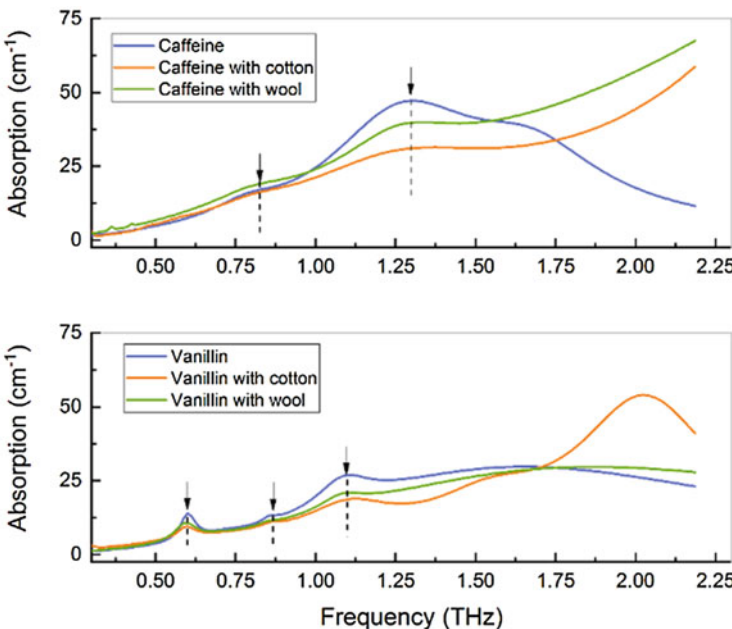


Fig. 5 THz absorption spectra of vanillin (upper) and caffeine (lower), pure or combined with cotton and wool. Resonances are labelled with a dashed line

Therefore, the identification by THz spectroscopy of the real-word illicit drug samples requires sophisticated automatic codes that analyze the recorded spectra. Most of them are derived from chemometrics, like principal component analysis [12] genetic codes [16], self-organization feature map (SOM) artificial neural network [17], etc. A review of these techniques is given in [18].

Packaging or clothes that hide these drugs, but also the explosive materials, may partly absorb the THz signal and add features in the THz spectra, which disturbs the own spectral signature of the material of interest. This makes the identification of the substance more complex [19]. As an example, we show here (Fig. 5) the THz absorption spectra of vanillin and caffeine, when the substance is pure or when it impregnates a textile (wood and cotton). The spectral lines of the pure materials (0.87, 1.27, 1.66 and 2.44 THz for caffeine, and 0.6, 0.87, 1.16, 1.76 and 2.44 THz for vanillin). Most of these lines are still observable when impregnated in the textiles, but they are less contrasted and some of them are no more detectable.

Gases (Chemical Warfare)

Detecting or sensing gases is efficiently performed in the mid-infrared region, where chemical-link vibrations lead to unique spectral signatures [20]. In the THz range, transitions between roto-vibrational energy states are involved, which results in very

reach absorption line spectra and is complementary to mid-infrared spectroscopy, enlarging the number of gases that can be investigated. Also, as already written, THz spectroscopy offers a better resolution and thus selectivity. In the case the molecule acts as a symmetric rotor (i.e. acetonitrile, cyanide hydrogen...), the energy levels are regularly spaced, leading to an absorption spectral comb. The frequency distance between successive absorption peaks could be as short as a few GHz (for example, 13 GHz in methyl chloride). When the molecule is more complex, other vibration modes are involved, involving torsion, wagging, stretching and in general deformations of the molecule skeleton, and consequently the absorption lines are more difficult to interpret. When dealing with security applications, and also for environmental studies, the measurements are performed under standard pressure and temperature values. In this case, and because the molecules showing a THz signature are light, the absorption line has a Lorentzian profile and its width is of the order of a few GHz, due to broadening by pressure effects. Therefore, one will be able to discriminate a mixture of gases only if the spectral lines of each gas are separated by more than a few GHz from the ones of the other species. Nevertheless, depending on the species, concentrations as small as a few ppb or even less are measurable with high sensitivity CW spectrometers [21].

The detection of lethal gases (e.g. hydrogen cyanide-HCN, phosgene- CCl_2O , mustard gas, cyanogen- CNCl , sarin- $\text{C}_4\text{H}_{10}\text{FO}_2\text{P}$...) is of great interest in the fight against terrorism, but also on the battlefield, and to verify that some countries do not use it during conflicts. Even if all the performed research studies are not published, and they are numerous, several open papers related to this topic are available. For example, the online-available report to the US-DARPA by F. C. De Lucia [21] gives an excellent synthesis of the researches performed in the years 2000–2010. Because of the toxicity of these gases, studies are performed either theoretically by modelling their FIR absorption spectra, or by using their simulants, i.e. molecules that have similar functional groups as the gases, for example DMMM (dimethyl methyl phosphonate) instead of sarin.

The FIR response of HCN is widely studied because, beside security and defense issue, this gas has been detected in intergalactic clouds, and also in the smoke of fires or even in the smoke of cigarettes [22]! HCN shows periodic absorption lines separated by 88.5 GHz.

The possibility of detecting the mustard gas has been theoretically evaluated [23]. This gas exhibits absorption lines at 1.02, 2.13, 2.31, 2.79, 2.94, 3.42 and 3.57 THz. As well, THz detection of phosgene seems possible [24].

Standoff Techniques

The above described spectroscopic results have been obtained in the laboratory, either in transmission or reflection through/by the sample. Performing spectroscopic data acquisition at a very long distance is more difficult. Nevertheless, this is compulsory to avoid any hazard when dealing with dangerous substances (lethal agents, explosives) or when detection/identification has to be performed in

dangerous places, like on the battlefields. The technical difficulties are: 1) the long distances between emitting/receiving antennas and the sample; 2) the attenuation, in the THz range, of air over these long distances due to water vapor and dusts; 3) the obligation to work in the back-scattering regime as emitter and receiver are installed at the same position. This makes the THz signal to be recorded extremely weak. Moreover, the spectral features to be identified may be hidden or distorted by the lines of water vapor or of any atmospheric pollutant.

A smart solution has been proposed by X.-C. Zhang and his team. A THz pulse propagates through the sample (for example a vapor of the substance to be detected). Using a powerful femtosecond laser, air-breakdown is produced at the focus of the laser beam just after the sample, simultaneously with the arrival of the THz pulse. It is shown that the fluorescence of this plasma is encoded by the spectrum of the THz pulse, and thus by the absorption line of the substance. After recording the fluorescence waveform, a numerical decoding of its spectrum leads to retrieve the absorption spectrum of the substance. In [25], the authors demonstrate the principle of this technique when the THz pulse is generated in a LiNbO₃ crystal and the sample is a pellet of explosive (4-DNT mixed with PEHD). The spectrum of 4-DNT was thus recorded at a distance of 10-m. In [26], the same authors generated the THz pulse from a first photo-induced plasma, and they studied NG, 2,4-DNT, and HMX. The great advantage of this “all air plasma” technique [26] is that the signals are conveyed to and from the tested area by means of the laser beams, and they do not suffer from air absorption at THz frequencies. However, such a technique is maybe difficult to implement in real conditions. Especially, it requires a bulky and expensive amplified femtosecond laser system.

Another solution could be to carry the THz spectrometer to the location of interest with a robot or a drone, i.e. without endangering humans. This has been demonstrated by Demers et al. [27], who recorded the absorption spectrum of the atmosphere a few tens of meters over ground in the region of Los Angeles, using a drone-mounted CW THz spectrometer. From the recorded data, they were able to determine the water vapor content of air.

Imaging for Security Application

Requirements for Remote Sensing Dedicated to Security

The main goal of THz imaging, for security and defense applications, is to image items that could be carried by terrorists or enemies, and that are hidden under clothes or inside packages. Also, inspection of what is inside mails and postal packets is an important issue. Classical imaging looks at getting an image of the items, and thus to identify these items from their shape, which could be easy for typical objects like guns. In hyper-spectral imaging, several images of the same scene are recorded simultaneously at different THz frequencies, which should permit to identify the chemical composition of the observed materials.

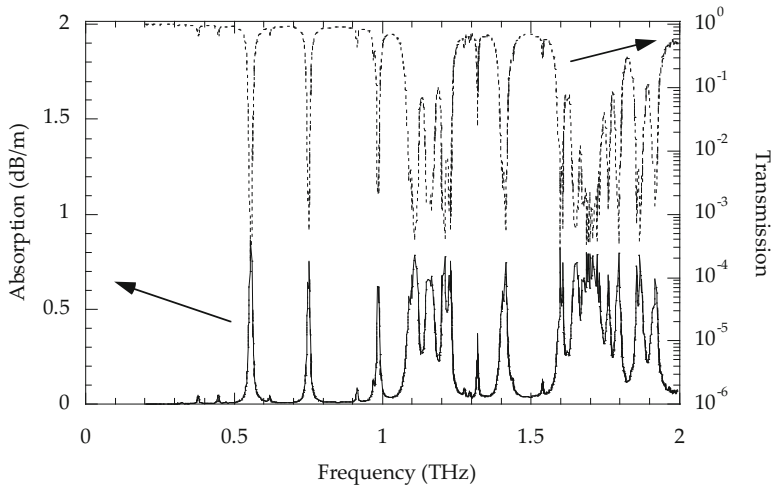


Fig. 6 Absorption of air at 21 °C and 51% relative humidity and transmission through a 50-m air distance. (Adapted from [28])

In any case, the observation of a scene is performed at a close distance (typically a meter or less) in special gates (like in airports or railways stations) or a more remote distance (more than 5~10 m) on the battlefield, at open-field borders, in the street or in large building halls. In the latter case, the long distance is compulsory to avoid any damage if the observed person is a terrorist or an enemy carrying a bomb. In airport or station gates, one desires to check that the traveler does not carry prohibited or dangerous weapons or substances.

Remote observation is limited by the attenuation of the atmosphere at THz frequencies. This attenuation is mainly due to absorption by water vapor. Below 1 THz, water vapor lines correspond to a few strong but rather narrow absorption peaks, while over 1 THz the lines are numerous and closer to each other, leading to a stronger overall absorption, even outside resonances. Typically, for moderately humid air, absorption is less than 0.1 dB/m below 1 THz in the transparency windows (0.21, 0.35, 0.41, 0.67, 0.84 THz), while it larger than 1 dB/m over 1.5 THz (see Fig. 6). Moreover, these values are at least ten times larger when the atmosphere is more humid or dusty. Therefore, performing THz remote control is unrealistic for frequencies higher than 0.7~1 THz, if the distance between the THz source and detector and the scene is larger than some tens of meters.

Getting images at video rates constitutes the second constrain in security applications. It is requested by a rapidly varying scene at the battlefield, and by the need of performing rapid inspections at gates, in view of avoiding long queues at the control. This makes not adapted to this purpose setups based on a single pixel sensor and a scanning mechanical system, even if some systems have been successfully tested in laboratories [29–31].

Finally, we remind the reader that the THz light coming from the scene towards the camera is strongly dependent on the surface state of the observed item. In the case of passive imaging, the thermal radiation signal will mostly depend on the orientation of the surface as regards to the camera. In the case of active imaging, the illuminating beam is either reflected or scattered (diffuse surface scattering) towards the camera. The efficiency of these latter phenomena has been treated in many publications, e.g. [32–33].

Passive Imaging

Basic Principles: Thermal Emission, THz Power Budget

Any body at a given temperature T emits a broadband incoherent radiation through the microscopic random movement (thermal agitation) of its elementary constituents (atoms, free electrons, molecules). The power radiated by an area ds of the body is given by the famous Planck formula, which can be approximated in the far infrared by the Rayleigh-Jeans one:

$$P(\nu, T) \approx 2k_B T \left(\frac{\nu}{c}\right)^2 d\nu d\Omega ds. \quad (2)$$

Here $P(\nu, T)$ is the power radiated in the solid angle $d\Omega$ at frequency ν and in the bandwidth $d\nu$. k_B is the Boltzmann constant.

Let us now suppose that one observes this body with a camera. We select the area ds at the surface of the body such as its image on the camera focal plane is equal to the size of a single pixel. In the limit of diffraction, the power collected by the pixel is:

$$P(\nu, T) \approx 2 k_B T d\nu. \quad (3)$$

Here $d\nu$ is the bandwidth of the detection pixel. The received power does not depend on the THz frequency ν , but only on the temperature of the emitting body. Thermal cameras are thus based on this expression: they can allow to determine the temperature of the observed scene. In the case of THz cameras for security applications, a hidden object could be “seen” thanks to its difference of temperature ΔT with the body of the person who carries it. The detected power difference is $\Delta P \approx 2 k_B \Delta T d\nu$. This power difference must be larger than the NEP of the detector. When it is equal to the NEP , it permits to define the noise equivalent differential temperature $NEDT$, i.e. the minimum temperature difference at the scene that we can record:

$$NEDT = \frac{NEP}{2 k_B d\nu}. \quad (4)$$

For a scene at room temperature, and assuming a realistic minimum $\Delta T = 0.1$ K, we obtain $\Delta P = 0.27$ pW for a 100-GHz bandwidth. At a video rate of 24 frame-per-second (fps), the maximum integration time is 40 ms. Therefore, to permit the discrimination of temperature inhomogeneity $\Delta T = 0.1$ K at the scene, the camera NEP must be smaller than $0.27/2\sqrt{24} \approx 0.03$ pW/ $\sqrt{\text{Hz}}$. Only superconducting cameras operating at cryogenic temperatures deliver this performance. However, if the constraints on the temperature and the image rate are less severe, the best room-temperature cameras are close to produce thermal THz images. For example, with $\Delta T = 2$ K and 1 fps, NEP should be smaller than 1.4 pW/ $\sqrt{\text{Hz}}$, which is less than one order of magnitude smaller than the NEP of the best room-temperature cameras. Note that here we do not take into account detection noises that are dependent on the incoming light power, like the shot noise.

Cameras for Passive Imaging

To our knowledge, video cameras for passive imaging are only based on superconducting detector arrays, which show an impressive NEP value (see Table 3), lower than the pW/ $\sqrt{\text{Hz}}$ threshold. They are derived from focal plane arrays used in radio-astronomy (see for example [34]). On the other hand, most of them operate below 1 K, and require liquid helium cryostat. Nevertheless, cryogenerators are nowadays available, which require no expensive and regular fillings with liquid helium. These video cameras are developed in common by laboratories and companies. One of them (Asqella) is commercially available. Demonstration of imaging of people at distances of 10~15 m has been performed, as well as imaging of persons who went in hiding in wooden crates (here the image was taken through the ~1-cm thick wood wall) [35].

Beside cryogenic cameras, attempts are done to employ room-temperature electronic detectors and cameras (see description in the next paragraph). Single HEMT transistor with a preamplifier shows a good enough $NEDT$ in the W band [36], and

Table 3 THz video-cameras for passive imaging

Laboratory / company	Sensor technol.	Array size pixel nb.	Frequency GHz	NEP pW/ $\sqrt{\text{Hz}}$	NEDT K	Video rate fps	References
QMC/Cardiff Univ. (UK)	KID	152	347	0.03	0.006	2	[27]
Supracon AG, Univ. Jena (G)	TES	128	350	0.0003	0.4	25	[28]
Asqella (Fin)	Micro-bridge bolometer	?	250, 420, 625	0.01	0.4	8	[29]

passive images have been obtained at 670 GHz with a single HEMT detector and scanning optics [31]. Blackbody emission has been recently imaged with a CMOS camera [37], but the beam was produced by a blackbody radiator at high temperature, and the signal was integrated over 10,240 frames! On the other hand, electronic cameras operate nicely at lower frequencies, typically below 250 GHz, and they are used in several commercial THz inspection systems that are described in the next paragraph.

Demonstration of Passive Remote THz Imaging

Both NIST at Boulder (USA), and VTT and Millilab in Finland, have built a passive system based on a superconducting camera (linear NB/NbN bridge sensors) and a scanning optical assembly [41]. Images at a rate of 5 fps of a $2 \times 4 \text{ m}^2$ scene at a standoff distance of 8 m were reported. A *NEDT* equal to 1.97 K was achieved, allowing to distinguish hidden objects carried by a person.

The THz system from IPTH Jena (now Leibniz-IPHT) [40], which includes a 64-pixels linear detector (superconducting transition-edge sensors – TES) and a scanning optics, is able to image at 350 GHz a scene up to 20 m, with a spatial resolution of 2 cm and a *NEDT* of 0.4 K at video rate (25 fps). Observation of hidden weapons has been demonstrated.

Below 250 GHz, several systems are commercial, based on electronic sensors and technologies derived from the microwaves. They are installed as body scanners at airport gates, in subway stations, etc. Some of them are listed in Table 4.

Active Imaging

Advantages and Drawbacks of Active Imaging

The main advantage of active imaging is the use of room temperature cameras. The focal plane array of these cameras is either made of electronic receivers or of microbolometers. Both of them are manufactured with the technology of microelectronics and MEMS, and they are relatively compact. Therefore, these cameras are easier to use in the real-world than the cryogenic ones, and in principle they should be cheaper. Moreover, active imaging is less sensitive to ambient temperature.

On the other hand, they require illuminating the scene with a rather strong THz beam. This limits the operation to distances of 10~20 m, and the illuminating beam can be detected by enemies. For civil applications, like at airport gates, people are frightened to be irradiated by electromagnetic waves, which are believed to be hazardous for the health. Finally, the way the person or the object reflects or scatters the THz beam, could make difficult the analysis of the THz image.

Table 4 Some THz and millimeter-wave scanners

Company	Website	Model	Technology	Frequency GHz	Standoff distance m	Spatial resolution cm ²	Video rate or image acquisition time
Thruvision	Thru-vision. Com	TS4-SC	Heterodyne detection	250	8	5 × 5	6 fps
Brijot	www.brijot.com	GEN2A	LNA	90	5	6 × 6	4–12 fps
Rohde & Schwarz	www.rohde-schwarz.com	R&S®QPS200		80–90	1		~ ms
Smiths detection	www.smithsdetection.com	EQO	Active	24.16	1	0.4 × 0.4	~ 10 s
L-3 Comm.	www.sds.l3.t.com	Pro-vision 2	Active 2 × 200 linear arrays (GaAs MMIC)		1		~ 1.5 s

Table 5 Commercially available THz video-cameras (list established in Jan. 2019)

Company	Country	Technology	Pixels	Sensitivity range (THz)	NEP (pW/Hz ^{1/2})
i2S	France	Microbololo.	320 × 240	0.4–3	30
INO	Canada	Microbololo.	384 × 288	0.1–4.2	—
TeraSense	USA	FET	64 × 64	0.01–1	1000

Cameras and Systems for Active Imaging

As already explained, cameras for active imaging are not supposed to exhibit the extraordinary performance of cryogenic cameras. Thus, in this purpose, 2 types of video-rate THz cameras are currently available. They are built with room-temperature micro-bolometers or make use of FET or CMOS transistors. Other cameras exist, for example with pyroelectric sensor arrays (Spiricon, Ophir, etc.), but they do not operate at video rate, and their NEP is rather high (tens of nW/√Hz).

We first list in Table 5 the commercially available cameras and their characteristics.

Other cameras still at the stage of development in laboratories are listed in Table 6. These cameras include either electronic sensor arrays (HBT, diodes, FET...) or micro-bolometers. Electronic arrays are more adapted to the sub-THz range, while micro-bolometers are sensitive above 1 THz. Typically, the best NEP is of the order of tens of pW/√Hz, and the bandwidth is some tens of GHz for electronic sensors up to about 100 GHz for micro-bolometers. However this bandwidth is also limited by filters in front of the camera, and it could be much narrower. The optics of the camera is single focus. It can be a sophisticated aberration-corrected lens, usually made in high-resistivity silicon, or a simple plano-convex element made in plastic (TPX, HDPE...). These optics are very fast (*f*-number ~ 1) [42]. Let us notice that we do not list here cameras for the low frequency regime (< 200 GHz), which are derived from the microwaves and are characterized by quite huge optics, in view of optimizing the spatial resolution. Also, some cameras have been announced (for example by Algiltron, USA: 1–6 THz, 75 pW/√Hz, 130 × 90 pixels, 30 fps), but to the best of our knowledge, are not commercially available.

The sources required for illuminating the scene could be quantum cascade lasers (QCL), generally used with micro-bolometer cameras. For sub-THz imaging, high-power single frequency are employed, like IMPATT diodes.

Table 6 THz video-cameras for active imaging technol

	Laboratory/company	Frequency THz	Respon-sivity kV/W	NEP pW/ $\sqrt{\text{Hz}}$	Array size pixel nb.	Rate (max) fps	References
HBT diodes	University of Notre Dame (USA)	0.45–0.65	9.8	3	6 × 2	–	[43]
Schottky diode	Univ. Texas Cornell Univ. (USA)	0.28 0.22	5.1 2.5	29 30	4 × 4 6 × 6	– 143	[44] [45]
NMOS FET	Univ. Texas Cornell Univ. (USA)	0.82	3.4	15.5	8 × 8	–	[46]
CMOS FET	Univ. Wuppertal (D) ST Microelectronics (F)	0.79–0.96	115	100	32 × 32	500	[47]
NMOS FET	Leti-CEA (F) Traycer (USA)	0.2–0.6 0.6–1.2	300 100–1000	18.7 5000	31 × 31 200 × 200	100 200	[48] [49]

Demonstration of Active Remote THz Imaging

The published reports on experimental active remote THz imaging are not so numerous.

Micro-bolometer cameras were first employed, as early as in 2005, by A. Lee and Q. Hu [50] at MIT to produce movies of a hidden razor blade, which was illuminated at 2.52 THz by a QCL laser. The same team published 1 year later the first demonstration of remote imaging with a THz camera [51]. A QCL at 4.9 THz illuminates a room-temperature micro-bolometer camera located at ~26 m from the QCL. An off-axis parabolic mirror ($f = 2$ m) serves to form the image of a sample placed in its focal plane. Great images in transmission of a dried seed pod were obtained, with a lateral resolution of 0.75 mm. The security issue was not addressed in this pioneering paper. More recently [52], J. Meilhan et al. have imaged at 2.4 THz the signal reflected by pellets of explosives. They have shown that the specularly reflected signal is stronger than the scattered one, but no clear evidence of identification of explosives was demonstrated.

The Batelle Company, under a contract with the U. S. Department of Energy, has demonstrated imaging at 350 GHz up to a distance of 20 m [53]. The illuminating beam is provided by GaAs Schottky diode multipliers and mixers, and its power is 4 mW. The signal reflected back by the scene is about 10 times weaker. It is recorded using a heterodyne scheme. The system is based around a single emitter and a single receiver. The image is obtained by scanning the scene with a movable reflector in approximately 10 s. Weapons hidden under the cloth of a person are clearly visible on the images. More or less at the same time, a rather similar system has been developed by the Jet Propulsion Lab [29] at 0.67 THz. Thanks to a confocal Gregorian optical system including a 100-cm reflector, imaging at 25 m was demonstrated. Here again, nice images of hidden weapons were obtained, in a total scanning time of 5 s. The heterodyne detection technique was also employed at 0.645 GHz by the team of H. Roskos in Germany [54], but together with a focal plane array Si-MOSFET camera. This system was used to inspect postal envelopes containing drugs, but not to perform remote detection.

Future Prospects

While below 0.3~0.5 THz, body-scanners are commercially available and are already installed in some airports, this is not the case at higher frequencies, for which the technology is less mature and needs improvement. Also reducing the image acquisition time is still a challenge even at millimeter wavelengths.

Beside the goals of THz imaging that we described above, other useful applications merit a development.

Hyper-Spectral Imaging

First, the Holy Grail of security and defense specialists is recording “color” THz movies of a scene at a remote distance, i.e. to record simultaneously images at

different THz frequencies. This is called hyper-spectral or multi-spectral imaging. It is expected to give spectroscopic information of any point of the observed scene, and thus to real-time identify the substances at the scene. This idea of recording images at different frequencies and then to identify materials was nicely demonstrated by K. Kawase and co-workers in a very famous publication [55]. The authors used a THz wave parametric oscillator (OPO) to record the spectra of THz signals transmitted through a postal envelop. The image was obtained by mechanically scanning the envelope in the THz beam. Sachets containing methamphetamine, MDMA, and aspirin were clearly identified by changing the probing THz frequency. Since this pioneering work, many papers have been published on this topic, for which researchers mostly employed THz-TDS or OPO systems. A good review of present state-of-the-art achievements is given in [56]. Because of the rather long scanning time, this technique is adapted to mail inspection, but not to a rapidly-varying scene. Also, it is noticeable that researchers are able to identify substances they already know to be hidden. But identifying a totally unknown product has not been demonstrated so far.

The use of cameras for multi-spectral THz imaging is scarcely reported. Most of the reports are based on electronic systems. Statnikov et al. [57] used the different harmonics of a chain of multipliers (SiGe HBT BiCMOS technology) to cover the band 165–990 GHz with a discrete set of 6 frequencies, and the heterodyne detection was realized by a single receiver based on the same technology as the emitter. The whole system included 6 emission/reception modules at 6 different frequencies. The images were produced by scanning a sample in the beam. The paper was devoted to biology-oriented imaging. Rather similar systems were developed later on, for example by Chi et al. [58] using a 45-nm CMOS SOI technology to produce a signal and images continuously tunable from 120~300 GHz. Here again the paper does not address the security issue. The team of H. Roskos [59] has used a set of FET transistors, which different spectral sensitivity, to record images in transmission or reflection of pellets of explosive simulants. The system was based on a single receiver and a raster-scan imaging scheme. The illuminating THz beam was delivered either by a frequency-multipliers chain or by a molecular laser. Images are very convincing, but the system does not supply real-time films and does not work at a remote distance. More recently, Zhou and coworkers [60] have used a tunable QCL together with a micro-bolometer array equipped with an as-well tunable metamaterial filter. The good NEP (100 pW/ \sqrt{Hz}) and fast response time of the array (0.1 s) permitted the authors to record impressive images of a brain tumor at frequencies from 2.5 THz up to 4.2 THz. However, application of this system to defense and security was not addressed.

THz Imaging through Brownout

A well-known problem encountered by the air forces is the so-called “brownout effect”. When a helicopter is landing or taking off over an arid field, its rotor airflow generates a cloud of particles (sand, dust, etc.), called *brownout* (a similar phenomenon is observed over a snow-covered field, namely the *whiteout*). The brownout can

be as thick as tens of meters. Because of the induced lack of visibility, the pilot can no more see the ground, and in between the helicopter and the ground. Different accidents, like collisions between helicopters, have already been reported. Systems that can deliver an image through the brownout, at the video rate, are highly looked-for. Microwave systems could supply such images and movies, but they are too bulky (1-m diameter optics) to be installed in helicopters. On the other hand, visible and infrared light cannot propagate through the brownout because of scattering by the brownout particles that are bigger than the wavelength. A good compromise is to select the THz technology. First studies on the feasibility of THz imaging through a brownout have been realized, showing that, in the future, active imaging could present the requested performance, especially if the technology is progressing [61–62].

Conclusion

Imaging or sensing systems based on THz technology are expected to deliver unrivalled information in the area of security and defense. Discovering objects hidden under a cloth, inside an envelope or packet, has been definitively demonstrated. For this application, frequencies below 0.5 THz are sufficient, because the corresponding theoretical spatial resolution is ~ 0.7 mm. Moreover, these rather low frequencies propagate over long distance in air, and they easily go through covering layers like papers, cotton fabrics, plastic films, etc. In addition, signals at these frequencies are efficiently generated and detected by electronic components that are rather cheap and compact. Therefore, THz imaging below 0.5 THz will certainly be performed with all-electronic systems.

Identifying substances requires higher frequencies, typically over 1.5 THz, and the necessary spectroscopic or at least multi-spectral techniques necessitate several narrow band THz beams, or very broadband beams, like the ones corresponding to ultra-short THz pulses. In this case, the present THz technology merits improvement in terms of delivered power, size and price. Also, it is desired that video-rate THz cameras make progress in terms of sensitivity and *NEP*, while it would be fine that their prices decrease.

References

1. Emerson DT (1997) The work of Jagadis Chandra Bose: 100 years of millimeter wave research. *IEEE Trans Microwave Theo Techn* 45:2267
2. Rubens H (1892) Ueber dispersion ultranrother strahlen. *Wied Ann* 45:238
3. Nichols EF, Tear JD (1923) Joining the infra-red and electric wave spectra. *Proc Nat Acad Sci U S A* 9:211
4. Loewenstein EV (1966) The history and current status of Fourier transform spectroscopy. *Appl Opt* 5:845
5. Smolenskaya OA et al. (2018) Terahertz biophotonics as a tool for studies of dielectric and spectral properties of biological tissues and liquids. *Prog Quant Electron* 62:1–77
6. Pedersen JE, Keiding SR (1992) THz time-domain spectroscopy of nonpolar liquids. *IEEE J Quant Electron* 28:2518–2522

7. Hillger P, Grzyb J, Jain R, Pfeiffer U (2019) Terahertz imaging and sensing applications with silicon-based technologies. *IEEE Trans THz Sci Technol* 9:1–19
8. Rowe S et al. (2016) A passive terahertz video camera based on lumped element kinetic inductance detectors. *Rev. Scient Instrum* 87:033105
9. Soylu G et al. (2018) Detection of weak terahertz pulsed signals using kinetic inductance detectors. *J Infrared, Milli THz Waves*:1–7
10. Chen J et al. (2007) Absorption coefficients of selected explosives and related compounds in the range of 0.1–2.8 THz. *Opt Express* 15:12060–12,067
11. Giles Davies A, Burnett AD, Fan W, Linfield EH, Cunningham JE (2008) Terahertz spectroscopy of explosives and drugs. *Mater Today* 11:18–26
12. Burnett AD et al. (2009) Broadband terahertz time-domain spectroscopy of drugs-of-abuse and the use of principal component analysis. *Analyst* 134:1658–1668
13. Hu Y, Huang P, Guoa L, Wang X, Zhang C (2006) Terahertz spectroscopic investigations of explosives. *Phys Lett A* 359:728–732
14. Leahy-Hoppa MR, Fitch MJ, Zheng X, Hayden LM, Osiander R (2007) Wide-band terahertz spectroscopy of explosives. *Chem Phys Lett* 434:227–230
15. Shen YC et al. (2005) Detection and identification of explosives using terahertz pulsed spectroscopic imaging. *Appl Phys Lett* 86:241116
16. Chen Y et al. (2011) Quantitative analysis of terahertz spectra for illicit drugs using adaptive-range microgenetic algorithm. *J Appl Phys* 110:044902
17. Pan R, Zhao S, Shen J (2010) Terahertz Spectra Applications in Identification of Illicit Drugs Using Support Vector Machines. *Proc Eng* 7:15–21
18. El Haddad J, Bousquet B, Canioni L, Mounaix P (2013) Review in terahertz spectral analysis. *Trends Analyt Chem*, Elsevier 44:98–105
19. Herault E, Garet F, Coutaz J-L (2016) On the possibility of identifying substances by remote active THz spectroscopy. *IEEE Trans THz Sci Techn* 6:12–19
20. Killinger D (2006) Detecting chemical, biological, and explosive agents. SPIE Newsroom <https://doi.org/10.1117/2.1200609.0383>
21. De Lucia FC (2010) THz technology and molecular interactions. Report DAAD19-00-1-0109, U.S. Army Research Office
22. Bigourd D et al. (2006) Detection and quantification of multiple molecular species in mainstream cigarette smoke by continuous-wave terahertz spectroscopy. *Opt Lett* 31:2356–2358
23. Deng X-J et al. (2018) Terahertz spectroscopy and vibrational analysis of sulfur mustard by quantum chemical calculations. *Comput Theo Chem* 1142:21–27
24. Tang L et al. (2011) The study on the vibrational spectra of THz/IR absorbance and Raman scattering for phosgene. *Inf Technol* 2:004
25. Clough B, Liu J, Zhang X-C (2011) “All air–plasma” terahertz spectroscopy. *Opt Lett* 36:2399
26. Liu J, Dai J, Chin SL, Zhang XC (2010) Broadband terahertz wave remote sensing using coherent manipulation of fluorescence from asymmetrically ionized gases. *Nat Photonics* 4:627

27. Demers JR, Garet F, Coutaz J-L (2017) Atmospheric water vapor absorption recorded ten meters above the ground with a drone mounted frequency domain THz spectrometer. *IEEE Sensor Lett* 1:3500803
28. Yang Y, Shutler A, Grischkowsky D (2011) Measurement of the transmission of the atmosphere from 0.2 to 2 THz. *Opt Exp* 19:8830
29. Cooper KB et al. (2010) Fast high-resolution terahertz radar imaging at 25 meters. *Proc SPIE* 7671:76710Y
30. Zhao G, Shen Y, Wang J, Yu J (2016) New progress of active and passive terahertz imaging. *Proceedings of SPIE* 10030, Infrared, Millimeter-Wave, and THz Technol. IV, 10030Q
31. Grossman EN et al. (2014) Low-frequency noise and passive imaging with 670 GHz HEMT low-noise amplifiers. *IEEE Trans THz Sci Technol* 4:749–752
32. Liu HB, Chen Y, Bastiaans GJ, Zhang XC (2006) Detection and identification of explosive RDX by THz diffuse reflection spectroscopy. *Opt Express* 14:415
33. Schecklman S, Zurk LM, Henry S, Kniffin GP (2011) Terahertz material detection from diffuse surface scattering. *J Appl Phys* 109:094902
34. Farrah D et al. (2017) Far-infrared instrumentation and technology development for the next decade. Preprint arXiv:1709.02389
35. Rowe S et al. (2016) A general purpose terahertz camera based on kinetic inductance detectors for commercial/industrial applications. 41st International Conference on Infrared, Millimeter, THz Waves (IRMMW-THz), Copenhagen
36. Lynch JJ et al. (2008) Passive millimeter-wave imaging module with preamplified zero-bias detection. *IEEE Trans Microwave Theory Techniques* 56:1592–1600
37. Malz S, Jain R, Pfeiffer U (2016) Towards passive imaging with CMOS THz cameras. 41th International Conference Infrared on Millimeter THz Waves – IRMMW-THz
38. Rowe S et al. (2016) A passive terahertz video camera based on lumped element kinetic inductance detectors. *Rev. Sci. Instrum.* 87:033105
39. Enestam S et al. (2016) Phenomenology of passive multi-band submillimeter-wave imagery. *Proc. SPIE* 9830:98300B
40. Heinz E et al. (2015) Passive 350 GHz video imaging systems for security applications. *J Infrared, Millimeter, THz Waves* 36:879–895
41. Grossman E et al. (2010) Passive terahertz camera for standoff security screening. *Appl Opt* 49:E106
42. Marchese L et al. (2018) Overcoming the challenges of active THz/MM-wave imaging: an optics perspective. *Proc SPIE* 10639:106392B
43. Rahman SM et al. (2014) Design, fabrication and characterization of 585 GHz integrated focal plane arrays based on heterostructure backward diodes. *Proc 39th IRMMW-THz*
44. Han R et al. (2013) Active terahertz imaging using Schottky diodes in CMOS: array and 860-GHz pixel. *IEEE J Solid-State Circuits* 48:2296
45. Fleet EF et al. (2017) Design and performance of a THz block camera with a 130 nm CMOS focal plane array. *Proc SPIE* 10189:101890A

46. Kim DY, Park S, Han R, Kenneth K (2013) 820-GHz imaging array using diode-connected NMOS transistors in 130-nm CMOS. Proc Symposium on VLSI Circuits (VLSIC, Kyoto, Japan):C12–C13
47. Al Hadi R et al. (2012) A 1 k-Pixel video camera for 0.7–1.1 terahertz imaging applications in 65-nm CMOS. IEEE J Solid State Circuits 47:2999–3012
48. Boukhayma A et al. (2016) A low-noise CMOS THz imager based on source modulation and an In-Pixel High-Q passive switched-capacitor N-Path filter. Sensors 16:325
49. <http://www.traycer.com>.
50. Lee AWM, Hu Q (2005) Real-time, continuous-wave terahertz imaging by use of a micro-bolometer focal-plane array. Opt Lett 30:2563
51. Lee AWM, Qin Q, Kumar S, Williams BS, Hu Q (2006) Real-time terahertz imaging over a standoff distance (>25 meters). Appl Phys Lett 89:141125
52. Meilhan J et al. (2011) Active THz imaging and explosive detection with uncooled antenna-coupled microbolometer arrays. Proc SPIE 8023:80230E
53. Sheen DM et al. (2009) Active wideband 350 GHz imaging system for concealed-weapon detection. Proc SPIE 7309:73090I
54. Lissauskas A et al. (2009) Terahertz imaging with Si MOSFET focal-plane arrays. Proc SPIE 7215:72150 J
55. Kawase K, Ogawa Y, Watanabe Y (2003) Non-destructive terahertz imaging of illicit drugs using spectral fingerprints. Opt Exp 11:2549
56. Murate K, Kawase K (2018) Perspective: Terahertz wave parametric generator and its applications. J Appl Phys 124:160901
57. Statnikov K et al. (2015) 160-GHz to 1-THz multi-color active imaging with a lens-coupled SiGe HBT chip-set. IEEE Trans Microwave Theory Techn. 63:520–532
58. Chi T, Huang M-Y, Li S, Wang H (2017) A packaged 90-to-300 GHz transmitter and 115-to-325 GHz Coherent Receiver in CMOS for Full-Band Continuous-Wave mm-Wave Hyper-spectral Imaging. IEEE Intern Solid-State Circuits Conf. paper 17–7
59. Bauer M et al. (2014) Antenna-coupled field-effect transistors for multi-spectral terahertz imaging up to 4.25 THz. Opt Express 22(19252)
60. Zhou Z et al. (2018) Multicolor T-Ray imaging using multispectral metamaterials. Adv Sci 5:1700982
61. Fiorino ST et al. (2012) A technique to measure optical properties of brownout clouds for modeling terahertz propagation. Appl Opt 51:3605
62. Prophète C et al. (2018) Modeling of an active terahertz imaging system in brownout conditions. Appl Opt 57:6017

Multi-Year Project: Technology of High-Selective Imprinted Nanoantenna for Explosives Detection

Sergey Piletsky

University of Leicester, Leicester, UK

e-mail: sp523@leicester.ac.uk

Volodymyr Chegel

V.E. Lashkaryov Institute of Semiconductor Physics, National Academy of Sciences of Ukraine, Kiev, Ukraine

Andrii Lopatynskyi

V.E. Lashkaryov Institute of Semiconductor Physics, National Academy of Sciences of Ukraine, Kiev, Ukraine

Vitalii Lytvyn

V.E. Lashkaryov Institute of Semiconductor Physics, National Academy of Sciences of Ukraine, Kiev, Ukraine

Juan Martinez Pastor (✉)

University of Valencia, Valencia, Spain

e-mail: Juan.Mtnez.Pastor@uv.es

Rafael Abargues

University of Valencia, Valencia, Spain

e-mail: Rafael.Abargues@uv.es

Pedro Rodríguez

Intenomat SL, Valencia, Spain

e-mail: p.rodriguez@intenomat.es

Project Goals

The present project addresses the growing need in development of highly sensitive and robust explosives detectors for counter-terrorist measures based on molecularly imprinted polymers (MIPs) integrated with Localized Surface Plasmon Resonance (LSPR) nanoantennas. The scientific and technological aim of proposed project is to develop long-life MIP with expressed specificity to selected explosives and integrate them with plasmonic (gold or silver) nanoparticle (MIP-PNP). The final aim of the project is to design robust portable device used by police officers capable of detecting and identification a range of explosive materials. This aim will be achieved through the systematic work planned in accordance with two main objectives. The first objective includes design and synthesis of MIP-PNP with specificity to real selected explosives (trinitrotoluene (TNT) and pentaerythritol tetranitrate (PETN))

using their chemical analogues, as a recognition system capable of overcoming poor stability and short shelf life problems inherent to antibody-based detection systems. The second objective of this project includes development of a basic prototype of portable optoelectronic explosives detector based on LSPR optical setup, which allows real-time ultrasensitive detection of small size molecules in liquid or gas phases. During the project, British team produces MIP-PNP for integration with LSPR explosives detector, Spanish team works on integration of MIP-PNP with transducer and testing/validation of developed LSPR explosives detector, Ukrainian team conducts computer modelling of MIP-PNP composite sensitivity and is responsible for the development and testing of portable optoelectronic LSPR explosives detector system.

Current status of the project. LSPR response of the MIP-PNP system upon the detection of TNT molecules was simulated and optimized for different parameters of gold nanoparticle and MIP shell. The design of MIP-PNP nanoparticles should include large gold cores (>100 nm) with at least 50 nm MIP shell. A one-step procedure to synthesize in-situ nanocomposite thin films of Ag nanoparticles embedded in a polyethyleneimine (PEI) polymer with MIP capability was developed. Ag-PEI films synthesized with 3-nitrotoluene as a template exhibit a limit of selective detection around 10 nM in gas phase. Two-channel explosives detector was designed for quantitative determination of interaction of the analyte molecules with the MIP-PNP nanochip by registering the variation of light extinction in the 400–750 nm wavelength range. A differential measurement scheme is proposed, in which the intensity of the radiation fluxes of the light passing through the measuring and reference channels is considered.

Deliverables

- Elaboration of optimized parameters for MIP-PNP composite obtained according to computer models that yield target molecules detection sensitivity in the picomolar concentration range: model for core-PNP/shell-MIP structure, model for LSPR nanoantenna, sensitivity modelling.
- Synthesis of optimised MIP-PNP composite using an immobilised template for MIP formation, able to confer specificity to target molecules in LSPR experiments. The polymerisation conditions including choice of monomers, optimum polymerisation time, temperature as well as size and concentration of noble metal nanoparticles will be optimized according to characterization results and sensitivity testing of LSPR signal.
- Development of sensor chip with target molecules detection sensitivity in the picomolar concentration range and compatible with mass-manufacturing of sensor devices: development of sensor chip based on MIP-PNP composite and its experimental evaluation, sensitivity testing and feedback for MIP-PNP optimization.

- Development of explosives detector prototype with target molecules detection sensitivity in the picomolar concentration range for TNT and PETN and their chemical analogues: design, prototyping, testing and optimization of the detector.
- Development of commercial portable explosives detector with target molecules detection sensitivity in the picomolar concentration range for TNT and PETN and their chemical analogues: design, fabrication and testing of portable detector (at small scale production).

Security Relevance

Globally, there is a problem concerning growing terrorism activity and lack of suitable tools for sensitive and selective detection of explosives by police force. Additionally, a fast, portable and inexpensive detector for explosives is needed for various disciplines including humanitarian demining, remediation of explosives waste sites, homeland security, and forensic applications. A number of attempts were made to address this problem using various recognition elements and sensor principles. Each of such methods has advantages, but overall they suffer from the fact that it is extremely difficult to combine sensor robustness, required for police operation, with high sensitivity necessary for detecting trace quantities of explosive material. Obviously, it is not a simple task to satisfy these requirements, especially in the case of a detection technique that should also be inexpensive. The last requirement becomes very important when recognition elements are sensitive to exploitation and storage conditions. The present proposal addresses these issues by integrating LSPR nanoantennas with MIP nanoparticles into a MIP-PNP composite in order to develop novel sensitive elements for use in portable and inexpensive explosives detectors capable of sensing trace amounts of explosive substances.

Science Relevance.

The main scientific and technological impact from the implementation of the proposed project will come from the development of a new technology for the picomolar detection of selected explosives (TNT and PETN) and their chemical analogues exploiting MIPs and plasmonic gold nanoparticles nanoantenna. A portable optoelectronic sensor for the detection of chosen explosives will be designed that needs minimal sample volumes and which can potentially operate continuously in the public hazard areas.

Partnership Relevance

Implementation of the proposed project will enhance the connections between scientific centers of NATO countries and consolidate their efforts concerning urgent

security challenges. Experience exchange with Ukrainian scientists and their training in leading laboratories specializing in nanoscience will extend and strengthen the partnership between NATO and Ukraine.

End Users

MIP Diagnostics (UK) will be a provider of MIP nanoparticles and InteNanoMat S.L. (Spain) will be responsible for commercialisation of the explosive detector prototype.

Technical Summary

The research developed around the first milestone of the project is centered on:

1. Computer models have been developed and applied for the simulation of spectral response of the “spherical gold core-MIP shell” system during the TNT detection.
2. LSPR sensor chip fabrication protocol based on a nanocomposite containing Ag-nanoparticles in a MIP matrix: tests upon sensor chip exposure to vapor of explosive analogues, resulting in a selective sensing of 3-nitrotoluene with a limit of detection in the range 10–100 nM.
3. Design of explosives detector prototype, including specification, tentative list of electronic components&modules and assembly drawing. Noise analysis of photometric converter for the explosive detector prototype was performed.

Simulation of Spectral Response of the “Spherical Gold Core-MIP Shell”

An analytically solvable computer model for the simulation of light extinction properties of the “spherical gold core-MIP shell” (GNP-MIP) system was developed based on the Mie scattering theory and the Bruggeman effective medium theory in order to estimate the spectral response of this system during the analyte detection. Specifically, Mie theory was used to calculate the light extinction cross-section spectrum of the single spherical nanoparticle with a homogeneous shell, and Bruggeman effective medium theory was applied to consider the MIP shell on the nanoparticle surface as a heterosystem consisting of polymer, ambient medium (e.g. water), imprinted sites and analyte molecules in different ratios in order to estimate the effective refractive index of the MIP shell. The model is also considering the possible swelling of the MIP shell due to the interaction with analyte molecules, which leads to an increase of its thickness and an additional contribution of the ambient medium to the effective refractive index.

The developed model is highly customizable and can be used to predict the spectral response of “spherical gold core-MIP shell” system during the detection of analyte molecules with a large number of input parameters of the gold nanoparticle (diameter), ambient medium (refractive index), polymer shell (thickness, refractive index, imprinted sites volume fraction, imprinted sites occupation degree with analyte molecules, swelling ratio), analyte (refractive index). The model is characterized by a moderate computer time requirement, which is of importance for conducting the trend analysis for multiple input parameters in a reasonable time and optimization of the “spherical gold core-MIP shell” system parameters for achieving the maximum analyte detection sensitivity. This model is consistent with more sophisticated, but more computer time consuming, numerical modelling, as the case of finite element method (FEM). This method enables calculations of light extinction spectra and electric field intensity distributions in the vicinity of the metal nanostructure at different wavelength of incident light. The comparison of simulated light extinction spectra for a single MIP-GNP nanoparticle upon its interaction with TNT molecules obtained with the analytical (Mie theory described above) and the numerical (FEM) models for the same geometrical and optical configuration shows that while they are close to each other (see Fig. 1a), further FEM model refinement is needed to achieve better coincidence of simulated spectra.

The use of Mie theory in our model allows the estimation of the shift in the maximum of the light extinction spectrum (i.e., the LSPR shift) of the “spherical gold core-MIP shell” system upon the detection of TNT molecules for different gold nanoparticle size and MIP shell thickness. The simulations were extended for different fractions of imprinted sites occupied with TNT molecules, for different porosity values of the imprinted polymer (MIP shell imprinted sites volume fraction) in the range 5–30%. A MIP shell swelling (by volume) fraction of 10% was assumed after interaction with TNT molecules. The most favorable GNP-MIP shell structure

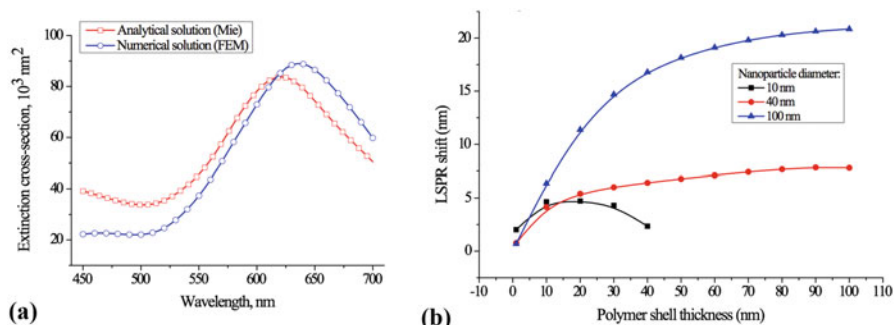


Fig. 1 (a) Simulated light extinction spectra of the “spherical gold core-MIP shell” system obtained using analytical Mie and numerical FEM methods. (b) Simulated shift of LSPR of the “spherical gold core-MIP shell” system upon the detection of TNT molecules for different gold nanoparticle size as a function of the MIP shell thickness. The fraction of imprinted sites occupied with TNT molecules after detection was equal to 100%, the MIP shell imprinted sites volume fraction (porosity) and its swelling percentage (by volume) were fixed to 30% and 10%, respectively

will consist of large Au nanoparticles (100 nm) and MIP shell thicker than 50 nm, as shown in Fig. 1b. In order to enhance the positive LSPR shift, the MIP shell porosity and imprinted sites availability for analyte molecules should be as large as possible (30% was considered in calculated values shown in Fig. 1b).

LSPR Sensor Chip Fabrication and Characterization Based on Ag(Nanoparticles)-MIP

Nanocomposites materials based on polymer matrices represent an adequate solution to many present and future technological demands, because they combine the novel properties of metallic or semiconductor nanoparticles (i.e., tunable LSPR or photoluminescence) with the properties of polymers. Polymers exist both natural and synthetic, with different backbone composition made up of carbon-carbon bonds such as polythene, polystyrene and poly acrylates, and carbon-hetero elements (e.g. oxygen, sulfur, nitrogen) bonds such as polyamides, polyesters, polyurethanes, polysulfides and polycarbonates. Moreover, polymers can also have different pendant groups like, thiols, amines, carboxylic acid, phenols etc., which confer to them a broad range of physico-chemical properties.

Two different strategies are mainly used to obtain metal–polymer nanocomposite films: ex-situ and in-situ methods. In the ex-situ method, plasmonic metal nanoparticles (PNPs) are synthesized by wet chemistry as a colloidal solution for spin coating deposition to form thin films over a given substrate [1]. However, this approach lacks from producing homogeneous films since NPs easily agglomerate, especially when high NP concentrations are required. In the in-situ approach (Fig. 2a), PNPs, particularly silver ones, can be generated inside the polymer matrix during the bake step, due to a solid-state chemical reduction in the thin film of the metallic precursor present in the initial polymer solution [2–5]. The in-situ approach is a very fast and one-step procedure for the production of PNP-MIP chips using a similar approach (see Fig. 2b) with a good control of the PNPs size, other than their concentration inside the polymer matrix.

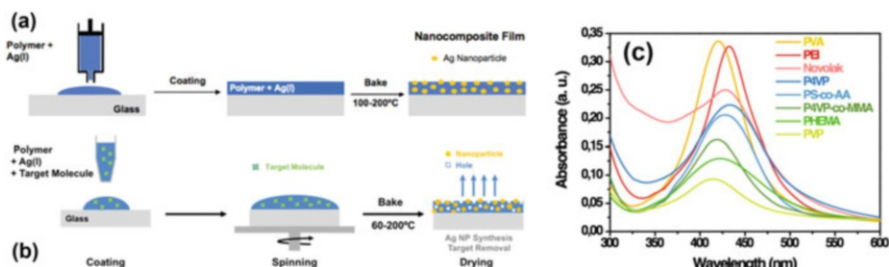


Fig. 2 (a) In-situ approach to fabrication of Ag–polymer nanocomposite films by spincoating and baking. (b) Idem as (a) including the molecular imprinting of the nanocomposite. (c) UV-Vis Localized Surface Plasmon Resonance (LSPR) spectra of different Ag–polymer nanocomposite thin films.

Several polymers such as poly(vinylalcohol) (PVA), poly(ethyleneimine) (PEI), poly(4-vinylphenol) (P4 VP), Poly(4-vinylphenol-co-methyl methacrylate) (P4 VP-co-MMA), Poly(2-hydroxyethyl methacrylate) (PHEMA), poly(styrene-co-allylalcohol) (PS-co-AA), poly(vinylpyrrolidone) (PVP) and Novolak are considered excellent candidates as host matrices for the *in-situ* synthesis of Ag and Au PNP s during the thermal annealing of the thin films. Apart from excellent solubility in water and many organic solvents, other than excellent film forming properties, these polymers contain functional groups able to reduce Ag(I) to Ag(0) that will form the PNPs. Ag PNPs are *in situ* synthesized inside the host polymers by a one-step procedure.

In a first step, a solution containing the target polymer and the Ag(I) precursor (AgNO_3 or AgClO_4) is deposited by spin coating and baked (Fig. 2a). As a result, Ag (I) is reduced to Ag(0) by means of the polymer and Ag-PNPs are generated inside the host polymeric matrix, after a thermal baking of 100–200 °C for 10 min. The thickness of the nanocomposite films is around 130 nm. The presence of Ag-PNPs in the different polymer matrices is confirmed by UV-Vis spectroscopy because of the observation of the characteristic LSPR peak of the Ag-PNPs in the range 400–440 nm, as shown in Fig. 2c. Particularly interesting are Ag-PVA and Ag-PEI nanocomposites, because they exhibit the highest LSPR intensity.

In some previous works we had demonstrated that Ag-PVA nanocomposite is a good optical sensor based on the LSPR signal, especially for the chemosensing of thiol- and amino-based analytes [3–5]. However, efforts for sensing nitro-containing analytes (nitro-groups are contained in organic compounds with explosive properties) with Ag-PVA were unfruitful. Most probably, diffusion of nitro-containing compounds is somehow hindered in PVA matrix due to unfavorable molecular interaction between NO_2 groups and OH groups of PVA. As an alternative, we have proposed within this project to use Ag-PEI as the basis for the plasmonic sensor of explosive analogues in vapor phase. The LSPR intensity decreases by 20% and slightly shift to the red ($\Delta\lambda_{\text{LSPR}} = 2 \text{ nm}$) after the exposure of this nanocomposite to 3-Nitrotoluene (3-NT) analyte in vapor phase for 10 h, as shown in Fig. 3a. The sensor sensitivity and selectivity to nitro-containing analytes can be improved by the

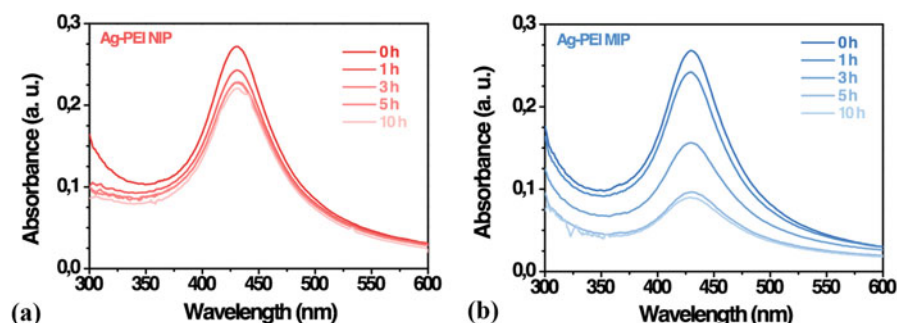


Fig. 3 Response of Ag-PEI films fabricated without (a) and with MIP treatment using 3-NT vapor upon exposure to 3-NT vapor

Molecularly Imprinted Polymer (MIP) approach, as proposed in our project. The fabrication process consists of the in-situ synthesis of Ag NPs inside PEI in the presence of template molecules (e.g., 3-NT), which are removed during the baking process (needed to form the Ag-PEI nanocomposite) leaving behind complementary cavities, as it was illustrated in Fig. 2b. The new MIP-based nanocomposite containing the Ag PNPs have a noticeable LSPR response upon exposure to 3-NT in vapor phase: the LSPR intensity decreases in a 70% after 10 h exposure, as shown in Fig. 3b.

The transduction mechanism of the sensor is based on the interaction of 3-NT molecules in specific MIP sites with Ag PNPs via covalent bonds that fix free electron gas inside them, which is the reason to the reduction of the LSPR intensity upon adsorption of molecules at the surface of Ag PNPs. The LSPR intensity (i.e., the sensor response) with the concentration of 3-NT analyte for a constant exposure time of 3 h is sensitive above the limit of detection (LOD) of the sensor, which is in the range 10–100 nM, as shown in Fig. 4a. Furthermore, Ag-PEI sensors molecularly imprinted with 3-NT, DMDNB, 4NP and PA were fabricated and subject to 3-NT vapor exposures. As observed in Fig. 4b, only the Ag-PEI nanocomposite molecularly imprinted with 3-NT shows an important response, which confirms the sensor selectivity to this analyte.

In summary, we have demonstrated that molecularly imprinted Ag-PEI films can be used for selective sensing of nitro-containing molecules in gas phase with a LOD in the range 10–100 nM, which is not bad, but it will be necessary to improve it. Furthermore, the response time is too much slow and it should be reduced drastically. Therefore, it will be necessary to optimize the MIP processing of the polymer and/or using other kind of nanoparticles (quantum dots, for example).

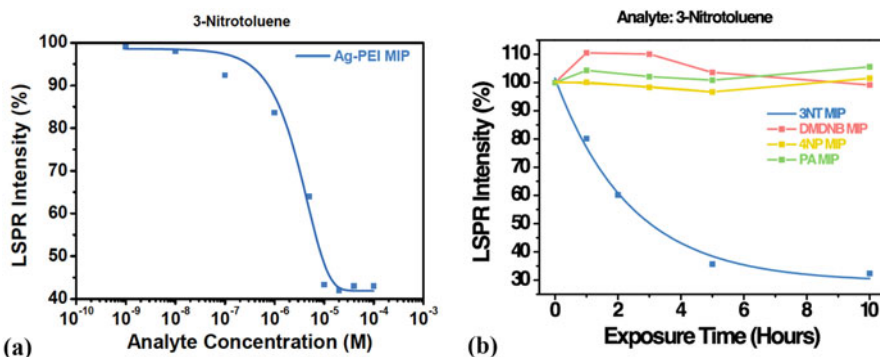


Fig. 4 (a) Absorption decay response of Ag-PEI sensor molecularly imprinted with 3-NT as a function of the 3-NT concentration for an exposure time of 3 h. Blue continuous curve is the best fitting to the 4PL function [5]. (b) Selectivity of Ag-PEI sensor molecularly imprinted with 3-NT, DMDNB, 4NP and PA. Blue continuous curve is the best fitting to the kinetic saturating function $A_t = A_\infty + B e^{-kt}$

Design of Explosives Detector Prototype

The explosives detector is designed for quantitative determination of adsorption of the analyte molecules on the surface of the nanochip (array of nanoparticles created over a transparent substrate) in flow mode. The adsorption value is determined by the level of absorption (extinction) of light in the 400–750 nm wavelength range. This process is achieved using selective light sources and photodetectors. A differential measurement scheme is used, in which the intensity of the radiation flux of the light passing through the measuring channel and through the reference channel is measured. Changes in the optical density are defined as the difference in the two measured channels:

$$\Delta OD = \lg\left(\frac{I_0}{I_m}\right) - \lg\left(\frac{I_0}{I_{ref}}\right).$$

I_0 – the radiation flux of the incident light, I_{ref} – light transmitted through the reference channel, I_m – light transmitted through the measuring channel, respectively.

Signals from photodetectors (in the form of a photocurrent) are converted by photo-amplifiers into a voltage and then by an analog-to-digital converter (ADC) into digital form, and then processed by an appropriate microprocessor (MP), from which measurement data are transferred to the personal computer (via serial interface) or to smartphone via bluetooth. Controlling the operating modes of the detector is carried out by means of mechanical switches connected to the digital inputs of the MP.

The first part of the work will consist in the definition of requirements for the photometric converter path, intended to determine changes in optical density of the analyzed sample (i.e. changes in the extinction coefficient in the visible spectral region). The photometric converter performs registration and algorithmic processing of the output signals (filtration and transformation of numerical values of voltages into numerical values of the optical density) referred above and main quality criteria for its development are modularity, simplicity of connections and replacement of individual units. The functional diagram of the converter is shown on Fig. 5 that contains several blocks/components: the optical system, mechanical system for probe delivery, sample-chip holder, two-channel flow cuvettes, two-channel photodetectors (photodiodes or spectrometer) and photo-amplifiers, the ADC, the electronic control system (Microprocessor – MP) and the Power Supply Unit (PSU). The optical system includes a light source with continuous spectrum for excitation of localized surface plasmon resonance (LSPR) in nanostructures, beam focusing system and optical fiber. The use of a white LED as the light source opens up the possibility for a significant reduction in energy consumption compared to the sensors using halogen light bulbs.

The changes in the extinction spectra can be detected by two methods. The first one is the measurement of the LSPR response of the sensor chip by detecting the

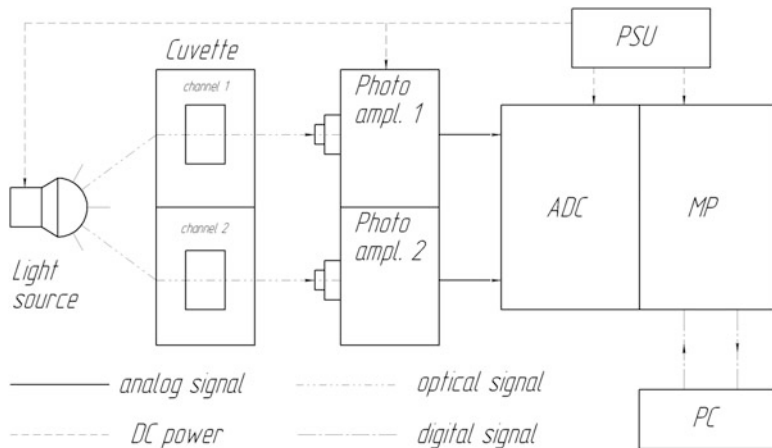


Fig. 5 Simplified functional diagram of the detector of explosive vapors

wavelength shift in the extinction spectra using a compact external spectrometer. The second one will consist in monitoring the changes in the extinction intensity of the sensor chip at a fixed wavelength using photodiodes conveniently amplified.

In the absence of analyte in the cuvette, the photo-amplifier should provide the output signal level, possibly covering as much as possible the input dynamic range of the ADC. The measurement path, in total, should provide resolution of the conversion not worse than 10^{-4} (-80 dB) relative to the maximum signal level.

The basic approach in noise error calculations is to identify the noise sources, segment them into conveniently handled groups (in terms of the shape of their noise spectral densities), compute the rms value of each group, and then combine them by root-sum-squares to get the total noise. Major noise sources in our prototype would be:

- radiation source noise;
- concentration fluctuations of analyte in cuvette;
- photodetector noise;
- OA noise;
- ADC noise.

Noise from the radiation source, the photo-amplifier and the ADC are caused by the intrinsic noise of these elements, the noise of the power supply and the noise of the passive components of the circuit. The ADC noise is also caused by the reference voltage noise. The actual noise level is also determined by its spectral composition and frequency characteristic of the measuring path. Noise of some components can be estimated from their datasheets, others can only be estimated experimentally or indirectly. Noise calculations of the photo-amplifier will be made following the recommendations in Ref. 6. Concentration fluctuations of analyte in the cuvette will be considered to be lower than the required resolution of the analysis; the radiation

source noise is compensated by a two-channel measuring scheme. In fact, an evaluation of the impact of these discarded factors may require additional research.

Broader Impacts

From the practical point of view, the proposed project addresses 30 most important capabilities requirements underlined by ESRAB falling into the Function “Detection, identification and authentication” with the capability to detect and identify specific dangerous goods as drugs and explosives. The basic concepts and knowledge to be developed have widespread applicability also in fields outside of explosives detection, such as monitoring of drugs or environmental pollutants. Technologies delivered through the project can be applied in other security, civilian or military fields, with a spill-over effect boosting the technological and industrial base of NATO and Partner countries.

Young Researcher Participation

Eduardo Aznar Gadea was participating in the present project between June and end of December 2018, preparing and testing sensor chips based on Ag nanoparticles and semiconductor quantum dots (more recently) into molecularly imprinted polymer matrices. Now he is beginning a joint financed industrial PhD between our group and our spin-off company Intenanomat SL. He will continue to collaborate partially in the project until recruiting a new graduated student.

Petro Demydov is participating in the present project as a PhD student of the Ukrainian team. He is working on modelling the sensitivity of MIP-GNP nanoparticles and designing the explosives detector prototype.

Contributions

No contributions until now.

References

1. Khanna v, Singh N, Charan S, Subbarao VVVS, Gokhale R, Mulik UP (2005) Synthesis and characterization of Ag/PVA nanocomposite by chemical reduction method. Mater Chem Phys 93: 117
2. Abargues R, Abderrafi K, Pedrueza E, Gradiess R, Marqués-Hueso J, Jimenez E, Valdés JL, Martinez-Pastor JP (2009) Optical properties of different polymer thin films containing *in situ* synthesized Ag and Au nanoparticles. New J Chem 33: 1720–1725

3. Gradišek R, Abargues R, Habbou A, Canet-Ferrer J, Pedrueza E, Russel A, Valdés JL, Martínez-Pastor J (2009) Localized surface plasmon resonance sensor based on Ag-PVA nanocomposite thin films. *J Mater Chem* 19: 9233–9240
4. Marqués-Hueso J, Abargues R, Valdés JL, Martínez-Pastor J (2010) Ag and Au/DNG-novolac nanocomposites patternable by ultraviolet lithography: a fast route to plasmonic sensor microfabrication. *J Mater Chem* 20: 7436–7443
5. Abargues R, Rodríguez-Canto PJ, Albert S, Suárez I, Martínez-Pastor JP (2014) Plasmonic optical sensors printed from Ag-PVA nanoinks. *J Mater Chem C (Materials for optical and electronic devices)* 2: 908–915
6. Yang Zhen (2013) Using MCP6491 Op Amps for Photodetection Applications // AN1494 (DS01494A), Microchip Technology Inc. See <https://www.microchip.com/wwwAppNotes/AppNotes.aspx?appnote=en560825>

Stepped-Frequency Noise Radar for High Resolution 2D and 3D SAR Imaging

K. Lukin (✉)

LNDES, O.Ya. Usikov Institute for Radiophysics and Electronics, Kharkov, Ukraine

D. Tatyanko

LNDES, O.Ya. Usikov Institute for Radiophysics and Electronics, Kharkov, Ukraine

V. Palamarchuk

LNDES, O.Ya. Usikov Institute for Radiophysics and Electronics, Kharkov, Ukraine

P. Vyplavkin

LNDES, O.Ya. Usikov Institute for Radiophysics and Electronics, Kharkov, Ukraine

S. Lukin

LNDES, O.Ya. Usikov Institute for Radiophysics and Electronics, Kharkov, Ukraine

O. Zemlyaniy

LNDES, O.Ya. Usikov Institute for Radiophysics and Electronics, Kharkov, Ukraine

Yu. Shiyan

LNDES, O.Ya. Usikov Institute for Radiophysics and Electronics, Kharkov, Ukraine

O. Mishchenko

LNDES, O.Ya. Usikov Institute for Radiophysics and Electronics, Kharkov,
Ukraine

L. Yurchenko

LNDES, O.Ya. Usikov Institute for Radiophysics and Electronics, Kharkov,
Ukraine

P. Sushchenko

LNDES, O.Ya. Usikov Institute for Radiophysics and Electronics, Kharkov,
Ukraine

Introduction

Ground Based Synthetic Aperture Radar (SAR) are used for microwave coherent imaging of an area of interest and may be used in many applications, such as: detection of small objects Ground Penetrating Radar; Through-the-Wall radar; and for generation of real time microwave “video”, and many others. Stepped frequency (SF) technique is common technique for SAR design [1]. A narrow frequency bandwidth of the transmitted signals enables application of ADC with slow sampling rate, which may provide rather high dynamic range since they have up to 32–48 bits of amplitude resolution. However, this technique also has some drawbacks, such as: ambiguity in range measurements; high level of range side lobes and low resistance against narrowband coherent interferences.

We have proposed application of random waveforms [2–5] for SAR imaging. Later on we have suggested application of random waveforms with synthesized Power Spectral Density (PSD) for application in ground penetrating radar and Software Ground SAR to go around the drawbacks typical for SF radar with a regular steps of regular waveform. The required for the implementing of the approach suggested, an ensemble of random realizations of random probing signals may be generated as follows: (1) Step-like random jumps of Tx single frequency signal over a defined frequency mesh according to a random law, i.e. *frequency hopping* with random hops; (2) Step-like increase of the PSD central frequency of Tx narrow band random signal, i.e. *stepped frequency noise radar* (SF NR); (3) Step-like random jumps of the PSD central frequency of Tx narrow band random signal according to a random law, i.e. *random frequency hopping of random signals* [6, 7].

When using the first method the frequency of Tx single-frequency signals is discrete random quantity with given probability distribution. It has a finite number of values on a given regular frequency mesh. For instance, frequency can be random quantity with normal probability distribution and given expectation and variance. In this case, we obtain the resulting signal with Gaussian-shaped spectrum. Correlation function of such a signal is also Gaussian-shaped without any side lobes in range

profile [2]. In the case of uniform distribution of the frequency of Tx signal the synthesized signal PSD will have a rectangular shape. Correlation function in this case has sinc-function shape, and additional weighting procedure is required for minimizing the range side lobes. Random variation of frequency steps (hops in this case) allows eliminating ambiguity in the velocity measurements. At a single point of the frequency mesh the maximal range is defined by signal duration provided sufficient level of the transmitted power.

The second method uses a narrow-band noise signal which has its PSD central frequency being increased discretely according to a linear law. Resulting signal which is formed in this way has its PSD of almost rectangular shape. Because of continuity of probing signal PSD, the use of the second approach also allows eliminating ambiguity of range measurements, which is inherent drawback of conventional SF radar.

The third method is a combination of the first and the second ones. Narrowband noise signal is transmitted with random hopping of its PSD central frequency over a finite mesh of the fixed equidistant frequencies. Application of this approach allows performing of unambiguous range measurements. If the central frequency of the transmitted narrow-band noise signals is a random quantity with normal distribution and given expectation and variance, it allows avoiding range side lobes.

In the Chapter, we present our theoretical consideration of SF Noise Radar concept, design of hardware and software SF NR and some experimental results obtained with the help of hardware and software implementation of SF Noise Radar based on the second approach from the above ones. Section “Probing signals for stepped frequency noise radar and signal processing” is devoted to the brief description of the theory of SF random signal generation and processing of radar returns in SF Noise Radar. In the following sections, we describe design and main performance of the developed hardware and software SF Noise Radars. Software Noise Radar was designed on the basis of AWG and combines SF theory and analog reception of radar returns with the help of I/Q phase detector. The next section is devoted to developing algorithm for 3D tomographic SAR imaging using MIMO SF Noise Radar. In the last section some results of 2D SAR imaging of indoor scene are presented and discussed. In Conclusion we briefly describe prospective of many applications of the suggested approach.

Probing Signals for Stepped Frequency Noise Radar and Signal Processing

The probing signal for SF noise radar is compound of N noise pulses (steps) with close central frequencies at the adjacent time intervals. From step to step the carrier frequency is stepwise changed according to the chosen way. Herein after we consider linearly growing stepwise frequency growing. Duration of each step is equal to T so the duration of the transmitted signal is $T_N = NT$. We designate as $x_n(t)$

the signal transmitted within one step. Then for the n -th step at the time interval of $nT \leq t \leq (n + 1)T$ the sounding signal $x_n(t)$ could be written as follows

$$x_n(t) = \Pi_T(t - nT) A_0 \cos [\omega_n t + \phi(t)], \quad (1)$$

where t is current time; $\omega_n = 2\pi f_n$; $f_n = f_0 + n \Delta f f_0$ and Δf is central frequency and frequency step, respectively, which may be generated in either hardware or in software signal generators;

$$\Pi_T(t) = \begin{cases} 1 & \text{if } |t - nT| \leq T/2 \\ 0 & \text{if } |t - nT| > T/2 \end{cases}$$

$\phi(t) = \int_0^t \delta f(t') dt'$ is random phase due to random modulation of the signal frequency $\delta f(t)$ around its central value f_n of the n -th step.

Figure 1 shows time realization, Fig. 1a, and power spectral density (PSD), Fig. 1b, of a narrowband noise waveform with stepped increasing of its central frequency generated in Matlab environment.

In SF radar, a stepped frequency probing signal is transmitted towards a target with the help of Tx antenna; part of the Tx signal is coupled out to be used as a reference in I/Q phase detector; the reflected signal (radar returns) is received with the Rx antenna and is fed into the I/Q phase detector for estimation of both amplitude and phase of the received signals. In case of SF Noise Radar, the order of the frequency manipulation is the same, but as a probing signal the random signal (1) is used.

The Matlab algorithm for generation of the signal (1) was elaborated which allowed also varying the duration of the signal segments related to every central

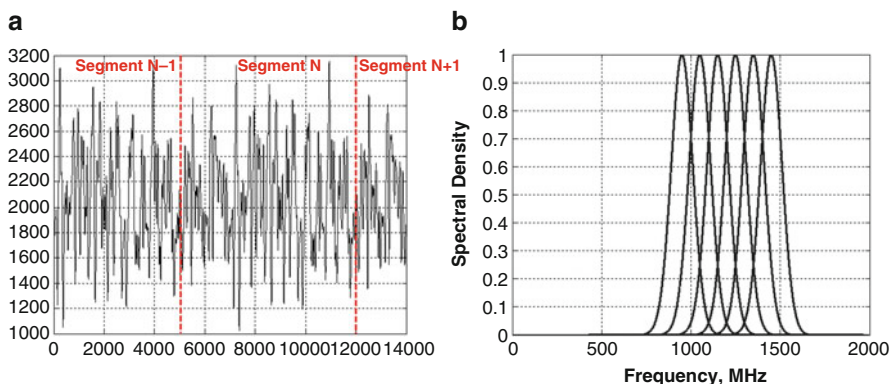


Fig. 1 Time realization, (a) and power spectral density (PSD), (b), of a narrowband noise waveform with stepped increasing of its central frequency

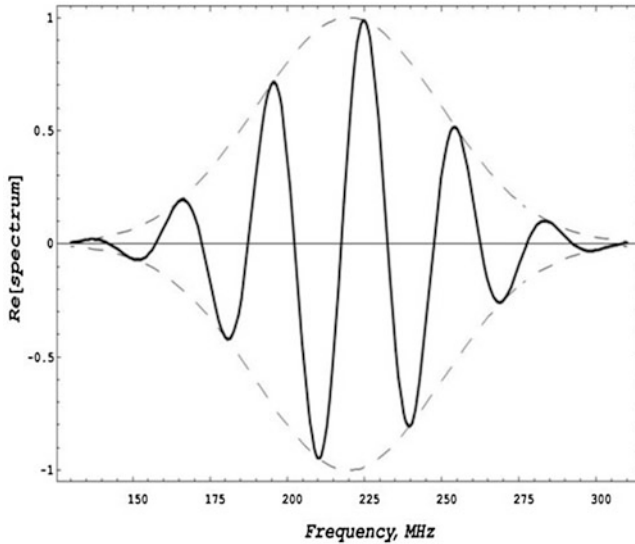


Fig. 2 Frequency dependence of the inphase output of the phase detector/correlator of Stepped Frequency Noise Radar

frequency of the narrowband noise signal with Gaussian PSD. Frequency step Δf and PSD bandwidth of the narrowband noise signal might be chosen in the proper way providing -3 dB overlay of the PSDs of successive steps, as it is shown in Figs. 1b. This allows setting the time of single frequency radiation and, hence, integration time in the receiver. In addition, the algorithm enables also application of frequency windowing for synthesized PSD aiming elimination of range sidelobes (Figs. 2 and 3).

During experiments the digitally generated waveform is to be uploaded to AWG memory, read out, converted to the analog form and transmitted towards a target.

In case of SF noise Radar, the order of the operations is the same, but random signal (1) is used as a probing signal and I/Q phase detector now is treated as a correlator to estimate cross-correlation between the reference x_{ref} and radar return x_{rr} signals

$$D_n(\tau_0, f_n, T) = \frac{2}{T} \int_0^{T/2} x_{ref}(t; f_n) x_{rr}(t; f_n; \tau_0) dt \quad (2)$$

When the estimation of cross-correlations is done for the scene at all N frequency steps we may restore the scene range profile applying inverse Fourier transform to Eq. (2):

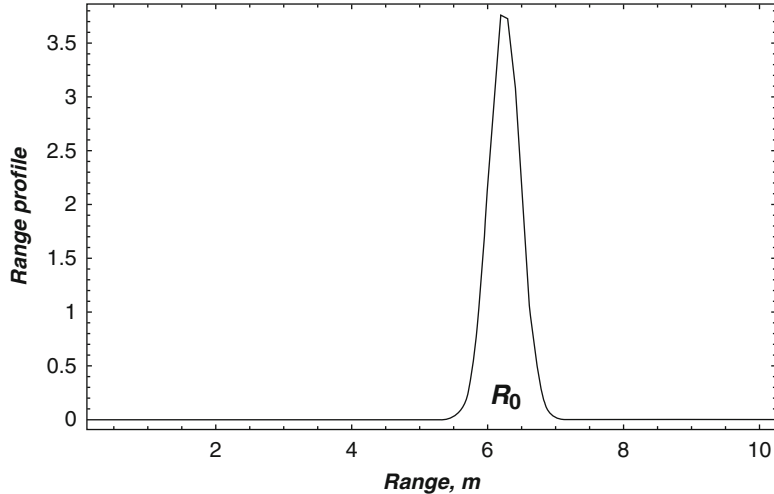


Fig. 3 Range profile for a single target scene obtained with the help of SF Noise Radar

$$R(\tau_0, NT) = \frac{1}{2\pi} \sum_{n=1}^N D_n(\tau_0, f_n, T) e^{-i2\pi f_n \tau_0} \quad (3)$$

For example, if for a scene with a single point-like target one obtains frequency responses with real parts shown in Fig. 2 then application of inverse Fourier transform (3) results in the range profile shown in Fig. 3, where $R_0 = 2\tau_0/c$ is the distance to the target. Note that in our case, a Gaussian windowing was applied in frequency domain which is shown with dashed curves in Fig. 2. This gave no sidelobes in range profile in Fig. 3.

In the following sections, we describe design and main performance of the developed hardware and software SF Noise Radars.

Hardware Stepped-Frequency Noise SAR

We have designed a SF Noise Radar with hardware generation of probing signals, which is compound of transmit and receive antennas, transmitter, receiver, control unit and processing unit. Noise signal is generated by the synthesizer, amplified by power amplifier and radiated by the transmit antenna. Transmitted signal of SF Noise Radar is a sequence of narrowband noise signals with PSD central frequency randomly hopping over a discrete frequency mesh. The PSD width of noise signal is chosen to be coherent to the radar returns within the Noise Radar working range. Part of the probing signal is coupled out and fed into the reference channel of the receiver. Radar returns are fed into the second channel of the receiver. Additive

mixture of signal from targets, passive interference and receiver noise comes out of the second receiver channel. In-phase and quadrature components of the received signals are extracted from the receiver quadrature detector. These signals are proportional to the phase difference between the reference and reflected signals. They are amplified filtered and fed into the dual-channel ADC. Sampled signal is stored in a memory device, processed using signal processor and displayed. Detection of the reflected signal on the background of the additive noise is done by estimation the likelihood ratio and comparison with corresponding thresholds. Control unit with a programmable synchronizer generates control signals for the probing noise signal synthesizer, ADC, storage device and signal processor that allows to coordinate the interaction of all radar subsystems.

Structurally, the SF Noise radar is designed as a set of separate modules, which include an antenna system, transmitter, receiver, processing unit and power supply unit. The control unit is a separate board and included in the transmitter unit. Maximum power probing signal reaches 600 mW and can be regulated by an attenuator. Reference signal power is 28 mW. Range resolution in free space is about 0.31 m.

In the transmitter, probing noise signals with specified statistical characteristics are synthesized. The noise signal synthesis is done with the help of voltage-controlled oscillator (VCO) oscillations, the oscillations of the frequency synthesizer and a mixture of these oscillations, which is formed by frequency converters. Frequency mesh is formed using a synthesizer with the reference frequency of 999.5 MHz. For this purpose, the method of direct digital synthesis (DDS) is used. The output signal of the frequency synthesizer can be tuned within the frequency range 130 ... 380 MHz. The minimal time step is 1 μ s, while the maximal time step may be as long as 8000 μ s. The minimal frequency step is 1 MHz. The frequency switching is determined by the control digital code combinations, which are prepared in advance and stored in the memory of the control unit. In order to obtain random signals, the VCO is frequency modulated by the analog signal of the noise source. Analog noise signal of p-n junction of a transistor is used for formation of modulating noise signal with normal distribution of amplitudes and “rectangular” PSD shape within the frequency range 0.1 ... 14 MHz at -3 dB level. To ensure the high stability of the spectral characteristics of the probing signal, the VCO noise generator has a threshold automatic gain control (AGC) system and VCO is covered by a PLL with a time constant of 5 μ s. The PSD bandwidth of VCO random signal can be smoothly varied from 1.8 to 100 MHz via adjusting the threshold of AGC system. Carrier frequency of the probe signal can be switched step-by-step within the range 950 ... 1430 MHz with a minimal frequency step of 1 MHz. The duration of the transients in a discrete switching of the central frequency does not exceed 0.1 μ s.

Dynamic range of the analog wideband UHF receiver is higher than 110 dB. Receiver noise figure is 4.5 dB; the flatness of amplitude-frequency response is less than 1 dB; bandwidth of the quadrature low pass filter is 5 MHz. In-phase and quadrature signals are sampled with the help of slow ADC with sampling rate of (0.044 ... 10) MHz and high dynamic range (>100 dB). Digitizing of the received signals was done using GageScope 82 ADC.

The laboratory tests carried out with the aim of evaluating the SF Noise radar performance. We investigated behavior of the phase of the synthesized noise signal during switching of PSD central frequency, switching speed, spectral characteristics of the sounding signal, output signals of the quadrature detector. In addition, we have estimated range profile and Doppler signal registration.

In order to estimate performance and transients in the transceiver during switching of the PSD central frequency the reference signal was fed into converter, while a highly stable signal from a standard signals generator was fed into the receiver input. Frequency of the generator was adjusted manually. It was set to about 950 MHz. Output of the transmitter was varied with period 1 μ s taking two values 950 and 1200 MHz. Transients in the transceiver are determined by the duration of the receiver signal front-edge. It depends on the switching time, on the both IF filter and quadrature low-pass filter bandwidths. It has been shown the following: the output signal front-edge duration in the transmitted signal does not exceed 100 ns; maximal spike amplitude is 10% of the nominal value; duration of the signal at half level reaches 900 ns for 1 μ s step duration. The transient's duration at the receiver output may be done shorter of 10 ns and the minimum duration of the step may be as short as 100 ns if to make switching time shorter of 10 ns, provided IF band-pass filter and quadrature low-pass filter having bandwidths of 100 MHz and 50 MHz, respectively. As an example, the random signals in the inphase and quadrature channels of the SF Noise Radar are shown in Fig. 4.

The probing noise signal PSD was investigated for the step of 1 μ s duration. The bandwidth may be switched within the range (1.8...100) MHz. As an example, five noise signals PSD, with the same central frequency of 950 MHz, but different PSD bandwidth are shown in Fig. 5. Each power spectrum was averaged over 100 realizations and normalized to their maximum values. Curve 1 represents PSD of single frequency pulse of 1 μ s duration. It's – 3 dB width equals to 1 MHz, and the shape can be described approximately by $\sin x/x$ function. The curves 2, 3, 4, and

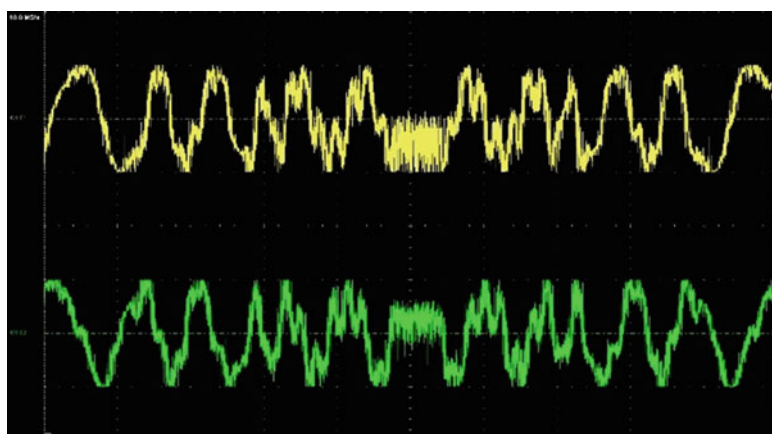


Fig. 4 Output signal of inphase (upper) and quadrature (lower) channels of SF Noise Radar

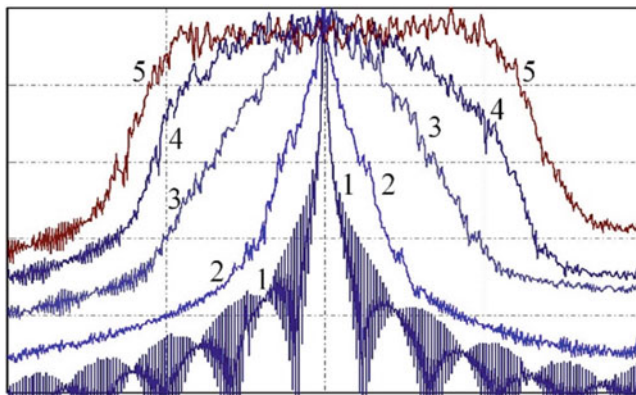


Fig. 5 Power spectral density of the noise sounding signal having different PSD bandwidth: 1 – 1 MHz; 2–1.8 MHz; 3–27 MHz; 4–54 MHz; 5–100 MHz

5 shows PSD of the signals with frequency modulation by normal noise with PSD rectangular shape within the frequency range of 0.1 ... 14 MHz.

The PSD widths of those signals at -3 dB level are as follows: 1.8; 27; 54 and 100 MHz, respectively. The Fig. 5 also shows that with PSD width increasing their shape varies from the Lorentz (curve 2), to the bell-shape (curve 3) then to truncated bell-shape (curve 4) and finally it transforms to rectangular one. For the cases of the curves 2 ÷ 5, the measurements have shown that increase in the step duration doesn't affect the shape and width of their PSDs, which is a consequence of the fact that correlation interval for all 4 cases does not exceed $1\mu\text{s}$ step duration. However, in case of single frequency signal, curve 1, power spectrum width of the Tx signal varies inversely proportional to step duration.

Figure 6 shows three experimental plots of coherence function. Their 0.5 width can be used for estimation of coherence length (correlation interval) of the sounding random signal of a single step duration. Curve 1 represents ambiguity function for the non-modulated signal, and its width equals 300 m. For the frequency modulated signal with 27 MHz bandwidth the correlation interval equals $L_c = 11$ m (curve 2), while for the signal having 54 MHz bandwidth the correlation interval equals $L_c = 5.6$ m (curve 3).

We have investigated a possibility of localization of the desired areas in range together with range selection and measurement of targets ranges within this zone using for sounding noise signals with synthesized spectrum. For that we used a cable transmission line which connected the transmitter output and the receiver input. An irregularity of the cable line placed at 2.2 m distance has been used as a target and another regularity at 7.8 m was used as passive interference. Reference signal of the transmitter was fed into the second input of the receiver. The probing signal consisted of 1024 steps. The central frequency of the Tx signal was increased from 950 MHz up to 1430 MHz with 1 MHz steps and then was decreased in the reverse order down to 950 MHz. The duration of the step was 1 μs . During the

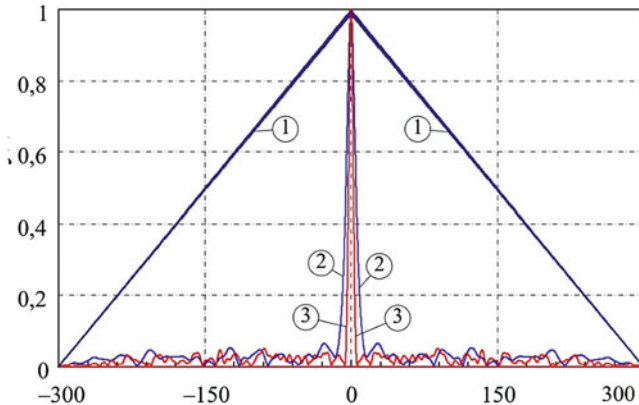


Fig. 6 Ambiguity function of a single step signal with different PSD bandwidth: 1 – 1 MHz; $L_c = 300$ m 2–27 MHz; $L_c = 11$ m 3–54 MHz; $L_c = 5.6$ m

measurement each frequency except the maximal one was repeated twice. The maximal frequency was kept during 66 steps. We used two types of signals: with frequency modulation for each step and without it. In the case of absence of frequency modulation, we obtained the well-known conventional SF Radar [1].

Figure 7 shows three range profiles within the 0 ... 12 m range interval with the solid curves and the related correlation intervals with the dashed ones, 1,2,3. The profile marked by circles (\circ) corresponds to the single frequency SF signal; triangles (Δ) – to noise signals with 27 MHz PSD bandwidth and squares (\square) – to noise signals with 54 MHz PSD bandwidth.

Numbering of correlation intervals corresponds to that in Fig. 6. It can be seen from the Fig. 7 that at the absence of frequency modulation the levels of signals reflected by the first target at 2.2 m and by the second one at 7.8 m are nearly equal because of weak attenuation of the signals in the cables. If the PSD bandwidth of the noise signal is 27 MHz, then reflection from the second target at 7.8 m is substantially weakened. If the PSD bandwidth of the noise signal is 54 MHz this reflection is suppressed almost completely. At the same time, the reflections from the first target at 2.2 m range decreases with the coefficient of 0.87 and 0.63, respectively.

Comparison of the obtained range profiles shows that a narrowband random signal significantly reduces the response from a target placed beyond the correlation length, L_c , of the Tx signal. This property of the SF Noise radar enables limiting of its working range, which could be a desirable performance, for instance, in Through-The-Wall radar. Variation of the PSD bandwidth of the TX signal gives a possibility to vary the working range or, in other words, tune the SF Noise Radar sensitivity interval. In SF Noise Radar cross-correlation of Tx narrowband noise signal and radar returns is estimated in I/Q phase detector having its output signals with a frequency not exceeding Doppler frequency interval for the chosen central frequency, which allows application of slow ADCs with high depth resolution (32–48 bits). This exclude application of fast ADCs, as it is needed in high resolution

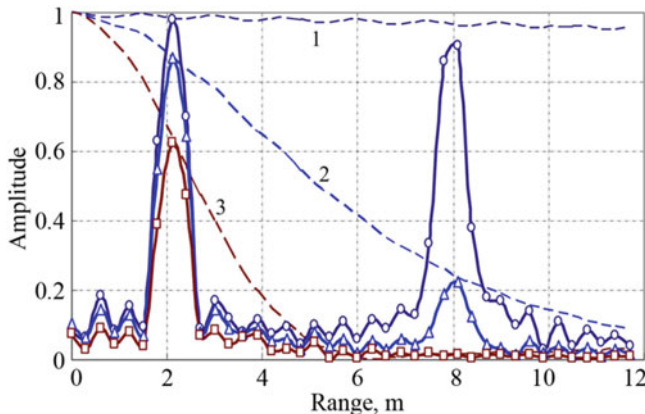


Fig. 7 Range profiles obtained with: (○) – SF signal ($L_c = 300$ m); (Δ) – Noise signal: 27 MHz PSD bandwidth ($L_c = 11$ m); (\square) – Noise signal: 54 MHz PSD bandwidth ($L_c = 5.6$ m)

Noise Radars [2–5]. In this way, SF Noise Radar has unique performance, such as high dynamic range, flexible control and wide range of probe signal parameters. This opens up a good prospective for the use of SF noise signals with synthesized spectrum in many realistic radar applications.

Software Stepped Frequency Noise Radar

We have designed and tested a Software stepped frequency noise radar based on Arbitrary Waveform Generator (AWG) that is a device enabling fast digital-to-analog converting of digital signals stored in a fast enough memory. In our experiments we have been using AWG-472 arbitrary waveform generator from EUVIS, Inc. [8]. This device has two synchronous channels with 4 Mb onboard memory for each channel and external clock frequency up to 4GHz. These performance enables design of Stepped frequency noise radar with synthesis of a narrow-band noise signal with central frequency being varied discretely according to an arbitrary law. In this approach the target range can be measured within the range limited by correlation function width (coherence length) of the transmitted noise signal. The finite duration of the correlation interval of the transmitted signal allows usage of this approach for eliminating ambiguity in range measurements, which is inherent drawback of conventional stepped frequency radar. Part of the processing is to be done in analog way using a wideband I/Q phase detector which may be treated as a correlator in our case: the radar returns are to be mixed up with the transmitted noise signal giving the output at the current central frequency. The I/Q phase detector output should be sampled with a slow multi-bit ADC and transferred to a PC for its further processing. Radar returns from targets placed at the ranges exceeding the noise radar correlation interval gives zero output from the phase detector/correlator.

Further processing consists in applying inverse Fourier transform over the whole frequency mesh resulting in getting of range profile (3) [2, 7]. Resulting signal which is formed in this way has almost rectangular synthesized spectrum shape which give range side lobes. It can be avoided by means of using an appropriate weighting of the synthesized energy spectrum of the transmitted signal or proper varying in the transmitted signals power.

Two types of wideband stepped-frequency waveforms in 1000–1500 MHz frequency band were being formed in the Software Stepped-frequency radar suggested. Generation of the first type of waveform is based on stepped changing of single frequency signal within the given bandwidth. Frequency step and signal bandwidth are the prescribed parameters in this case. The waveform of the second type is formed by means of stepped changing of PCD central frequency of narrowband random signal with bell-shaped or rectangular shaped spectrum. For the second type of waveform the PSD bandwidth of narrowband random signal and degree of overlap of neighboring spectrum shapes are to be defined, as well. This radar has been used for SAR imaging of a room containing multiple targets, which is described in section “Laboratory tests of software stepped frequency noise SAR”.

SAR Imaging Using Software Stepped Frequency Noise Radar

Stepped frequency noise radar enables obtaining range profiles (3) using the described above approach. After applying Fourier transform to the acquired signals one obtains information not only on the amplitude, but also on the reflected signals phase. This enables combining the stepped frequency noise radar with concept of synthetic aperture radar. In order to use this approach one needs to perform operation of stepped frequency noise radar at varying antenna position with respect to the scene. One can achieve this by moving the antenna (or the radar as a whole unit) along a special positioning system. All positions of antenna phase center with respect to the scene form the synthetic aperture. It can be either one dimensional or two dimensional. In the first case obtaining of 2D images in the “range – cross-range” coordinates is possible, while in the second case one can obtain 3D image with additional cross-range axis resolution.

Principle of SAR operation is based on processing of signal received by radar at various positions of Tx and Rx antennas with respect to the objects of interest. Antenna positions form certain virtual antenna aperture. SAR imaging can be considered as matched filtration of the signals obtained from different antenna positions. Signal from a point-like scatterer placed at the point of interest is used as a reference function. Such matched filtration can be described in spectral domain as follows. Relation for a Fourier-components of the received signal scattered by a point-like target is

$$E_{\vec{R}'}(f, \vec{R}) = E_0(f, \vec{R}) \cdot \xi(\vec{R}') h(\vec{R}' | f, \vec{R}), \quad (4)$$

where $E_0(f, \vec{R})$ is a Fourier component of the signal radiated at the antenna position \vec{R} ; $\xi(\vec{R}')$ is the reflection coefficient of the scene element with coordinates \vec{R}' ; $h(\vec{R}' | f, \vec{R})$ is a linear operator describing propagation of the signal towards the target and back, f is frequency of the Fourier harmonic.

Relation for estimation of the reflectivity of the given point of the scene $\xi(x, y)$ will have form

$$\begin{aligned} \xi(\vec{R}') &= \iint_{-\infty} E_{rec}(f, \vec{R}) \cdot E_{\vec{R}}^*(f, \vec{R}) df dR = \\ &\iint_{-\infty} E_{rec}(f, \vec{R}) \cdot \left(E_0(f, \vec{R}) \cdot h(\vec{R}' | f, \vec{R}) \right)^* df dR, \end{aligned} \quad (5)$$

where $E_{rec}(f, \vec{R})$ is a Fourier-component of the signal received by the radar at the given antenna position. Stepped frequency radar acquires the product $E_{rec}(f, \vec{R}) \cdot E_0(f, \vec{R})^*$ thus there is no need in Fourier transform of the sounding and reference signal and their multiplication.

For the far zone of the physical antenna the propagation operator can be written as

$$h(\vec{R}' | f, \vec{R}) = \frac{P \left(\frac{\vec{R}' - \vec{R}}{|\vec{R}' - \vec{R}|} \right)^2 \cdot \exp \left(-\frac{4\pi i |\vec{R}' - \vec{R}| \cdot f}{c} \right)}{|\vec{R}' - \vec{R}|^2} \quad (6)$$

where $P \left(\frac{\vec{R}' - \vec{R}}{|\vec{R}' - \vec{R}|} \right)$ is the physical antenna pattern; c is microwave propagation velocity in the medium. Normally, only the phase part of the propagation operator is used for SAR imaging. When SAR antennas move with low velocity and transmitting-receiving is done at certain positions, it is possible to substitute integral over \vec{R} by a sum over all antenna positions. Besides, due to finiteness of the signal energy spectrum, the integral over frequency may be substituted by the sum over frequency spectrum elements. This leads to following expression in discrete form:

$$\xi\left(\vec{R}'\right) = \sum_{a=0}^A \sum_{m=1}^M E_{rec}(m, a) \cdot E_0^*(m, a) \times \exp\left(\frac{4\pi i |\vec{r}_a| \cdot (F_{car} + m\Delta f)}{c}\right) \quad (7)$$

where \vec{r}_a is a vector joining the given antenna position with point scatterer, m is a number of a signal frequency component; M is a quantity of frequency components according to Nyquist criterion; Δf is frequency difference between two nearest frequency components; f_0 is PSD central frequency; $f_m = f_0 + m\Delta f$.

Laboratory Tests of Software Stepped Frequency Noise SAR

Block diagram of L-band Software Stepped frequency noise radar described in section “Software stepped frequency noise radar” is shown in Fig. 8. AWG output signal (CH1) is fed into the power amplifier unit where it is being filtered and amplified. Part of the sounding signal is coupled out to the reference channel while its main part is transmitted via Tx antenna towards the scene. Radar returns are received by the same antenna. Radar returns go to the phase detector where it is convolved with the reference signal. Output of the phase detector goes through the low pass filter and then sampled with low sampling rate ADC. AWG enables generating signals of any form. In current series of the experiments we generated two types of signals: single frequency stepped frequency signal and stepped frequency with narrowband noise modulation.

Stepped frequency signal was generated as 500 frequency steps with 1 MHz spacing and 1 μ s signal repetition period. SF Noise signal was generated in a PC as a

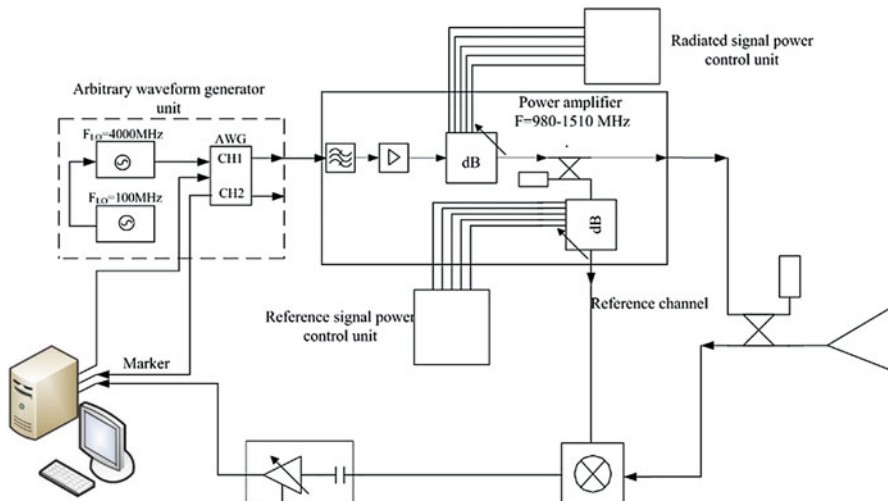


Fig. 8 Block diagram of experimental setup of Software stepped frequency noise radar

narrowband random signal with constant bandwidth and step-like varying of its central frequency and was uploaded into AWG memory. Its central frequency is varied according to the same law as in usual stepped frequency radar.

Step-like linear variation of frequency in time enables to obtain estimation of radar returns in frequency domain, where complex amplitude of the averaged product of sounding and reference signals is a function of frequency. Actually, we obtained the phase dependence of the reflected signal as function of the probing signal frequency. Application of inverse Fourier transform to this dependence gives the range profile (3) of the scene similar to the case of double spectral processing [2,9].

Poor decoupling of Tx and Rx antennas of the radar of Fig. 8 leads to presence of strong echoes in near range zone (maximum at 0.8 m). In addition, complex scene produces complicated image which is difficult to analyze. This can be cancelled by making two measurements – with and without target of interest and by subtraction of one image from another. Proper choosing of noise signal PSD bandwidth and adding a delay line in the reference channel enables limiting of radar sensitivity range. Combination of this range limiting with SF noise radar concept enables obtaining images within the desirable range intervals, only. In addition, application of slow ADCs with 32–48 bits enabled achieving a 96 dB dynamic range.

The L-band Software SF Noise Radar has been tested in indoor imaging experiment. The picture of the LNDES interior is shown in Fig. 9. in the room, such as: metallic.

There are many various objects in the room, such as: racks with measuring equipment along the wall; laboratory and office desks; metallic chairs and large safe-case; two tripods with antennas and TX and Rx units of Ka-band Ground Noise SAR, etc. In the front part of the picture one may see (from left to right) monitor, PC with ADC board, power supply unit, power meter, all placed on the top of the desk. Further one may see the L-band Tx/Rx Unit based on AWG-472 placed inside the box with horn antennas mounted on its sides. As targets we used two plastic balls of different diameters covered with metal foil. Tx/Rx Unit was placed on a truck that was able to move with an appropriate velocity along the cross-range direction. In this way SAR mode was implemented for the SF Noise Radar. Figure 10 shows 2D SAR Images of LNDES room without spherical targets and Fig. 11 shows similar images, but with two spherical targets at 2.5 m range from antenna which have been obtained with the help of L-band Software Stepped-Frequency Noise SAR described above.

In Figs. 10 and 11 there are three images obtained for three different PSDs bandwidths of the Tx waveforms. The images in the left column were obtained with a single frequency Tx waveform at every step, i.e. the usual SF mode, which had a correlation interval (coherence length) about 1500 m that made the SF radar sensitive to reflections from any object in the room including the walls, ceiling and floor. In spite of having strong reflections from tripods with antennas and TX and Rx units of Ka-band Ground Noise SAR and devices on the racks along the wall, we still may identify the spherical targets at the 2.5 m range in the image of Fig. 11.

The images in the middle column are obtained with the help of noise signal having PSD bandwidth of 10 MHz. Now we may see much lower reflections from



Fig. 9 Experimental setup of L-band Software stepped frequency noise radar in the LNDES room

the devices on both the desk and the racks at the wall. This is because of random waveform correlation interval was about 15 m, which limited sensitivity range of the radar. Similar images are shown in the right column of Figs. 10 and 11 obtained with random waveforms having the PSD bandwidth of 30 MHz which gives 5 m correlation interval, that does not allow to detect even the spherical targets placed at the 2.5 m range from the antenna. The obtained results are in complete agreement with theoretical description of the main performance of SF Noise SAR.

Tomographic Imaging with MIMO Stepped Frequency Noise SAR

There are several methods for generation of tomographic 3D SAR. Phased Antenna Array (PAA) is the most general approach to 3D image formation though it has some limitations in observation angles. However, the major disadvantage of PAA consists in a necessity of application of very complicated and expensive phase shifters, feeding and controlling systems to perform fast beam scanning. In addition, it requires both off-line and on-line calibrations, which makes its maintenance also very expensive.

Application of SAR approach though leads to certain loss in dynamic range of the system, but the beam scanning is done through a simple movement/switching of a small antenna, which makes the microwave circuits much simpler. Beam scanning

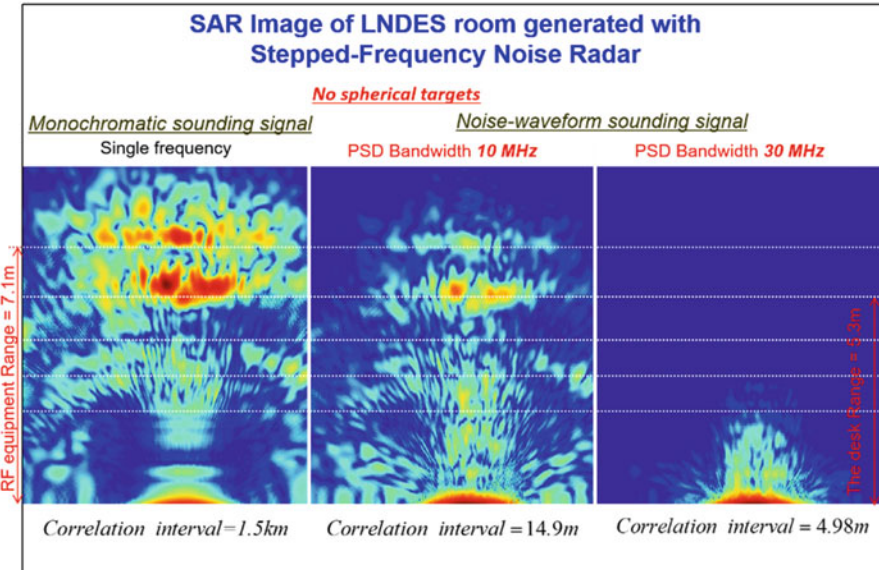


Fig. 10 2D Image of LNDES room obtained with L-band Software Stepped-Frequency Noise SAR: no spherical targets

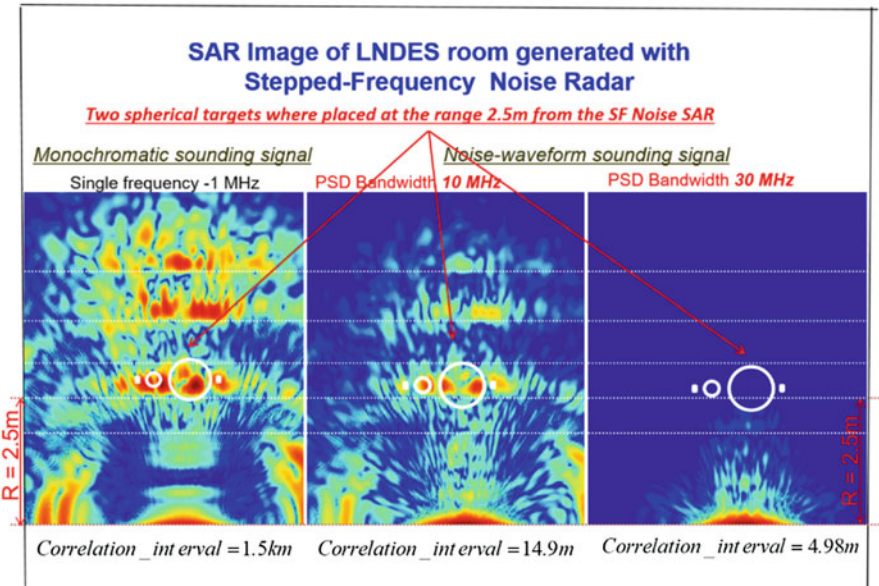


Fig. 11 2D Image of LNDES room obtained with L-band Software Stepped-Frequency Noise SAR: two spherical targets are placed at 2.5 m range from the radar

and/or SAR imaging is done via post processing of the acquired data. For 2D and 3D imaging the scan can be done either by shifting one of the antennas (Tx or Rx) or both of them. The latter mode provides twice higher angular resolution for the same aperture size compared to the former approach.

The most cost-efficient approach in terms of hardware is the cross- or L-shaped antenna configuration. In this case, one linear antenna (either Tx or Rx) switches/shifts its position by one step at a time, waiting for the other antenna accomplished full switching/moving through a full cycle before shifting by another step, and then the process is repeated until all the combinations of Tx and Rx antennas positions are visited. Thus, a dataset is obtained that is reasonably sufficient to form a 3D image (compared to a simultaneous scan of the entire 2D plane). We will call this mode as a *MIMO mode with time-division of TX/Rx channels*.

The principle of tomographic 3D imaging consists in illumination of an object of interest with a wideband signal enabling high enough range resolution and in formation of 2D aperture for providing cross-range (angular) resolution required. Having the reference signal sampled we can vary its delay and thereby perform range focusing. This enables generation of 2D images (tomographic slices) for every range bin inside transparent/semitransparent scene. In this way, application of noise or SF waveform with wide enough PSD bandwidth enables layer-by-layer visualization of a semitransparent scene and, therefore, generation of its tomographic 3D image [11–13].

SF Noise SAR transmits set of narrowband random signals at every position of Tx positions and coherent reception of the scattered waves at all Rx antenna positions. Estimation of cross-correlations of the Tx and Rx signals contains information on the amplitude and phase of every range bin of the illuminated area. The range bin is defined by range resolution which depends on the PSD bandwidth B : $dz = c/2B$, where c is the velocity of light. SF noise waveform with a variable PSD bandwidth enables controlling the radar range resolution, which is the 3rd coordinate of the tomographic image.

2D aperture synthesis is the next step in 3D tomographic image formation. 2D aperture synthesis may be performed via either real or virtual motion of Tx and/or Rx antennas over a planar synthetic aperture along with performing transmission and reception of SF random signals at the equidistant grid nodes, as was described above. Positioning system for such 2D movement may be complex and expensive. To simplify this process, we have suggested generation of virtual 2D synthetic aperture via moving of both Tx and Rx antennas, but along only two orthogonal directions forming either Cross- or L-shape antenna arrays. 2D scan is done in the following way: Tx antenna takes the first position, and Rx antenna performs SAR scan along a horizontal path. After that, Tx antenna is displaced to another position along vertical path, and a new SAR scan is performed by the Rx antenna. Every scan of the Rx antenna enables generation of a 2D image in the plane of Rx synthetic aperture. Those images for different Tx antenna positions will contain information on phase shift of the signal due to movement of the Tx antenna phase center which may be used for angular(cross-range) compression.

The MIMO noise SAR developed in LNDES IRE NASU contains transmit (Tx) and receive (Rx) Antennas with Pattern Synthesizing (APS) [10]. In these antennas the phase centres of a radiator/receiver (which is a resonant slot) in both antennas can be moved along their apertures. Radar returns are sampled when varying the radiator /receiver positions for the scene imaging.

The first step in the signal processing is a standard one for the SF noise SAR imaging is so called range compression which gives range profiles (3) related to every realized combination of the Tx and Rx radiator/receiver positions. This can be done via estimation of cross-correlations between the received and reference signals. In case of SF noise radar the IF copy of the transmitted signal $S_{m, n, l}$ is to be used as the reference function:

$$R(\tau, r_T, r_R) = \frac{1}{T} \int_{\tau}^{T+\tau} X_{Ref}(t, r_T, r_R) X_{RR}(t, r_T, r_R) dt \quad (8)$$

where τ is mutual delay between the reference signal and the radar returns acquired when signal propagating from transmitter towards a scene point and back to the receiver:

$$\tau = \tau(r, r_T, r_R) = \{|r - r_T| + |r - r_R|\}/c \quad (9)$$

which is the function of the coordinates r of the point of interest and the Tx/Rx antennas positions are: r_T, r_R .

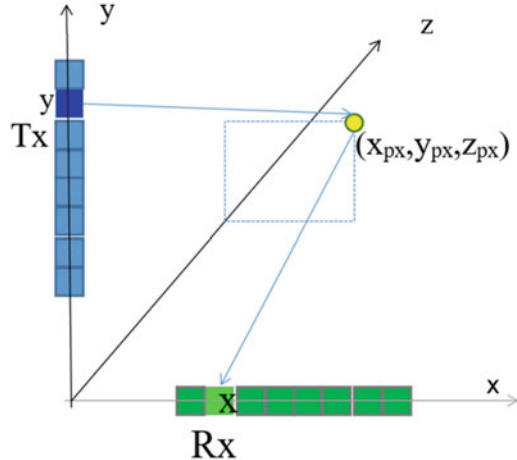
The second step in the processing is the angular compression. It can be done either separately for azimuth and elevation planes, or alternatively, as a single procedure. The idea of the processing can be explained as follows. We choose a point of interest in the scene. If a target is present at this point, it will leave responses in the range profiles acquired at all the antenna positions. Compensation of the phase shifts acquired by signals when propagating towards the point and back to every position of Rx receive antenna and further summation of the radar returns will result in a peak if the target really existed in the point of interest. In this way, the resulting value, assigned to the 3D pixel is:

$$I(r) = \frac{1}{L_T L_R} \iint_{L_T L_R} R[r_T, r_R, \tau(r, r_T, r_R)] e^{i\omega\tau(r, r_T, r_R)} dr_T dr_R \quad (10)$$

where ω is the angular carrier frequency of RF signal.

So for the imaging with the help of such a system one has to trace the signal transmitted by Tx antenna, reflected by the scene and received by the Rx antenna and after that apply an appropriate signal processing. It is seen from Eq. (10) that in order to form a 3D image with the help of the MIMO SF noise SAR the angular compressions (*azimuth and elevation*) are to be applied to the range compressed data (*range profiles*), $R(\tau, r_T, r_R)$ (3) previously prepared for every combinations of Tx and Rx antennas positions, provided proper phase compensation according

Fig. 12 Scheme of 3D Imaging via combination of 2D aperture synthesis (2D image focusing) in XY plane and radar range compression along Z axis



to Eq. (10). Actually, Eq. (13.10) sums up all the range profiles with accounting the phase shifts acquired by transmitted, scattered and received signals when propagating towards a scene and back. Figure 12 shows a geometrical illustration to the above description of antenna configuration and the signals propagation in 3D imaging experiments.

Suppose, that Tx radiator phase centre was placed in one by one fashion at N positions along its aperture. At each of these positions, radiator of the Tx antenna did not move when transmitting CW noise signal. Part of the transmitted signal was sampled and used as a reference signal, while Rx antenna phase center was sequentially placed at M positions along Rx antenna aperture where the radar returns have been received during the integration time. Both the reference and the received radar return are down converted, digitized and saved in the on-board memory of ADC board. Assume that every record of both the reference and the radar returns contains L samples. This gives two 3D arrays of samples: $S_{m, n, l}$ for the reference signal $X_{Ref}(t, r_T, r_R)$ and $C_{m, n, l}$ for the radar returns $X_{RR}(t, r_T, r_R)$; $m = 1 \dots M$, $n = 1 \dots N$, $l = 1 \dots L$.

For implementation of the 3D imaging algorithm it is suitable to use a discrete representation of the Eq. (10):

$$I(x, y, z, f) = \sum_{m, k} R_{m, k} \left(\frac{r(x_{px}, y_{px}, z_{px}, m, k)}{c} \right) e^{\frac{2\pi j f r(x_{px}, y_{px}, z_{px}, m, k)}{c}} \quad (11)$$

where

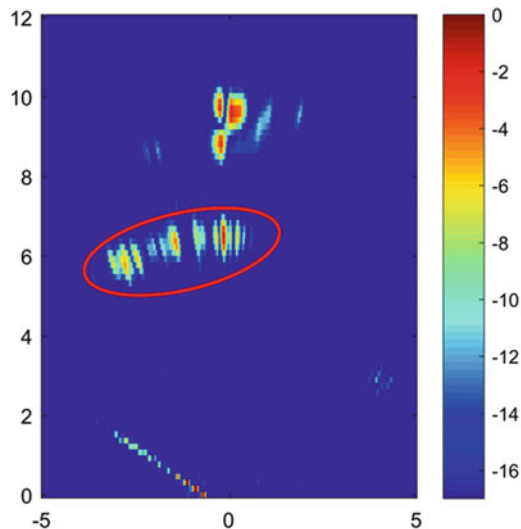
$$r(x_{px}, y_{px}, z_{px}, m, k) = \sqrt{x_{px}^2 + (y_{tx} - y_{px})^2 + z_{px}^2} + \sqrt{(x_{px} - x_{rx})^2 + y_{px}^2 + z_{px}^2} \quad (12)$$

- $y_{tx} = m * \Delta y$, $x_{rx} = k * \Delta x$;
- m is the number of Tx antenna resonant slot position;
- k is the number of Rx antenna resonant slot position;
- $r(x_{px}, y_{px}, z_{px}, m, k)$ stands for the overall path of the Tx and Rx signals equals to the sum of the distances from Transmitter to the scene pixel and from the pixel to the Receiver.

Equation (11) enables formation of tomographic SAR image and its cross section along any plane provided proper transformation of the coordinates. For estimation of range profile in SF noise SAR the algorithm (3) is to be used. Knowing properties of sounding signal enable application of detection rule to the generated. Thus 2D aperture synthesis in combination with range resolution capability of wideband noise signals gives a possibility of performing tomographic SAR images in both active and radiometric modes. Usage of random waveform gives such benefits as absence of range ambiguity and improving immunity against external electromagnetic interferences, providing high EMC performance [1–5].

The noise SAR designed was able to image even a slowly moving target. One of such 2D Noise SAR images is shown in Fig. 13 [14]. The response from the moving

Fig. 13 Image of experimental scene with a target moving towards the SF Noise SAR antenna: the target responses is marked with red ellipse



target (marked with red ellipse) is spread widely along azimuth and across the range strip due to its motion.

As it may be seen from the presented results, SF noise SAR is capable of 2D image generation, including mapping of moving targets, provided fast enough antenna scanning.

The developed MIMO Ground Noise SAR has been used for 3D imaging experiments of outdoor scenes and the data acquired has been used for generation 3D coherent images with the help of Eq. (11) and Eq. (12). Some details of that experiments may be found in [11,12].

Conclusions

We have presented approach for obtaining range profiles in noise radars which enable achieving high both dynamic range and range resolution, using analog convolution of Tx random signals and slow multibit ADCs. It is based upon stepped frequency radar concept but with narrowband random sounding signal. This enables combination of advantages of both stepped frequency and noise radar concepts such as low frequency radar returns to be sampled, on the one hand, and high electromagnetic compatibility and interference immunity performance, on the other hand. We have carried out experimental tests of this approach and investigated its basic performance, such as: spectral characteristics of probing signal, switching time of its central frequency, output signal of quadrature detector, range profile, etc. Possibility of range limiting has been experimentally shown in the observation area jointly with selection and measuring of the target distance within this area when using sounding noise signals with the synthesized spectrum. This can substantially reduce the interference level during detection, tracking and measurements of target coordinates. Besides, we have explained possibility of 2D and 3D tomographic SAR imaging using this signal and validated capability of the SF NR to measure Doppler frequency shift which is important for SAR imaging. The approach described being properly modified enables generation of the images with multistatic passive systems, as well.

We have approved microwave tomographic imaging technology experimentally, which gave a good background for application of the suggested MIMO SF Noise SAR technology for design of cost efficient and technically effective high resolution and fast 3D Imagers needed when developing of reliable security systems for detection of hidden firearm and explosives.

References

1. Iizuka K, Freundorfer A (1983) Detection of nonmetallic buried objects by a step frequency radar. *Instit Electr Electron Eng* (71): 277–279
2. Lukin K (1999) Noise radar technology. *Radiophysics and electronics*, Kharkov. Institute for Radiophysics and Electronics of NASU. 4(3): 105–111 (In Russian). Translation is published in *Telecommunications and Radio Engineering* 55(12) 2001: 8–16
3. Lukin K (2005) Noise Radar Technology: the principles and short overview. *Appl Radio Electron* 4(1): 4–13
4. Tarchi D, Lukin K, Fortuny-Guasch J et al. (2010) SAR imaging with noise radar. *IEEE Trans Aero Elec Sys* V 46(3): 1214–1225
5. Lukin K et al. (2008) Ka-band bistatic ground based Noise-Waveform-SAR for short range applications. *Radar Sonar Navigation, IET* 2(4): 233–243
6. Bandhauer B (2007) Frequency hopping radar, US Patent No. US 7,215,278 B2, Int. Cl. G01S 7/28. Date of Patent 08.05.2007, <http://www.patentstorm.us>
7. Lukin K, Mogyla A, Palamarchuk V, Kravchuk A, Cherniy B (2010) Noise radar with synthesizing of sounding signal spectrum. *Radiophysics and Electronics*, Kharkiv, IRE NASU 15(1): 62–71 (2010) (In Russian); Translation in *TELECOMMUNICATIONS and RADIO ENGINEERING* 70(10): 883–898, (2011)
8. <http://www.euvis.com/>
9. Mogyla A, Lukin K, Kulyk V (2001) Statistical errors of ranging in the spectral interferometry technique. *Telecommun Radio Eng* 55(10–11): 67–77
10. Lukin K (2005) Sliding antennas for synthetic aperture radar. *Appl Radio Electron* 4(1): 103–110
11. Lukin K et al. (2015) SAR tomography for short range applications using MIMO ground based noise waveform SAR. *Appl Radio Electron* 4(1): 103–110
12. Lukin K et al. (2011) 2D and 3D imaging using S-band noise waveform SAR. *Proceedings of third International Asia-Pacific Conference on Synthetic Aperture Radar. (APSAR-2011)*. pp. 1–4
13. Baselice F, Ferraioli G, Lukin S, MatuozzoG, Pascazio V, Schirinzi G (2016) A new meth odology for 3D target detection in automotive radar applications. *Sensors* 16: 614
14. Lukin S (2018) 3D imaging in automotive radar using stepped frequency and random waveforms. PhD Thesis. University of Napoli “Parthenope” 139 p

Dual Sensor ALIS (Advanced Landmine Imaging System) and Its Operation in Cambodia

Motoyuki Sato (✉)

Center for Northeast Asian Studies, Tohoku University, Sendai, Japan

e-mail: Motoyuki.sato.b3@tohoku.ac.jp

Introduction

Humanitarian demining has gathered interest all over the world last 20 years, however, it is still quite important activity in many mine affected countries. Since the Ottawa treaty established in 1997, land mine problems have been widely known, and we have continued efforts to demolish all the landmines including buried mines in mine affected countries. However, we have noticed that in many mine affected countries, mine clearance is not an easy task and we are continuing this effort. It is reported that accidents caused by landmines occurred in 56 countries in 2016, and more than 9000 people were killed or injured. As of November 2017, landmines remains in 61 countries [1].

Most of the humanitarian demining activities are supported by ODA (Official Development Assistance), and the cost to effect ratio is an important issue. Although humanitarian demining operation has been conducted for more than 20 years, in most mine affected countries, buried mines still remain in relatively difficult sites for such as mountainous areas. At the same time, types of mines that we have to detect is not only plastic mines that contain small amount of metal part which is normally detonator, but also non-metallic mines, which is typically produced by guerrilla in countries such as Colombia.

In conventional humanitarian demining operation, landmine detection was carried out by EMI (Electromagnetic Induction) sensors (also referred as Metal detector), which is capable of detecting very small metal objects included in plastic mines. United Nation (UN) and domestic organization of demining determine the SOP (Standard Operation Procedure) for humanitarian demining, and normally all the metal material buried shallower than 20 cm must be removed. Currently, detection of landmines by EMI sensors is almost perfect, and can detect very small metal objects. However, problem of detection of mines by EMI Sensor in mine fields is the large amount of metal debris which have to be removed together with land mines. In order to increase the efficiency of land mine detection and clearance, GPR (Ground Penetrating Radar) has been introduced. Since GPR is also sensitive to non-metal material included in the landmines, it has a possibility to discriminate landmines from metal debris. A combined sensor of EMI and GPR is called “Dual Sensor” in humanitarian demining. We have developed ALIS (Advanced Landmine Imaging

System) dual sensor since 2002 and have deployed it in mine affected countries. In this paper, we introduce the technology used in ALIS and its achievements.

EMI Sensor and GPR

EMI sensors, which is also called as a metal detector, has widely been employed in detection of buried landmines, UXO and explosive substances. EMI sensors can detect only electrically conducting material included in these explosive objects. In contrast, Ground Penetrating Radar (GPR) can also be used not only for metallic objects, but also for non-metallic objects. GPR is sensitive to even very small targets such as gravels and tree roots in soil, and even detect inhomogeneous soil moisture. Therefore, if we use only GPR for detecting landmines, we will be confused by numerous images of subsurface material. Therefore the idea of Dual sensor is that we use EMI sensor as a primary sensor, and then we use GPR as a secondary sensor for classifying the detected objects. Tohoku University has developed a dual sensor ALIS since 2002 [2–9].

The ALIS prototype was equipped with a camera which is set on the pole of the sensor head, which looks down on the ground surface, and the movement of the sensor head was estimated from the captured images of the ground. Therefore it could track the position of the sensor, while it is moved by a hand of an operator for survey. The GPR system used in ALIS uses cavity back spiral antennas and operates at 1–3 GHz. We found that GPR can image deeper than 20 cm, which is required by the UN standards. The GPR data and EMI sensor acquired with the sensor position information are recorded on a PC and are processed simultaneously to visualize the data. One of the unique technical points of ALIS is that it can use Synthetic Aperture Radar (SAR) processing for GPR image reconstruction [3]. As far as we were concerned, there is no other dual sensors which can use SAR processing for obtaining GPR images for hand held GPR sensor, which can be used for landmine detection. It should be noted that SAR processing is equivalent to migration processing used in GPR signal processing [10, 11].

ALIS Development

The development of ALIS started in 2002, and the first prototype of ALIS was completed in 2004. We conducted field tests of ALIS operation in an evaluation test site prepared in Afghanistan in 2004, using inert mines [5]. In this test we could confirm that SAR processing is quite useful for GPR under the real mine field condition. If we test GPR performance in sandpit of laboratory condition, most GPR systems can image the buried landmines clearly, because sand is homogeneous and there is no clutter. In contrast, in real mine field conditions, very strong clutter which is caused by the gravel and tree roots in the soil, and inhomogeneity of soil



Fig. 1 ALIS (Second generation prototype) operated in a mine field in Cambodia

moisture distort the GPR image of buried landmines. However, we found that SAR processing reduces the clutter drastically, and we could recover clear GPR images.

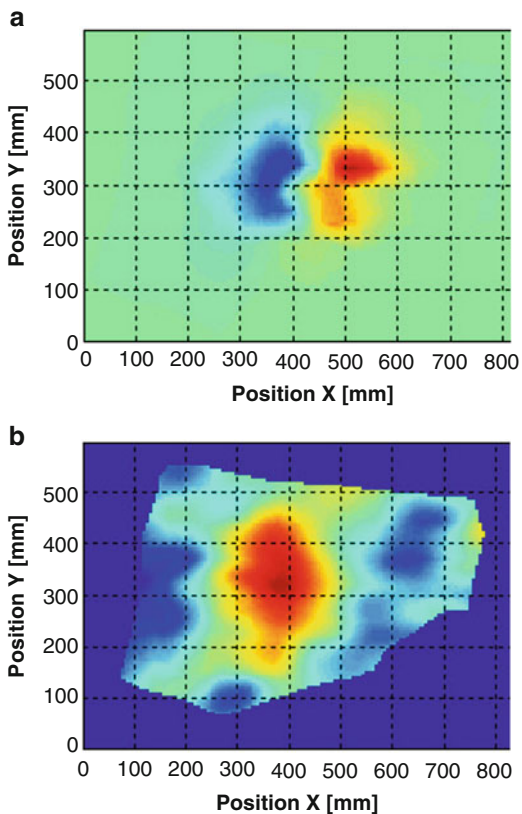
The initial test in Afghanistan has to be quitted, because of the unstable political situation, and then we continued the test in Cambodia in 2006.

Based on some field experiments, we developed the second-generation prototype ALIS. The first porotype of ALIS was operated by 2 operators. One of the operator scans the sensor head and the second operator processes the data and analyses the SAR images to detect buried mines. However, after evaluation tests, we found that the system should be operated by one operator in real mine fields, and we designed the second generation prototype of ALIS, which can be operated by one operator as can be seen in Fig. 1. The system is composed from 3 units, which include the sensor head, the PC for signal processing and display and the backpack including electrics board and batteries.

ALIS Field Tests in Mine Affected Countries

The second-generation prototype of ALIS has been used in Croatia in real mine fields in 2006 and 2007 for quality control (QC) operation in humanitarian demining operations [6]. Then we conducted the evaluation tests of the second-generation prototype ALIS in Cambodia in 2009 together with CMAC (Cambodian Mine Action Centre). Based on this evaluation test, CMAC gave the certificate to ALIS for operation for humanitarian demining, and decided to use the prototype of ALIS in mine clearance operation in mine fields. Tohoku University and CMAC agreed to

Fig. 2 Visualized EMI sensor and GPR data acquired by the prototype ALIS. (PMN-2, Mine field in Cambodia) (a) EMI response, (b) GPR response



organize a team for ALIS and 2 sets of the second-generation prototype ALIS systems have been used in mine fields during 2009 and 2016.

Figure 2 shows an example of images obtained by ALIS in a mine field in Cambodia. A PMN-2 anti-personnel mine, which is a plastic mine having diameter of 8 cm buried in soil is clearly imaged.

During 2009 and 2016, more than 254,867m² mine contaminated area has been cleared, and more than 80 mines have been detected by ALIS. Totally 15,621 metal fragments were detected, and demines have judged that 12,081 (77%) detected objects out of them are not mine. There was not case that mine was judged as a fragment.

Due to the UN regulation, all the objects detected by a EMI sensor have to be excavated, and excavation needs more time than detection of buried objects. This means, if ALIS is used for mine clearance operation, more than 70% of detected objects by metal detectors does not have to be excavated as possible mines. We believe this will drastically shorten the time for excavation, and increase the efficiency of the whole mine clearance operation.

ALIS

Based on the experience of operation of prototype ALIS in mine affected countries including Croatia and Cambodia, we have continued hardware development of ALIS and it was completed in 2017. This ALIS is composed from one unit, which includes EMI and GPR sensor head and its electronics and batteries, and a tablet PC which is used for SAR processing and data display.

One of the major technical change compared to the conventional prototype ALIS systems is its senior position tracking function. Conventional prototype ALIS systems have used a camera and image based sensor position tracking system. However, ALIS is now using an accelerometer equipped within the sensor head for the sensor position tracking. For the signal processing, we use a tablet PC (Panasonic Toughpad), which works on Android. Other technical specifications of ALIS including EMI and GPR performance have not been changed from the prototype ALIS. Therefore, we believe that the technical performance of the advanced ALIS has already been validated by ALIS prototype operations in mine fields.

The system is powered by Ni-MH rechargeable battery, and works more than 6 h. The size of the system is shown in Fig. 3, and it is not much different from most of the conventional EMI sensors (metal detectors) used for humanitarian demining. The total weight of the equipment including the battery is 3.1 kg (Fig. 4).

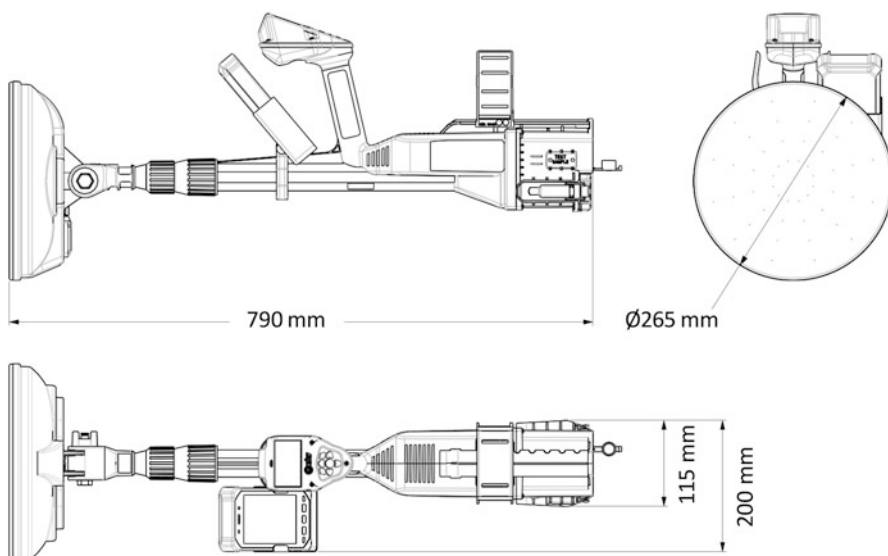


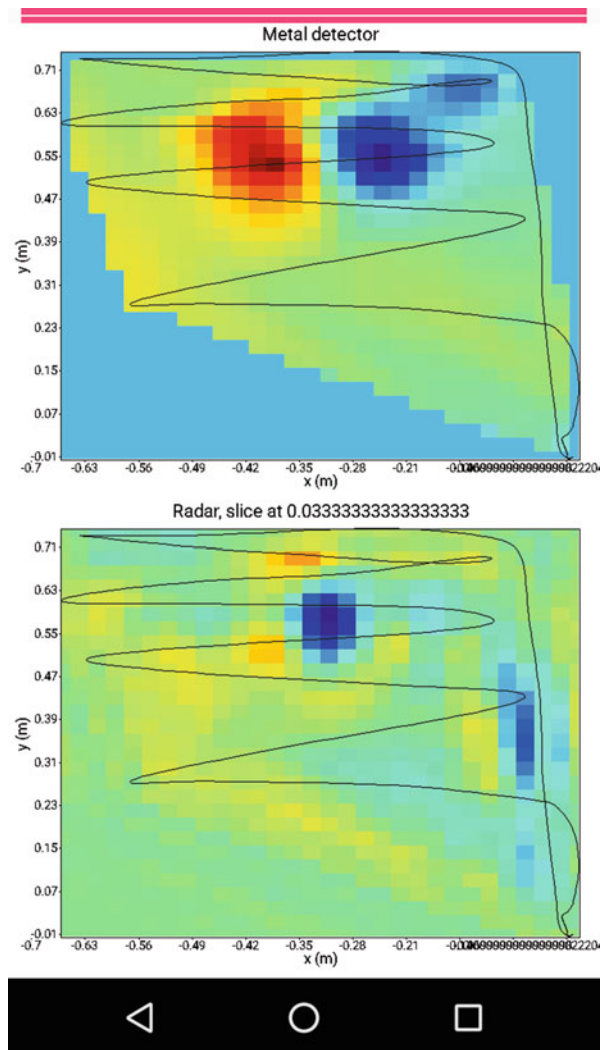
Fig. 3 ALIS. (Size for transportation is shown)

Fig. 4 ALIS system

A typical operation procedure of ALIS is as follows. At first, a deminer uses EMI sensor and detect a metal object. Then the deminer uses GPR of ALIS and acquires dense data in an area typically around 50 cm by 50 cm, which the deminer can scan the sensor head without moving the body. The deminer will sweep the search head to acquire the data. The interval of each sweep should be around 5 cm, and the scan must cover the area of the object. After the data acquisition, signal processing automatically starts, and EMI and GPR horizontal image (C-scan) will be displayed on the color LCD display of the tablet PC as shown in Fig. 5. The deminer can change the depth of the C-scan image by sliding the display by a figure, then can judge the shape of the buried objects. After the data acquisition, signal processing takes only a few second, and the deminer can judge the images immediately after the scanning.

The scanning operation of the ALIS sensor head is not much different from the conventional EMI sensors. Therefore we believe the introduction of ALIS is easy for deminers who have experience on EMI sensor operation.

Fig. 5 ALIS display on a tablet PC



Evaluation Test in Cambodia

We conducted evaluation test of ALIS at a mine detector test lanes at CMAC R&D site at DU4, which is located near Siem Reap, Cambodia in February 2018. This site was prepared in 2006 for evaluation test of GPR and EMI sensors under the support of the Japanese government. The first prototype of ALIS was also evaluated in this site in 2006, and the second prototype of ALIS was evaluated in 2009.

Table 1 Soil type

Lane #	Soil Type
4	Sand (dry)
5	Clay (dry)
6	Laterite

Each lane has 180 cm width and 25 m length. The soil property of each lane is different, and 4 lanes which we used for the test are shown in Table 1.

Several kinds of targets, including Type-72, PMN-2 and metal fragments such as screw are buried at different depth in this site. In this time, we used known objects as targets, in order to obtain the standard data sets (Fig. 6).

ALIS EMI sensor is equipped with a soil compensation function, which can adjust the performance of the EMI sensor to soil properties. Some soil types such as Laterite contain Ferromagnetic material and EMI sensors responded to the soil itself. If a landmine is buried in such magnetic soil, it is very difficult to detect the metal included in the mine by EMI sensor, because the response from soil is not much different from the metal in the mine in intensity. In order to avoid this problem, ALIS EMI sensor records the response from magnetic soil, and discriminate from metal contained in the mine.

Figure 7 shows one of the images, which were obtained by ALIS. EMI data is raw signal, and GPR image is obtained by synthetic aperture radar (SAR) signal processing.

In order to use SAR processing, we have to determine the velocity of electromagnetic wave in soil. The velocity of electromagnetic wave is given by

$$v = \frac{c}{\sqrt{\epsilon_r}} \quad (1)$$

where $c = 3 \times 10^8$ (m/s) is the velocity of electromagnetic wave in vacuum and ϵ_r is the dielectric constant, which is dominantly determined by soil moisture. Therefore, we have to know the soil moisture to obtain high quality ALIS GPR images.

Figure 8 shows two GPR images processed by using different dielectric constant value. We can understand that the selection of the appropriate dielectric constant can focus the image of the targets. The soil moisture can be changed dependent on the climate condition. However, we found that the small variation of the velocity used for SAR processing changes the depth of the image, but the shape of the images have not much been affected.

We can obtain nominal value of the dielectric constant by using a TDR (Time Domain Reflectometer) on site, but we are developing software which determines the dielectric constant from acquired GPR data.

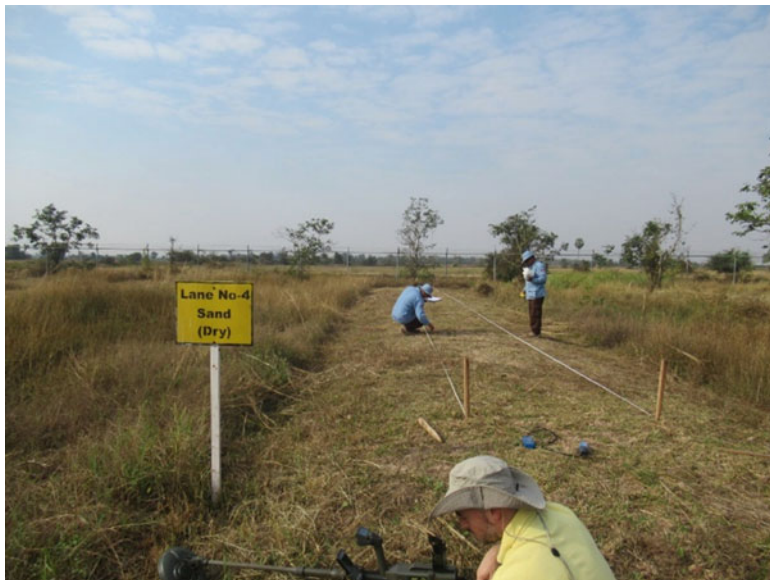


Fig. 6 CMAC DU4 R&D site, Test Lane #4 (Sand)

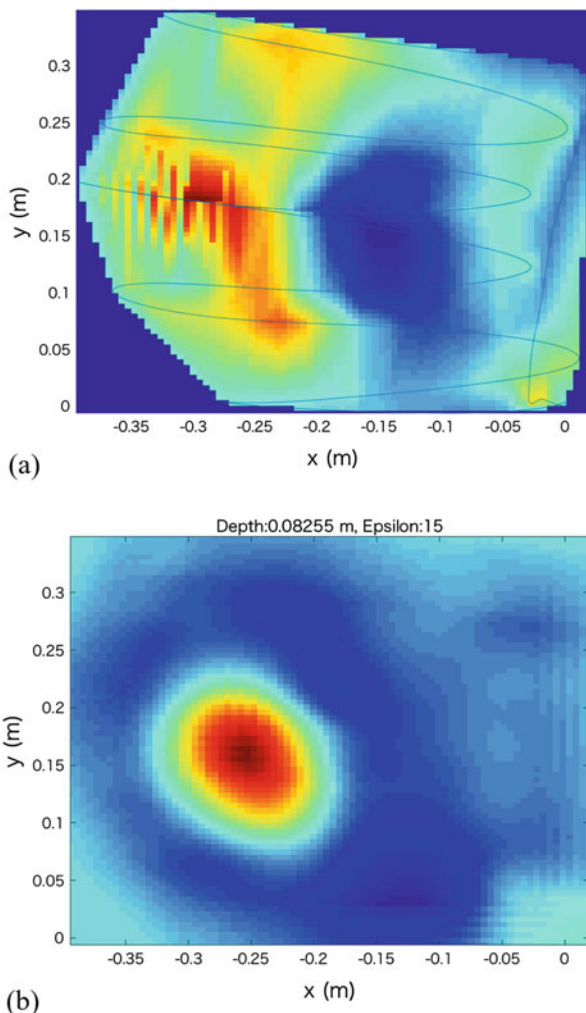
ALIS Operation in Cambodia

In October 2018, we trained 4 Cambodian deminers for ALIS operation. Two of them have ever used the prototype ALIS and the other two have never used. At first we explained the technical principle of ALIS and showed the difference of detection performance of GPR and EMI sensors. We used 4 days for this basic training of ALIS operation. We found that all four operators learned the basic operation of ALIS and they could discriminate the mines from metal fragments by observing the ALIS GPR images for known targets.

Then CMAC conducted an evaluation test of ALIS for field operation. The evaluation of the accuracy of the detection and location of the buried metal objects was the main issue in this test. This is to guarantee the safe operation of ALIS as a mine detection sensor (Fig. 9).

After conducted performance trial on ALIS dual sensors detector for period of 6 working days in CMAC test lanes of mine detector, CMAC trial team summarized the performance of ALIS as follows:

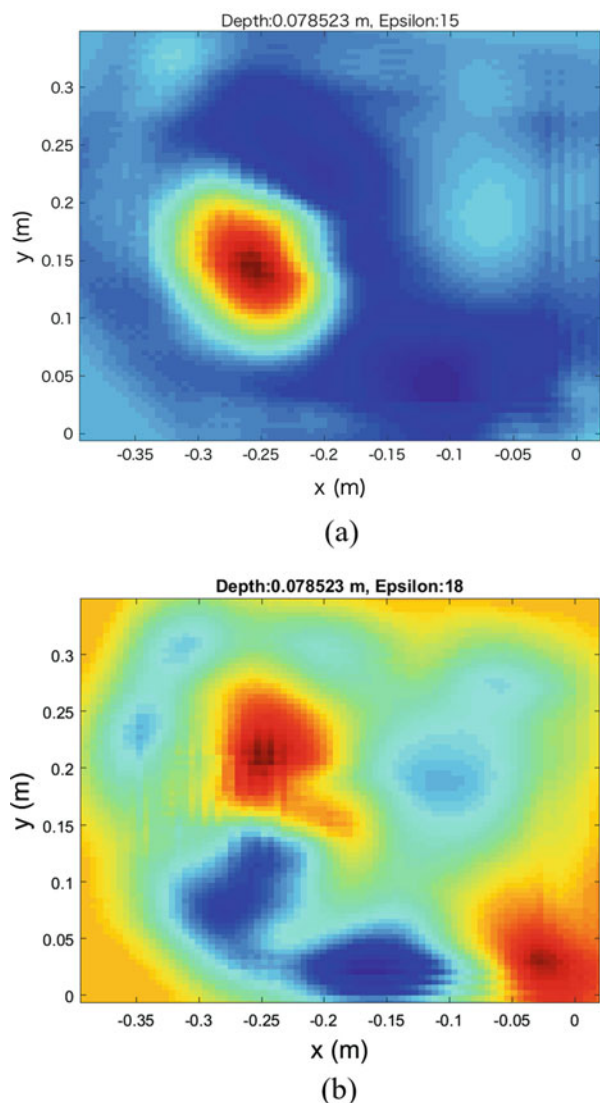
Fig. 7 ALIS image (Type 72, depth = 10 cm, Laterite, data#810, sixth Feb 2018).
a EMI sensor, **b** GPR



Advantage

- ALIS is the dual sensors detector and could be judged mine or metal.
- ALIS is in good detection for pinpointed
- ALIS is simple in operation (not complicated functions for operations)
- ALIS is recorded data of operations (data logger).
- ALIS saved time on investigation of detected metal objects by GPR with experienced operator.

Fig. 8 ALIS GPR image.
 (Type 72, depth = 10 cm,
 Laterite, data#810, 6 Feb
 2018). **a** $\epsilon_r = 15$, **b** $\epsilon_r = 18$



Disadvantage

- ALIS is little heavy than CMAC existing metal detector.
- ALIS is in hot conditions need reset frequently.
- ALIS is some time features of scan received not-clear.
- ALIS is not able to scan the big boundary of detection object like Anti-tank mine at depth of 50 cm.
- ALIS is scanned in good results requires the flat ground.



Fig. 9 ALIS operation training in CMAC DU4 site, Siem reap, Cambodia

Then CMAC concluded as follows. "It should be mentioned that ALIS dual sensors detector was completed test and evaluation in safe area (test lanes) as schedule planned, no faced any major technical troubles."

The following recommendations were made by CMAC based on the discussion with members of trial team.

1. The ALIS dual sensors detector should be considered the next step on Operational Field Evaluation (OFE). CMAC Technical Survey Clearance (TSC) team with five persons should be tasked to conduct OFE.
2. The first draft of ALIS SOP, should be approved, for improvement in temporary use of OFE.
3. If Researcher team of Tohoku University and CMAC decide to implement recommendation above, then they should consider starting OFE from January to September 2019, on the purpose of evaluation ALIS Ground-penetrating Radar on dry and wet soil condition,

Following the recommendation by the research and development division of CMAC, CAMC gave the certificate of ALIS operation in mine fields in Cambodia in January 2019, and established the SOP for ALIS.

Two units of ALIS were rented to CMAC from Tohoku University and CMAC has started the operation test of ALIS in mine fields in Cambodia from January 2019 (Fig. 10).



Fig. 10 ALIS operation in a mine field in Battambang province, Cambodia

Conclusion

We described the development of ALIS, which is a dual sensor for humanitarian demining in this paper. ALIS technology has been established based on the evaluation test of operation in real mine fields in Cambodia since 2009.

In January 2019, CMAC gave the certificate to ALIS for its operation in mine-fields, and CMAC started its operation.

It visualization capability is unique among dual sensors, and its performance will be evaluated in the long-term test in minefields in Cambodia. Clutter rejection by SAR processing of GPR data is the most important technical features of ALIS.

The performance of EMI sensor and GPR strongly depends on the soil physical properties and targets, *i.e.*, landmine types. EMI sensor is affected by magnetic soil, but the soil compensation function of ALIS solved this problem. Soil inhomogeneity due to moisture is the most important reason which cause the clutter image in GPR. It is also strongly dependent on the soil type and its *in-situ* conditions. Therefore field evaluation tests in various soil conditions must be conducted, and the acquired data should be scientifically analyzed to optimize the performance of ALIS capability of landmine detection.

Acknowledgments

This work was supported by the JSPS Grant-in-Aid for Scientific Research (A) 26,249,058. The field tests were supported by CMAC Cambodian Mine Action Centre) and IMCCD (International Mine Clearance and Community Development Supporters).

References

1. <http://www.the-monitor.org/en-gb/reports/2017/landmine-monitor-2017.aspx>
2. Sato M (2010) Evaluation test of ALIS in Cambodia for humanitarian demining. Proceedings of SPIE – The International Society for Optical Engineering 7664.
3. Feng X, Fujiwara J, Zhou Z, Kobayashi T, Sato M (2005) Imaging algorithm of a Hand-held GPR MD sensor (ALIS). Proc SPIE 5794: 1192–1199
4. Sato M, Fujiwara J, Feng X, Zhou Z, Kobayashi T (2005) Development of a hand-held GPR MD sensor system (ALIS). Proc SPIE 5794: 1000–1007
5. Sato M (2005) Dual sensor ALIS evaluation test in afghanistan. IEEE Geosci Remote Sens Soc Newslett: 22–27
6. Sato M (2009) ALIS evaluation tests in Croatia. Proc SPIE.7303, 73031B-1-73031B-12
7. Sato M, Fujiwara J, Takahashi K (2007) The development of the hand held dual sensor ALIS. Proc SPIE, 6553, 65531C-1-65531C-10
8. Sato M, Takahashi, K (2007) The evaluation test of hand held sensor ALIS in Croatia and Cambodia. Proc SPIE, 6553, 65531D-1-65531D-9
9. Sato M, Takahashi K (2007) Development of the hand held dual sensor ALIS and its evaluation. Proc 4th International Workshop on Advanced Ground Penetrating Radar, pp. 3–7
10. Sato M (2018) Introduction of the advanced ALIS: advanced landmine imaging system. Proc vol 10,628, SPIE Defense + Security, Orlando, Florida, USA.
11. Sato M (2011) ALIS: a handheld multisensor system for landmine detection, Ch11.1 In Subsurface Sensing, Wiley, ISBN978-0-470-13388-0

Explosive Detection: Growing of the Threat and New Approaches in Suicide Bombers Detection

Pierre Charrue (✉)
NATO/ISEG, Brussels, Belgium
e-mail: pierre.charrue@cea.fr

From the beginning of the twenty-first century, the terrorist threat has changed on many aspects with the implementation of modus operandi involving both more or less sophisticated techniques and rather often the completion of the attacks by suicide bombers.

These phenomena have increased with the development of war zones over the world and the terrorism training of young and fanatic persons within special clandestine training camps.

The consequences of such situation are now more and more impacting the society's ways of working as the citizens themselves which tend to feel insecure when attacks are occurring in any country.

The answer to this kind of evolution is not simple and has to be examined on the different aspects of the steps which are overcome from the attack decision up to the implementation of the final attack. Many of these attacks are fortunately stopped during upstream preparation phases thanks to the intelligence services actions and cooperation which represent the best protection of the society against this kind of threat.

In some cases, self-radicalized and generally isolated people can decide by themselves to implement an attack. These attacks coming from unknown people by security services are not easy to identify and prevent. In such case, the last barrier to defeat the attack tentative is the detection of the terrorist when he tries to enter in a critical infrastructure.

The critical infrastructure checking of the whole accesses without disturbing the normal working of it is a real challenge.

The purpose of this paper is to propose some improvements both in detection strategies and in the implementation of sensors to obtain more flexible, adaptable and efficient detection systems to counter as far as possible most of attack tentatives.

The homemade explosive detection is very complex because of the various constituents used to prepare such materials and the wide possibilities which exist to prepare HMEs. Moreover these materials can be used in different physical state (solid, liquids, gels, gases,...). The possibilities of combination of constituents and configurations of use are almost infinite (bomb carriers, left behind luggage, body trapped vehicles (cars, trucks, boats, planes, drones, etc....)).

The first strategy implemented consisted in improving already existing technologies to obtain the best possible detection results and sensitivity in optimized configurations. Such strategy is today developed for X-Rays detection machines which associate different X-Ray technologies associated with high power calculation technologies which allow to both checking many luggage in rather short time (hundreds luggage per hour) with a very high resolution. The main international airports are now equipped with such systems. This kind of strategy is also developed to associate various kinds of sensors in portable detectors for example for vapor traces detection.

Another strategy was developed within the NATO/STANDEX program from 2010.

The basic idea consisted in associating different kinds of detection technologies based on different physical way of working in order to get an orthogonal detection configuration to limit the false alarm rate as far as possible. In fact the challenge was to apply such detection system in a metro station to check moving people in corridors without stopping them. The implementation of this configuration of detection was only possible by plugging the different real time working sensors on a data merging

and analysis system containing both a data processing module for alert triggering and a sophisticated video tracking system to track the suspicious people having triggered an alert when moving among the crowd.

Such system has been demonstrated in Paris metro in June 2013. Some of the technologies developed in the frame of this program have been transferred to industry and are now commercialized.

Hundreds of runs in different configurations were performed using both explosive simulants and explosive traces. The tests were performed in real configuration of use of the metro station in order to evaluate the environment configuration effects on the detection performances (temperature variations, dust, vibrations, electromagnetic noise, etc...). During the different runs, more than 2000 people equivalency passed through the detection system. Each of the components of the system were controlled by official agencies to guarantee that the whole system was complying with the health and safety French and European regulations before authorizing the implementation of detection trials.

The real time and contactless detection feasibility being demonstrated, the further improvements will consist in developing alert management systems to control the critical infrastructure access whether alert is triggered and stop the attack tentative.

An example of a possible configuration strategy which could be adopted is described in the Fig. 1 thereafter:

Question addressed: what could be further detection systems?

People checking will be more and more frequent in the future because of the increase and evolutions of the terrorism threat using explosive materials. Whatever be the further detection systems architecture, CONOPS and technologies implemented they will have to comply with the applicable regulations and ethical rules to be accepted by the citizens which will be submitted to several time a day checking even for their private activities to access show or sport event places for example.

The today evolutions tend to fuse detection sensors and electronic devices. These hybrid systems will become probably very familiar in the next few years because integrated within smart phones and other mobile electronics. Such sensors could be

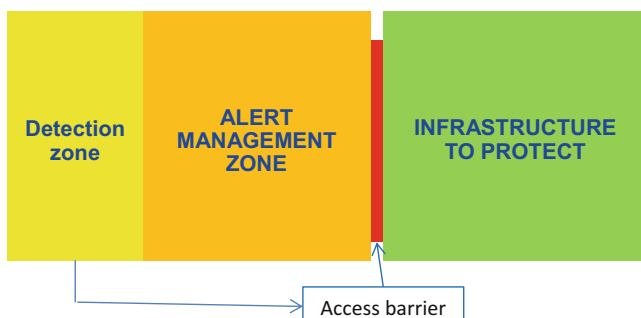


Fig. 1 An example of protection strategy which could be implemented

used to check the air pollution level for example and so contribute to the building of real time pollution maps. It could be also used in the frame of chemical air contamination to trigger alert.

This miniaturization of sensors could be used also in association with micro drones coordinated in cloud configuration, each drone being equipped with a specific sensor. Such configuration could be imagined to remote control a suspicious object or a left behind luggage in a train station for example.

Today micro drones are also developed for specific applications. The Rolls Royce Company associated with the Harvard University are developing a very small drone named SWARM⁵ (4,5 cm) to inspect airplane engines. We can imagine other applications of such technology for example to check truck payloads which are often not easy accessible.

Such technology configuration needs, to be realistic, to have a rather great autonomy which means that the drone should have enough electrical energy to work a long time. This constrain is not compatible with the mass limitation of the drone except if the drone is continuously electrically reloaded by electromagnetic waves when working. This kind of technology already exists and is developed in France by the QUINTEQ Company⁶.

The data processing will have to be developed using Artificial Intelligence machines capabilities the drones will have only to transfer rough data which will have to be real time processed.

Other families of sensors are also developed using bio-electronic configurations. Such work is developed in North Carolina University in the USA⁷. Rather little information is available on such technologies.

Other breakthrough technologies could deeply modify the development of further sensors. For example a team of King's College, London, UK published recently interesting results related to room temperature working masers⁸.

Such technology could provide low cost and effective coherent microwaves sources which could be used in the explosive detection. The use of microwaves sensors has been demonstrated during the STANDEX trials in 2013.

The future configuration of the detection systems will be very different of what is today implemented. Some of the further key technologies and potential breakthroughs are discussed in the presentation.

⁵Revue Sciences et Avenir, N°859, Septembre 2018, P 23

⁶La Recherche, Octobre 2017, N°528

⁷Sciences et Avenir- Avril 2017,N°842

⁸Jonathan D.BREEZE & All., Nature 555, 493-496, (22nd March 2018)

The other key point will be the adaptability of detection systems to the evolution of the threat combining explosives and other hazardous products or materials.

Protection of critical infrastructures will have to be considered in different configurations, the most promising being to detect as far as possible upstream of the entrances to stop any attack tentative and limiting the potential consequences on the infrastructure so protected.

The further detection strategies will probably consider the 3 spatial dimensions and the time dimension to manage the alerts. That's the purpose of the next NATO / DEXTER programme which will be launch very soon.

Findings of the Advanced Research Workshop



As reported in previous chapters, the “Advanced Research Workshop on Explosives Detection” (the Workshop) represented an important gathering of scientists, engineers, policy-makers, and administrators working within the framework of the NATO Science for Peace and Security (SPS) Programme. The three pillars of SPS are Science, Partnership, and Security, and this workshop thoroughly embodied all three in ways that will be discussed in this chapter. However, participants also identified avenues to strengthen these pillars – especially in Partnership – and we reserve discussion of this pillar for last.

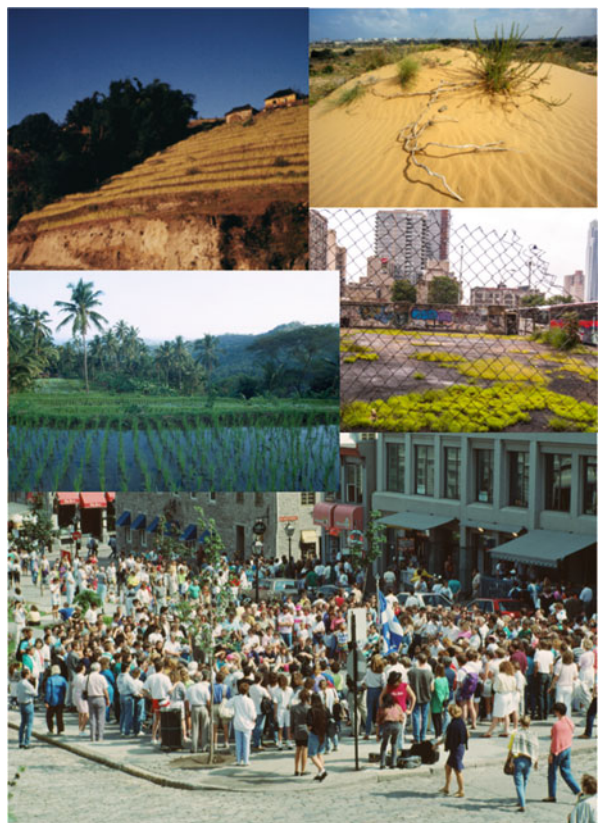
Multidisciplinary Approach

One of the findings of the workshop was the multidisciplinary and cross-cutting approach inherent in all the projects presented at the workshop. It is worth noting the range of scientific disciplines represented (physics, chemistry, biology, geoscience, computer science, mathematics, etc.), as well as many fields of engineering (electrical/electronic, mechanical, informatic, communications, robotic, etc.). In many projects, practitioners from diverse disciplines collaborated closely – foreshadowing the coming discussion of partnership.

Threat Diversity

The science and technologies described in this volume cover a necessarily wide range of application modes and environments. The explosives in the title of the workshop could represent landmines, UXO, and other explosive remnants of war (ERW) in post-conflict regions. Alternatively, they could be improvised explosive

Fig. 1 Impressions of a variety of possible settings for detection of explosive devices. (All photos public domain)



devices (IEDs) deployed in active war zones, former war zones, or non-conflict areas subject to terroristic attack. Furthermore, IEDs might be stationary or moving. A stationary IED might be similar to a landmine or other ERW, while a moving IED is very different – deployed as a car bomb, in a suitcase, or as an explosive vest, shoe, or any disguising article. The possibilities are limited only by the malicious imagination of the attacker. Furthermore, in all of these modes of deployment, the environment may be different. ERW-type threats could be buried in sand- versus clay-rich soils, in dry or wet climate, on a flat plain or a mountainside, and in an open farm field or a narrow city street (see, e.g., Fig. 1). Mobile explosive threats might have different speeds and movement patterns, and be delivered by a human or vehicle, but for maximum effect will probably threaten crowded places like busy city streets, festivals, concerts, transportation terminals, etc.

Even a brief consideration of possible explosive threats suggests a minimum of about 10 environmental and operational variables, with end-members as follows (with continuous spectra between of course) (Table 1):

Table 1 End-Members of 10 possible variables for explosive threat detection

End-Member 1	End-Member 2
Stationary Explosive Device	Fast-Moving Mobile Device
Peaceful Area	Active Conflict Zone
Affluent Region	Impoverished Region
Undeveloped Setting	Urban Setting
Easy Access to Power and Communications	Remote and Isolated
Arid Climate	Wet Climate
Flat Terrain	Rugged Terrain
Granular Soils	Cohesive Clay Soils
Uniform Particle Size	Long-Graded Aggregate
Dominantly Fine	Dominantly Cobbles

The reader may immediately think of others and may realize that some of these are probably not entirely independent. However, this simply reinforces the incredible range of conditions under which detection of explosive threats must be undertaken. Figure 1 depicts just a few possible settings.

This range of variables drives the need for the range of technologies, and therefore the range of science and engineering disciplines required for a comprehensive global program of threat reduction and security enhancement. A single technology or system, or even a single set of systems, is likely to be applicable to no more than a few particular threats in rather specific combinations of settings.

Partnerships

Of course, the need for a wide variety of technologies to provide global security, and their coordinated development and deployment, will require many levels of partnership. Projects represented at the Workshop displayed excellent internal partnerships – between people of different nationalities, different levels of age, experience, and education (older PhDs working with young undergraduate students), different genders/identities (male, female, and non-binary team members) to name a few. Partnership between project teams already exists at some levels, and will be increased by the connections made at the Workshop. Several formal discussion sessions, as well as social events, provided a forum for the exchange of ideas, recognition of natural synergies, and the exchange of contact details both for continued correspondence and collaboration and for new collaborative opportunities.

Recommendations

Based on the need for multiple combinations of technologies to address the global explosive threat, Workshop participants identified and discussed several desired manifestations and opportunities for enhancing partnership. These include:

1. *Modularity*: this would allow rapid integration of sensors/systems to address specific sets of threat conditions. This will require standardization:

1.1. *Standardization of*

1.1.1. *Connectors*

1.1.2. *Communications Protocols*

1.1.3. *Data Formats*

2. *Centralized Data Storage*: Easy access to data generated by various project teams would allow:

2.1. *Replication of Results*: This is a critical component of the Science pillar.

2.2. *System Testing and Validation*: Comparison of the performance of new systems with existing ones can demonstrate that projects are truly enhancing the Security pillar.

2.3. *AI Learning Data*: Artificial Intelligence/Machine Learning (AI/ML) is a fast-emerging, powerful method for rapid, high-speed target detection – and more importantly, discrimination (e.g., between threats and innocuous objects). However, development of effective intelligent systems (with necessarily very high probability of detection and low false alarm rate) requires a tremendous number of training images or datasets – probably far too many for a single research group, or even a consortium of institutions, to compile. Compilation of a global repository of shared training datasets is a great opportunity for partnership.

3. *Capacity Building*: Although great progress in demining and addressing IEDs has been realized in recent years,¹ the problem remains geographically widespread, and locally intense. There are multiple countries and territories with hundreds of IED incidents per year,² and hundreds of square kilometers of potentially mined land¹. Meaningful threat reduction/security enhancement will require scale-up and distribution of the experimental, emerging, and/or new technologies. This will surely require partnership between research groups, governments, and NGOs – which can be facilitated, or simply made possible, only with NATO SPS support.

We note a final point under partnership. One aspect of enhancing security in the face of explosive threats was mentioned briefly by at least two presenters at the Workshop; they indicated that their organizations/teams certainly work on detecting explosive threats, but also on detecting and disrupting the people and networks that train and support those who would build and deploy those threats. This is an important point, and one that is not often stated explicitly: *Detecting already-*

¹International Campaign to Ban Landmines (2018) Landmine & Cluster Munition Monitor – 2018, ICBL, Geneva.

²Overton, I., Dathan, J., Winter, C., Whittaker, J., Davies, R. & Kaaman, H. (2017) Improvised Explosive Device (IED) Monitor – 2017, Action on Armed Violence (AOAV), London.

deployed mines, IEDs, or moving explosive vectors is the last line of defense against catastrophic events. In this section, we imagine stopping a catastrophe by detecting an explosive device at the last line of defense (a near-miss in the language of safety and forensic engineering), and then applying a “5-Whys”³ Root Cause Determination of the type commonly applied in product failure analysis and safety incident (or, in this case, near-miss) debriefs.⁴ After detecting, responding to, and neutralizing the threat, the root cause determination could start at different points or focus on different failures; e.g., “how did this device get through previous levels of security screening?”, or “why didn’t the AI target identifier recognize this as an explosive device?”

However, if we start just with the situation, with no inference about the engineering- or systems-level failure, we may end-up with a very different and very broad root cause:

1. Q: Why is this explosive device here?

A: Someone put it there.

2. Q: Why did they put it there?

A: Because they wanted to harm or terrorize _____.

3. Q: Why did they want to harm or terrorize_____?

A: Because they believe that _____ has/have wronged them egregiously.

4. Q: Why do they believe that _____ has wronged them?

A: Because _____ has something (resource, land, honor, security, privilege, etc.) that rightly belongs to them.

5. Q: Why do they feel that it rightly belongs to them?

A: _____.

There is a massive body of psychological, historical, religious, cultural, etc. literature providing Answer 5 for various peoples, at different places and times. We conclude that to achieve the highest and earliest-stage level of safety/security effectiveness on a global scale, we will need cooperation amongst the physical sciences and engineering, as well as political and social sciences. This requires a coordinating framework with global reach – a role that can only be filled by an international organization such as NATO SPS.

³Ohno, T. (1988). Toyota Production System: Beyond Large-Scale Production, CRC Press, Boca Raton.

⁴Tuli, R. W., & Apostolakis, G. E. (1996). Incorporating Organizational Issues into Root-Cause Analysis. Process Safety and Environmental Protection, 74(1), 3–16.

Special Call for Proposals

According to the findings of this workshop, the NATO SPS Programme issued a special call for proposals in October 2019 in the field of explosives detection. The call encouraged long-term research in the hard sciences, as well as in social disciplines (such as political science, anthropology, sociology, psychology, etc.). Social science applications could be in the form of long-term studies, case studies with practical applications (i.e. sharing best practices, developing recommendations, identifying gaps), field studies, etc.

The SPS Programme addresses the following key priorities and areas in the field of Mine and Unexploded Ordnance Detection and Clearance:

- (a) Development and provision of multi-sensor systems, new and advanced technologies, methodologies and best practice
- (b) Ensuring end users are given sufficient relevant information and included in the decision-making process.
- (c) Active and ongoing review of past projects to drive future works
- (d) Fostering the integration of devices and methods from different project and technologies into other and future projects
- (e) Data analysis
- (f) Preparation for Actual Field Conditions
- (g) Dissemination and Capacity Building

The findings of the Advanced Research Workshop have helped define the following areas of interest in a systematic way:

- **Multi-Sensor Systems**
 - Standardization of communications protocols
 - Development of modular sensors and other components
 - Integration of existing detection technologies
 - Testing and evaluation of the effectiveness of various combinations of sensors
 - Field procedures or algorithms for pin-pointing of targets
- **Data Analysis**
 - Advancement of post-processed detection systems to real-time results
 - Novel data fusion methods
 - Application of artificial intelligence/machine learning to explosive object identification
 - Compilation of test results and target signatures or images into a widely-accessible database
 - Identify common shapes or elements of IEDS to enhance detection and discrimination
 - Automation of threat detection and response

- **New or Rapidly Developing Technologies**

- Development of drone-mountable systems
- Adapt technologies for remote robotic operations
- Identification of emerging technologies
- Integrate systems using “smart” cyber-physical components
- Elevate technology readiness level for existing but under-developed methods
- Methods for search area or clearance area reduction
- Enhance portability and field applicability of direct explosives detection technologies

- **Preparation for Actual Field Conditions**

- Develop scalability for promising approaches
- Develop or adapt promising lab/test bed technologies to realistic terrain
- Organization of realistic field trials for promising technologies

- **Dissemination and Capacity Building**

- Commercialization and distribution of well-developed technologies
- Enhancement of communication between researchers and end-users
- Exchange of equipment for synergistic co-development or integration
- Exchange of young researchers